18TH
INTERNATIONAL
BRYOZOOLOGY
ASSOCIATION
CONFERENCE

BRYOZOAN STUDIES 2019

Edited by
Patrick Wyse Jackson & Kamil Zágoršek

Czech Geological Survey

Dedication

This volume is dedicated with deep gratitude to Paul Taylor.

Throughout his career Paul has worked at the Natural History Museum,
London which he joined soon after completing post-doctoral studies in Swansea
which in turn followed his completion of a PhD in Durham.
Paul's research interests are polymatic within the sphere of bryozoology – he has
studied fossil bryozoans from all of the geological periods, and modern bryozoans
from all oceanic basins. His interests include taxonomy, biodiversity,
skeletal structure, ecology, evolution, history to name a few subject areas;
in fact there are probably none in bryozoology that have not been the subject of his
many publications. His office in the Natural History Museum quickly became a magnet
for visiting bryozoological colleagues whom he always welcomed:
he has always been highly encouraging of the research efforts of others,
quick to collaborate, and generous with advice and information.
A long-standing member of the International Bryozoology Association,
Paul presided over the conference held in Boone in 2007.

Contents

Foreword

The 18th International Conference of the International Bryozoological Association was held in the Technical University of Liberec, in the beautiful city of Liberec in the Czech Republic, from Sunday 16 June to Saturday 22 June 2019. The meeting was presided over by Tim Wood.

The meeting was attended by 82 delegates from 17 different countries. 64 oral communications, together with 23 posters were presented. Of particular significance was the participation of younger delegates some of whom were supported through the IBA Travel Awards and The Palaeontological Association Grant-in-Aid.

This volume contains sixteen papers presented at the Conference, and the editors and Association are most grateful to the Czech Geological Survey for willingness to publish these proceedings. The IBA conference volumes are a valued source of primary research on bryozoans and collectively have added considerably to the body of knowledge on this group since the first conference volume was published in 1968.

The conference followed the usual organisational scheme and began with a pre-conference fieldtrip that visited many geological and cultural sites in Bohemia and Moravia. Led by Kamil Zágoršek the trip started from Budapest, Hungary where the group visited the Hungarian Natural History Museum before spending seven days travelling through central Europe. Devonian, Cretaceous and younger Eocene and Miocene successions were examined. Cultural activities included visits to significant mediaeval castles such as at Filakovo, the UNESCO World Heritage locations at Vlklinec and Rajsna, and two battlefields. The trip finished in Prague with a city tour.

On arrival at Liberec the delegates congregated in a disused cinema for an ice-breaking party sponsored by the micro-brewery Albrecht, and the following morning the scientific sessions commenced in the AULA lecture theatre in Building G on the University campus. In total thirteen sessions were delivered during the programme, on different bryozoological topics including evolution and ecology, growth and morphology, bryozoans and climate change, bryodiversity, phylogeny, southern hemisphere bryozoans, reproduction and development, and fossil studies. The diversity of papers and posters covered all aspects of bryozoology with a wide geographical and geological coverage. On the first morning of the conference Eckart Hakansson delivered a keynote address on free-living cheilostome bryozoans.

The mid-Conference trip took in a circular route that highlighted a number of important geological locations close to Liberec, as well as places of cultural and more-recent historical significance. The First stop was to Jested Hill where the party ascended a volcanic cone on top of which is perched a television and communications mast and centre. Following this, a cave system in local sandstone was visited – this is now a favoured haunt of local motorbike enthusiasts. Lunch was at the Cvikov Brewery where the operations were explained, and some of the resultant products drunk afterwards over a meal. In the afternoon the IBA group visited the breath-taking Panská Skála locality which is the most visited tourist site in the district – here columnar basalts erupted during the Paleogene cropout in spectacular fashion. While there the President took the opportunity to collect freshwater bryozoans in an adjacent pond. On the return journey to Liberec a short visit was made to a local glass producer.

The Conference Dinner, which was held early during the meeting, took place in the atmospheric cavernous vaulted basement of the City Hall. Ellis Medals were presented by the President, Tim Wood to Dennis Gordon and Mary Spencer Jones; these are awarded to members who have made a major contribution to the bryozoological community. The announcement of the recipients was met by resounding cheering and clapping.

At the close of the meeting the outgoing President instituted Antonietta Rosso the incoming President who in turn presented him with an IBA Presidential Medal. Three Gilbert Larwood Awards were presented: to Marianne Nilsen Haugen for her poster on *Reptadeonella* in European waters, to Katerina Achilleos for her paper on biochemical pathways in calcification of marine invertebrates focussed on *Cellaria immersa*, and to Carolann Schack for her paper on depth gradients characterising polymorphism in New Zealand cheilostomes.

The Post-Conference Field Excursion took place along the Croatian coast of the Adriatic Sea where participants led by Maja Novosel spent a week on the board of a research vessel diving, collecting and studying modern bryozoans. A number of cultural and scientific visits were made on land: these included a trip to the Palace of the Roman Emperor Diocletian, and the Institute of Oceanography and Fisheries, both in Split, and a viewing of making jewellery from red coral on the island of Zlarin. The pictures from Conference events can be found in http://18iba.tul.cz/photos.

The overriding benefit of the IBA International Conferences is to provide bryozoologists a forum to present and discuss new research, and to develop new collaborations. This volume provides a permanent record of the proceedings which we believe will serve to stimulate on-going and future studies into fossil and modern bryozoans.

The IBA and the bryozoological community is most grateful to our host Kamil Zágoršek who organised the meeting with huge efficiency, and who delivered an event that will live long in the memory. As host Kamil warmly thanks the Rector of the Technical University of Liberec Doc. Miroslav Brzezina, the Dean of the Faculty of Science, Humanities and Education Professor Ján Picek, and the Head of the Liberec District Martin Půta, for their support leading up to, and during the meeting. He is most grateful to all of his colleagues, students and members of other organisations and institutions whose assistance and cooperation made the conference and fieldtrips successful, namely: Ilona Sovová, Helena Lánská and Martin Mašek, together with the students Kristýna Vobejdová, Jáchym Krček and Filip Dirigl. The following people are warmly thanked for their help during the running of the field excursions: Alfréd Dulai, Miklós Kázmér and Jan Doucek.

The International Bryozoology Association and host Kamil Zágoršek are most grateful for the support of various sponsors: the Palaeontological Association, the University of Zagreb Department of Biology, and the Ministerstvo žívotního prostředí ČR (Ministry of the Environment, Czech Republic) and Albrecht – chateau brewery Frýdlant.

1st December 2019

Kamil Zágoršek, editor and conference host
Patrick N. Wyse Jackson, editor

Group photo
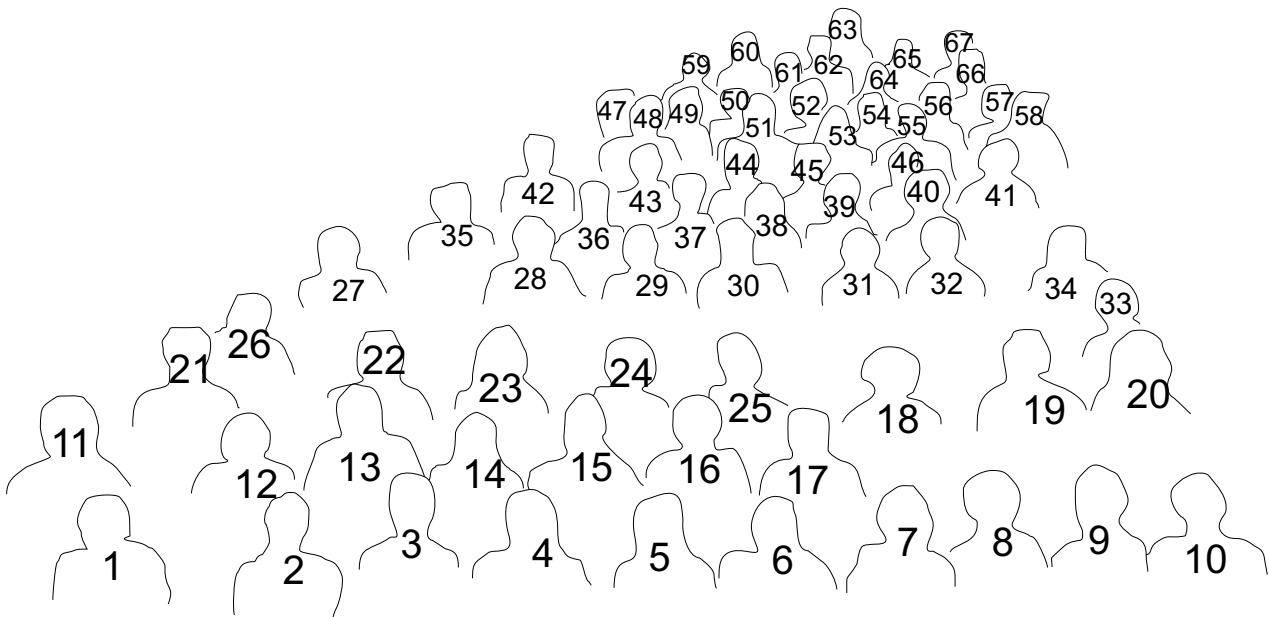
The list of participants

1) Kamil Zágoršek, 2) Carolann Schack, 3) Karine Nascimento, 4) Ana Carolina Almeida,

5) Nadezhda Karagodina, 6) Andrew Ostrovsky, 7) Elena Belikova, 8) Olga Kotenko,

9) Anna Kvach, 10) Vladimir Kutiumov, 11) Helena Lánská, 12) Philip Bock,

13) Steven J. Hageman, 14) Vanessa Yepes-Narvaez, 15) Leandro Manzoni Vieira,

16) Dennis P. Gordon, 17) Mary E. Spencer Jones, 18) Antonietta Rosso,

19) Nina V. Denisenko, 20) Ji Eun Seo, 21) Marcus M. Key, Jr., 22) Mali Hamre Ramsfjell,

23) Maja Sannum, 24) Yuta Tamberg, 25), Catherine Reid, 26) Eckart Håkansson,

27) Scott Lidgard, 28) Patrick Wyse Jackson, 29) Juan Luis Suárez Andrés,

30) Mark A. Wilson, 31) Ekaterina Shevchenko, 32) Uliana Nekliudova,

33) Urszula Hara, 34) Norbert Vávra, 35) Julian Bibermair, 36) Lara Baptista,

37) Ania Piwoni-Piórewicz, 38) Katerina Achilleos, 39) Hannah Mello,

40) Maja Novosel, 41) Timothy S. Wood, 42) Sebastian Decker, 43) Paola Florez,

44) Judith E. Winston, 45) Lee Hsiang Liow, 46) Abby Smith, 47) Emanuela Di Martino,

48) Loic Villier, 49) Chiara Lombardi, 50) Paul Taylor, 51) Hans Arne Nakrem,

52) Noga Sokolover, 53) Laís V. Ramalho, 54) Joanne Porter, 55) Sergio Gonzalez Mora,

56) Andrea Waeschenbach, 57) Caroline Buttler, 58) Piotr Kuklinski, 59) Björn Berning,

60) Marianne Nilsen Haugen, 61) Andrej Ernst, 62) Arthur Porto,

63) Beth Okamura, 64) Junye Ma, 65) Thomas Schwaha,

66) Joachim Scholz, 67) Masato Hirose.

Review of symbioses between bryozoans and primary and secondary occupants of gastropod shells in the fossil record

Caroline J. Buttler[1*] and Paul D. Taylor[2]

[1] Department of Natural Sciences, Amgueddfa Cymru -National Museum Wales, Cardiff, CF10 3NP, UK
[*corresponding author Caroline.Buttler@museumwales.ac.uk]
[2] Department of Earth Sciences, Natural History Museum, London SW7 5BD, UK
[p.taylor@nhm.ac.uk]

ABSTRACT

Gastropod shells have been used as substrates by bryozoans since Ordovician times. Their use falls into three categories: (1) empty shells of dead gastropods; (2) shells of living gastropods; and (3) shells of dead gastropods housing secondary occupants (conchicoles). We here identify criteria to recognise these different categories in the fossil record; some are strong and unequivocal; others are weak and can only tentatively identify the category. The categories are not exclusive: bryozoans encrusting the shells of living gastropods can continue to grow after the gastropod has died and the shell is empty or contains a conchicole. Categories (2) and (3) represent symbioses between the bryozoans and the primary and secondary shell occupants, respectively. The most common conchicoles today are hermit crabs (paguroids). Numerous Cenozoic examples of inferred bryozoan-paguroid symbioses are known, along with a few Mesozoic examples, the earliest of which comes from the Middle Jurassic soon after the first appearance of paguroids in the fossil record. Identities of Palaeozoic conchicoles are equivocal, but may include sipunculan worms and possibly non-paguroid arthropods. There are benefits and costs to the bryozoans, gastropods and conchicoles participating in the various symbioses.

Most individual bryozoan-conchicole symbioses are facultative, have short geological durations, and provide little or no evidence for coevolution.

INTRODUCTION

The larvae of most species of bryozoans attach to hard or firm substrates, such as shells or rocks. From the Ordovician period to the present day, gastropod shells have been common attachment substrates for bryozoans.

The oldest probable gastropods are recorded from the Cambrian (Parkhaev 2017), and the earliest bryozoans are known from the Tremadocian stage of the Ordovician (Ma *et al.* 2015). Marine gastropods are found in a range of environments, include infaunal, epifaunal and planktonic species, and grazing, browsing, detritivorous and carnivorous species. Epifaunal gastropods in particular furnish suitable hard substrates for bryozoan larvae to attach to and grow over.

Bryozoans play an important role in preserving mollusc shells. During the Late Ordovician, aragonitic mollusc shells were rapidly dissolved before final burial in the 'calcite sea' pertaining at the time (Palmer and Wilson 2007). Large calcitic bryozoans very commonly used molluscs as substrates, preserving

them as moulds after aragonite dissolution. This process has been termed bryoimmuration (Wilson *et al.* 2018). The bryozoans involved are commonly unilamellar encrusting trepostomes which overgrew the entire mollusc shell, leaving an impression of the fine details of the shell surface on their basal walls.

The aims of this paper are to review symbioses between bryozoans and primary and secondary occupants of gastropod shells in the fossil record, and to assess criteria for recognising the different types of association.

TYPES OF ASSOCIATION

Associations between bryozoans and gastropod shell substrates can be divided into three categories:

- bryozoan colonies growing on shells of living gastropods
- bryozoan colonies growing on empty shells of dead gastropods
- bryozoan colonies growing on shells of dead gastropods housing secondary occupants (conchicoles)

These associations are not exclusive. Colonies which began as encrusters of living gastropod shells could continue to grow after the mollusc had died and the shell was either empty or occupied by a conchicole. Although involving coralline red algae rather than bryozoans, a good modern example of this dynamic change was described by Zuschin and Piller (1997). These authors recognised that the degree of algal encrustation on gastropod shells from the northern Red Sea in Egypt reflected the identity of the different inhabitants. Encrustation by algae started on living gastropods, with the area of the aperture remaining free of growth. Once the gastropod had died, the shells were colonized by hermit crabs and tended to become more heavily encrusted with algal growth extending around the aperture. Further algal growth after abandonment of the shell by the last hermit crab resulted in the formation of a rhodolith (i.e., a spheroidal algal nodule).

RECENT BRYOZOAN/GASTROPOD/ CONCHICOLE ASSOCIATIONS

All three types of associations between bryozoans and gastropods are known today. Bryozoans commonly encrust living gastropod shells in benthic communities. However, they can also be found encrusting planktonic gastropods; for example, the cheilostome genus *Jellyella* sometimes leads a pseudoplanktonic mode of life on floating shells of the caenogastropod *Janthina* (Taylor and Monks 1997). In addition to bryozoans encrusting the surfaces of mollusc shells, boring bryozoans have been observed as endobionts within the shells of living gastropods (Smyth 1988).

Bryozoans are among the most diverse symbionts associated with hermit crabs living in gastropod shells. Symbiotic bryozoans develop evenly thick colonies on the external surfaces of these shells, contrasting with the uneven encrustation of unoccupied shells resting on the sea-bed and having one side against the sediment surface. In addition, bryozoan colony growth is able to extend onto inner shell surfaces where mantle tissues prohibit growth when the gastropods are alive. The symbiotic bryozoan colonies also commonly grow outwards from the shell aperture, constructing a crude extension of the helicospiral chamber of the gastropod and leaving the gastropod shell deeply embedded within the bryozoan colony (e.g., Taylor 1991; Carter and Gordon 2007). In fossil examples, the aragonitic mineralogy characterizing most gastropods means that the shell is typically represented by a mould in the bryozoan colony, the mould sometimes later infilled with diagenetic calcite cement.

While most tube-building bryozoan/paguroid symbioses involve only one bryozoan species, in some examples from the Otago Shelf of New Zealand the helicospiral tube is commenced by one bryozoan species but continued by a second species following exactly the same growth trajectory (Taylor 1991). Rarely, two colonies belonging to different species grow simultaneously outwards from the aperture to build a single tube. In the Pliocene of Florida, helicospiral tubes begun by the cheilostome bryozoan *Hippoporidra*

were sometimes continued by the scleractinian coral *Septastrea* (Darrell and Taylor 1989).

The majority of bryozoan/conchicole symbioses are facultative for both participants. For example, a study of bryozoan and hermit crab associations from the Otago Shelf (Taylor *et al.* 1989) noted that most of the bryozoan species could be found encrusting other living substrates, including living gastropods, as well as the shells of dead molluscs.

Bell (2005) found that intertidal hermit crab shells from the south Wales coast were more heavily encrusted by bryozoans than were the shells of living gastropods, which were fouled by barnacles. These differences were considered to be due to different microhabitats. In contrast, subtidal hermit crabs from Delaware Bay (Karlson and Shenk 1983) had fewer encrusting bryozoans, which was suggested to be due to these shells being occupied by hydroids and slipper limpets that outcompeted bryozoans.

Occupancy of gastropod shells by hermit crabs in modern environments can be so pervasive that almost all undamaged shells may be tenanted by hermit crabs or other conchicoles (e.g., Kellogg 1976).

CRITERIA FOR RECOGNISING DIFFERENT TYPES OF ASSOCIATION IN THE FOSSIL RECORD

Without the presence of the living animals in fossils, it can be difficult to identify the type of interaction occurring when bryozoans encrust gastropod shells. Some evidence is strong and unequivocal, but in many cases available indicators of interaction type are weak and ambiguous.

The only unequivocal evidence that a bryozoan colony was associated with a living gastropod is if the skeleton of the fouling bryozoan colony is partly overgrown and immured within the shell of the gastropod (Palmer and Hancock 1973). This can be seen in thin sections of colonies of the cyclostome *Reptomultisparsa incrustans* (d'Orbigny) from the Middle Jurassic (Bathonian) of Calvados, France, where bryozoan zooids can be observed sandwiched between the layers of the mollusc shell (Fig. 1).
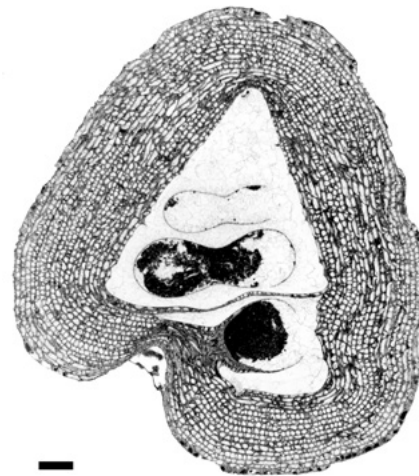
Figure 1. Thin section of the cyclostome *Reptomultisparsa incrustans* with zooids sandwiched between layers of molluscan shell, indicating that in this association the gastropod and bryozoan were alive at the same time (NHMUK D58654 Jurassic, Bathonian, Calvados, France). Scale bar = 1 mm.

There are several criteria that indicate an encrusted fossil gastropod shell was occupied by a living organism – either the gastropod itself or a conchicole – but it may be difficult to ascertain the identity of the shell occupant. If the bryozoan colony does not grow across the gastropod shell aperture, then the shell may have been occupied. Alternatively, when bryozoan colony growth covers only the apex of the shell, this may also indicate occupancy by the living gastropod or a conchicole. Coverage of the entire shell by the bryozoan colony, but with significantly less growth and/or with thickened walls and fewer apertures on the 'underside', indicates a shell that was maintained in a fixed orientation, either by the gastropod or a conchicole.

The strongest evidence of an association between a bryozoan and a conchicole is the preservation of the animal inside the shell. Unfortunately, fossil hermit crabs are rarely preserved *in situ*, which is understandable given the feeble calcification of the hermit crab cuticle, chelae excepted, and the tendency of the crabs to vacate their shells prior to burial.

The oldest example of an *in situ* hermit crab is preserved within the conch of an amaltheid ammonite from the upper Pliensbachian (Lower Jurassic) of Banz in southern Germany (Jagt *et al.* 2006). The same paper described remains of hermit crabs in volutid gastropods from the upper Maastrichtian (Upper Cretaceous) of Kunrade in the Netherlands, the Middle Eocene of Yantarnyi, Kaliningrad district, Russia, and the Miocene of Liessel, Netherlands. Hyden and Forest (1980) described from the Miocene of New Zealand another *in situ* hermit crab. However, in none of these examples are there associated bryozoans, and fossils of putative symbioses between bryozoans and paguroids invariably lack the hermit crabs (cf. Aguirre-Urreta and Olivero 2004: see below). However, patterns of encrustation by bryozoans and other sclerobionts in fossil gastropod shells can be used to infer the former presence of a hermit crab (Walker 1992).

Fossil gastropod shells evenly encrusted by bryozoans on their external surfaces and in which colony growth extends onto the inner surfaces of the shell suggest occupancy of the shell by conchicoles. This evidence is particularly strong when growth of the bryozoan outward from the aperture constructs a helicospiral extension of the shell chamber (Fig. 2)

The presence of 'pagurid facets' has also been used as evidence for hermit crab occupancy. These are worn patches near the base of the shell caused by the hermit crab dragging its home along the sea-bed. In contrast, living gastropods tend to hold their shells more upright and do not produce drag marks. Progressive thinning of the layers of bryozoan zooids towards the facet, with kenozooids replacing autozooids as in *Reptomultisparsa incrustans*, implies that the facets were created when the bryozoan was alive and actively growing.

Encrustation of an infaunal gastropod shell indicates unequivocally that the gastropod was no longer living when colonised. Walker (1988) showed that shells of the infaunal gastropod *Olivella biplicata* developed a unique community of suspension-feeding epibionts, including bryozoans, near the shell aperture when occupied by *Pagurus granosimanus*.
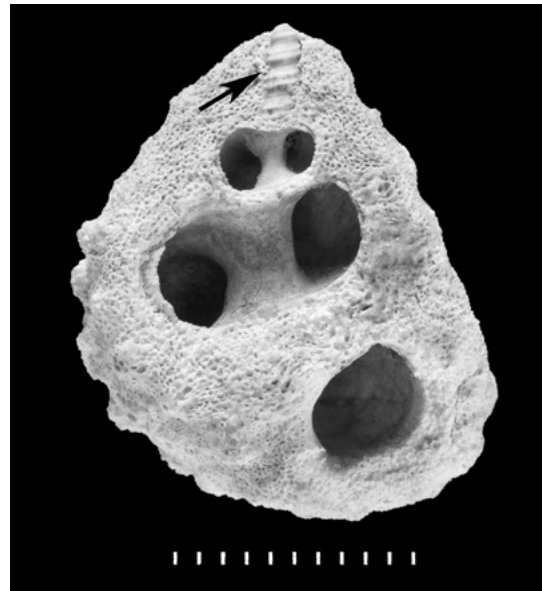
Figure 2. Helicospiral extension of the shell chamber formed by a colony of the cheilostome *Hippoporidra edax* colony growing outwards from the aperture of a gastropod (NHMUK 23459a, Pliocene, Coralline Crag, Formation, Suffolk, UK). Arrow points to the gastropod shell. Scale bar = 1 cm.

The presence of other diagnostic symbionts can be used as evidence that a shell was occupied by a paguroid. For example, the boring ichnofossil *Helicotaphrichnus* is found in the columella of some gastropod shells. This has been used to infer the former presence of a hermit crab as *Helicotaphrichnus* is identical to holes made by a polychaete symbiont found living exclusively with hermit crabs (Taylor 1994; Ishikawa and Kase 2007).

Bryozoan-encrusted gastropod shells occasionally furnish strong evidence that the bryozoan grew on an empty gastropod shell. This includes growth across the aperture to seal the entrance to the shell, or bryozoan colony growth covering one side of the shell only and developing a skirt-like, free lamina around the edge of shell where the colony expanded across the sediment surface (Fig. 3). However, in both cases it is impossible to know if initial bryozoan colonization began while the mollusc was alive, or when the shell was occupied by a conchicole.
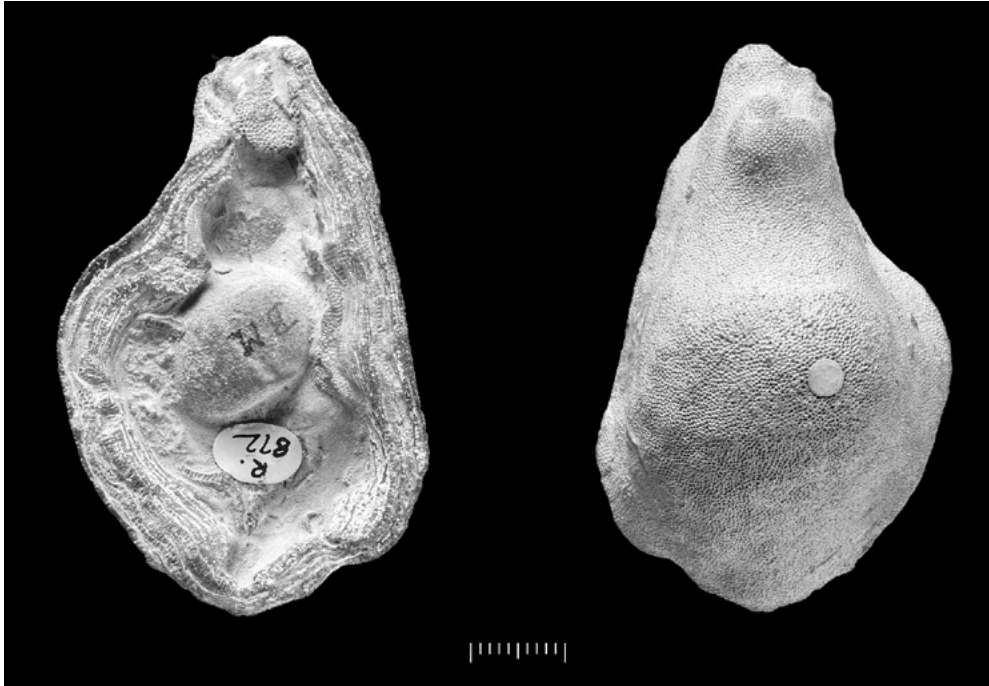
Figure 3. Colony of the cystoporate *Favositella interpuncta* covering one side of a gastropod shell and developing a skirt-like, free lamina around the edge where it is likely to have rested on the sediment surface (NHMUK R872, Silurian, Wenlock Limestone, Dudley, UK). Scale bar = 1 cm.

ASSOCIATIONS IN THE FOSSIL RECORD
Ordovician–Devonian

Bryozoans have commonly been observed encrusting gastropod shells in rocks of the Lower Palaeozoic. In many cases the mollusc was very obviously dead when encrusted because the bryozoan completely covers the shell (e.g. *Favositella*: Oakley 1966; Snell 2004) (Fig. 3). It is impossible to know in these cases if the encrustation began when the gastropod was alive.

The oldest bryozoan/gastropod association suggestive of the presence of a conchicole of unknown identity occurs in the trepostome *Leptotrypa calceola* from the Upper Ordovician of the Cincinnati region, USA. When sectioned, the small colonies of this bryozoan show little or nothing of the gastropod shell on which the bryozoan is presumed to have recruited, and have a spiral bryozoan-constructed chamber leading to a wide circular aperture (Fig. 6). As this association antedates the oldest fossil of paguroids by almost 250 million years, the nature of the conchicole remains a matter of speculation.

McNamara (1978) observed examples of symbioses between different bryozoan and gastropod species in the Coniston Limestone Group (Ashgill) of Cumbria, UK. All specimens were decalcified and the gastropods are preserved as external and internal moulds. McNamara (1978) suggested that the bryozoans did not encrust empty shells but were symbionts of living gastropods, which he thought was advantageous to both partners and caused modification in the growth of some of the trepostome colonies. In associations between the bryozoan *Diplotrypa* and the gastropod *Sipoecus*, bryozoan encrustation is located on the dorsal parts of the shells and the earlier whorls are free of bryozoans. The colonies are domed on the abapertural side of the shells and thinner on the apertural sides. In other specimens, however, *Diplotrypa* colonies appear to be growing on empty shells of *Sipoecus* and outwards across the sediment surface. The bryozoan *Montotrypa* is observed only encrusting the abapertural surface of the gastropods *Lophosira* and *Spiroecus*, so colonies

would not have been in contact with the sediment. In an association between *Diplotrypa* and *Euryzone*, bryozoan encrustation is located on the distal part of the shell. McNamara (1978) considered examples where the aperture remained free of encrustation to be evidence of symbiosis with a living gastropod. No gastropods were found not associated with bryozoans, and no other organisms in the fauna were encrusted, leading to the suggestion that the bryozoans were host specific to the gastropods. However, the lack of gastropods without associated bryozoans may simply reflect the potency of bryoimmuration in the preservation of these molluscs, with any unencrusted gastropods being lost to the fossil record.

Shells of the Silurian gastropod *Murchisonia* from the Upper Leintwardine Formation of the Ludlow Series at Delbury Quarry, Shropshire, UK, can be found encrusted by the trepostome *Asperopora*. No colonies of *Asperopora* were found encrusting other shells in the fauna, suggesting that this bryozoan preferentially recruited onto gastropod shells. As with the Coniston Limestone associations described above, the lack of unencrusted gastropods may be explained by bryoimmuration: in the absence of encrustation by calcitic bryozoan colonies, the aragonitic shells of these and other molluscs were dissolved and therefore lacking in the fossil fauna, providing another example of the under-representation of aragonitic molluscs in Silurian and other fossil faunas (the 'missing molluscs' of Cherns and Wright 2000). The trepostome colonies encrust the entire external surface of the *Murchisonia* shells, although not equally. On the apertural side of the shells, colonies are often thin and there are no autozooecial apertures, indicating a lack of feeding zooids in this area of the colony. Although the colonies are not found growing across the shell apertures, they did grow a short distance into the aperture, indicating that the shell was no longer occupied by a living gastropod. One specimen appears to have bryozoan skeleton sandwiched between whorls of the gastropod shell, implying that in this case the gastropod was alive at the time of encrustation (Fig. 4). Therefore, we propose that the bryozoans encrusted the shells of living gastropods but continued to grow after the deaths of the molluscs. One colony of *Asperopora* has an erect branch on the apertural side of the shell with an orientation suggesting that the shell may have been occupied by a conchicole (Fig. 5). Owen (1961) described gastropods from the Lower Leintwardine Formation (Ludlow Series) of Perton Quarry, Herefordshire, UK, with a similar overall pattern of encrustation by another trepostome, *Orbignyella fibrosa*.

Examples of the trepostome *Leptotrypella* were described encrusting the gastropod *Palaeozygopleura* in the Devonian Hamilton Group of New York state by Morris *et al.* (1991). Colonies covered all surfaces of the shells including the apertural lips, indicating that the shells were no longer occupied by a living gastropod. The thickest part of the colonies is on the abapertural sides of the shells, suggesting that a conchicole dragged the shells, the thin bryozoan layer on the apertural side developing because the shell was lifted from the substrate. These authors pointed to sipunculan worms as potential modern analogues for the conchicole. A similar symbiosis observed in the same rocks involves the tabulate coral *Pleurodictyum* encrusting shells of *Palaeozygopleura* occupied by a conchicole of unknown identity (Brett and Cottrell 1982).

Carboniferous–Triassic
There are scarcely any records of bryozoan/gastropod associations from the late Palaeozoic and Triassic. This could be due to the relative paucity of encrusting bryozoans, especially trepostomes, through this interval of time. One example has been described from the Upper Carboniferous Bird Spring Group, Arrow Canyon, Clark County, Nevada (Lipman and Langheim 1983). Here, the upper surfaces of the patellid gastropod *Lepetopsis* are found partly or totally encrusted by bryozoans. Small encrusting auloporids are also found on these gastropod shells.

Jurassic–Cretaceous
The fossil record of hermit crabs extends back to the Early Jurassic (Collins 2011), whereas the oldest

inferred bryozoan symbiont of hermit crabs is the Middle Jurassic cyclostome *Reptomultisparsa incrustans* (Buge and Fischer 1970; Palmer and Hancock 1973). Colonies of this species in the Late Bathonian of Normandy form thick, multilaminar encrustations on the gastropod *Ataphrus labadyei*, comprising up to 40 layers of zooids (Taylor 1994). Thin layers of bryozoan skeleton bioimmured between whorls of gastropod shell in some specimens provide evidence that these particular colonies were initially symbionts of living gastropods. Bryozoan growth evidently continued after death of the gastropod when the shell was occupied by a conchicole presumed to be a hermit crab. Evidence for a secondary occupant includes the colony growing onto the internal surfaces of the shells, short tubular extensions to the living chamber, and 'pagurid facets' (Taylor 1994). However, no hermit crabs have been found *in situ* in these moderately common associations.

A broken specimen of another cyclostome, *Reptomulticlausa* sp. from the Cenomanian of Devon, UK, with features suggesting that it may have been a paguroid symbiont (Taylor 1994) is one of only two specimens of this association recorded from the Cretaceous. The other is from the Late Campanian of James Ross Island, Antarctica, where the external

Figure 5. Branch of the trepostome *Asperopora* developed on the apertural side of a *Murchisonia* shell suggesting occupation of the shell by a conchicole (NMW 2019.21G.2.3, Silurian, Ludlow Series, Upper Leintwardine Formation, Delbury Quarry, Shropshire, UK). Scale bar = 5 mm.

mould of a shell of the gastropod *Taioma* encrusted by a cheilostome bryozoan colony has been described containing the hermit crab *Paguristes* (Aguirre-Urreta and Olivero 2004). Although the cheilostome was identified as an ascophoran, the figure given by Aguirre-Urreta and Olivero (2004, fig. 3c) appears to depict a calloporid anascan.

Cenozoic

While the Mesozoic fossil record of inferred bryozoan/paguroid symbioses is sparse, the diversity of these associations increased steeply in the Oligo-Miocene, with at least 15 species known by the early Miocene (Taylor 1994; Pérez *et al.* 2015). These and later Cenozoic examples were listed by Taylor (1994, appendix). Of particular note is the Forest Hill Formation (early Miocene) of Southland, New Zealand, where bryozoan symbionts of paguroids can be found in almost rock-forming abundance. Colonies of the eleven species of cyclostome and cheilostome bryozoans involved constructed long
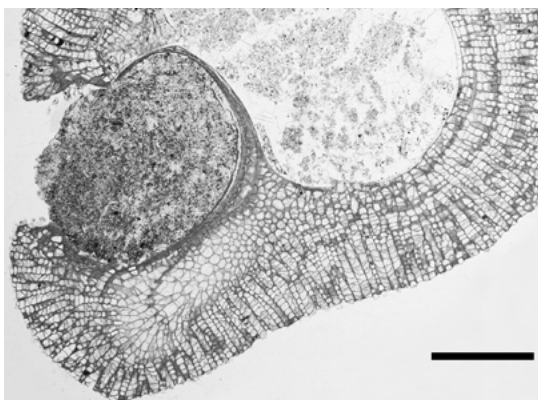

Figure 4. Skeleton of trepostome *Asperopora* apparently sandwiched between gastropod whorls, implying that the bryozoan and gastropod were alive at the same time (NMW 2019.21G.5.2, Silurian, Ludlow Series, Upper Leintwardine Formation, Delbury Quarry, Shropshire, UK). Scale bar = 5 mm.
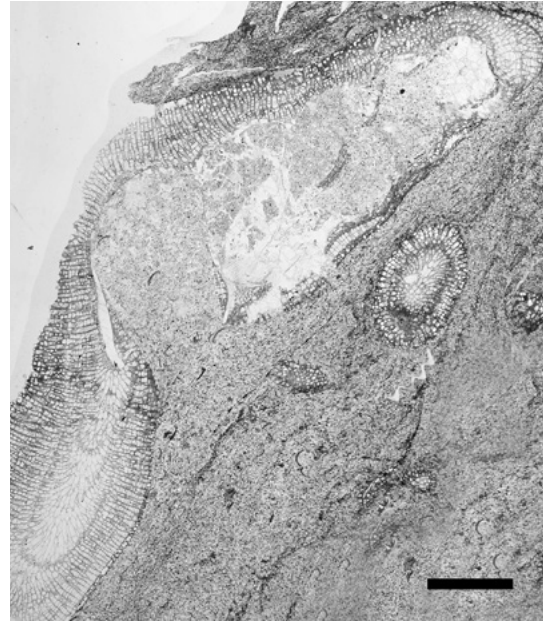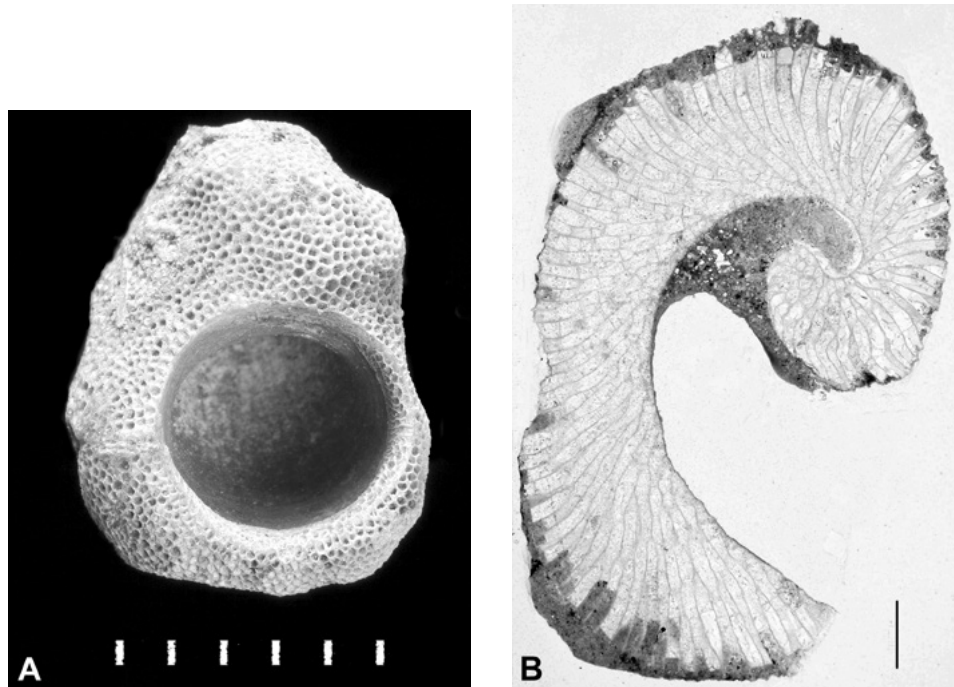
Figure 6. Characteristic colony-form of the trepostome *Leptotrypa calceola* with a large, circular aperture that possibly housed an unknown symbiont; (A) hand specimen, (NHMUK D7120a) (B) thin section (NHMUK D7120b) Ordovician, Cincinnatian, Cincinnati, USA). Scale bar (A) = 5 mm; (B) = 1 mm.

involute or evolute extensions from gastropod shells. The gastropods themselves were only a few millimetres in size, and their moulds can be found embedded within the apices of sectioned or broken bryozoan colonies.

The ascophoran cheilostome genus *Hippoporidra* is one of the most widely distributed paguroid symbionts today. Although the aragonitic mineralogy of most species of *Hippoporidra* biases against its more widespread occurrence in the fossil record, there are numerous records in the Miocene–Pleistocene of Europe and North America. The earliest species of this genus – *H. portelli* from the late Eocene of Florida – is unusual in apparently having had a skeleton of calcite (Taylor and Schindler 2004).

In the Red Crag Formation (Pleistocene) of Essex, UK, another ascophoran, *Turbicellepora*, encrusts shells of the gastropods *Neptunea* and *Nucella* (Harrison 1984). Colonies mostly occur on the spires of the shells but can also be found at the anterior ends over the siphonal canal (Fig. 7).

This pattern of encrustation suggests that the shells were occupied, although there is no conclusive evidence as to whether this was by the gastropod or a conchicole.

Boring ctenostome bryozoans have been described in gastropod shells from the middle Miocene Korytnica Clays of Poland (Baluk and Radwanski 1979). Colonies are most common around the shell aperture, and the absence of borings that were subsequently overgrown by the gastropod led the authors to suggest that these shells were occupied by hermit crabs rather than living gastropods.

DISCUSSION

There are numerous potential benefits and costs to the bryozoans, gastropods and conchicoles from the various associations reviewed above. Most of these advantages and disadvantages are untested in living symbioses and must remain speculative in fossil examples.
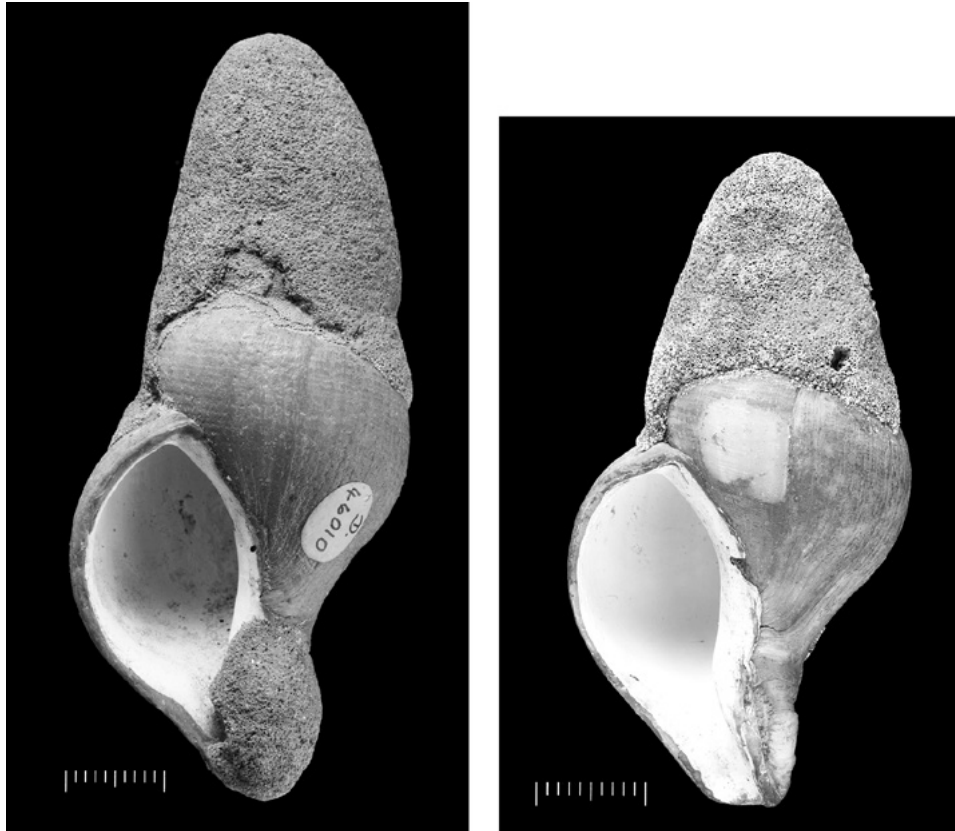
Figure 7. Cheilostome *Turbicellepora* encrusting shells of the sinistral gastropod *Neptunea angulata*, covering the spires of the shells and, in the case of the specimen on the right, the anterior ends of the shell over the siphonal canal (NHMUK P46010, P1626, Pleistocene, Red Crag Formation, Essex, UK). Scale bar = 1 cm.

Bryozoans encrusting a live gastropod or one occupied by a conchicole have the advantage of being on a mobile substrate, which lessens the chances of the colony being buried by sediment compared with static substrates. This is reflected in the large size of the colonies in terms of number of zooids relative to the size of the substrates they encrust. The bryozoans can also benefit from having a long-lived substrate that they are often able to monopolize to the exclusion of other sclerobionts. Encrusting a gastropod shell elevates a bryozoan colony above the turbid layer on the sea floor and gives it access to faster flowing ambient currents and enhanced feeding opportunities. One bryozoan has been shown to protect itself and its host from predation: colonies of the South African ctenostome *Alcyonidium nodosum* encrusting the shells of the living gastropod *Burnupena papyracea*

produce secondary metabolites that protect the host gastropod from predation by the rock lobster *Jasus lalandii* and thereby improve their own survival (Gray et al. 2005).

The presence of encrusting bryozoans may perhaps benefit living gastropods by camouflaging them against certain kinds of predators. Colonies can also potentially strengthen the gastropod shell and make it less vulnerable to boring and durophagous predators. Large bryozoan colonies, however, could adversely affect the hydrodynamics of living gastropods, leading to destabilisation of these snails, especially in high energy environments.

The advantages and disadvantages to bryozoans and their symbiotic conchicoles are similarly not well understood. The powerful feeding and respiratory currents of hermit crabs create a high flux of suspended

food for the bryozoan symbionts, especially in the vicinity of the tube aperture where the growth rate of the bryozoans is greatest. For example, Morris et al. (1989) in a study of hermit crabs from Texas and California recognised encrustation sites on the inner surface of the outer and inner lips of the shells where concentrations of food would be high.

Bell (2005) suggested that increased dispersal could be an advantage for epibionts on shells if they had short-lived larval stages, such as *Alcyonidium gelatinosum*. It is also possible that in bryozoans having male zooids with long tentacles, such as the ascophoran *Hippoporidra*, sperm could be delivered to other colonies when they were brought together by the hermit crabs on whose shells they were carried.

Hermit crabs symbiotic with bryozoans may benefit from having homes that enlarge in size with their growth, thus avoiding the need for the crabs to move to larger shells. Domicile exchange is a time when hermit crabs are particularly vulnerable to destruction or damage by predators or physical forces. However, hermit crabs kept in the laboratory were found to switch homes despite living in tubes constructed by bryozoans (Taylor 1991). As paguroids are unable to repair any damage to the gastropod shells they occupy, the symbiotic bryozoans may be important in maintaining these shelters. Bryozoan symbionts could exclude destructive boring organisms, as well as manufacturing thick domiciles that are difficult for durophagous predators to break into. Paguroid symbionts may be camouflaged by the mottled pigmentation seen in some colonies of *Hippoporidra*, as well as the branching outgrowths that make domiciles look less like gastropod shells. On the other hand, branched and excessively thick bryozoan colonies may significantly increase the weight of the domiciles, make them unbalanced, and reduce the fitness of the hermit crab (Buckley and Ebersole 1994). It has been demonstrated that some hermit crabs are highly selective over their choice of gastropod shells, and may reject shells that are too heavy or have symbionts located in

positions affecting the centre of gravity of the shell (Conover 1976).

SUMMARY

Bryozoan/gastropod associations can be recognised throughout the fossil record from the Ordovician to the present day. These may have involved bryozoans colonizing shells occupied by living gastropods, empty shells, or shells housing secondary occupants (conchicoles). Careful interpretation of these associations can enhance knowledge of the biodiversity and palaeoecology of ancient benthic communities. Today, bryozoans are common symbionts of paguroids inhabiting gastropod shells. Ancient symbioses between fossil bryozoans and paguroids (or unknown conchicoles) are typically of short geological duration, not obligatory for the bryozoans concerned, and provide little or no evidence for coevolution between the symbionts.

ACKNOWLEDGEMENTS

REFERENCES

AGUIRRE-URRETA, M.B. AND OLIVERO, E.B. 2004. A Cretaceous hermit crab from Antarctica: predatory activities and bryozoan symbiosis. *Antarctic Science* **4**, 207–214.

BALUK, W. AND RADWANSKI, A. 1979. Boring ctenostomate bryozoans from the Korytnica Clays (Middle Miocene; Holy Cross Mountains, Central Poland. *Acta Geologica Polonica* **29**, 243–252.

BELL, J.J. 2005. Influence of occupant microhabitat on the composition of encrusting communities on gastropod shells. *Marine Biology* **147**, 653–661.

BRETT, C.E. AND COTTRELL, J.F. 1982. Substrate specificity in the Devonian tabulate coral *Pleurodictyum*. *Lethaia* **15**, 247–262.

BUCKLEY, W.J. AND EBERSOLE, J.P. 1994. Symbiotic organisms increase the vulnerability of a hermit crab to predation. *Journal of Experimental Marine Biology and Ecology* **182**, 49–64.

BUGE, E. AND FISCHER, J.-C. 1970. *Atractosoecia incrustans* (d'Orbigny) (Bryozoa Cyclostomata) espèce

bathonienne symbiotique d'un Pagure. *Bulletin de la Société Géologique de France* **12**, 126–133.

CARTER, M.C. AND GORDON, D.P. 2007. Substratum and morphometric relationships in the bryozoan genus *Odontoporella*, with a description of a new paguridean-symbiont species from New Zealand. *Zoological Science* **24**, 47–56.

CHERNS, L. AND WRIGHT, V.P. 2000. Missing molluscs as evidence of large-scale, early aragonite dissolution in a Silurian sea. *Geology* **28**, 791–794.

CONOVER, M.R. 1976. The influence of some symbionts on the shell-selection behaviour of the hermit crabs, *Pagurus pollicarus* and *Pagurus longicarpus*. *Animal Behavior* **24**, 191–194.

CONOVER, M.R. 1979. Effect of gastropod shell characteristics and hermit crabs on shell epifauna. *Journal of Experimental Marine Biology and Ecology* **40**, 81–94.

DARRELL, J.G. AND TAYLOR, P.D. 1989. Scleractinian symbionts of hermit crabs in the Pliocene of Florida. *Memoir of the Association of Australasian Palaeontologists* **8**, 115–123.

GRAY, C.A., MCQUAID, C.D. AND DAVIES-COLEMAN, M.T. 2005. A symbiotic shell-encrusting bryozoan provides subtidal whelks with chemical defence against rock lobsters. *African Journal of Marine Science* **27**, 549–556.

HARRISON, M.D. 1984. *A computer aided palaeoecological study of selected Red Crag (Lower Pleistocene) gastropods*. Unpublished PhD thesis, Polytechnic of North London.

HYDEN, F.M AND FOREST, J. 1980. An *in situ* hermit crab from the Early Miocene of southern New Zealand. *Palaeontology* **23**, 471–474.

ISHIKAWA, M. AND KASE, T. 2007. Spionid bore hole *Polydorichnus subapicalis* new ichnogenus and ichnospecies: a new behavioral trace in gastropod shells. *Journal of Paleontology* **81**, 1466–1475.

JAGT, J.W.M., VAN BAKEL, B.W.M., FRAAIJE, R.H.B. AND NEUMANN, C. 2006. *In situ* fossil hermit crabs (Paguroidea) from northwest Europe and Russia. Preliminary data on new records. *Revista Mexicana de Ciencias Geológicas* **23**, 364–369.

KARLSON R.H. AND SHENK, M.A. 1983. Epifaunal abundance, association, and overgrowth patterns on large hermit crab shells. *Journal of Experimental Marine Biology and Ecology* **70**, 55–64.

KELLOGG, C.W. 1976. Gastropod shells: a potentially limiting resource for hermit crabs. *Journal of Experimental Marine Biology and Ecology* **22**, 101–111.

LIPMAN, E.W. AND LANGHEIM, R.L. 1983. *Lepetopsis franae*, n. sp. a new patellid gastropod from the Bird Spring Group, Virgilian, at Arrow Canyon, Clark County, Nevada. *Journal of Paleontology* **57**, 602–605.

MCNAMARA, K.J. 1978. Symbiosis between gastropods and bryozoans in the late Ordovician of Cumbria, England. *Lethaia* **11**, 25–40.

MA, J., TAYLOR, P.D., XIA, F. AND ZHAN, R. 2015. The oldest known bryozoan: *Prophyllodictya* (Cryptostomata) from the lower Tremadocian (Lower Ordovician) of Liujiachang, south-western Hubei, central China. *Palaeontology* **58**, 925–934.

MORRIS, P.J., LINSLEY, R.M. AND COTTRELL. J F. 1991. A Middle Devonian symbiotic relationship involving a gastropod, a trepostomatous bryozoan, and an inferred secondary occupant. *Lethaia* **24**, 55–67.

MORRIS, P.A., SOULE, D.E. AND SOULE, J.D. 1989. Bryozoans, hermit crabs, and gastropods: life strategies can affect the fossil record. *Bulletin of the Southern Californian Academy of Sciences* **88**, 45–60.

OAKLEY, K.P. 1966. Some pearl-bearing Ceramoporidae (Polyzoa). *Bulletin of the British Museum (Natural History), Geology Series* **14**, 1–20.

OWEN, D.E. 1961. On the species *Orbignella fibrosa* (Lonsdale). *Geological Magazine* **98**, 230–234.

PALMER, T.J. AND HANCOCK, C.D. 1973. Symbiotic relationships between ectoprocts and gastropods, and ectoprocts and hermit crabs in the French Jurassic. *Palaeontology* **16**, 563–566.

PALMER. T.J AND WILSON, M.A. 2007. Calcite precipitation and dissolution of biogenic aragonite in shallow Ordovician calcite seas. *Lethaia* **37**, 417–427.

PARKHAEV, P., YU. 2017. On the position of Cambrian archaeobranchians in the system of the Class Gastropoda. *Paleontological Journal* **51**, 453–463.

PÉREZ, L.M., GRIFFIN, M., PASTORINO, G., LÓPEZ-GAPPA, J. AND MANCEÑIDO, M.O. 2015. Redescription and palaeoecological significance of the bryozoan *Hippoporidra patagonica* (Pallaroni, 1920) in the San Julián Formation (late Oligocene) of Santa Cruz province, Argentina, *Alcheringa* **39**, 1–7.

TAYLOR, P.D. 1991. Observations on symbiotic associations of bryozoans and hermit crabs from the Otago Shelf of New Zealand. *Bulletin de la Société des Sciences Naturelles de l'Ouest de la France* **H.S. 1**, 487–495.

TAYLOR, P.D. 1994. Evolutionary palaeoecology of symbioses between bryozoans and hermit crabs. *Historical Biology* **9**, 157–205.

TAYLOR, P.D. AND MONKS, N. 1997. A new cheilostome bryozoan genus pseudoplanktonic on molluscs and algae. *Invertebrate Biology* **116**, 39–51.

TAYLOR, P.D., SCHEMBRI, P.J. AND COOK, P.L. 1989. Symbiotic associations between hermit crabs and bryozoans from the Otago region, southeastern New Zealand, *Journal of Natural History* **23**, 1059–1085.

TAYLOR, P.D. AND SCHINDLER, K.S. 2004. A new Eocene species of the hermit-crab symbiont *Hippoporidra*

(Bryozoa) from the Ocala Limestone of Florida. *Journal of Paleontology* **78**, 790–794.

SMYTH, M.J. 1988. *Penetrantia clionoides*, sp. nov. (Bryozoa), a boring bryozoan in gastropod shells from Guam. *Biological Bulletin* **174**, 276–286.

SNELL, J. 2004. Bryozoa from the Much Wenlock Limestone Formation (Silurian) of the West Midlands. *Monograph of the Palaeontographical Society, London* **621**, 1–136.

WALKER, S.E. 1988. Taphonomic significance of hermit crabs (Anomura: Paguridea): epifaunal hermit crab–infaunal gastropod example. *Palaeogeography, Palaeoclimatology, Palaeoecology* **63**, 45–71.

WILSON, M.A., BUTTLER, C.J. AND TAYLOR, P.D. 2018. Bryozoans as taphonomic engineers, with examples from the Upper Ordovician (Katian) of Midwestern North America. *Lethaia*, **52**, 403-409.

Chemical and microbiological characterization of metabolites from *Cryptosula zavjalovensis* Kubanin, 1976 – preliminary report

H. Fortunato[1]*, L. Gonzaga[2] and S. Quaiyum[3]

[1] Department of Natural History Sciences, Faculty of Science, Hokkaido University, N10 W8 Kita-ku,
Sapporo 060-0810, Japan [*corresponding author: e-mail: helenaf@sci.hokudai.ac.jp]
[2] Department of Chemistry, University of Southern Mindanao, Kabacan, Cotabato, 9407 Philippines
[3] National Institute of Advanced Industrial Science and Technology, Hokkaido University,
2-17-2-1 Tsukisamu Higashi, Sapporo 062-0052, Japan

ABSTRACT

The marine environment is an abundant and diverse source of biologically active compounds, with great potential in pharmaceutics and medicine. Though still underused, the last decades have seen several studies showing the potential of bryozoans in this respect. We report preliminary data concerning the activity and identification of secondary metabolites from the marine bryozoan *Cryptosula zavjalovensis* from Japan. Water and ethanol extracts exhibited medium/high activity towards 11 laboratory stoke bacterial strains shown by the zone of inhibition diameter in the tested bacteria. Moreover, cytotoxicity profiling using MTT colorimetric test revealed that ethyl acetate extract exhibited cytotoxicity toward human MCF-7 breast cancer cells. Further separation of this extract yielded three fractions: E1 80:20 v/v, E2 100:0 v/v; E3 methanol/chloroform 50:50 v/v. Cytotoxicity profiling showed that E2 (concentration 10 µg/mL) exhibited 79% activity, whereas E3 (1 µg/mL concentration) displayed 58% activity. The active metabolite was isolated using liquid chromatography-mass spectrometry and its preliminary structure determined by tandem mass spectrometry. Results show that *C. zavjalovensis* can be a source for novel metabolites with potential in clinical oncology and bacteriology. Further studies should confirm obtained results, reveal the exact structure of the studied metabolite, and determine its mechanism of action.

INTRODUCTION

Allelochemicals are specific natural substances produced by organisms and used in defense to improve the organisms' survival by exerting physiological effects on competing or predatory organisms (Williams *et al*. 1989). These substances have attracted interest because of their possible applications in drug discovery and particularly in pharmacology. Although most allelochemicals have been isolated from terrestrial plants (Joffe and Thomas 1989), the last several decades have seen research turning to the marine realm as a possible source of novel products, resulting in the discovery of several thousands of promising molecules, mostly from algae, sponges, cnidarians and mollusks, demonstrating the value of oceans as source of many novel chemical classes. Several of these compounds have pharmaceutical and medical properties, and some of them have already been approved as new drugs (Mathur 2000; Bulaj *et al*. 2003; Jha and Zi-rong 2004; Cragg

and Newman 2013; Blunt *et al.* 2016; Lefranc *et al.* 2019).

The diversity of allelochemicals in the more than 8000 living species of bryozoans (Ryland 2005) has scarcely been surveyed (Figuerola and Avila 2019). Most of the known products are alkaloids (Blunt *et al.* 2004; 2011), but several other molecules (i.e., macrolide lactones, indole alkaloids, isoquinoline quinones, sterols) have also been detected, showing a wide variety of compounds (Sinko *et al.* 2012; Tian *et al.* 2018). One of the best-studied bryozoan species is *Bugula neritina* (L.), from which a series of compounds called bryostatins, with potent anti-cancer properties (Pettit *et al.* 1982), has been isolated and characterized. These compounds modulate the signal transduction enzyme protein kinase-C (PKC) and show remarkable selectivity against several human cancers (Pettit 1991; Lilies 1996; Morgan *et al.* 2012). Bryostatins also seem to enhance learning and memory in animal models (Sun and Alkon 2005; Kuzirian *et al.* 2006) and are being tested for the treatment of Alzheimer's and other neurodegenerative problems (Hongpaisan and Alkon 2007; Sun *et al.* 2014).

From the viewpoint of ecology, these metabolites are valuable for the organisms' defence as documented in several studies (Sharp *et al.* 2007). Bryostatins for example, play an important role in protecting *B. neritina* larvae against fish predation (Lopanik *et al.* 2004). Interestingly, the natural products in *B. neritina* vary among populations (Davidson and Haygood 1999). Bryostatins are produced by a bacterial symbiont, *Endobugula sertula*, and we need to consider the variable presence of symbionts and the environmental factors under which these metabolites are produced.

Another widely studied bryozoan is *Flustra foliacea* (L.), which has yielded several flustramines (brominated and indole alkaloids) that show strong antimicrobial activity as well as moderate cytotoxicity against the HCT-116 cell-line (Carle and Christophersen 1980, 1981; Wulff *et al.* 1982; Wright 1984; Holst *et al.* 1994; Lysek *et al.* 2002). Among other very promising bryozoans under study

are *Amathia convoluta* (Lamarck) (tribrominated alkaloids with potent and selective activity against ruminant nematods; γ-lactam alkaloids with in-vitro cytotoxicity against L1210 murine leukemia cells and KB human epidermoid carcinoma cells) (Zhang *et al.* 1994; Narkowicz *et al.* 2002); *Watersipora subtorquata* (d'Orbigny) (bryoanthrathiophene with potent anti-proliferation activity towards bovine aorta endothelial cells (BAEC)) (Jeong *et al.* 2002); *Cribricellina cribraria* (Busk, 1852) (carboline alkaloids with cytotoxic, antibacterial, antifungal and antiviral activity) (Prinsep *et al.* 1991); and *Pterocella vesiculosa* (Lamarck) (alkaloids and bromocarbolines exhibiting potent antitumor activity towards the murine leukemia cell line) (Till and Prinsep 2009; Wang *et al.* 2016).

Up to now, of the five species of the ascophoran cheilostome bryozoan genus *Cryptosula*, only *C. pallasiana* (Moll, 1803) has been studied in relation to the possible presence of potential useful natural metabolites. Tian *et al.* (2014, 2017) detected several alkaloids in this species including the new natural products p-methylsulfonylmethyl-phenol and 7-bromo-2,4-(1H,3H)-quinazolineione, which exhibits strong cytotoxicity against leukemia cell lines. The Pacific species *Cryptosula zavjalovensis* Kubanin, 1976 is morphologically similar to *C. pallasiana*, but uniquely emits a strong, pungent odor when alive. As far as is known, *C. zavjalovensis* is restricted to the North Pacific rim, extending from Ketchikan, Alaska, northward and westward across the Aleutian Islands to the Kurile Islands, far-eastern Russia (Vladivostok), and northern Japan (Dick *et al.* 2005; Grischenko *et al.* 2007).

Whereas most rocky-intertidal bryozoans inhabit cryptic microhabitats under boulders and in crevices, *C. zavjalovensis* frequently encrusts exposed hard substrates, and its colonies are often scarcely fouled (Grischenko *et al.* 2007), leading to speculation that the odor-producing compound (or some other substance) might inhibit larvae from other organisms from settling on the colony, interfere with the surficial bacterial film (i.e., that it might have antibacterial activity) or defend against predators. Preliminary

studies showed the presence of antibacterial properties in extracts of *C. zavjalovensis* (Quaiyum *et al*. 2018), leading to interest in the source of these properties, and in their potential function both in nature and as a novel metabolite. The aim of this study was to isolate and identify natural products produced by *Cryptosula zavjalovensis* and test their antibacterial and cytotoxic activity using water and ethanol extracts.

MATERIALS AND METHODS

Cryptosula zavjalovensis was collected at several locations around the Akkeshi Marine Station, Hokkaido, Japan, during low tides in July 2015 and July-August 2016. Algae and rocks with encrusting bryozoan colonies were placed in containers with seawater and taken to the laboratory for separation. Bryozoans were scraped from the substrates and kept in running sea water while being cleaned and prepared. Colonies were identified under a stereoscopic microscope (Olympus). During identification, it was noted that the material emitted the pungent odor distinctive of the species.

Chemical extraction

Material for chemical analyses was placed in 10 g vials filled with ethanol (30 ml) and stored at -15 °C for transport to Hokkaido University, Japan, and the University of Algarve (UAlg), Portugal. Preliminary tests for the possible presence and bioactivity of secondary metabolites were conducted at Hokkaido University, and further work was done at University of Algarve. Natural products were isolated from *C. zavjalovensis* by means of solvent extraction. Samples were homogenized and extracted using ethanol, which was then evaporated to dryness. The solute was fractionated in ethyl acetate and water to obtain organic and aqueous fractions, respectively. During this process, the hydrophilic components of the natural compounds stayed in the aqueous layer while the hydrophobic ones will be in the organic layer. The process was repeated for the separated organic and aqueous layers to enhance the separation and followed by fractionation of the organic and aqueous extracts using solid phase extraction and reversed-phase chromatography. To narrow the search for bioactive compounds, the ethyl acetate extract was separated into three major fractions by solid phase extraction. Three major fractions were obtained from the ethyl acetate extract using solid phase extraction with a methanol-water (**E1,** 80:20 v/v; **E2,** 100:0 v/v) and methanol-chloroform gradient (**E3**, 50:50 v/v). These fractions were further used in the toxicity tests. Aqueous fractions H1–H4 and organic fractions E1–E3 were separated into their components by means of liquid chromatography-mass spectrometry (LC-MS), in both positive and negative ionization modes (Ho *et al*. 2003; Waters 2017). LC-MS chromatograms for aqueous fractions H1–H4 revealed no promising peaks in either the positive or negative mode. Post-processing of chromatograms was done by using HyStar®. Potential peaks were noted and their m/z values were compared to previously isolated and identified natural products from other marine organisms using the MarinLit® database, an extensive database of marine natural products, for possible identification.

All reagents used for extractions were obtained from Sigma-Aldrich (Japan) and Carlo Erba Reagents (Portugal). All were analytical or HPLC grade and were used without further purification. In Japan, an Agilent 1100 Series HPLC System coupled with a Bruker Daltonics micrOTOF-HS mass spectrometer (ESI) was used for the LC-MS analyses. In Portugal, the LC-MS and tandem mass spectrometry (MS/MS) analyses were done using a Bruker® QqTOF Impact II Mass Spectrometer with ESI and CaptiveSpray nanoBooster™ with a ThermoScientific™ Dionex™ UltiMate™ WPS-3000TPL RSLCnano autosampler.

Cytotoxicity tests

Preliminary screens of the extracts for bio-active compounds were done using the MTT (3-(4,5-dimethyl-2-thiazolyl)-2,5-diphenyl-2H-tetrazolium bromide) assay against the MCF-7

breast cancer cell line (Culture Collections, Public Health England). In the mitochondria of living cells, MTT is reduced to purple-colored formazan, but upon cell death the ability to metabolize MTT is lost. Consequently, color formation is a marker of cell viability. MTT was dissolved in Dulbecco's phosphate-buffered saline (DPBS) at a concentration of 5 mg/ml. The wells of the test plate were seeded with 90 µL of the cell suspension to give a concentration of 1 x 10⁴ cells per well. After a 24-hour incubation, 10 µL of the extracts were added at a concentration of 1 µg/mL or 10 µg/mL. Cisplatin, a known chemotherapeutic drug against various types of tumors such as bladder, head and neck, lung, ovarian and testicular cancers (Dasari and Tchounwou 2014), was used as a positive control. Cisplatin has been used against breast cancer cells, sometimes in combination with other drugs such as taxanes, vinca alkaloids, and 5-fluorouracil for synergistic effects as well as to minimize cisplatin resistance (Prabhakaran *et al*. 2013). Moreover, cisplatin-related toxicities are dose dependent (Florea and Büsselberg 2011), making it an ideal positive control. Incubation was done for 72 hours, after which the medium was aspirated from the plate. An MTT solution (100 µL) was added to each well and incubated for 3 hours. Healthy cells would have adhered at the bottom of the well and manifested purple formazan crystals. The MTT solution was then aspirated, DMSO (100 µL) added to dissolve the formazan crystals, and the plate incubated for 10 minutes at 37 °C and shaken for 10s before it was read under a Thermo Labsystems Multiskan JX plate reader at an absorbance of 570 nm. As this is a colorimetric assay, formazan crystals need to be dissolved so its color is imparted in the solution before reading with the plate reader. The reader does not assess the state or color of the cells by itself, but rather the level of color of the solution which reflects the proportion of healthy cells in the wells. It should be noted that MTT reduction relies on mitochondrial reductase to convert tetrazole to formazan and the assumption is that the conversion is dependent on

the number of viable cells. Nevertheless, it may alter mitochondria enzymatic activity (without affecting cell number or cell viability) and in longer incubation times increase sensitivity and color accumulation which may result in over 100% viability results (Riss *et al*. 2004; Wang *et al*. 2011). As such MTT can be used as a marker of viable cell metabolism and not specifically cell proliferation. It is advisable to complement it with cell counts, which was not the aim of this study.

The cytotoxic effect was calculated as:

$$\%Cell\ Cytotoxic\ Effect = \left[1 - \frac{Optical\ density\ of\ treated\ cells}{Optical\ density\ of\ control\ cells}\right] \times 100$$

Microbiological tests

Colonies for microbiology were pulverized with a mortar and separated into 15 g samples that were then each mixed with 135 ml of deionized water (9:1 ratio). These were termed 'water extracts'. Ethanol extracts used in the microbiological essays were obtained as described in the preceding section. Both the water and the ethanol extracts were tested for antimicrobial activity against 11 different gram-positive and gram-negative bacterial strains. A pure bacterial culture was prepared for each strain by inoculating 2 ml of Mueller Hinton broth medium (Oxford Ltd., Basingstoke, Hampshire, England) followed by a 24-hour incubation at 37°C. The bacterial suspension density was adjusted to 106 colony cfu/ml (colony forming units per milliliter), equivalent to a 0.5 McFarland standard turbidity. For the assays, an approximately equal amount of each bacterial broth suspension was spread onto Mueller-Hinton agar medium in an 8 cm Petri dish and dried for 10 minutes. Two wells per dish (diameter 6 mm, volume 8 mm³ and 2.6 cm apart) were prepared, one for the test extract and one for the negative control. Bryozoan extract (100 µL; water or ethanol) was then added to one of the test wells in each assay. As a negative control, 100 µL of distilled water (for water-extract assays) or 100 µL of 30% ethanol in distilled water (for the ethanol-extract assays) was added to the other well. The assay plates were then

incubated for 24 hours at 37°C. The water-extract assays were done with 10 replicates, whereas the ethanol-extract assays were done with five replicates. The degree of antimicrobial activity of the extract was assessed through the size (diameter, including the size of the well itself) of the zone of inhibition (ZOI) of bacterial growth, evident as the clear zone surrounding the test well (Fig. 1). Mean ZOIs greater than 15 mm were considered to represent strong antimicrobial activity.

RESULTS

Chemical extraction and identification

The organic fractions separated using LC-MS yielded several peaks, in both the positive and negative ionization modes. Some of the peaks identified in the negative mode were: retention time RT = 4.23 minutes, m/z = 586.04; RT = 5.38 min, m/z = 612.12; RT = 6.56 min, m/z = 565.99 (Fig. 2). In the positive ionization mode, two additional peaks were: RT = 5.37 min, m/z = 568.26 and RT = 6.18 min, m/z = 225.20. For identification, an initial search for matches in the

MarinLit® database yielded no results. Further searches showed that the peak with RT = 6.56 min and m/z = 565.99 (Fig. 2) was similar to that of the

Figure 1. Microbiological assay showing the zone of inhibition (ZOI) (black bar across the B well between sample and edge of growth medium) in a microbiological assay for an extract from *Cryptosula zavjalovensis*. B, test well; C, control well.
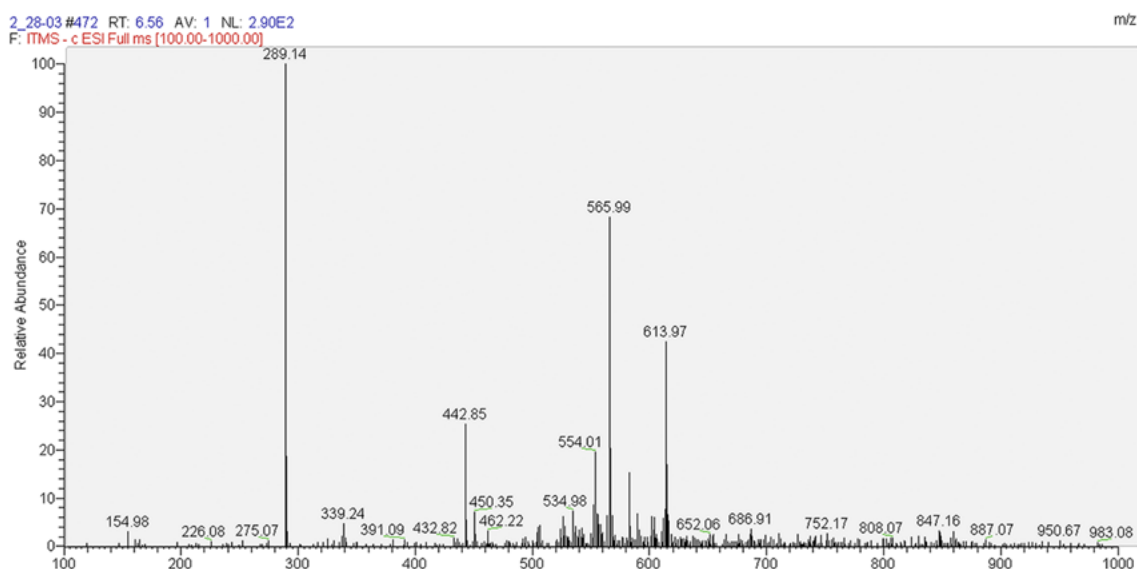

Figure 2. Mass spectrogram with peak m/z = 565.99, RT = 6.56 min obtained using the organic fraction from *Cryptosula zavjalovensis* and separated using LC-MS in the negative ionization mode.

alkaloid pterocellin E isolated from the New Zealand bryozoan *Pterocella vesiculosa* (Prinsep 2008). Using this structure as a basis, a preliminary structure was proposed for this peak (Fig. 3).

Cytotoxicity assays
Figures 4 and 5 show preliminary cytotoxicity results for the aqueous and organic extracts. The organic fraction exhibited moderate levels of cytotoxicity toward human MCF-7 breast cancer cells (Fig. 4).
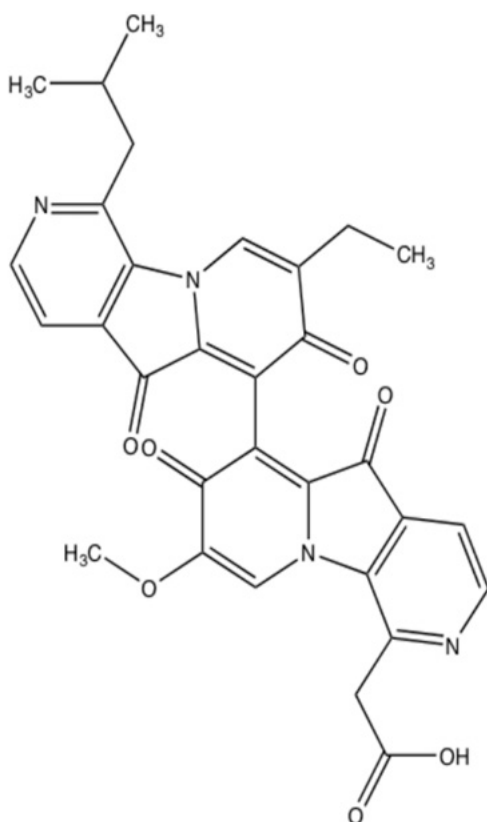
Figure 3. Preliminary structure proposed for a novel compound from *Cryptosula zavjalovensis*.
Peak 566 (negative mode): m/z: 566.1801 (100.0%), 567.1835 (33.5%), 568.1869 (2.7%), 568.1869 (2.7%), 567.1772 (1.5%), 568.1844 (1.4%). Chemical formula, C31H26N4O7; exact mass, 566.1801 g; molecular weight, 566.5700 g/mol; elemental analysis, C – 65.72%, H – 4.63%, N – 9.89%, O – 19.77% .

An increase in the extract concentration from 1 to 10 µg/mL resulted in an increase in cytotoxicity from 9% to 23%. In contrast, the aqueous extract fractions strangely exhibited negative cytotoxicity, that is, there were more viable cells in the plates with the test extracts than in the control plates. Increasing the extract concentration from 1 to 10 µg/mL resulted in a decrease in cytotoxicity from –10% to –36%.

The three fractions of the organic extract (**E1**, **E2**, **E3**) showed varying levels of cytotoxicity (Fig. 5). Fraction **E1**, like the aqueous fractions, exhibited negative cytotoxicity, as did fraction **E2** at lower concentration. However, at a concentration of 10 µg/ml, **E2** exhibited 79% cytotoxicity, indicative of the presence of bioactive compounds (Fig. 5). At concentrations of 1 and 10 µg/ml, fraction **E3** exhibited cytotoxicity at 58% and 107%, respectively (see above the possible reasons for a greater than 100% result).

Microbiology assays
Water extracts of *C. zavjalovensis* showed activity (ZOI > 15 mm) against eight of the 11 tested bacterial strains. ZOI values varied between 19.80 mm (*Salmonella* strain SkS02) and 15.31 (*Staphylococcus* strain SkS02). For ethanol extract essays, *Bacillus* strain A10 showed the highest zone of growth inhibition (ZOI = 20.83 mm), and *Staphylococcus* strain SkS02 the lowest (ZOI = 16.92). Interestingly, ethanol extracts showed higher inhibitory effects against most of the microorganisms tested, with ZOI values above 20.00 mm in four of the eight positive cases. All microorganisms tested showed statistically different ZOIs between the water and the ethanol extracts (p < 0.05), except for *Shigella* strain SkS01 and *Staphylococcus* strain SkS02 (Quaiyum *et al*. 2018).

DISCUSSION
Several alkaloids isolated from *Cryptosula pallasiana* (Tian *et al*. 2014) were the first to be compared with those detected in the congener *C. zavjalovensis*. However, none of the *C. pallasiana* isolates matched
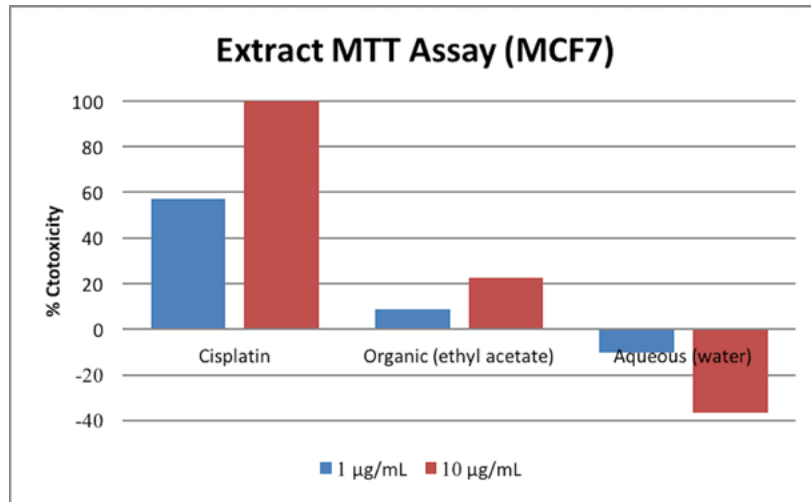
Figure 4. Cytotoxicity assay results using the MTT test for the aqueous (water) and organic (ethyl acetate) fractions from
Cryptosula zavjalovensis **towards MCF-7 breast cancer cell line.**

Figure 5. Cytotoxicity assay results using the MTT test for the organic fractions E1 (80:20 v/v methanol:water), E2 (100:0 v/v methanol:water), and; E3 (methanol:chloroform 50:50 v/v) from *Cryptosula zavjalovensis* towards MCF-7 breast cancer cell line.
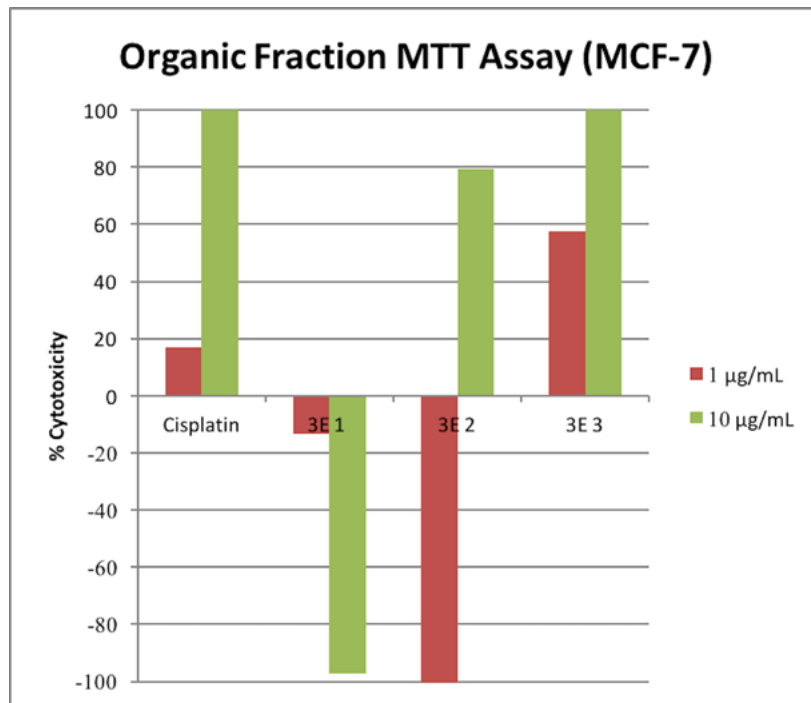
any of the m/z data from this study, and no matches were found in the MarinLit® database. This suggests that the peaks found here represent compounds that have not previously been detected, nor recorded in the available databases, and consequently could be novel compounds.

Interestingly, the peak with m/z = 566 (Fig. 2) was similar to that of pterocellin E isolated from *Pterocella vesiculosa* from New Zeland (Prinsep 2008). This helped to build up a preliminary chemical structure for this secondary metabolite of *C. zavjalovensis* (Fig. 3). However, the elucidation of the structure of this compound remains in the early stages of tandem mass spectrometry and is thus not definitive. The structure proposed is based merely on the similarities of the properties of the identified compound and that of pterocellin E. Further methods that can be used to elucidate the structure include infrared (IR) spectroscopy and carbon-13 nuclear magnetic resonance (^{13}C NMR) to identify functional groups, and proton nuclear magnetic resonance (H NMR) to identify molecular fragments.

Preliminary testing for cytotoxicity of the extracts using the MTT assay against human MCF-7 breast cancer cells showed that *Criptosula zavjalovensis* compounds have bioactivity. Bioactivity was present in the organic fractions (increasing from 23% to 95% when concentration was increased from 1 to 10 μg/ml), but it was most evident in organic fractions E2 and E3. Indeed, fraction E2 exhibited 79% cytotoxicity at a concentration of 10 μg/mL, whereas fraction E3 at a concentration of 1 μg/mL exhibited 58% cytotoxicity, and 107% with the increase in concentration to 10 μg/ml. As mentioned earlier, the MTT assay is a relative test of cell viability and does not indicate cell proliferation. It may alter mitochondria metabolism so its response is increased compared to untreated cells leading to over 100% viability values in the formation of formazan (Riss *et al*. 2004; Wang *et al*. 2011). These results are very promising, as even at a lower concentration the extracts show higher activity than the Cisplatin control. Future studies should combine MTT assays with more

direct viability tests (such as LDH assay) and cell counts to better assess cytotoxicity.

The aqueous extracts exhibited negative cytotoxicity, that is, there were more viable cells in the treatment plates than in the control ones. This effect was even more evident with an increase in extract concentration. Although this result seems to indicate a proliferation of the cancer cells, it should be noted that MTT reduction is only an indicator of cell viability and does not specifically indicate cell proliferation, although with the proper controls, it could be used as an assay for cell proliferation (Huyck *et al*. 2012). Indeed, the MTT assay alone is not enough to assess if the tested extract has any proliferative properties. Factors such as metabolic and energy perturbations, cell line, oxidative stress, and others may affect the reduction of MTT (Stepanenko and Dmitrenko 2015). It is possible that the action of the extract on the cell line could result in an enzymatic activity increase without actually affecting the cell number or the cytotoxicity. This could then result in the under- or overestimation of the cell viability, or in the case of this study, the cytotoxicity of the extract tested. To clarify these results, it is recommended that the MTT assay be supplemented with non-metabolic methods (Jaszczyszyn and Gasiorowski 2008; Wang *et al*. 2011; Angius and Floris 2015). Moreover, some chemical constituents may activate genes encoding growth factors which could mask the cytotoxicity of certain metabolites. Further cytotoxicity tests using other assays are needed in order to investigate these findings and better assess the properties of the tested extracts.

The microbiological tests showed that both water and ethanol extracts from *Cryptosula zavjalovensis* exhibit potential as bacterial inhibitors. Although the antibacterial activity of the extracts varied considerably across the microorganisms tested, both exhibited a broad spectrum of antibacterial activity against gram-negative and gram-positive strains, which attests to their potential utility in developing new antibacterial drugs. The ZOI size indicative of meaningful biological activity is open to question.

Whereas some authors consider that a meaningful ZOI should have a minimum size (Bergquist and Bedford 1978; Lippert *et al*. 2003), others agree that any ZOI should be considered as positive evidence, as it reflects the ability of the metabolite to actually inhibit bacterial growth (Kelman *et al*. 2001; Figuerola *et al*. 2014). It is important to note that the observed ZOI may depend on the capillarity and diffusion rates of both the studied metabolites and the medium used (Walls *et al*. 1993; Jensen *et al*. 1996; Jenkins *et al*. 1998). As this was a preliminary study, we used a conservative approach and followed the traditional view considering ZOI > 15 mm as a significant cut-off value, and most bacterial strains we assayed showed distinct and relatively high ZOI values.

It is noteworthy that only specimens from Akkeshi were used in the microbiological and cytotoxicity assays. This could explain some of the results (i.e., the negative results in water-extract cytotoxicity tests), as bryozoans from different localities can produce metabolites with quite different properties (Lippert *et al*. 2003; Figuerola *et al*. 2014). Studies from other localities are needed for more definitive conclusions. In addition, no marine bacteria were tested, and it is possible that different results would be obtained if microorganisms from the marine realm were used in assays.

Though these are preliminary results and more tests are necessary, both the cytotoxicity and the microbiology assays indicated that *Cryptosula zavjalovensis* produces novel metabolites with potential utility in pharmacology. In a time when bacterial resistance is increasing and many diseases are becoming more broadly distributed, it is important to search for novel products that could expand the range of possible cures.

ACKNOWLEDGMENTS

REFERENCES

ANGIUS, F. AND FLORIS, A. 2015. Liposomes and MTT cell viability assay: An incompatible affair. *Toxicology in Vitro* **29**, 314–319.

BERGQUIST, P.R. AND BEDFORD, J.J. 1978. The incidence of antibacterial activity in marine Demospongiae. Systematic and geographical considerations. *Marine Biology* **46**, 215–221.

BULAJ, G., BUCZEK, O., GOODSELL, I., JIMENEZ, E.C., KRANSKI, J., NIELSEN, J.S. AND OLIVERA, B.M. 2003. Efficient oxidative folding of conotoxins and the radiation of venomous cone snails. *Proceedings of the National Academy of Sciences of the United States of America* **25** (100), 14562–14568.

BLUNT, J.W., COPP, B.R., KEYZERS, R.A., MUNRO, M.H.G. AND PRINSEP, M.R. 2016. Marine natural products. *Natural Product Reports* **33**, 382–431.

BLUNT, J.W., COPP, B.R., MUNRO, M.H.G., NORTHCOTE, P.T. AND PRINSEP, M.R. 2004. Marine natural products. *Natural Products Reports* **21**, 1–49.

BLUNT, J.W., COPP, B.R., MUNRO, M.H., NORTHCOTE, P.T. AND PRINSEP, M.R. 2011. Marine natural products. *Natural Products Report* **28**, 196–268.

CARLE, J.S. AND CHRISTOPHERSEN, C. 1980. Marine alkaloids. 2. Bromo alkaloids from a marine bryozoan *Flustra foliacea*. Isolation and structure elucidation. *The Journal of Organic Chemistry* **45**(9), 1586–1589.

CARLE, J.S. AND CHRISTOPHERSEN, C. 1981. Marine Alkaloids. 3. Bromo-Substituted Alkaloids from the Marine Bryozoan *Flustra foliacea*, Flustramine C and Flustraminol A and B. *The Journal of Organic Chemistry* **46**(17), 3440–3443.

CRAGG, G.M. AND NEWMAN, D.J. 2013. Natural Products: A Continuing Source of Novel Drug Leads. *Biochimica et Biophysica Acta – General Subjects* **1830**(6), 3670–3695.

DASARI, S. AND TCHOUNWOU, P. 2014. Cisplatin in cancer therapy: molecular mechanisms of action. *European Journal of Pharmacology* **740**(5), 364–378.

DAVIDSON, S.K. AND HAYGOOD, M.G. 1999. Identification of Sibling Species of the Bryozoan *Bugula neritina* That Produce Different Anticancer Bryostatins and Harbor Distinct Strains of the Bacterial Symbiont "*Candidatus Endobugula sertula*". *The Biological Bulletin* **196**, 273–280.

DICK, M.H., GRISCHENKO, A.V. AND MAWATARI, S.F. 2005. Intertidal Bryozoa (Cheilostomata) of Ketchikan, Alaska. *Journal of Natural History* **39**, 3687–3784.

FIGUEROLA, B. AND AVILA, C. 2019. The Phylum Bryozoa as a Promising Source of Anticancer Drugs. *Marine Drugs* **17**(8), 477–500.

FIGUEROLA, B., COMORERA, L.S., PRECKLER, C.A., VAZQUEZ, J., MONTES, M.J., GARCIA-ALJARO, C., MERCADE, E., BLANCH, A.R. AND AVILA, C. 2014. Antimicrobial activity of Antarctic Bryozoans: An ecological perspective with potential for clinical application. *Marine Environmental Research* **101,** 52–59.

FLOREA, A.M. AND BÜSSELBERG, D. 2011. Cisplatin as an Anti-Tumor Drug: Cellular Mechanisms of Activity, Drug Resistance and Induced Side Effects. *Cancers* **3**, 1351–1371.

GRISCHENKO, A.V., DICK, M.H. AND MAWATARI, S.F. 2007. Diversity and taxonomy of intertidal Bryozoa (Cheilostomata) at Akkeshi Bay, Hokkaido, Japan. *Journal of Natural History* **41**, 1047–1161.

HO, C., LAM, C., CHAN, M., CHEUNG, R., LAW, L., LIT, L. AND TAI, H. 2003. Electrospray Ionisation Mass Spectrometry: Principles and Clinical Applications. *The Clinical Biochemist Reviews* **24**(1), 3–12.

HOLST, P.B., ANTHONI, U., CHRISTOPHERSEN, C. AND NEILSON, P.N. 1994. Marine alkaloids 15. Two alkaloids, flustramine E and debromoflustramine B, from the marine bryozoan *Flustra foliacea*. *Journal of Natural Products* **57**, 997–1000.

HONGPAISAN, J. AND ALKON, D.L. 2007. A structural basis for enhancement of long-term associative memory in single dendritic spines regulated by PKC. *Proceedings of the National Academy of Sciences USA* **104**, 19571–19576.

HUYCK, L., AMPE, C. AND VAN TROYS, M. 2012. The XTT Cell Proliferation Assay Applied to Cell Layers Embedded in Three-Dimensional Matrix. *Assay and Drug Development Technologies* **10**(4), 382–392.

JASZCZYSZYN, A. AND GASIOROWSKI, K. 2008. Limitations of the MTT Assay in Cell Viability Testing. *Advances in Clinical and Experimental Medicine* **17**(5), 525–529.

JENKINS, K.M., JENSEN, P.R. AND FENICAL, W. 1998. Bioassays with marine microorganisms. In: K.F. Haynes & J.G Millar (eds.), *Methods in Chemical Ecology, Vol. 2, Bioassay Methods*. New York, Chapman and Hall Publishers, pp. 1–38.

JENSEN, P.R., HARVELL, C.D., WIRTZ, K. AND FENICAL, W. 1996. Antimicrobial activity of extracts of Caribbean gorgonian corals. *Marine Biology* **125**, 411–419.

JEONG, S.J., HIGUCHI, R., MIYAMOTO, T., ONO, M., KUWANO, M. AND MAWATARI, S.F. 2002. Bryoanthrathiophene, a new antiangiogenic constituent from the bryozoan *Watersipora subtorquata* (d'Orbigny, 1852). *Journal of Natural Products* **65**, 1344–1345.

JHA, R. K. AND ZI-RONG, X. 2004. Biomedical Compounds from Marine Organisms. *Marine Drugs* **2**(3), 123–146.

JOFFE, S. AND THOMAS, R. 1989. Phytochemicals: a renewable global resource. *AgBiotech News and Information* **1**, 697–700.

KELMAN, D., KASHMAN, Y., ROSENBERG, E., ILAN, M., IFRACH, I. AND LOYA, Y. 2001. Antimicrobial activity of the reef sponge *Amphimedon viridis* from the Red Sea: Evidence for selective toxicity. *Aquatic Microbial Ecology* **24**, 9–16.

KUZIRIAN, A.M., EPSTEIN, H.T., GAGLIARDI, C.J., NELSON, T.J., SAKAKIBARA, M., TAYLOR, C., SCIOLETTI, A.B. AND ALKON, D.L. 2006. Bryostatin enhancement of memory in *Hermissenda*. *Biological Bulletin* **210**, 201–214.

LEFRANC, F., KOUTSAVITI, A., IOANNOU, E., KORNIENKO, A., ROUSSIS, V., KISS, R. AND NEWMAN, D. 2019. Algae metabolites: From in vitro growth inhibitory effects to promising anticancer activity. *Natural Products Report* **36**, 810–841.

LILIES, G. 1996. Gambling on marine biotechnology. *Bioscience* **46**, 250–253.

LIPPERT, H., BRINKMEYER, R., MULHAUPT, T. AND IKEN, K. 2003. Antimicrobial activity in sub-Arctic marine invertebrates. *Polar Biology* **26**, 591–600.

LOPANIK, N., LINDQUIST, N. AND TARGETT, N. 2004. Potent cytotoxins produced by a microbial symbiont protect host larvae from predation. *Oecologia* **139**(1), 131–139.

LYSEK, N., RACHOR, E. AND LINDEL, T. 2000. Isolation and Structure Elucidation of Deformylflustrabromine from the North Sea Bryozoan *Flustra foliacea*. *Zeitschrift für Naturforschung C* **57**(11-12), 1056–1061.

MATHUR, V.S. 2000. Ziconotide: a new nonopioid intrathecal analgesic for the treatment of chronic pain. *Seminars in Anesthesia, Perioperative Medicine and Pain* **19**(2), 67–75.

MORGAN, R.J., LEONG, L., CHOW, W., GANDARA, D., FRANKEL, P., GARCIA, A. AND DOROSHOW, J.H. 2012. Phase II trial of bryostatin-1 in combination with

cisplatin in patients with recurrent or persistent epithelial ovarian cancer: a California cancer consortium study. *Investigational New Drugs* **30**(2), 723–728.

NARKOWICZ, C.K., BLACKMAN, A.J., LACEY, E., GILL, J.H. AND HEILAND, K. 2002. Convolutindole A and convolutamine H, new nematocidal brominated alkaloids from the marine bryozoan *Amathia convoluta*. *Journal of Natural Products* **65**, 938–941.

PETTIT, G.R. 1991. The Bryostatins. In: W. Herz, G.W. Kinby, W. Steglich and C. Tamm (eds.), *Fortschritte der Chemie organischer Naturstoffe / Progress in the Chemistry of Organic Natural Products*. Vienna, Springer Publishers, **57**, pp. 153–195.

PETTIT, G.R., HERALD, C.L., DOUBEK, D.L. AND HERALD, D.L. 1982. Isolation and Structure of Bryostatin 1. *Journal of the American Chemical Society* **104**(24), 6846–6848.

PRABHAKARAN, P., HASSIOTOU, F., BLANCAFORT, P. AND FILGUEIRA, L. 2013. Cisplatin induces differentiation of breast cancer cells. *Frontiers in Oncology* **3**(134), 1–10.

PRINSEP, M.R. 2008. Further Pterocellins from the New Zealand Marine Bryozoan *Pterocella vesiculosa*. *Journal of Natural Products* **71**(1), 134–136.

PRINSEP, M.R., BLUNT, J.W. AND MUNRO, M.G.H. 1991. New Cytotoxic ß-Carboline Alkaloids from the Marine Bryozoan *Cribricellina cribraria*. *Journal of Natural Products* **54**(4), 1068–1076.

RISS, T.L., MORAVEC, R.A, NILES, A.L., DUELLMAN, S., BENINK, H.A., WORZELLA, T.J. AND MINOR, L. 2004. Cell Viability Assays. In: G.S. Sittampalam, A. Grossman, K. Brimacombe, M. Arkin, D. Auld, C. Austin, J. Baell, B. Bejcek, J.M.M. Caaveiro, T.D.Y. Chung, N.P. Coussens, J.L. Dahlin, V. Devanaryan, T.L. Foley, M. Glicksman, M.D. Hall, J.V. Haas, S.R.J. Hoare, J. Inglese, P.W. Iversen, S.D. Kahl, S.C. Kales, S. Kirshner, M. Lal-Nag, Z. Li, J. McGee, O. McManus, T. Riss, O.J. Trask, Jr., J.R. Weidner, M.J. Wildey, M. Xia and X. Xu (eds.), *Assay Guidance Manual*. Bethesda (MD), Eli Lilly & Company and the National Center for Advancing Translational Sciences, pp. 289–314.

RYLAND, J.S. 2005. Bryozoa: an introductory overview. *Denisia* **16**, 9–20

QUAIYUM, S., FORTUNATO, H., GONZAGA, L.J. AND OKABE, S. 2018. Antimicrobial Activity in the Marine Cheilostome Bryozoan *Cryptosula zavjalovensis* Kubanin, 1976. *Journal of Antimicrobial Agents* **4**(3), 178–182.

SHARP, J.H., WINSON, M.K. AND PORTER, J.S. 2007. Bryozoan metabolites: An ecological perspective. *Natural Products Report* **24**, 659–673.

SINKO, J., RAJCHARD, J., BALOUNOVA, Z. AND FIKOTOVA, L. 2012. Biologically active substances from water invertebrates: a review. *Veterinarni Medicina* **57**(4), 177–184.

STEPANENKO, A.A. AND DMITRENKO, V.V. 2015. Pitfalls of the MTT assay: Direct and off-target effects of inhibitors can result in over/underestimation of cell viability. *Gene* **574,** 193–203.

SUN, M.K. AND ALKON, D.L. 2005. Dual effects of bryostatin-1 on spatial memory and depression. *European Journal of Pharmacology* **512**, 43–51.

SUN, M.K., HONGPAISAN, J., LIM, C.S. AND ALKON, D.L. 2014. Bryostatin-1 Restores Hippocampal Synapses and Spatial Learning and Memory in Adult Fragile X Mice. *The Journal of Pharmacology and Experimental Therapeutics* **349**, 393–401.

TIAN, X.R., GAO, Y.Q., TIAN, X.L., LI, J., TANG, H.F., LI, Y.S., LIN, H.W. AND MA, Z.Q. 2017. New Cytotoxic Secondary Metabolites from Marine Bryozoan *Cryptosula pallasiana*. *Marine Drugs* **15**(4), 120–130.

TIAN, X.R., TANG, H.F., LI, Y.S., LIN, H.W., ZHANG, X.Y., FENG, J.T. AND ZHANG, X. 2014. Studies on the Chemical Constituents from Marine Bryozoan *Cryptosula pallasiana*. *Records of Natural Products* **9**(4), 628–632.

TIAN, X.R., TANG, H.F., TIAN, X.L., HU, J.J., HUANG, L.L. AND GUSTAFSON, K.R. 2018. Review of bioactive secondary metabolites from marine bryozoans in the progress of new drugs discovery. *Future Medicinal Chemistry* **10**(12), 1497–1514.

TILL, M. AND PRINSEP, M.R. 2009. 5-Bromo-8-methoxy-1-methyl-β-carboline, an Alkaloid from the New Zealand Marine Bryozoan *Pterocella vesiculosa*. *Journal of Natural Products* **72**(4), 796–798.

WALLS, J.T., RITZ, D.A. AND BLACKMAN, A.J. 1993. Fouling surface bacteria and antibacterial agents of four Bryozoan species found in Tasmania, Australia. *Journal of Experimental Marine Biology and Ecology* **169**, 1–13.

WANG, A.T., PRINSEP, M.R. AND MARTINUS, R.D. 2016. Pterocellin A isolated from marine the bryozoan *Pterocella vesiculosa* is cytotoxic to human HeLa cells via mitochondrial apoptotic processes. *SpringerPlus* **5**(742), 1–11.

WANG, S., YU, H. AND WICKLIFFE, J.K. 2011. Limitation of the MTT and XTT assays for measuring cell viability due to superoxide formation induced by nano-scale TiO_2. *Toxicology in Vitro* **25**, 2147–2151.

WATERS. 2017. Beginner's Guide to SPE [Solid-Phase Extraction]. Retrieved from Waters: http://www.waters.com/waters/en_US/Beginner%27s-Guide-to-SPE-%5BSolid-Phase-Extraction%5D/nav.htm?locale=en_US&cid=134721476 (accessed on August 13, 2019).

WILLIAMS, D., STONE, M., HAUCK, P. AND RAHMAN, S. 1989. Why are secondary metabolites (natural products) biosynthesized? *Journal of Natural Products* **52**(6), 1189–1208.

WRIGHT, J. 1984. A New Antibiotic from the Marine Bryozoan *Flustra foliaceae. Journal of Natural Products* **47**(5), 893–895.

WULFF, P., CARLE, J. AND CHRISTOPHERSEN, C. 1982. Marine alkaloids 5. Flustramide A and bromo-Nb-methyl-Nb-formyltryptamine from the marine bryozoan *Flustra foliacea. Comparative Biochemistry and Physiology Part B: Compa-rative Biochemistry* **71**(3), 523–524.

ZHANG, H., SHIGEMORI, H., ICHIBASHI, M., KOSAKA, T., PETTIT, G.R., KAMANO, Y. AND KOBAYASHI, J. 1994. Convolutamides A-F, Novel γ-lactam alkaloids from the marine bryozoan *Amathia convoluta. Journal Tetrahedron* **50**, 10201–10206.

Palaeocorynid-type structures in fenestellid Bryozoa from the Carboniferous of Oaxaca, Mexico

**Sergio González-Mora[1*], Patrick N. Wyse Jackson[2], Adrian J. Bancroft[3]
and Francisco Sour-Tovar[4]**

[1] Posgrado en Ciencias Biológicas, Universidad Nacional Autónoma de México, Ciudad Universitaria, 04510 CDMX, México [*corresponding author: e-mail: gioser@ciencias.unam.mx]

[2] Department of Geology, Trinity College, Dublin 2, Ireland [wysjcknp@tcd.ie]

[3] 51 Westbury Drive, Pandy, Wrexham, Wales, United Kingdom [palaeozoic@gmail.com]

[4] Museo de Paleontología, Departamento de Biología Evolutiva, Facultad de Ciencias, Universidad Nacional Autónoma de México, Ciudad Universitaria, 04510 CDMX, México [fcosour@ciencias.unam.mx]

ABSTRACT

In order to protect themselves from predation many modern living bryozoans develop variety of polypides with different protective functions, grow skeletal structures such as spines, or produce chemical metabolites. Skeletal structures that are inferred to have been developed as a response to potential predation have been recognized in the fossil record. Outcrops of the Ixtaltepec Formation (Mississippian–Pennsylvanian) in the Santiago Ixtaltepec area, Oaxaca State, southern Mexico, have yielded fenestrate bryozoans with two distinct forms of such skeletal structures preserved on the obverse surface of colonies. Both morphotypes originate from pillar-like structures, one forming simple straight radial arm-like expansions, the other forming a much larger reticulate meshwork. These distinctive structures known as palaeocorynid-type appendages, have historically been considered to be hydrozoans, algae, or independent bryozoans attached to fenestellid bryozoans and reputed distinctive forms were formally designated as the genera *Palaeocoryne*, *Claviradix* or *Macgowanella*. The latter two are junior synonyms of the former, but the status of all of these genera is untenable as their skeletal structure has been shown to be contiguous with the main bryozoan skeleton they arise from. These palaeocorynid-type appendages are described from Mexico for the first time, and the reticulate form is the first recorded occurrence outside of Great Britain.

INTRODUCTION

Fenestellid bryozoans frequently have skeletal extensions such as long spines, high keels and superstructures developed on obverse surfaces (McKinney *et al*. 2003); palaeocorinid-type structures which are contained within this group are distinctive for their diversity, rarity and peculiar shape. Palaeocorynid-type structures have been the focus of studies by several authors for one hundred and fifty years (Duncan and Jenkins 1869; Duncan 1873; Young and Young 1874; Vine 1879a, b; Elias and Condra 1957; Ferguson 1961, 1963; Bancroft 1988). The genus *Palaeocoryne*, with the type species *P. scoticum*, was erected by Duncan and Jenkins (1869) on the basis of specimens from the Carboniferous of Ayrshire and Lanarkshire, that were attached to the margins of the bryozoan *Fenestella s.l.* and they suggested that they were closely related to hydrozoans. Allman (1872) contradicted this view on account of the ornamentation of their surface and instead proposed that they were related

to Rhizopoda protists. Young and Young (1874) observed that these structures were connected to the skeleton of the branch from which they emerged and demonstrated using thin-sections the continuity of the skeletal tissue between the bryozoan branch and the palaeocorynid structure. Vine (1879a, b) argued that these are appendages of the colony that might have a supportive and reproductive function. Elias and Condra (1957) also considered that these structures were overgrowths of *Fenestella* and rejected the earlier argument that these appendages were related in some way with red algae. Ferguson (1961, 1963) established the genus *Claviradix* for the forms of palaeocorynidae from the Pennsylvanian of Durham, England that had root-type processes, and concluded that both *Palaeocoryne* and *Claviradix* were separate organisms from the colony that hosted them. He considered that both host and attached structure maintained a relationship of commensalism, however recognizing that they had a certain affinity with

bryozoans on account of the similarity of the skeletal structure. In addition, Ferguson (1963) reported that some of the species contained within these genera were associated with more than a single taxon of fenestellids, recording for example that *Palaeocoryne scoticum* occurred with both *Fenestella frutex* M'Coy, 1844 and *Fenestella* cf. *quadidecimalis* M'Coy, 1844. This may have influenced his conclusion that *P. scoticum* was an independent biological organism.

Bancroft (1988) in the most recent major review of the palaeocorynid-type structures reported new material well preserved *in situ*, and documented more complex appendages that formed a reticulate meshwork on the obverse surface of some fenestellids. Critically his study included an analysis of skeletal microstructure which unequivocally demonstrated that palaeocorynid-outgrowths are part of the bryozoan zoarium. Additionally, he postulated that these skeletal developments were a form of specialized appendages that provided protection to the feeding polypides.
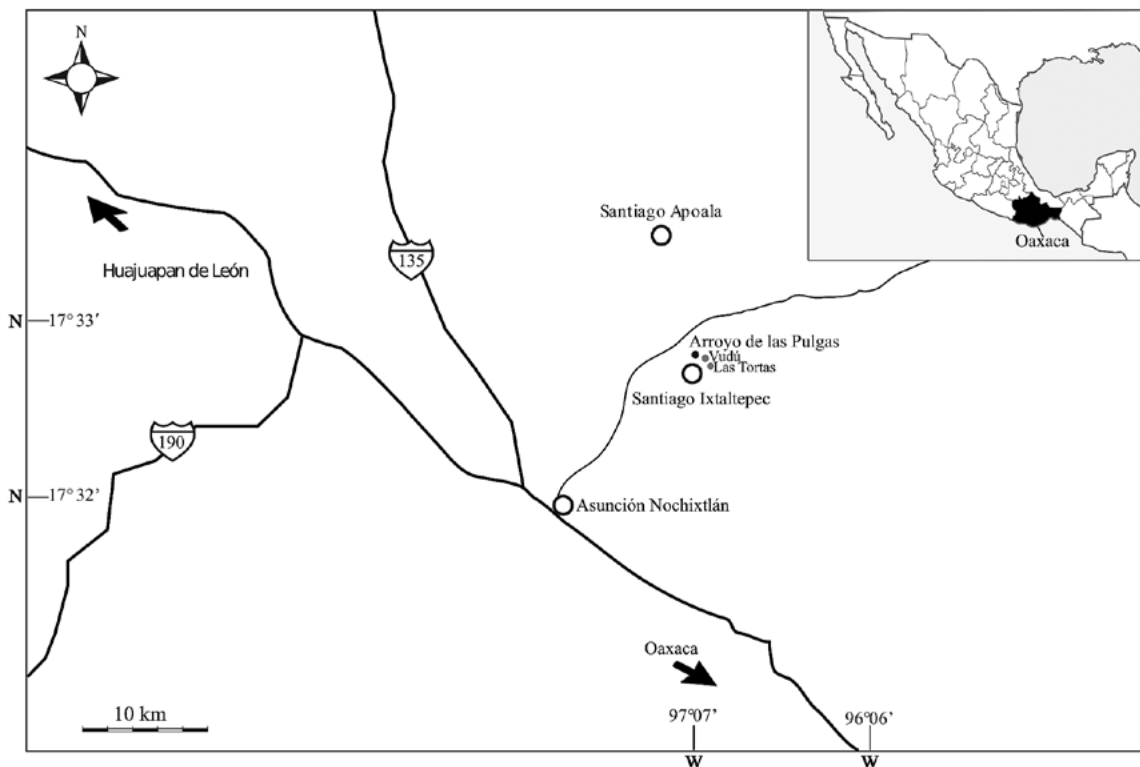

Figure 1. Geographical location of the Ixtaltepec Formation.

In addition to the genera *Palaeocoryne* and *Claviradix*, the genus *Macgowanella* was erected by Nelson and Bolton (1980) from the Upper Carboniferous of Alberta, Canada, who interpreted the radiating form, previously described as the cystoporate bryozoan *Evactinopora*? *tenuiradiata* Warren, 1927, as bryozoan holdfasts. However, it is clear from a reassessment of the morphology of *Evactinopora* that this material that it is not an evactinoporid (Yancey *et al.* 2019) and that they conform to palaeocorynid-type appendages.

In the present work we report the occurrence of two kinds of palaeocorynid-type structures associated with fenestellid bryozoans in outcrops of the Ixtaltepec Formation (Mississippian-Pennsylvanian), Oaxaca, Mexico, as discuss their taxonomic status and assess their functional biology.

GEOLOGICAL SETTING

The Santiago Ixtaltepec region is located 19 km northwest of the city of Asunción Nochixtlán, State of Oaxaca in southern Mexico. The specimens were collected in the Ixtaltepec Formation whose type section is located at Arroyo de las Pulgas, approximately 500 m north of the town of Santiago Ixtaltapec (17º32´–17º33´N; 97º06´–97º07´W) (Fig. 1).

The Carboniferous succession overlies the Tinú Formation (Cambrian-Ordovician) and it is divided into two formations (Robison and Pantoja-Alor 1968). The 'Santiago Formation', an informally named unit that is considered to be Mississippian (Tournaisian–Serpukhovian) in age (Quiroz-Barroso *et al.* 2000; Navarro- Santillán *et al.* 2002; Castillo-Espinoza 2013), and the Ixtaltpec Formation comprising 430m of rocks of Late Mississippian–Middle Pennsylvanian age. The base of this formation contains 90 m of siltstones, intercalations of shale, fine-grained calcareous sandstone, and thin layers of slightly clayish calcarenite and is followed by units of slightly sandy shale with fine-grained sand beds and fine-grained micaceous strata. Above these beds are thick layers of sandy shale interbedded with fine-grained shale. For palaeontological analysis being carried out by the senior author as part of on-going studies, the Ixtaltepec Formation has been informally divided into eight levels (API-1 to API-8), each characterized by its fossil content and lithology. Strata from levels API-1 to API-4 contain fossils of Mississippian age (Visean–Serpukhovian) (Torres-Martínez and Sour-Tovar 2016a) and levels API-5 to API-8 yield a Pennsylvanian fauna (Bashkirian–Moscovian) (Torres-Martínez and Sour-Tovar 2016b). The palaeocorynid type-structures were collected in "Las Tortas"(17°33´16´´N, 97º06´35´´W) and "Vudú" (17°33´15´´ N, 97°06´ 36´´W) outcrops that correlate with the API-2 and API-7 levels, respectively (Fig. 2).

MATERIAL

The material described herein is housed in the collection of the Museo de Paleontología, Facultad de Ciencias, Universidad Nacional Autónoma de México. Figured specimens are designated in the descriptions by the prefix FCMP.

MORPHOLOGY OF PALAEOCORYNID-TYPE STRUCTURES FROM MEXICO

The palaeocorynid-type 1 structure (Figs 3, 5) was found in the API-1 level of the Ixtaltepec Formation and is associated with a colony of fenestrate bryozoan (specimen FCMP 1380). This structure forms a cylindrical stem 1 mm in length and 0.4 mm in thickness, on top of which is a barrel-shaped body slightly elevated in its center. A series of cylindrical spines emerge from it; while 7 fragmented spines are observed, the number of spines could reach between 8 and 10, whose sizes range from 0.8–1.0 mm in length and 0.25–0.3 mm in thickness. The surface ornamentation is striated with a grainy texture and it is present throughout all the appendage.

Several examples of palaeocorynid-type 2 (Figs 4, 5, 7) are present in the API-7 level of the Ixtaltepec Formation, all developed from a colony of a fenestellid bryozoan preserved in shale. These form a reticulate meshwork on the reverse surface
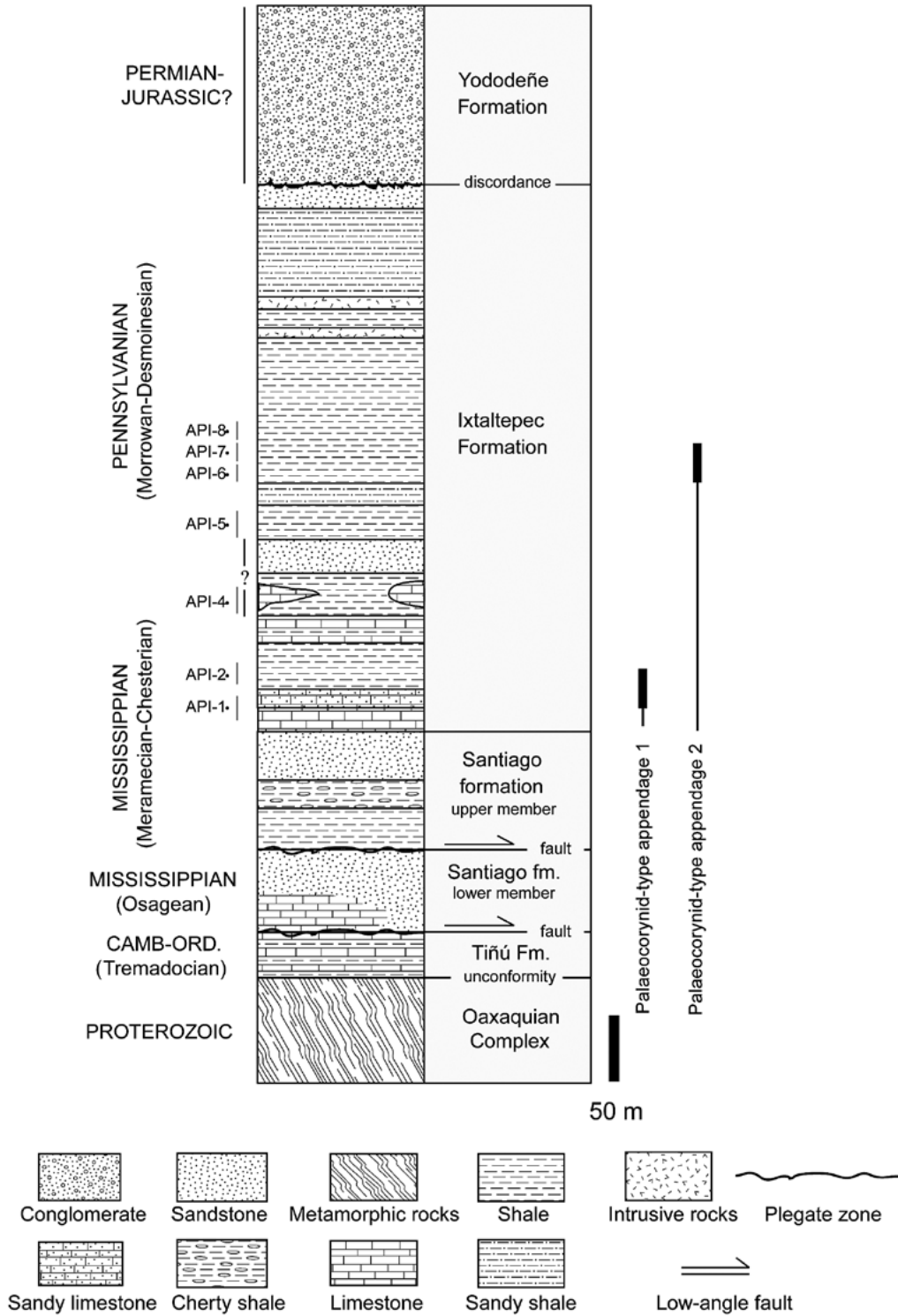
Figure 2. Stratigraphic column of the Paleozoic region of Santiago Ixtaltepec, Mexico. The bars indicate the levels where the palaeocorynid-type structures were found.
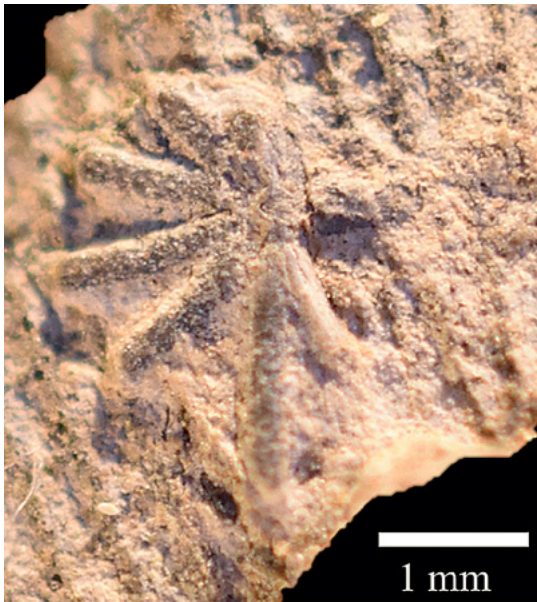
Figure 3. Palaeocorynid-type 1 structure (FCMP 1380) from API-2 level of Ixtaltepec Formation.
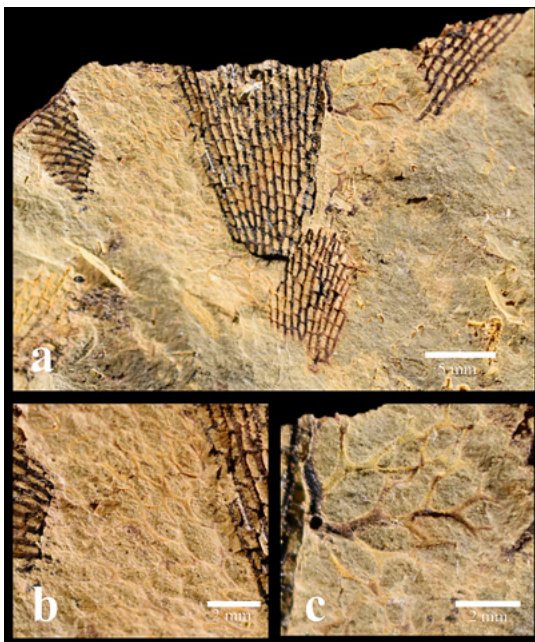
Figure 4. Palaeocorynid-type 2 structure (FCMP 1381) from API-7 level of Ixtaltepec Formation. (A) Fenestellid that displays a reticulate meshwork formed by the overlapping and fusion of palaeocoryne-type structures that have bifurcations; (B) Partial reticulate meshwork; (C) Body of the palaeocorynid-type structure with spines that form a meshwork.

(specimen FCMP 1381). As the bryozoan colony is preserved as a mold, only the external characteristics can be seen, and additionally only in two dimensions due to flattening of the sediment. On account of this poor preservation the length of the stem cannot be determined. Approximately four spines emerge from the circular body of palaeocorynid-type 2. Almost all the spines have bifurcations ranging from the 2nd to the 9th order. These spines in some points overlap and fuse, in some cases smaller lateral spines emerge from them. Their length is 0.5–1.5 mm, and thickness is 0.1–0.4 mm; the spines near the central pillar of the appendage are larger. The specimen is similar to the reticulate palaeocorynid-type appendages described by Bancroft (1988) and to the specimens assigned to *Claviradix cruciformis* by Ferguson (1963).

DISCUSSION

Taxonomic status of the genus Palaeocoryne

While McKinney and Wyse Jackson (2015, p. 30) informally retained the genus *Palaeocoryne,* it is now considered that there is no biological basis for its distinction; neither it or its junior synonyms *Claviradix* and *Macgowanella* are independent biological entities from the colony from which they develop, since both the external ornamentation and skeleton of the branches are continuous with these structures (Bancroft 1988).

Functional biology considerations

Recent bryozoans develop a range of different responses to the activity of predators, ranging from an increase in the production of secondary metabolites (Lindquist and Hay 1996) to the development of skeletal spine-like structures with differing morphologies (Harvell 1984). Evidence throughout the fossil record has also shown fenestrate bryozoans evolved a number of strategies to counteract the effects of predation including the production of spine-like structures that allows the inference of such prey-predator relationships (McKinney *et al.* 2003). Bancroft (1988) suggested that the palaeocorynid-type structures provided protection to the feeding

polypides by providing a passive defensive structure against predators. These structures are more abundant in some horizons than others (Bancroft 1988) which could perhaps be correlated with times of higher incidence of predators in the fossil record. Throughout the Palaeozoic a number of fenestrate taxa developed superstructures, most of which belong to the Family Semicosciniidae (Suárez Andrés and Wyse Jackson

2015). The earliest examples are seen in *Loculipora* and *Unitrypa* from the Silurian, while the incidence of keel-bearing and superstructure-bearing genera rose significantly in the Devonian with up to twelve being reported (Ernst 2013). The number of genera with such structures declined though the Carboniferous (*Fenestella s.l.*, *Hemitrypa*) and into the Permian (*Cervella*). The intermittent appearance both in time
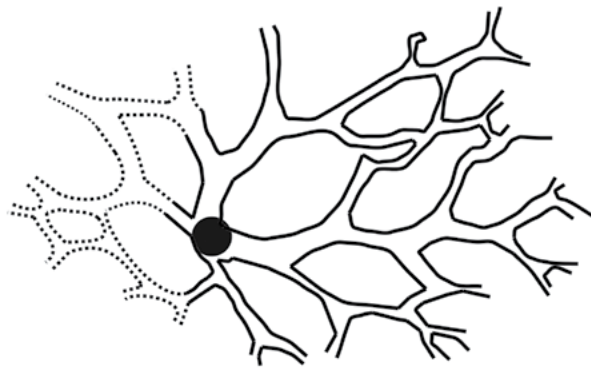
Figure 5. Sketch of palaeocorynid-type 2 structure (FCMP 1381) from API-7 level of Ixtaltepec. The dotted lines indicate a possible reconstruction of the missing spines and the black dot indicates the body of the structure.
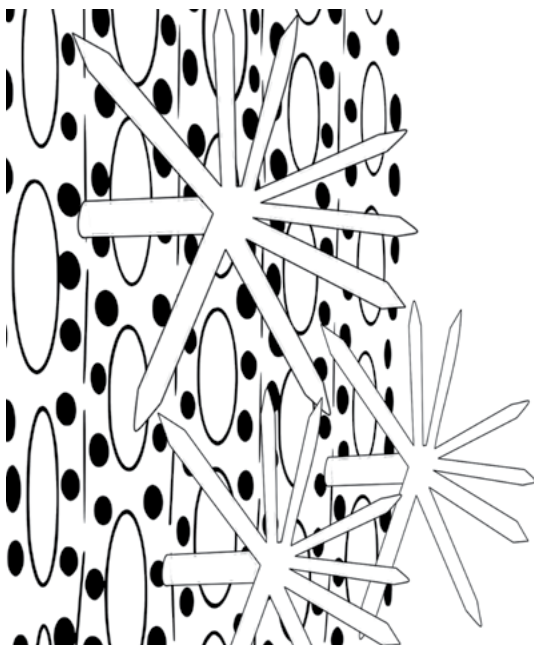
Figure 6. Sketch of the life position of palaeocorynid-type 1 structure.
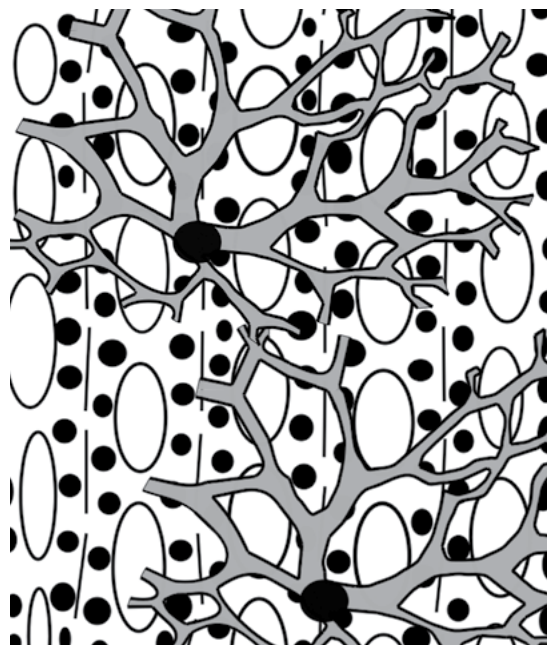
Figure 7. Sketch of the life position of palaeocorynid-type 2 structure.

and in taxa of palaeocorynid-type appendages during the Carboniferous, coupled with their diversity of forms and the rarity of finding them *in situ*, strongly suggests that palaeocorynid-type appendages could be an example of phenotypic plasticity of some fenestellid bryozoans.

Phenotypic plasticity is the ability of the same ontogenetic system (organism) to produce different phenotypes under the pressure of different environmental conditions. These phenotypes can be expressed as changes in form, status, movement or activity rate (West-Eberhard 2003). A plastic response is distinguished in a pathological way, since in the first one there is an adaptive phenomenon, which results in responses that improve the adaptation under specific selective contexts. Two types of phenotypic plasticity have been recognized: one where morphological or functional variation is continuous (reaction norms) and another where variation is discontinuous (polyphenisms) (Gilbert 2012). Both types of plasticity are present in bryozoans (Taylor 2005).

Polyphenisms are a type of discontinuous phenotypic plasticity, where specific conditions of an environment result in a particular discrete phenotype (Gilbert 2012). A very common polyphenism that is manifest in bryozoans is the presence of spines, which occur in a great variety of forms. Some of these can be solid, others are hollow; however, in a colony not all zooids are necessarily associated with them. They develop as a morphological response induced by the environment, whether physical or biological (Taylor 2005). In the first case, it has been demonstrated that the spines of *Electra pilosa* develop as a result of the exposure of the zooids to abrasion caused by the waves, where the spines allow the protection of the lophophore against high energy conditions (Bayer *et al*. 1997). In the case of polyphenisms caused by biological entities, Harvell (1984) in a series of laboratory experiments on colonies of *Membranipora membranacea*, found that the activity of predatory nudibranchs induced rapid formation of spines in some of the zooids. This strategy is very effective in reducing the effects of predation within the colony, however it has a great cost in the development of zooids, since its growth rate slows down (Taylor 2005).

We suggest that palaeocorynid-type structures can be a polyphenism in which a skeletal structure is formed above the level of autozooecial apertures on branches so that the autozooids are afforded protection (Figs 6, 7) against predation or the impact of large sediment particles that could affect their ability to feed efficiently.

CONCLUSION

Palaeocorynid-type appendages were until recently considered to be hydrozoans, algae, or independent bryozoans attached to fenestellid bryozoans and were assigned to the genera *Palaeocoryne*, *Claviradix* or *Macgowanella*. The latter two are junior synonyms of the former, but their generic status is untenable as their skeletal structure has been shown to be contiguous with the main bryozoan skeleton they arise from. The palaeocorynid-type appendages can form an open barrier that protects the bryozoan autozooids from predation or the impact of particles that affect their feeding activities, those kind of appendages are an example of phenotypic plasticity of some fenestellid bryozoans. The preservation of these relatively delicate structures is very rare in the fossil record, and hitherto were known only from several species of fenestrate bryozoans from the Carboniferous of Britain (Bancroft 1988) and Canada (Nelson and Bolton 1980). For the first time these palaeocorynid-type appendages are described from Mexico, and the reticulate form is recorded for the first time outside of Britain.

ACKNOWLEDGEMENTS

REFERENCES

ALLMAN, G.J. 1872. *A monograph of the gymnoblastic or tubularian Hydroids: the genera and species of the Gymnoblasta. Part II.* Ray Society.

BANCROFT, A. 1988. Palaeocorynid-type appendages in Upper Palaeozoic fenestellid Bryozoa. *Palaeontology* **31**, 665–675.

BAYER, M.M., TODD, C.D., HOYLE, J.E. AND WILSON, J.F. 1997. Wave–related abrasion induces formation of extended spines in a marine bryozoan. *Proceedings of the Royal Society of London. Series B: Biological Sciences* **264**(1388), 1605–1611.

CASTILLO-ESPINOZA, K. 2013. *Sistemática de braquiópodos, cefalópodos y crinoideos del Misisípico Medio de la Formación Santiago, Santiago Ixtaltepec. Oaxaca.* Tesis de Maestría, Mexico City, Universidad Nacional Autónoma de México, 119 p.

DUNCAN, P.M. 1873. On the genus *Palaeocoryne*, Duncan & Jenkins, and its affinities. *Quarterly Journal of the Geological Society* **29**, 412–417.

DUNCAN, P.M. AND JENKINS, H.M. 1869. On *Palaeocoryne*, a genus of tubularine Hydrozoa from the Carboniferous Formation. *Philosophical Transactions of the Royal Society of London*, **159**, 693–699.

ELIAS, M.K. AND CONDRA, G.E. 1957. *Fenestella* from the Permian of West Texas. *Memoirs of the Geological Society of America* **70**, 1–158.

ERNST, A., 2013. Diversity dynamics and evolutionary patterns of Devonian Bryozoa. *Palaeobiodiversity and Palaeoenvironments* **93**, 45–63.

FERGUSON, J. 1961. *Claviradix*, a new genus of the Family Palaeocorynidae from the Carboniferous rocks of County Durham. *Proceedings of the Yorkshire Geological Society* **33**, 135–148.

FERGUSON, J. 1963. British Carboniferous Palaeocorynidae. *Transactions of the Natural History Society of Northumbria* **14**, 141–162.

GILBERT, S.F. 2012. Ecological developmental biology: environmental signals for normal animal development. *Evolution & Development* **14**, 20–28.

HARVELL, C. D. 1984. Predator-induced defense in a marine bryozoan. *Science* **224**(4655), 1357–1359.

LINDQUIST, N. AND HAY, M.E. 1996. Palatability and chemical defense of marine invertebrate larvae. *Ecological Monographs* **66**, 431–450.

MCKINNEY, F.K., TAYLOR, P.D. AND LIDGARD, S. 2003. Predation on bryozoans and its reflection in the fossil record. In: P.H. Kelley, M. Kowaleski & T.A. Hansen (eds.), *Predator-prey interactions in the Fossil Record*. New York, Kluwer Academic/Plenum Publishers, pp. 239–261.

MCKINNEY, F.K. AND WYSE JACKSON, P.N. 2015. Part G, revised, Volume 2, Chapter 8A: Order Fenestrata: morphology and growth. *Treatise Online* **66**, 1–91.

NAVARRO-SANTILLÁN, D., SOUR-TOVAR, F. AND CENTENO-GARCÍA, E. 2002. Lower Mississippian (Osagean) brachiopods from the Santiago Formation, Oaxaca, Mexico: Stratigraphic and tectonic implications. *Journal of South American Earth Sciences* **15**, 327–336.

NELSON, S.J. AND BOLTON, T.E. 1980. *Macgowanella* gen. nov., possible bryozoan holdfasts, Mississippian of southern Canadian Rocky Mountains, Alberta. *Canadian Journal of Earth Sciences* **17**(10), 1431–1435.

QUIROZ-BARROSO, S.A., POJETA, J., JR., SOUR-TOVAR, F. AND MORALES-SOTO, S. 2000. *Pseudomulceodens*: a Mississippian Rostroconch from Mexico. *Journal of Paleontology* **74**, 1184–1186.

ROBISON, R.A. AND PANTOJA-ALOR, J. 1968. Tremadocian trilobites from the Nochixtlán region, Oaxaca, Mexico. *Journal of Paleontology* **42**, 767–800.

SUÁREZ ANDRÉS, J.L. AND WYSE JACKSON, P.N. 2015. Feeding currents: a limiting factor for disparity of Palaeozoic fenestrate bryozoans. *Palaeogeography, Palaeoclimatology, Palaeoecology* **433**, 219–232.

TAYLOR, P.D. 2005. Bryozoans and palaeoenvironmental interpretation. *Journal of the Palaeontological Society of India* **50**, 1–11.

TORRES-MARTÍNEZ, M.A. AND SOUR-TOVAR, F. 2016a. Braquiópodos discínidos (Lingulida, Discinoidea) de la Formación Ixtaltepec, Carbonífero del área de Santiago Ixtaltepec, Oaxaca. *Boletín de la Sociedad Geológica Mexicana* **68**, 313–321.

TORRES-MARTÍNEZ, M.A. AND SOUR-TOVAR, F. 2016b. New Productide Brachiopods (Productoidea) from the Carboniferous of Ixtaltepec Formation, Oaxaca, Mexico. *Journal of Paleontology* **90**, 418–432.

VINE, G.R. 1879a. Physiological character of *Fenestella*. *Hardwicke´s Science Gossip* **15**, 50–54.

VINE, G.R. 1879b. On *Palaeocoryne*, and the development of *Fenestella*. *Hardwicke´s Science Gossip* **15**, 225–229, 247–249.

WEST-EBERHARD, M.J. 2003. *Developmental Plasticity and Evolution*. Oxford University Press, New York.

YANCEY, T.E., WYSE JACKSON, P.N., SUTTON, B.G. AND GOTTFRIED, R.J. 2019. Evactinoporidae, a new family of Cystoporata (Bryozoa) from the Mississippian of North America: growth and functional morphology. *Journal of Paleontology* **93**, 1058–1074.

YOUNG, J. AND YOUNG, J. 1874. On *Palaeocoryne* and other polyzoal appendages. *Quarterly Journal of the Geological Society* **30**, 684–689.

Euthyriselloidea and Mamilloporoidea – expanded superfamily concepts based on the recognition of new families

Dennis P. Gordon[1*] and JoAnn Sanner[2]

[1] National Institute of Water & Atmospheric Research, Private Bag 14901 Kilbirnie, Wellington, New Zealand
[*corresponding author: email: dennis.gordon@niwa.co.nz]
[2] Department of Paleobiology, National Museum of Natural History,
Smithsonian Institution, Washington, DC 20650, USA

ABSTRACT

Current knowledge of the cheilostome superfamily Euthyriselloidea Bassler, 1953 is that it is mono-familial, has a restricted Indo-West Pacific–Australasian geographic range and no known fossils. Here we report that the discoidal North American Eocene fossil, *Schizorthosecos radiatum* Canu and Bassler, 1920 represents not only a new taxon (*Clathrolunula* gen. nov.) unrelated to the type species of *Schizorthosecos* Canu and Bassler, 1917, but constitutes the earliest record of Euthyriselloidea, differing from the five nominally included genera in colony form. Currently unplaced as to family, *Schizorthosecos* Canu and Bassler, 1917 includes four nominal species. Of these, the type species, *S. interstitia* (Lee, 1833), differs markedly from *S. radiatum* Canu and Bassler, 1920, which has a radiate suboral process ('radiate bar'), associated with a subfrontal hypostegal coelom in life, almost identical to that in the erect, branching euthyrisellid genus *Pseudoplatyglena* Gordon and d'Hondt, 1997. Clathrolunulidae fam. nov. is created for *Clathrolunula* and *Pseudoplatyglena* and a new family of Mamilloporoidea, Schizorthosecidae, is established for *Schizorthosecos* and *Stenosipora* Canu and Bassler, 1927. Neoeuthyrididae fam. nov. is included in Euthyriselloidea, which now comprises three families. The origin of Euthyriselloidea is discussed in relation to Cook's (1975) comparison of the frontal shield of *Tropidozoum* and the foraminate cryptocyst in the cupuladriid genus *Discoporella*. *De novo* evolution of an ascus by intussusception is inferred in the earliest euthyrisellid or its immediate ancestor.

INTRODUCTION

D'Hondt (1985) established the superfamily Euthyriselloidea solely for Euthyrisellidae Bassler, 1953 [posthumously and independently also named by Harmer (1957)], which currently has four included genera – *Pleurotoichus* Levinsen, 1909, *Euthyrisella* Bassler, 1936, *Tropidozoum* Harmer, 1957 and *Pseudoplatyglena* Gordon and d'Hondt, 1997. All have erect, rooted colonies in which the calcified walls are interior and have generally limited contact with the investing extrazooidal cuticle (Cook and Chimonides 1981; Cook *et al.* 2018). External ovicells and avicularia are lacking. *Tropidozoum* has two species; the others are monospecific. Whereas *Euthyrisella* and *Pleurotoichus* are characterised by colonies that are branching and somewhat flustrine, colonies in *Tropidozoum* and *Pseudoplatyglena* are cellariiform, being jointed. One other genus – *Neoeuthyris* Bretnall,

1921 – has been included in the Euthyrisellidae in the past (Cook and Chimonides 1981). As in *Euthyrisella*, the frontal shield has processes that can abut against the outer membranous epitheca and, while also lacking areolar-septular pores, the hypostegal coelom communicates physiologically with the proximal zooid via rosette pores in the transverse wall. The sole species of *Neoeuthyris* is encrusting, however, lacks a basal coelom and has avicularia. Cook *et al*. (2018) suggested separation as a monogeneric family but did not formally establish it.

One unique feature of Euthyrisellidae is the presence of a subfrontal hypostegal coelom, comprising an extension of the frontal hypostegal coelom (or part of it) beneath the calcified frontal shield. This coelomic extension appears in *Euthyrisella* as a small transverse expansion proximal to the orifice. Small pores in the distal part of the shield, plus mural septular pores, allow communication between the hypostegal coelom and its laterobasal expansion. In *Pleurotoichus* and *Tropidozoum*, on the other hand, the subfrontal hypostegal coelom is much more extensive, occurring beneath the entire frontal shield with openings in shield calcification connecting the frontal and subfrontal parts of the coelom. Unlike most ascophoran frontal shields, there are no marginal areolar-septular pores in these two genera to allow physiological communication between the hypostegal/subhypostegal coelom and visceral coelom. Whereas interzooidal communication pores high in the distal zooid wall in *Euthyroides* and *Pleurotoichus* communicate with the hypostegal coelom of the distal zooid, this arrangement is lacking in *Tropidozoum*; here, the hypostegal coelom and its basal expansion appear to be completely isolated from the visceral coelom.

In *Pseudoplatyglena*, the subfrontal hypostegal coelom is strikingly different from that in the other genera. The proximal margin of the orifice is defined by a crescentic bar that inserts at each proximolateral corner beside the condyles. It is also connected to the distal rim of the frontal shield by four radiating struts. The whole apparatus is covered by a cuticular epitheca in life and the space underneath it constitutes a moderately capacious subfrontal hypostegal coelom. However, in contrast to the other euthyrisellid genera, the hypostegal coelom associated with the radiate bar seems to be disconnected from the frontal hypostegal coelom, which, also contrasting with the other genera, communicates physiologically with an axial coelom via analogues of marginal areolar-septular pores. The basal walls of the autozooids are interior and surround the axial coelom.

When first described, the radiate bar in *P. mirabilis* appeared unique in Cheilostomata. Here we describe a seemingly homologous structure in the fossil discoidal species *Schizorthosecos radiatum*, which differs from the type species of *Schizorthosecos*, *S. interstitia* (Lea, 1833), in several important features. We redescribe *S. radiatum* as the type of a new genus and family of Euthyriselloidea. In comparing its features, we also discuss the status of *Neoeuthyris*, erecting a new family for it as a third family of Euthyriselloidea. We also suggest an evolutionary scenario for Euthyriselloidea. In discussing the relationships of *Schizorthosecos sensu stricto*, we erect a new family of Mamilloporoidea for it and *Stenosipora* Canu and Bassler, 1927.

MATERIAL AND METHODS

Where appropriate, living and fossil specimens described herein were cleaned by bleach (aqueous sodium hypochlorite) of any organic material or adherent debris and thoroughly washed before drying under a heat lamp. Scanning electron microscopy of type material was carried out at the Smithsonian National Museum of Natural History, Washington, D.C., USA, using a FEI (Field Electron and Ion Company) SEM at 15 kV (material uncoated). Additional material was examined by a Philips SEM at the Institute of Geological and Nuclear Sciences, Lower Hutt, New Zealand, and Hitachi TM3000 Tabletop SEM at the National Institute of Water and Atmospheric Research, Wellington, New Zealand (material sputter-coated with Au-Pd).

Measurements were made directly from SEM images using Fiji [(Fiji Is Just) ImageJ], an open-

source image-processing package based on ImageJ (Schindelin *et al*. 2012).

Repositories of examined specimens: MNHN = Muséum National d'Histoire Naturelle, Paris; NIWA = National Institute of Water and Atmospheric Research, Wellington; USNM = United States National Museum, i.e. Smithsonian National Museum of Natural History, Washington, D.C. Morphological abbreviations: ZL, ZW = length and width of limited area of zooid visible at colony surface; ZD = vertical depth of zooid including peristome; OL, OW = orifice length and width; FAvL, FAvW = length and width of frontal avicularium/heterozooid; AAvL, AAvW = length and width of avicularium on abfrontal colony surface; OvL, OvW, length and width of ovicell; KL, KW, length and width of abfrontal cancellate kenozooid; KD = depth (thickness) of cancellate kenozooid; RD = diameter of funnel-shaped rootlet pore in abfrontal colony surface. Measurements are in micrometres, given in the text as range, followed by mean and standard deviation in parentheses. N = 15 for all measurements except where otherwise indicated in text.

SYSTEMATICS

Superfamily Euthyriselloidea Bassler, 1936

Diagnosis: Encrusting, discoidal or erect. Interior-walled frontal shield with lepralioid ascus. Hypostegal coelom typically not in communication with visceral coelom of same zooid via frontal septular pores, but with proximal zooid via transverse wall and/or laterobasal or basal coelom. Hypostegal coelom with subfrontal extension in some taxa. No hyperstomial ovicells; internal brooding in brood sac in unmodified zooids or in dimorphic zooids with vestigial or endozooidal ooecium. Avicularia present or absent.

Family Clathrolunulidae n. fam.

Diagnosis: Colony discoidal and cupuliform with exterior basal walls, or erect and cellariiform with interior basal walls abutting an axial coelom. If discoidal, zooids vertically to obliquely erect, radiating from colony centre in linear series and frontal surface of zooids much reduced. Orifice with rounded antral part separated from poster by rounded condyles. Proximal orificial rim defined by broadly transverse bar, the proximal side of which has 3–5 struts radiating toward a very narrow area of frontal shield proximally. Hypostegal coelom of this suboral area discontinuous with rest of frontal shield and with subhypostegal extension. Frontal shield flanked by marginal pores; these communicating with visceral coelom in discoidal colonies but with axial coelom in cellariiform colonies. A pair of round heterozooids distolateral to orifice in discoidal form only. No oral spines. No ovicells.

Type Genus: *Clathrolunula* nov.

Stratigraphic Range: Middle Eocene (North America) to Recent (New Caledonia).

Remarks: The suboral radiate bar in *Clathrolunula* n. gen. is so similar to that in *Pseudoplatyglena mirabilis* Gordon and d'Hondt, 1997 that we are compelled to take the parsimonious view that the two taxa are more closely related to one another than either is to core Euthyriselloidea (i.e. Euthyrisellidae). Not only do they share the radiate suboral bar, but its associated hypostegal coelom (and subfrontal extension) are disconnected from the hypostegal coelom of the remainder of the frontal shield. Additionally, both genera have interzooidal pores (analogous to areolar-septular pores but probably not homologous with them – see discussion) that are not found in Euthyrisellidae. Further, no external evidence of brooding (neither ovicells nor dimorphic zooids) has yet been found in either genus. Accordingly, we unite the two genera in one new family, each in its own subfamily owing to the very different colony form. Our interim hypothesis is that the foraminate part of the frontal shield in an ancestral form (colony type uncertain) became reduced to a radiate suboral bar, the coelom of which became discontinuous with that of the rest of the frontal shield.

Subfamily Clathrolunulinae n. subfam.

Diagnosis: Colony discoidal and cupuliform with exterior basal walls. Zooids vertically to obliquely erect, radiating from colony centre in linear series and frontal surface of zooids much reduced. Orifice with rounded antral part separated from poster by rounded condyles. Proximal orificial rim defined by broadly transverse bar, the proximal side of which has 3–5 struts radiating toward a very narrow area of frontal shield proximally. Hypostegal coelom of this suboral area discontinuous with rest of frontal shield and with subhypostegal extension. Frontal shield very small, lateral to orifice and/or with small proximal area, flanked by marginal pores communicating with visceral coelom. A pair of round heterozooids distolateral to orifice. No oral spines. No ovicells. Interzooidal communication pores simple, occurring in a horizontal row low on transverse and lateral walls just above junction with basal wall.

Type Genus: *Clathrolunula* nov.

Stratigraphic Range: Middle Eocene, Lutetian–Bartonian, North America.

Remarks: The family is monogeneric and monospecific (see below) and therefore known only from the Eocene North American localities where the type species is found.

Genus *Clathrolunula* nov.

Type Species: *Schizorthosecos radiatum* Canu and Bassler, 1920, Gosport Sand and Lisbon Formation, Alabama, Middle Eocene (Lutetian–Bartonian) [see Bybell and Gibson (1985) for stratigraphic age]. Also Jackson, Mississippi, Late Eocene (Priabonian).

Etymology: Latin *clathrum*, lattice, grate + *lunula*, crescent, alluding to the radiate bar separating frontal and subfrontal parts of the hypostegal coelom. Gender feminine.

Diagnosis: Characters as for family.

Remarks: The genus is monospecific. It differs from the type species of *Schizorthosecos* in several important respects (Table 1), including having exterior-walled basal zooidal surfaces instead of porous interior-walled sectors, and lacking obvious cavities for the emergence of rootlets in life. *Schizorthosecos interstitia* also has ovicells and adventitious avicularia with pivot bars. Moreover, the most notable zooidal morphological feature in *C. radiata* is the presence of a suboral radiate bar nearly identical to that found in the euthyrisellid genus *Pseudoplatyglena*. Its structure is consistent with the existence of a subfrontal hypostegal coelom in life, a character found elsewhere only in the superfamily Euthyriselloidea.

Clathrolunula radiata (Canu and Bassler, 1920
Fig. 1 A–F, Table 1

Schizorthosecos radiatum Canu and Bassler, 1920: p. 628, pl. 18, figs 16–19.

Material Examined: USNM 63864A–C (syntypes), Gosport Sand, Middle Eocene, Alabama. Also NIWA 128750, based on previously unregistered topotypic material donated by R.S. Bassler to G.H. Uttley, now in collection of NIWA, Wellington.

Description: Colony discoidal, weakly cupuliform, small, up to 2.6 mm diameter and 0.7 mm height. Zooids radiating from colony centre in linear series (Fig. 1, A); vertically erect in colony centre, with orifices facing frontally, becoming somewhat more oblique towards margin where orifices are more angled toward periphery. Zooid depth shortest in colony centre, lengthening toward periphery: ZD = 303–463 (396, 46.192).

Frontal surface of zooids much reduced but having normal centrifugal orientation of orifice distad toward colony periphery. Orifice with circular antral part separated from broad shallow poster by narrow, rounded condyle-like projections that taper
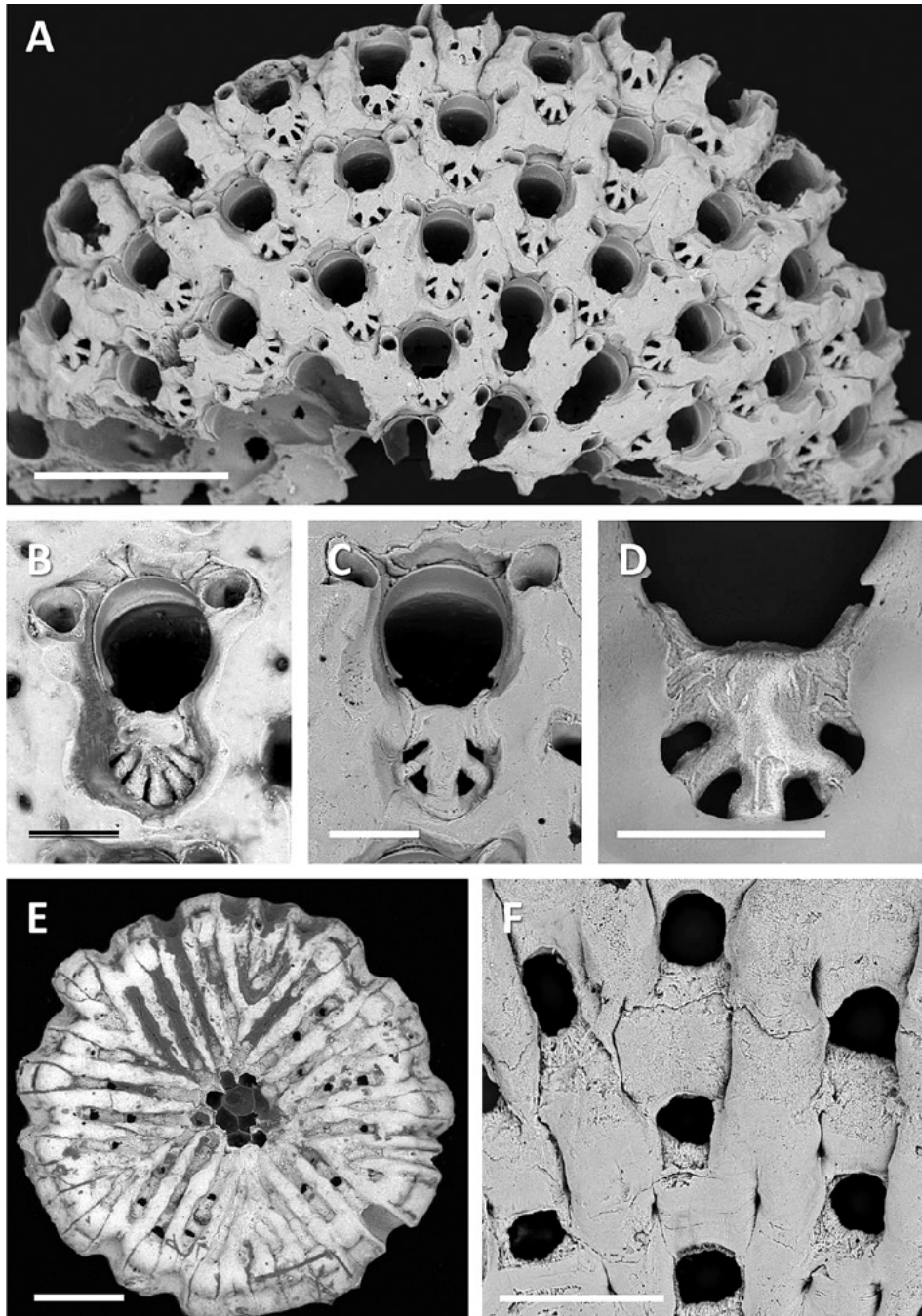
Figure 1 (A–F) *Clathrolunula radiata* (Canu and Bassler, 1920)
(A, C, D: NIWA 128750; B: USNM 63864A; E, F: USNM 63864B).
(A) Frontal view of half a discoidal colony; (B, C). Frontal view of suboral radiate bars with, respectively six
and four radial slits. Note the paired distolateral heterozooids and reduced frontal shield either side
of the orificial region; (D) Abfrontal view of suboral radiate bar with four slits;
(E) Exterior-walled basal surface of colony. Thick white radial series, some bifurcating,
are the fused laterobasal walls of adjacent zooid rows; (F) Part of basal surface showing uncalcified
areas of distobasal wall, typically one such hole per zooid, sometimes lacking or occluded.
Scale bars: A, E, 500 µm; B–D, 100 µm; F, 500 µm.

into sides of anter. Anter with narrow distal-oral ledge at lower level. Poster broad and wide, its proximal rim defined by a radiate bar, comprising a broad transverse bar, the proximal side of which has 3–5 struts and 4–6 slit-like or triangular lacunae (Fig. 1, B–D) radiating toward a very narrow area of frontal shield proximally; in life, the area under the radiate bar constituting a subhypostegal coelom. OL = 110–149 (137, 10.443), OW = 93–127 (117, 9.185). No oral spines.

Frontal shield (Fig. 1, A–C) short, its surface smooth and weakly undulating, slightly raised above level of orifice and radiating suborificial apparatus, but no actual peristome; shield widest on either side of oral-suboral area, each part with 1–3 round, sunken areolar-septular pores. Frontal ZL (measured orifice to orifice) 243–298 (271, 12.715); frontal ZW less than ZL, greatest distal to orifice at level of heterozooids: 179–238 (212, 17.534). A pair of circular or subrounded heterozooids (avicularia?) distolateral to orifice (Fig. 1 B, C).

These with smooth thin rims and no hint of condyles. FAvL = 38–52 (45, 4.137), FAvW = 38–53 (45, 4.512).

Basal surface (Fig. 1, E) exterior-walled. Each linear zooidal series recognisable by paired, slightly convex, thickened laterobasal wall surfaces. These are conspicuous, radiating in more or less straight lines from centre to periphery, sometimes Y-shaped where they diverge at bifurcation of zooid rows, which occurs as colony increases in diameter. These paired laterobasal wall surfaces separated by shallower mediobasal walls of successive zooids, also in linear series. Mediobasal wall of each zooid bipartite, comprising a thinner depressed proximal part and slightly bulging thicker distal part, the thinner part mostly missing (Fig. 1, F) and appearing as an opening. The size and shape of these openings varies.

Interzooidal communication pores simple, occurring in a horizontal row low on transverse and lateral walls just above junction with basal

Table 1. Morphological characters of *Schizorthosecos* (Mamilloporoidea) and the genera of a revised Euthyriselloidea.

Taxon	Colony form	Gaps in frontal shield allowing hypostegal/ subhypostegal continuity	Incubation of embryo	Avicularia	Hypostegal coelom	Subhypostegal coelom	Areolar pores	Visceral-hypostegal communication
Euthyrisella obtecta Euthyrisellidae	erect, flustrine, branching	few, tiny	ovisac in dimorphic zooids	absent	present	present	absent	via distal transverse wall
Pleurotoichus clathratus Euthyrisellidae	erect, flustrine, branching	extensive, linear	ovisac in dimorphic zooids	absent	present	present	absent	via distal transverse wall
Tropidozoum cellariiforme Euthyrisellidae	erect, cellariiform	numerous foramina	ovisac in dimorphic zooids	absent	present	present	absent	absent
Pseudoplatyglena mirabilis Clathrolunulidae	erect, cellariiform	either side of radiate bar only	unknown	absent	present	present	present	via areolar-septular pores
Neoeuthyris woosteri Neoeuthyrididae	encrusting	subhypostegal coelom absent	endozooidal ovicells	adventitious	present	absent	absent	via distal transverse wall
Clathrolunula radiata Clathrolunulidae	cupuliform	either side of radiate bar only	unknown	adventtious heterozooids (avicularia?)	present	present	present	via areolar-septular pores
Schizorthosecos interstitia Schizorthosecidae	cupuliform, rooted	subhypostegal coelom absent	in ovicells	adventitious	present	absent	present	via areolar-septular pores

wall. Ancestrula not clearly seen; shape of occluded orifice of centremost zooid at colony apex like that of other zooids, indicating that ancestrula probably resembled later zooids.

Remarks: There is no certain evidence that colonies of *Clathrolunula radiata* had anchoring rootlets. Holes in thinner parts of basal walls are somewhat inconstant in size and shape, but many are suggestive of foramina from which rootlets might have emerged, not as kenozooids but as zooidal extensions. Comparison of the morphological differences between *C. radiata* and *Schizorthosecos interstitia* (Table 1 and further below) shows that the two taxa cannot be confamilial.

Subfamily Pseudoplatygleninae n. subfam.

Diagnosis: Colony erect and cellariiform with interior basal walls abutting an axial coelom. Orifice with rounded antral part separated from poster by rounded condyles. Proximal orificial rim defined by broadly transverse bar, the proximal side of which has 3–5 struts radiating toward a very narrow area of frontal shield proximally. Hypostegal coelom of this suboral area discontinuous with rest of frontal shield and with subhypostegal extension. Frontal shield flanked by marginal pores; these communicating with axial coelom. No oral spines. No ovicells.

Type Genus: *Pseudoplatyglena* Gordon and d'Hondt, 1997.

Stratigraphic Range: Recent (New Caledonia).

Remarks: As explained above, the radiate suboral bar in *Clathrolunula radiata* (Fig. 1, A–D) and *Pseudoplatyglena mirabilis* (Fig. 2, A, B) are virtually identical in structure. Other shared characters are the bipartite division of the suboral and frontal parts of the hypostegal coelom (Figs 1, B–D, 2, B, C) and the presence of marginal communication pores. The most parsimonious hypothesis is that the two genera are more closely related to each other than to core Euthyrisellidae.

In describing *P. mirabilis*, Gordon and d'Hondt (1997) failed to note the axial coelom. It is evident in apical views of a branch bifurcation (Fig. 2, B), but in a stem cross section lower in an internode it was not apparent and it seems it may become obliterated (or nearly so) by secondary calcification of laterobasal walls. Re-examination of scanning electron micrographs of *P. mirabilis* show that the interzooidal pores do not communicate with zooidal visceral coeloms but with the axial coelom that abuts on basal walls that are fundamentally interior. In this respect too, *Pseudoplatyglena* differs from *Clathrolunula* n. gen. in that the latter has an exterior-walled basal surface and the marginal pores do communicate with zooidal visceral coeloms.

One other new family can be added to Euthyriselloidea. In a key and diagnoses of the genera of Euthyrisellidae, Cook and Chimonides (1981, p. 60) observed that embryos had been observed in all species, noting that they filled "the central and proximal parts of the cystid and are presumably contained in ovisacs". Strictly, however, while *Neoeuthyris* also has dimorphic orifices, it differs from the other genera in having actual ovicells, as well as avicularia, is encrusting and lacks a basal coelom. As noted above, Cook *et al.* (2018) suggested that *Neoeuthyris* could be accorded its own family. That suggestion is followed here.

Family Neoeuthyrididae nov.

Diagnosis: Colony encrusting, basal wall centrally uncalcified, closely adherent to substratum without intervening coelom. Frontal shield hyaline, thinly calcified, smooth with occasional protuberances. No visceral-to-hypostegal communication via marginal areolar septular pores in frontal shield; instead, hypostegal coelom, which is proximally deep, communicates with proximal zooid via multiporous septulum in transverse wall. Subfrontal hypostegal coelom lacking. Frontal adventitious avicularium occasional, latero-oral, with complete pivot bar. Female zooids with dimorphic orifice and brood chamber comprising large endozooidal ovicell, closed by zooidal operculum.
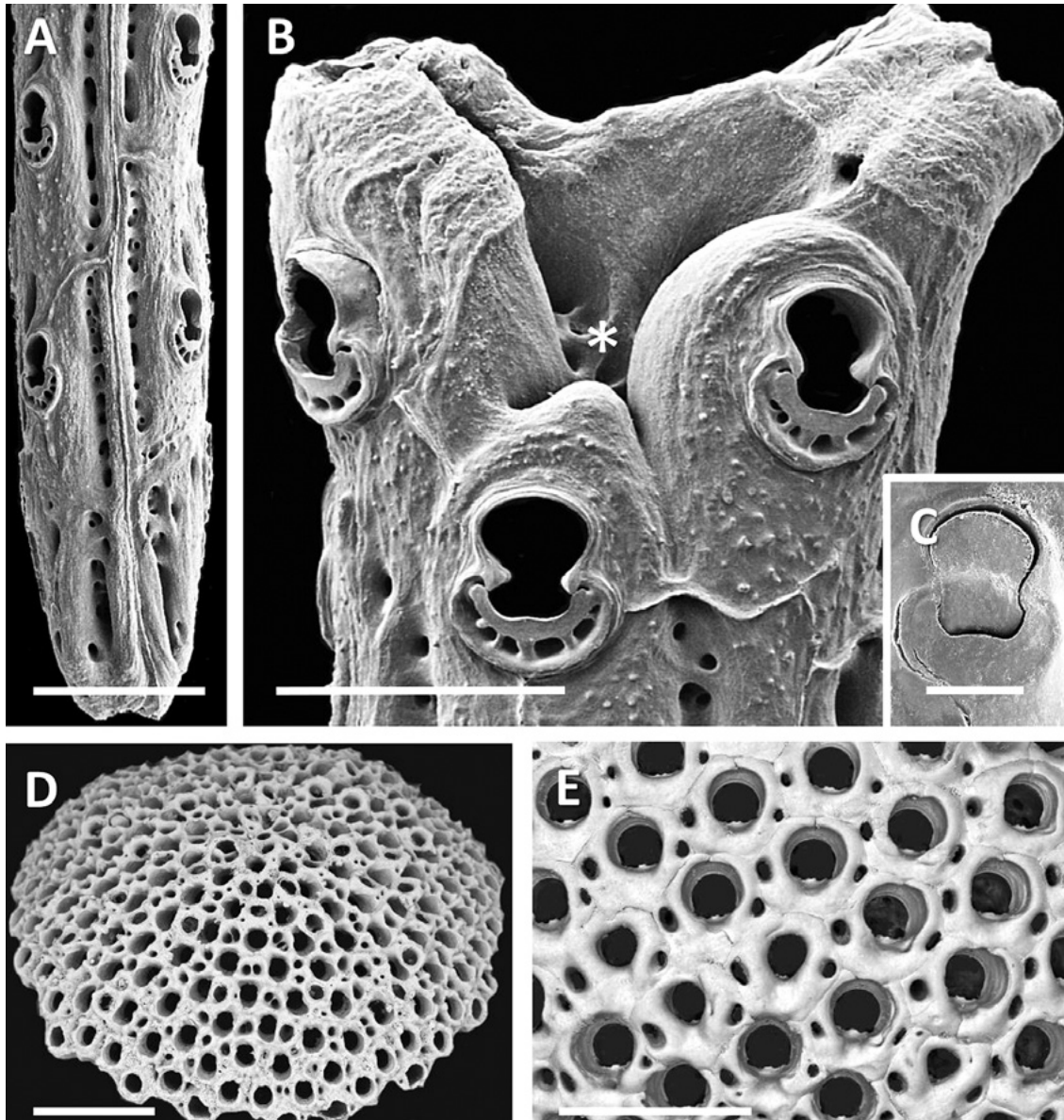
Figure 2. (A–C) *Pseudoplatyglena mirabilis* Gordon and d'Hondt, 1997 (MNHM-Bry 19962).
(A) Abfrontal part of branch internode showing a median strip of calcification flanked by furrowed pores
that connect the zooidal hypostegal coelom with the internal coelom of the internode;
(B) distal end of an internode showing an incipient branch bifurcation. An asterisk indicates the axial coelom,
extensive at this point. Note the radiate suboral bars proximal to autozooidal orifices;
(C) Orificial region, showing an operculum distal to the broadly crescentic area of membranous
frontal wall covering the suboral radiate bar that separates its associated hypostegal
coelom into frontal and subfrontal components; the frontal component is cut
off by a crescentic ridge from the rest of the zooidal frontal hypostegal coelom.
(D, E) *Schizorthosecos interstitia* (Lea, 1833) (D: NIWA 128749; E, USNM 62609J);
(D) Laterofrontal view of a whole colony;
(E) Frontal view of quincuncially arranged zooidal orifices, each surrounded by a limited area of frontal shield
and flanked by conspicuous areolar-septular pores that communicate with the visceral coelom.
Scale bars: A, 500 μm; B, 300 μm; C, 100 μm; D, 1000 μm; E, 400 μm.

Type Genus: *Neoeuthyris* Bretnall, 1921.

Stratigraphic and Geographic Range: Recent, Western Australia and Queensland, Australia.

Remarks: The diagnosis of the sole genus is as for the family. Although *Neoeuthyris* appears to have a different brooding structure, Harmer (1902, p. 270) noted that the distal zooidal wall in the dimorphic zooids of *Pleurotoichus clathratus* is separate from the proximal zooidal wall of the distal zooid, commenting, "This suggests that the B-zooecia possess a vestigial ovicell". He observed a similar double wall in *Tropidozoum cellariiforme* (Harmer 1957, pl. 67, fig. 17), likewise interpreting it as a vestigial ovicell and describing (p. 1107) "a large egg or embryo enclosed in an ovisac". If this is the case, then using the terminology of Cook and Chimonides (1981), the presumed "ovisac" in core Euthyrisellidae might be homologous with the "endozooidal ovicell" in Neoeuthyrididae. Cook and Chimonides (1981, p. 68) described the reproductive structure in *Neoeuthyris* thus: "ovicell apparently formed by an expansion of the lateral and distal walls, protruding into the cavity of the next zooid"; this needs clarification. Importantly, *Neoeuthyris* has in common with *Euthyrisella* not only dimorphic zooids but visceral-to-hypostegal communication via the proximal transverse wall, which supports inclusion in the Euthyriselloidea.

Superfamily Mamilloporoidea Canu and Bassler, 1927

Family Schizorthosecidae n. fam.

Diagnosis: Colony discoidal and cupuliform. Zooids vertically to obliquely erect, radiating from colony centre. Frontal surface of zooids much reduced. Orifice with round anter separated from smaller broad shallow poster by tiny condyles. Proximal orificial rim transversely sinuous to broadly U-shaped. Frontal shield short and broad, merging with peristome, imperforate. No oral spines. One to two pairs of areolar-septular pores flanking orifice. One or a pair of adventitious avicularia in distolateral position or lacking, with pivot bars. Ovicell hyperstomial, the visible skeletal layer imperforate. Basal surface comprising a layer of cancellate hexagonal sectors, one per zooid, each with interior basal wall; additionally with or without avicularia and 1–3 funnel-shaped loci for rootlets. Interzooidal communication pores simple, occurring in a horizontal row low on transverse and lateral walls just above junction with basal wall; additional pores in basal wall connecting with cancelli. Ancestrula apical.

Type Genus: *Schizorthosecos* Canu and Bassler, 1917.

Stratigraphic Range: Mid–Late Eocene, Lutetian–Priabonian, North America and Europe.

Remarks: When first introduced, *Schizorthosecos* was included in the Conescharellinidae, but this family comprises taxa with what is usually referred to as reversed frontal budding (Cook and Lagaaij 1976). Subsequently, Bassler (1935, 1953) included it in the Orbituliporidae, but, like *Conescharellina*, *Orbitulipora* is also characterised by reversed frontal budding and the erect colony is bilaterally compressed with a single adapical rootlet pit (Bock and Cook 2004). Cook and Chimonides (1994) discussed *Schizorthosecos* in the context of Mamilloporidae, stating: "*S. interstitia* … has radially budded colonies, with hyperstomial ovicells, and large basal cavities and avicularia like those of *Mamillopora*. However, the ovicells have paired entooecial areas frontally, and *S. radiatum* ... has autozooids with a small, costate suboral shield. It seems unlikely, therefore, that *Schizorthosecos* is a member of the Mamilloporidae." It is unclear what is meant by "large basal cavities". The abfrontal side of the type species of Mamilloporidae, *Mamillopora cupula* Smitt, 1873 is a single deep concavity lined by an irregular layer of blister-like kenozooids – 'bladders' in Smitt (1873), 'bubble-like' in Winston (2005) – with walls

in which are 1–2 tiny pores. Some of the kenozooids have small avicularian cystids ['calcified tubes' in Winston (2005)], evidenced by the tiny mandibular pivots in some. The kenozooidal walls appear to be exterior in Winston's (2005) micrographs, as also in *Mamillopora cavernulosa* Canu and Bassler, 1928 [see https://fossils.its.uiowa.edu/database/bryozoa/systemat/mamcav.htm (NMiTA)], but in the related genus *Anoteropora* Canu and Bassler, 1927, the abfrontal colony surface is composed of autozooidal basal walls and these are interior, with rootlets originating from laterobasal septula resembling pore-chambers (Cook and Chimonides 1994). In either case, the abfrontal colony surface of core Mamilloporidae (i.e. *Mamillopora*, *Anoteropora*) is not made up of thick cancellate sectors [presumably kenozooidal by analogy with a similar basal layer in *Conescharellina* (see Bock and Cook 2004)] as in *Schizorthosecos*. Additionally, core Mamilloporidae have dimorphic female zooids with large orifices and ovicells with a densely porous skeletal layer (endooecium?). The ooecium is formed by the distal kenozooid (Ostrovsky 2013). In spite of the differences between Schizorthosecidae nov. and Mamilloporidae, there are enough morphological characters in common (especially colony and zooid form and orificial characters) to include the former in Mamilloporoidea.

We also include in Schizorthosecidae nov. the genus *Stenosipora* Canu and Bassler, 1927. Although this genus is generally included in the Mamilloporidae, it has more in common with *Schizorthosecos*, viz imperforate ooecia, no sexual dimorphism, and a basal layer of cancellate sectors, each corresponding with the autozooid that budded it. These presumed kenozooids are well depicted in the original line drawings of the type species, *Stenosipora protecta* (Koschinsky, 1885), but not, unfortunately in published SEM images. Antolini *et al*. (1980) [photographs duplicated by Braga (2008)], show by SEM the frontal colony surface, which appears to be granular, not smooth. Autozooids are in quincunx, with the small area of frontal shield slightly elevated proximally, sloping inwards to the orifice, which is

longer than wide and nearly cleithridiate; the paired lateral-oral avicularia have pivot bars.

Genus *Schizorthosecos* Canu and Bassler, 1917

Type Species: *Orbitoloides interstitia* Lea, 1833, several localities in Alabama, Mississippi and Georgia, Middle–Late Eocene (Lutetian–Priabonian) [see Bybell and Gibson (1985) for stratigraphic age].

Diagnosis: Orifice with large round anter; proximal orificial rim transversely sinuous to U-shaped. A single adventitious avicularium adjacent to orifice or lacking. Basal surface of cancellate hexagonal sectors thickening with age; basal avicularia present or absent and 1–3 funnel-shaped loci for rootlets. Other characters as for family.

Remarks: The genus nominally comprises two additional species–*Schizorthosecos grandiporosum* Canu and Bassler, 1920 (Alabama and Mississippi, Lutetian–Priabonian) and *Schizorthosecos danvillensis* McGuirt, 1941 (Louisiana, Priabonian).

Schizorthosecos interstitia (Lea, 1833)
Fig. 2, D, E; Fig. 3, A, C, D, E), Table 1

Orbitolites interstitia Lea, 1833: p. 191, pl. 6, fig. 204.
Lunulites interstitia: Gabb and Horn 1862: p. 120.
Lunulites (*Cupularia*) *interstitia*: De Gregorio 1890: p. 249, pl. 42, figs 16–22.
Schizorthosecos interstitia: Canu and Bassler 1917: p. 75, pl. 6, figs 4, 5; Canu and Bassler 1920: p. 626, pl. 18, figs 1–9; McGuirt 1938: p. 139, pl. 28, figs 6, 7, 9, 10, pl. 29, figs 1, 2; McGuirt 1941: p. 99, pl. 28, figs 6, 7, 9, 10, pl. 29, figs 1, 2; Bassler 1953: p. 230, fig. 9; Cook and Chimonides 1994: p. 52.

Material Examined: USNM 62609A–N, syntype series, Gosport Sand, Jacksonian, Middle Eocene, Alabama. Also NIWA 128749, based on previously unregistered material donated by R.S. Bassler to G.H. Uttley, now in collection of NIWA, Wellington.

Description: Colony discoidal, weakly cupuliform (Fig. 2, D), up to 4.5 mm diameter and 1.2 mm height. Zooids arranged quincuncially; vertically erect in colony centre, with orifices facing frontally, becoming somewhat more oblique towards margin where orifices are more angled toward periphery. Zooid depth shortest in colony centre, lengthening toward periphery: ZD = 418–552 (489, 45.531), N = 11.

Frontal surface of zooids much reduced, averaging a little wider than long, with distinct hexagonal outline in best-preserved zooids prior to secondary calcification (Fig. 2, E); having normal centrifugal orientation of orifice toward colony periphery. Orifice nearly circular, averaging a little wider than long, proximal part truncated as broad shallow poster, its proximal margin sinuous with slight median convexity (Fig. 3, E); tiny rounded condyles tapering into sides of anter. OL = 98–110 (106, 3.477), OW = 98–112 (106, 4.063). No oral spines.

Frontal shield proportionately short and wide (Figs 2, E; 3, E), continuous with smooth even peristome that surrounds orifice at same elevated level. A conspicuous subcircular to oval areolar septular pore on each side of the frontal adjacent to poster. Secondary calcification produces raised peristomial margins and elevation of parts of proximal shield, sometimes forming median furrow that slopes inward to primary orifice, with proximolateral corners of shield umbonate and areolar pore areas increasingly sunken. Frontal-shield furrow sometimes transverse instead of longitudinal. Elevated peristome and shield tending to become fused with that of adjacent zoids, forming continuous network of smooth convex ridges, these sometimes becoming tubercular. Adjacent areolar pores of zooids slightly offset owing to the quincuncial arrangement, can appear as radially paired holes in thicker colonies, with their cavities seemingly merging into elongate furrows. ZL = 212–256 (230, 14.044), ZW = 238–284 (266, 13.498).

Frontal heterozooids not evident in neanic colonies lacking obvious secondary calcification. Heterozooids occur in one ephebic colony with obvious secondary calcification (USNM62609-I) in the vicinity of the apex, and some of them are avicularian in form. These are subcircular with a distinct pivot bar made of a single element, and a proximal tranverse opesial foramen. The rostral part, with a distinct, evenly rounded rim, is larger than a semicircle, with a proportionately large palatal foramen and no distal palate. NIWA 128749 includes a colony with broken avicularian cystids between the apex and margin having been budded from deep areolar cavities. Mimicking the avicularia in USNM62609-I are slightly larger arrangements that look like modified autozooidal openings; across each opening is a paired trabecula that simulates an avicularian crossbar but which is not always straight and an actual rostral rim is lacking. Perhaps the bars represent a stage in closure of a non-functional orifice. In the oldest colonies (e.g. USNM62606-A) the apex has numerous non-functional former autozooidal orifices occluded by secondary calcification. FAvL = 78–357 (168, 99.266), FAvW = 78–225 (139, 51.298).

Ovicells rare, evident only in one mature colony fragment (USNM62609-H) with much secondary calcification and somewhat chaotic surface topography; hyperstomial (Fig. 3, D), the opening extending vertically above primary zooidal orifice. Skeletal surface endooecial(?), smooth, nodular, imperforate. OvL = 101–150 (123, 13.675), OvW 152–190 (170, 14.728).

Abfrontal colony surface almost wholly covered by a layer of more-or-less hexagonal sectors (Fig. 3, A), each with 3–13 conspicuous pores (cancelli); porous sectors thicken, and cancelli tubes become longer, with age of colony (Fig. 3, C). In life this surface would have been covered by a coelom and cuticle, hence entire basal surface interior-walled. KL = 143–279 (223, 39. 354), KW 149–243 (198, 32.798), KD = 129–287 (234, 44.414); N= 11. Interspersed among porous sectors are 1–3 funnel-shaped concavities (Fig. 3, A), each smooth-walled with interior porous opening(s). In life these would have supported anchoring rootlets. USNM62609-G has three such concavities, none central, whereas
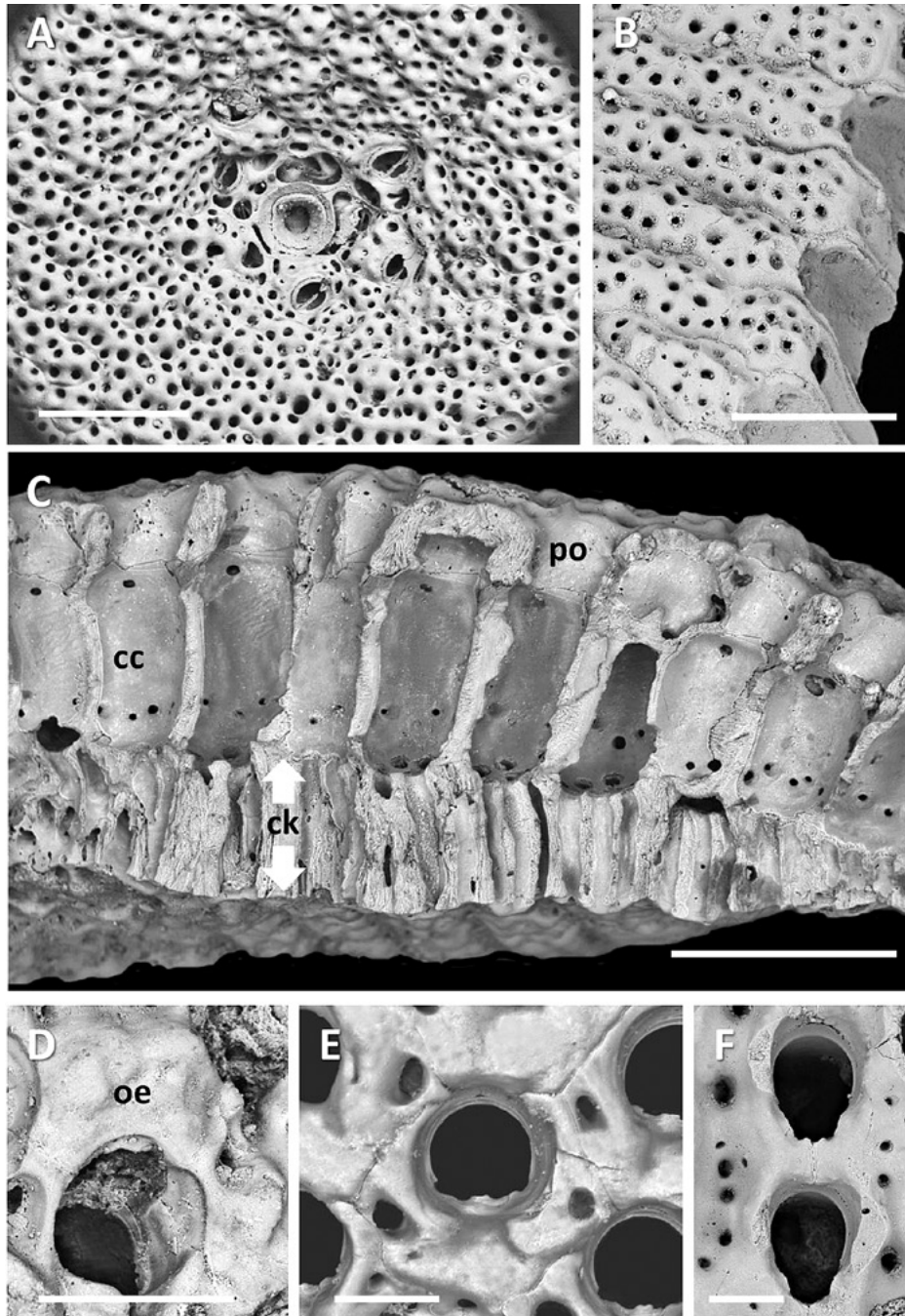
Figure 3. (A, C, D, E) *Schizorthosecos interstitia* (Lea, 1833) (A: USNM 62609C; C: USNM 62609L; D: USNM 62609H; E: USNM 6209J; (B, F) *Schizorthosecos danvillensis* McGuirt, 1941 (B, F: NIWA 132858). **(A)** Interior-walled basal surface of colony showing a large central rootlet aperture flanked by several avicularia with pivot bars. The basal surface is made up small hexagonal sectors, each with several cancelli. **(B)** Linear rows of cancellate sectors not externally divided into hexagons. **(C)** Cross section through centre of colony showing taller zooidal chambers in centre (po, peristomial orifice; cc, cystid chamber; ck, cancellate layer with arrows indicating thickness). **(D)** Imperforate hyperstomial ooecium (oe). **(E)** Autozooidal orifice, surrounded by others quincuncially. **(F)** Autozooidal orifices arranged in longitudinal radial series. Scale bars: A, 500 µm; B, C, 400 µm; D, 200 µm; E, F, 100 µm.

USNM62609-B has a moderately large central concavity only. RD = 166–374 (263, 74.175); N = 7.

There are several abfrontal avicularia, each of which appears to have been budded from an associated kenozooid (Fig. 3, A). Shape is like that of frontal avicularia near apex, except for USNM62609-E, in which the abfrontal avicularia are proportionately longer, being oval instead of near-circular. AAvL = 117–161 (138, 14.360), AAvW = 120–153 (136, 12.649).

Interzooidal communication pores simple, occurring in an uneven linear row low on transverse and lateral walls just above junction with basal wall (Fig. 3, C). Basal walls each have a cluster of communication pores that communicate with the cancelli. Ancestrular complex not clearly discernible.

Remarks: Schizorthosecos interstitia differs from *Clathrolunula* in several important respects, notably the absence of a suboral radiate bar, the presence of avicularia and ovicells, an abfrontal layer of cancellate sectors with interior basal walls, and the presence of 1–3 relatively large concave loci indicating anchoring rootlets in life. Canu and Bassler (1920, pl. 18, fig. 9) depicted the ovicells of *S. interstitia* as biperforate. SEM examination of the specimen shows that the ovicell is actually imperforate and that their light micrograph was retouched. It seems they mistook the irregular surface features as indicating foramina.

Schizorthosecos interstitia most closely resembles *Schizorthosecos danvillensis*, in which the autozooids are arranged not quincuncially but in radial linear rows; on the basal side, porous sectors are also arranged in radial linear series (defined by sinuous outlines), such that the boundaries of individual hexagons are much less apparent (Fig. 3, B). Orifices are proportionately longer and narrower (Fig. 3, F) and the short area of suboral frontal shield often has a median longitudinal suture. Areolar-septular pores are smaller, with two on either side of the orifice. Because zooids are arranged radially, areolar pores also occur in linear series, which, with secondary calcification, align in radial furrows.

Broken interzooidal heterozooid chambers indicate sparse adventitious avicularia in life; McGuirt (1941) mentions pivot bars. There are three concave loci for rootlets, one of which can be central.

Schizorthosecos grandiporosum not only lacks a radiate suboral bar, and hence is unrelated to *Clathrolunula radiata*, but it also appears to be unrelated to *S. interstitia*. In particular, it lacks an abfrontal layer of interior-walled cancellate sectors.. Two of the specimens illustrated by Canu and Bassler (1920, figs 11, 13) are missing. At present, both the generic and familial status of *S. grandiporosum* are unresolvable.

DISCUSSION

So far as is known, a subfrontal hypostegal coelom is known only in the superfamily Euthyriselloidea. It was first recognised in the genus *Tropidozoum* by Cook (1975, p. 161), who described the frontal shield as "a cryptocystal wall perforated by foramina and surrounded by a hypostegal coelom", i.e. the coelom appears on both sides of the wall/shield. She also noted (1975, p. 166) that the roof of the ascus "is formed by the membrane which is the basal wall of the hypostegal coelome [*sic*]". Cook (1975) hypothesised that *Tropidozoum* might be related to *Euthyrisella*, noting that both taxa shared colony-wide coeloms with interior basal walls and dimorphic zooids. This hypothesis was confirmed by a morphological study of all Euthyrisellidae then known, with *Tropidozoum* included in the family (Cook and Chimonides 1981).

Pseudoplatyglena mirabilis Gordon and d'Hondt, 1997 was discovered subsequent to Cook and Chimonides' (1981) study. Only two colonies were found, both lacking ovicells or dimorphic zooids. The lack of avicularia and the presence of a radiate suboral bar and subfrontal hypostegal coelom allied the genus with Euthyrisellidae. One additional character was overlooked by Gordon and d'Hondt (1997) in their description, viz the fact that zooidal basal walls can open into an axial coelom (Fig. 2, B). This is most evident at developing branch bifurcations; a zooidal basal coelom is another euthyrisellid character.

The discovery of a radiate suboral bar in a fossil species attributed to *Schizorthosecos* immediately suggested a relationship with *Pseudoplatyglena*. But *Clathrolunula radiata* has a discoidal colony whereas that of *P. mirabilis* is erect and articulated. Furthermore, *C. lunula* is Eocene in age whereas all other species attributed to Euthyrisellidae are Recent. This fact begs the question: Can *C. radiata* truly be included in the Euthyrisellidae, or is Euthyrisellidae actually an ancient family that diversified morphologically long before the Eocene?

The four core genera of Euthyrisellidae are admittedly disparate. Uniting them are dimorphic orifices and an erect colony form; and with respect to frontal-shield characters, Cook and Chimonides (1981, pp. 82–83) observed: "Within the Euthyrisellidae, there is great diversity in frontal shield calcification and in orifice shape which is not strongly correlated with colony form. This diversity suggests that the family has a long evolutionary history …". Harmer (1902) studied the frontal shield in *Pleurotoichus clathratus* and *Euthyrisella obtecta* and concluded that the "compensation sac develops in … the Lepralioid manner; that is to say, an invagination formed at the base of the operculum after the calcification of the front wall has been completed." Although examples of lepralioid-type shields are rare to absent in the Paleocene, they are common in several family-level taxa in the earliest Eocene (e.g. Gordon and Taylor 2015) so they must have developed more than once, presumably from umbonuloid-shielded ancestors (Gordon 2000), during the Paleocene. The unique combination of morphological features in Euthyrisellidae strongly suggests that the family is not closely related to other lepralioid superfamilies and we concur with Cook and Chimonides (1981) that morphological divergence occurred early in the family's history. Inasmuch as the radiate suboral bars in *Pseudoplatyglena* and *Clathrolunula* are so nearly identical, it is more parsimonious to consider them homologous.

In discussing the interior skeletal walls of core Euthyrisellidae, Cook and Chimonides (1981) noted that colonies with a high proportion of interior walls occur among free-living ('lunulitiform') anascans, several genera of which are characterised by species with extensive cryptocysts that appear allied with microporoidean taxa. Invoking the terminology of Banta (1970), they termed the frontal shield in Euthyrisellidae 'cryptocystidean'. Banta (1970) had sought to explain the origin of the ascophoran 'cryptocystidean' shield from a microporoidean-type cryptocyst. In contrast, Gordon and Voigt (1996) put forward a more parsimonious model, deriving the ascophoran shield and hypostegal coelom via the transformation of frontally contiguous transformed kenozooids, while acknowledging that Banta's hypothesis was at least conceptually possible. Even though the ascus in Euthyrisellidae is 'lepralioid' in its mode of formation as noted by Harmer (1902), the frontal shield exhibits two striking attributes: 1) it is an interior cryptocyst-like wall with a hypostegal coelom on both sides, and 2) has no areolar-septular pores in this wall to allow hypostegal–visceral communication. This arrangement suggests a different evolutionary pathway from the kenozooidal model, namely one that could be explained by Banta's (1970) model. In short, it is not inconceivable that Euthyriselloidea originated from a microporoidean-type ancestor, or a form resembling the cupuladriid genus *Discoporella* – Cook (1975, p. 165) perceptively remarked that, in *Tropidozoum*, the "depressed cryptocystal area is composed of fused spinules which can be seen to develop first proximally and laterally, forming the foramina by anastomoses, in a manner very similar to that seen in the Cupuladriidae, in *Discoporella umbellata* (see Cook, 1965, p. 179)". In this scenario, the ascus, which develops intussusceptively as an inward fold of the membranous frontal wall proximal to the operculum, would have originated independently of that in other ascus-bearing cheilostomes; such in any case seems to have happened several times in evolution (Gordon 2000). Parietal muscles would then insert on the underside of the intussuscepted ascus floor instead of the membranous frontal wall *per se*

(of which the ascus is an infold). The reduction of the foraminate area in a distal direction could conceivably have resulted in the radiate suboral bar seen in *Clathrolunulua* and *Pseudoplatyglena*, with the separation of this area of hypostegal coelom from the rest of the frontal shield. The interzooidal pores seen in *Clathrolunula* and *Pseudoplatyglena* would be non-homologous with the areolar-septular pores seen in other ascophorans.

Inter alia, Harmer (1902) remarked on the complex two-layered operculum with a strong vertical flange in *Pleurotoichus clathratus*, not dissimilar to that seen in cryptocystal Steginoporellidae (Gordon *et al.* 2017), Aspidostomatidae (Harmer 1926), *Monoporella* (Cheetham and Cook 1983), *Macropora* (Gordon and Taylor 2008) and *Cellaria* (Perez and Banta 1996) – plus a few ascophorans [e.g. *Didymosella* (Cook and Chimonides 1981) and *Margaretta* (Cheetham and Cook 1983)] – although whether the opercula all develop in the same way has not been determined.

With the addition of Neoeuthyrididae and Clathrolunulidae, Euthyriselloidea now comprises three families. With the addition of Schizorthosecidae, Mamilloporoidea now comprises five families (the others being Mamilloporidae, Ascosiidae, Cleidochasmatidae and possibly Crepidacanthidae).

REFERENCES

ANTOLINI, P., BRAGA, P. AND FINOTTI, F. 1980. I Briozoi dei Dintorni di Rovereto. Monte Baldo settentrionale e Valle di Gresta. *Pubblicacione della Società Museo Civico di Rovereto* **82**, 1–102.

BANTA, W.C. 1970. The body wall of cheilostome Bryozoa. III. The frontal wall of *Watersipora arcuata* Banta, with a revision of the Cryptocystidea. *Journal of Morphology* **131**, 37–56.

BASSLER, R.S. [1934] 1935. Bryozoa. *Fossilium Catalogus 1 Animalia* **67**, 1–229.

BASSLER, R.S. 1936. Nomenclatorial notes on fossil and Recent Bryozoa. *Journal of the Washington Academy of Science* **26**, 156–162.

BASSLER, R.S. 1953. *Part G. Bryozoa.* In: R.C. Moore (ed.), *Treatise on Invertebrate Paleontology*. Boulder and Lawrence, Geological Society of America and University of Kansas Press.

BOCK, P.E. AND COOK, P.L. 2004. A review of Australian Conescharellinidae (Bryozoa: Cheilostomata). *Memoirs of Museum Victoria* **61**, 135–182.

BRAGA, P. 2008. Atlas of Cenozoic Bryozoa of north-eastern Italy (Venetia region). *Lavori Società Veneziana di Scienze Naturali* **33**, 71–92.

BRETNALL, R.W. 1921. Studies on Bryozoa. Part 1. *Records of the Australian Museum* **13**, 157–162.

BYBELL, L.M. AND GIBSON, T.G. 1985. The Eocene Tallahatta Formation of Alabama and Georgia: its lithostratigraphy, biostratigraphy, and bearing on the age of the Claibornian Stage. *United States Geological Survey Bulletin* **1615**, 1–20.

CANU, F. AND BASSLER, R.S. 1917. A synopsis of American Early Tertiary cheilostome Bryozoa. *United States National Museum Bulletin* **96**, 1–87, 6 pls.

CANU, F. AND BASSLER, R.S. 1920. North American Early Tertiary Bryozoa. *United States National Museum Bulletin* **106**, 1–879, 162 pls.

CANU, F. AND BASSLER, R.S. 1927. Classification of the cheilostomatous Bryozoa. *Proceedings of the United States National Museum* **69** (14), 1–42, 1 pl.

CANU, F. AND BASSLER, R.S. 1928. Fossil and Recent Bryozoa of the Gulf of Mexico region. *Proceedings of the United States National Museum* **72** (14), 1–199, 24 pls.

CHEETHAM, A.H. AND COOK, P.L. 1983. General features of the class Gymnolaemata. In: R.A. Robison (ed.), *Treatise on Invertebrate Paleontology Part G. Bryozoa Revised. Volume 1*. Boulder and Lawrence, Geological Society of America and University of Kansas Press, pp. 138–207.

COOK, P.L. 1965. Notes on the Cupuladriidae (Polyzoa, Anasca). *Bulletin of the British Museum (Natural History) Zoology*, **13**, 153–187, 3 pls.

COOK, P.L. 1975. The genus *Tropidozoum* Harmer. *Documents des Laboratoires de Géologie de la Faculté des Sciences de Lyon*, h. s., **1** (1), 161–168, 3 pls.

COOK, P.L. AND CHIMONIDES, P.J. 1981. Morphology and systematics of some interior-walled cheilostome Bryozoa. *Bulletin of the British Museum (Natural History) Zoology*, **41**, 53–89.

COOK, P.L. AND CHIMONIDES, P.J. 1994. Notes on the genus *Anoteropora* (Bryozoa, Cheilostomatida). *Zoologica Scripta* **23**, 51–59.

COOK, P.L. AND LAGAAIJ, R. 1976. Some Tertiary and Recent conescharelliniform Bryozoa. *Bulletin of the British Museum (Natural History), Zoology* **29**, 317–376, 8 pls.

COOK, P.L., BOCK, P.E., HAYWARD, P.J. AND GORDON, D.P. 2018. Class Gymnolaemata, order Cheilostomata. In: P.J. Cook, P.E. Bock, D.P. Gordon and H.J. Weaver (eds),

Bryozoa of Australia Volume 2. Taxonomy of Australian Families. Melbourne, CSIRO Publishing, pp. 61–279.

DE GREGORIO, A. 1890. Monographe de la faune éocénique de l'Alabama et surtout de celle de Claiborne de l'étage parisien. *Annales de Géologie et de Paléontologie* **7** (8), 1–316, 46 pls.

GABB, W.M. AND HORN, G.H. 1862. The fossil Polyzoa of the Secondary and Tertiary Formations of North America. *Journal of the Academy of Natural Sciences of Philadelphia* **5**, 111–179, pls 19–21.

GORDON, D.P. 2000. Towards a phylogeny of cheilostomes – morphological models of frontal wall/shield evolution. In: A. Herrera Cubilla and J.B.C. Jackson (eds), *Proceedings of the 11th International Bryozoology Association Conference*. Panama City, Smithsonian Tropical Research Institution, pp. 17–37.

GORDON, D.P. AND HONDT, J.-L. D' 1997. Bryozoa: Lepraliomorpha and other Ascophorina, mainly from New Caledonian waters. In: A. Crosnier (ed.), *Résultats des Campagnes MUSORSTOM, Volume 18. Mémoires du Muséum National d'Histoire Naturelle* **176**, 9–124.

GORDON, D.P. AND TAYLOR, P.D. 2008. Systematics of the bryozoan genus *Macropora* (Cheilostomata). *Zoological Journal of the Linnean Society* **153**, 115–146.

GORDON, D.P. AND TAYLOR, P.D. 2015. Bryozoa of the Early Eocene Tumaio Limestone, Chatham Island, New Zealand. *Journal of Systematic Palaeontology* **13**, 983–1070.

GORDON, D.P. AND VOIGT, E. 1996. The kenozooidal origin of the ascophorine hypostegal coelom and associated frontal shield. In: D.P. Gordon, A.M. Smith and J.A. Grant-Mackie (eds), *Bryozoans in Space and Time*. Wellington, NIWA, pp. 89–107.

GORDON, D.P., VOJE, K.L. AND TAYLOR, P.D. 2017. Living and fossil Steginoporellidae (Bryozoa: Cheilostomata) from New Zealand. *Zootaxa* **4350**, 345–362.

HARMER, S.F. 1902. On the morphology of the Cheilostomata. *Quarterly Journal of Microscopical Science,* n. s., **46**, 263–350, pls 15–18.

HARMER, S.F. 1926. The Polyzoa of the Siboga Expedition. Part 2. Cheilostomata Anasca. *Siboga-Expeditie* **28b**, 181–501, pls 13–34.

HARMER, S.F. 1957. The Polyzoa of the Siboga Expedition. Part 4. Cheilostomata Ascophora II. *Siboga-Expeditie* **28d**, 641–1147, pls 42–74.

HONDT, J.-L. D' 1985. Contribution à la systématique des Bryozoaires eurystomes. Apports récents et nouvelles propositions. *Annales des Sciences Naturelles, Zoologie,* sér. 13, **7**, 1–12.

KOSCHINSKY, C. 1885. Ein Beitrag zur Kenntniss der Bryozoenfauna der älteren Tertiärschichten des südlichen Bayerns. I. Abtheilung. Cheilostomata. *Palaeontographica* **32**, 1–73, 7 pls.

LEA, I. 1833. *Contributions to Geology*. Philadelphia, Carey, Lea and Blanchard.

LEVINSEN, G.M.R. 1909. *Morphological and Systematic Studies on the Cheilostomatous Bryozoa*. Copenhagen, Nationale Forfatteres Forlag.

MCGUIRT, J.W. 1938. Louisiana Tertiary Bryozoa. Louisiana State University doctoral dissertation, Baton Rouge. https://digitalcommons.lsu.edu/gradschool_disstheses/7792

MCGUIRT, J.W. 1941. Louisiana Tertiary Bryozoa. *Geological Bulletin* **21**, 1–74.

OSTROVSKY, A.N. 2013. *Evolution of Sexual Reproduction in Marine Invertebrates. Example of Gymnolaemate Bryozoans*. Dordrecht, Springer.

PEREZ, F.M. AND BANTA, W.C. 1996. How does *Cellaria* get out of its box? A new cheilostome hydrostatic mechanism (Bryozoa: Cheilostomata). *Invertebrate Biology* **115**, 162–169.

SCHINDELIN, J. ARGANDA-CARRERAS, I., FRISE, E., KAYNIG, V., LONGAIR, M., PIETZSCH, T., PREIBISCH, S., RUEDEN, C., SAALFELD, S., SCHMID, B., TINEVEZ, J.-Y., WHITE, D.J., HARTENSTEIN, V., ELICEIRI, K., TOMANCAK, P. AND CARDONA, A. 2012. Fiji: an open-source platform for biological-image analysis. *Nature Methods* **9**, 676–682.

SMITT, F.A. 1873. Floridan Bryozoa, collected by Count L. F. de Pourtales. Part II. *Kongliga Svenska Vetenskaps-Akademiens Handlingar* **11** (4), 1–83, 13 pls.

WINSTON, J.E. 2005. Re-description and revision of Smitt's "Floridan Bryozoa" in the collection of the Museum of Comparative Zoology, Harvard University. *Virginia Museum of Natural History Memoir* **7**, 1–147.

The genus *Reptadeonella* (Bryozoa, Cheilostomatida) in European waters: there's more in it than meets the eye

Marianne Nilsen Haugen[1]*, Maja Novosel[2], Max Wisshak[3] and Björn Berning[4, 5]

[1] Natural History Museum, University of Oslo, Oslo, Norway
[*corresponding author: e-mail: m.n.haugen@nhm.uio.no]
[2] Faculty of Science, University of Zagreb, Zagreb, Croatia
[3] Marine Research Department, Senckenberg am Meer, Wilhelmshaven, Germany
[4] Oberösterreichisches Landesmuseum, Geowissenschaftliche Sammlungen, Leonding, Austria
[5] CIBIO, Centro de Investigação em Biodiversidade e Recursos Genéticos,
InBIO Laboratório Associado, Pólo dos Açores, Açores, Portugal

ABSTRACT

In European waters, the adeonid genus *Reptadeonella* Busk (Bryozoa, Cheilostomatida) is represented by two species: *R. insidiosa* (Jullien) from the Bay of Biscay and the western Channel, and the oft-cited *R. violacea* (Johnston), ranging from the southern British Isles to the Mediterranean Sea. Inspection of colonies previously reported as *R. violacea* from the central Mediterranean Sea and the central Atlantic Azores Archipelago, however, shows that these populations are specifically distinct, thus doubling the number of *Reptadeonella* species present in Europe. Accordingly, we here introduce two new species, the Mediterranean *Reptadeonella zabalai* sp. nov., and the Azorean *Reptadeonella santamariae* sp. nov.

INTRODUCTION

The adeonid genus *Reptadeonella* Busk, 1884 is a moderately diverse cheilostomatid genus, comprising 24 known species in tropical to warm temperate regions worldwide. Its fossil record stretches back to the lower Miocene (Aquitanian) of southwestern France (Pouyet and Moissette 1992, and references therein). Type species is *Reptadeonella violacea* (Johnston, 1847), which was originally described from the southern British Isles (cf. Hayward and Ryland 1999, p. 186). The type locality also marks its northernmost range of distribution while the species has since been reported to occur south along the European and NW African continental shelf as well as in the Mediterranean Sea (Hayward and McKinney 2002, p. 44) where the species can be easily recognised even by scuba divers owing to the distinctive deep purple colour of living colonies. Putative records from the western Atlantic and the Pacific coasts of North America (cf. Hayward and Ryland 1999, p. 186) have to be regarded as either non-native or specifically distinct.

Reptadeonella insidiosa (Jullien *in* Jullien & Calvet, 1903), which occurs offshore along the southern British Isles and northern France (Hayward and Ryland 1999, p. 188), is the only other *Reptadeonella* species currently known in European waters. However,

the results of recent taxonomic revisions show that the true biodiversity of bryozoan genera in European waters is often greatly underestimated (e.g. Berning *et al.* 2008, 2019; Reverter-Gil *et al.* 2015). Within a larger effort to better understand the evolution, systematics and ecology of the family Adeonidae Busk, 1884 (Orr *et al.* in press), we here present a morphological study of *Reptadeonella* populations from the central Atlantic archipelago of the Azores as well as from the central Mediterranean Sea that have hitherto been referred to as *R. violacea*.

MATERIAL AND METHODS

Bryozoan colonies analysed in this work are housed in the collections of the following institutions: Croatian Natural History Museum Zagreb (CNHM), Department of Biology at the University of the Azores (DBUA), Natural History Museum Oslo (NHMO), Biologiezentrum des Oberösterreichichen Landesmuseums Linz (OLL; collection Invertebrata varia), as well as the Senckenberg Museum und Forschungsinstitut Frankfurt (SMF). Specimens were prepared for scanning electron micrography (SEM) by soaking in diluted household bleach to remove chitinous parts and soft tissues. SEM images of *Reptadeonella zabalai* sp. nov. were taken at the Natural History Museum London using a LEO 1455VP while *Reptadeonella santamariae* sp. nov. was scanned at the GeoZentrum Nordbayern of the University of Erlangen (CamScan), at Senckenberg am Meer Wilhelmshaven (Tescan VEGA3 xmu), and at the Institute of Biomedical Mechatronics of the Johannes-Kepler-University Linz (Philips 525 M). Morphometric measurements were made on these micrographs using the software ImageJ.

SYSTEMATICS

Order Cheilostomatida Busk, 1852
Superfamily Adeonoidea Busk, 1884
Family Adeonidae Busk, 1884
Genus *Reptadeonella* Busk, 1884

Reptadeonella zabalai sp. nov.
Fig. 1A–E, Table 1

Adeona violacea – Levinsen 1909: p. 283, pl. 14, fig. 1a–g.
part *Reptadeonella violacea* – Novosel and Pozar-Domac 2001: p. 377 (listed); Novosel *et al.* 2004: p. 162 (listed); Chimenz Gusso *et al.* 2014: 223, fig. 121a–d.

Etymology: Named in honour of Mikel Zabala (Barcelona) for his contribution to our understanding of Mediterranean Bryozoa.

Material Examined: Holotype, Korčula Island (Croatia), 42°55'33.51"N 17°10'52.57"E, leg. M. Novosel, 04.07.2008, 4 m water depth, a single large colony formerly growing on a rhizome of *Posidonia oceanica* (Linné) Delile, 1813, which was originally kept in ethanol and that is now dried and split into several parts: CNHM 71, one large colony fragment free of a substratum; NHMO H 1431, one fragment on stub; OLL 2019/6, two small fragments free of a substratum. Paratype, CNHM 72, Lastovo Island (Croatia), 42°43'30"N 16°52'49.5"E, leg. M. Novosel, 05.03.2002, 10 m water depth, a large colony free of a substratum, dry. Paratype, OLL 2019/64, same locality information as CNHM 72, one colony on seagrass rhizome, dry.

Diagnosis: *Reptadeonella* with a single large adventitious avicularium and an elongated triangular rostrum pointing distally (seldom distolaterally) and slightly overarching the proximal orifice margin. Its colour is black in living and dried material. Spiramen single, round or oval, situated in a depression proximal to avicularium, usually in proximal third or fourth of zooid frontal; one or two rows of areolar pores, zooid surface finely granular. Secondary orifice oval to D-shaped (rarely suborbicular), peristome not raised above colony frontal. Tubular interzooidal kenozooids present also in late ontogeny. Gonozooid distinctly wider than autozooids; orifice much wider than long.

Table 1. Morphometric measurements (in µm) of *Reptadeonella zabalai* sp. nov.

Character	Mean	SD	Minimum	Maximum	N
Autozooid length	529	55	436	626	15
Autozooid width	343	31	294	390	15
Orifice length	81	5	72	87	15
Orifice width	114	8	92	124	15
Spiramen length	29	3	24	33	11
Spiramen width	38	4	32	42	11
Gonozooid length	629	–	–	–	1
Gonozooid width	412	–	–	–	1
Gonozooid orifice length	75	–	–	–	1
Gonozooid orifice width	162	–	–	–	1
Avicularium length	239	20	212	266	15
Avicularium width	81	9	65	93	15

SD = standard deviation; N = number of measurements.

Description: Colony encrusting unilaminar or occasionally multilaminar owing to self-overgrowth, occasionally growing free of a substratum, black when alive or dried, autozooids pyriform to regularly hexagonal, longer than wide (mean ZL/ZW = 1.54), with distinct lateral margins, frontal shield heavily calcified during ontogeny, flat or slightly convex, surface finely granular throughout; the single spiramen is placed in a depression, round to oval, generally about the same size or slightly larger than areolar pores and positioned proximal to the avicularium, usually in the proximal third or fourth of zooid; some 25–35 areolar pores arranged along the zooid margin in a single (usually in the proximal part) or double row.

Secondary orifice transversely oval, occasionally D-shaped or suborbicular, with a thin and slightly raised margin, widest at about mid-distance, the interior part of the distal orifice margin may be granular.

A large, single, adventitious avicularium with an elongate triangular rostrum positioned proximal to the orifice, directing distally (seldom distolaterally) and extending onto proximal part of the peristome; mandible hinged in small depressions proximal to the rostral margins that are distinctly raised; in some zooids or colony regions the large avicularia are replaced by small avicularia or oval kenozooids that may be associated with a suboral umbo.

Small tubular interzooidal kenozooids with a round to oval opesia (ø = 40–50 µm) occasionally present in the junction of three zooids, persisting even in late ontogeny when frontal calcification is well advanced.

Gonozooids broader than autozooids and with a larger D-shaped orifice that is much broader than wide; frontal surface between orifice and distal margin perforated by numerous areolar pores; no avicularium present, but a tubular kenozooid occasionally placed midlength of zooid.

Ancestrular complex of six autozooids similar in shape to adult ones but with small avicularia or kenozooids replacing them.

Discussion: *Reptadeonella zabalai* sp. nov. is mainly distinguished from *R. violacea* by its large avicularia. Small avicularia and oval kenozooids (often associated with a suboral umbo), however, may also occur in some colony parts in the new species (Fig. 1A at centre left), and the species

may then be distinguished by the presence of the small tubular kenozooids that are visible even in late ontogeny in the new species, which was already noted by Levinsen (1909, p. 284, pl. 14, fig. 1b). These kenozooids are occasionally also produced at the outer growth margin in *R. violacea* colonies but they are visible only in the zone of frontally uncalcified zooidal buds (cf. Hayward and Ryland 1999, p. 186), in which the frontal membrane is still exposed, and are overgrown when the frontal shield forms. Moreover, there are differences in colour: while *R. violacea* is deep purple when alive, living colonies of *R. zabalai* are black.

Within this study, numerous *Reptadeonella* colonies from along the Croatian Adriatic coast
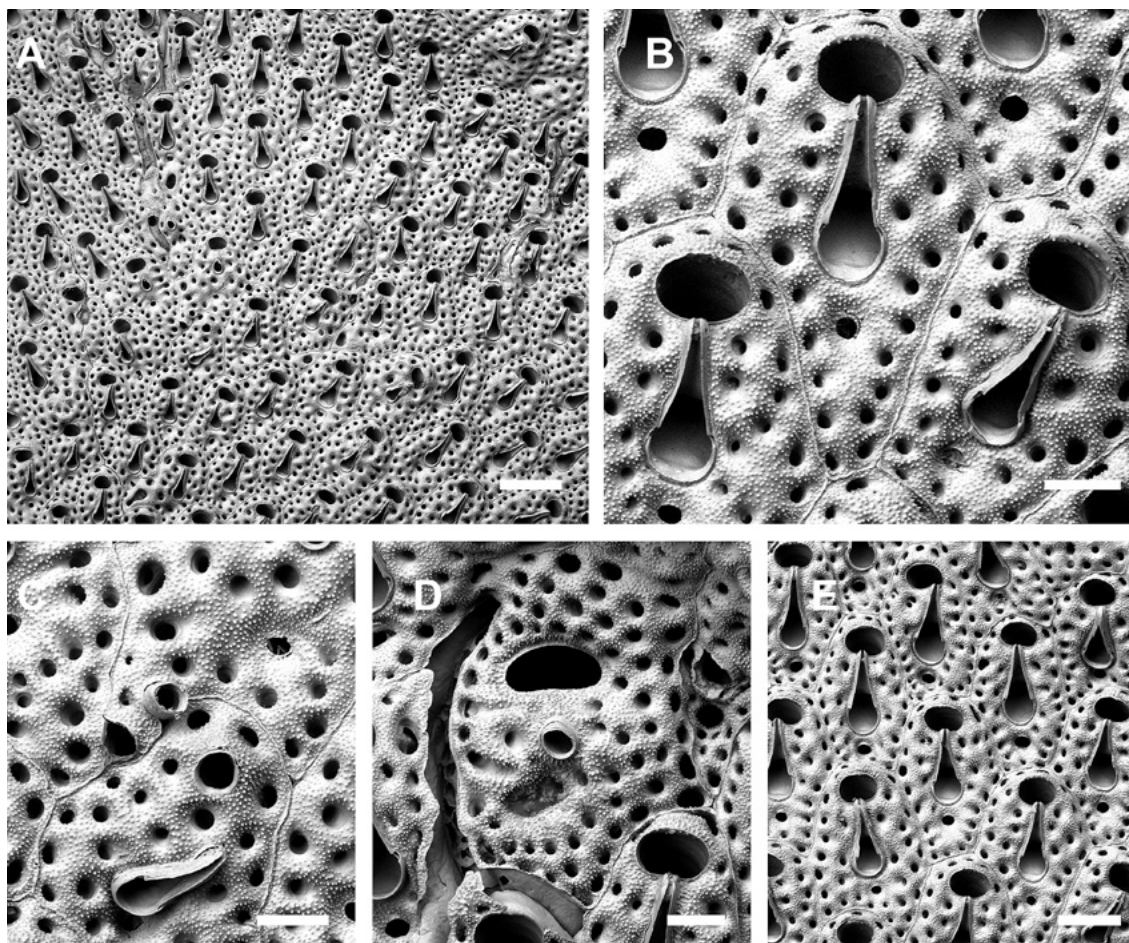
Figure 1. *Reptadeonella zabalai* sp. nov., holotype, Korčula, Croatia (NHMO H 1431).
(A) Overview of colony, note the presence of small avicularia at centre left;
(B) close-up of zooids showing orifices, adventitious avicularia and spiramina;
(C) interzooidal kenozooid in the junction of three zooids in a central region of the colony,
and a malformed autozooid with a kenozooid-like opesia;
(D) gonozooid with the avicularium replaced by a kenozooid, while the groove along
the left margin of the gonozooid is the bioclaustration
of a symbiotic zancleid hydroid (cf. McKinney 2009);
(E) overview of several autozooids.
Scale bars: A, E = 200 µm; B–D = 100 µm.

were optically examined and compared with the holotype of *R. zabalai*. While *R. violacea* occurs at least as far north as Rovinj (Hayward and McKinney 2002), *R. zabalai* has almost exclusively been found in Southern Adriatic sites (islands of Korčula, Lastovo and Sušac), with only one colony co-occurring with *R. violacea* in the Central Adriatic island of Kornati [for the exact localities and geographic distribution of the two species in the Croatian Adriatic see Novosel *et al*. (2020)]. Other unequivocal records of the species were reported from Sicily (Levinsen 1909) and other, albeit unspecified, Italian localities (Chimenz Gusso *et al*. 2014).

Reptadeonella zabalai is the species given as *Reptadeonella* aff. *violacea* in a molecular phylogenetic analysis of the family Adeonidae by Orr *et al*. (in press). A part of the holotype, which was formerly stored in ethanol, was used for the genetic analysis.

Distribution: *Reptadeonella zabalai* has been reported from the southeastern Adriatic Sea and Sicily, where it may co-occur with *R. violacea*, and is likely to be present also in other parts of the central and eastern Mediterranean Sea. Images or descriptions of the recorded *Reptadeonella* colonies from this region are, however, often wanting (e.g. Hayward 1974; Sokolover *et al*. 2016). Nevertheless, the *R. violacea* morphotype seems to be present in the eastern Mediterranean as well (e.g. Abdelsalam 2014). According to previous records and observations in the present study, *R. zabalai* occurs in depths between 4–45 m, growing on a wide range of substrata such as rocks, coralline algae, shells and other bioclasts as well as on seagrass rhizomes.

Reptadeonella santamariae sp. nov.
Fig. 2A–F, Table 2

Reptadeonella sp. – Wisshak *et al*., 2015: p. 95 (listed).
Reptadeonella violacea – Micael *et al*., 2019: p. 475 (listed).

Etymology: Named after its type locality, the island of Santa Maria (Azores).

Material Examined: Holotype, DBUA-BRY 001, Santa Maria Island, Baixa de Maia (Azores), 36°56'39.13"N 25°00'27.60"W, leg. B. Berning, 22.07.2015, 14 m water depth, one colony on rock, sputter-coated. Paratype, OLL 2019/65, same locality information as DBUA-BRY 001, one colony on rock, dry. Paratype, SMF 60074, Faial Island (Azores), 38°32'29"N 28°36'34"W, leg. M. Wisshak, 01.10.2008, 15 m water depth, two small colony fragments subsampled from a large colony on settlement panel, sputter-coated, on stub.

Diagnosis: *Reptadeonella* with a small adventitious avicularium pointing distally, most often not fully developed but seemingly replaced by a kenozooid; tip of rostrum not reaching proximal orifice margin if fully developed. Colour grey to black in living and dried material. Single round to oval spiramen positioned at about midlength of zooid frontal; one or two rows of lateral areolar pores; zooid surface finely granular. Secondary orifice oval to D-shaped, peristome not raised above colony surface. Tubular interzooidal kenozooids present also in late ontogeny. Length and width of gonozooids and their orifices distinctly greater than in autozooids.

Description: Colony encrusting, unilaminar, multiserial, forming relatively large patches, surface iridescent when alive and of a black to light grey colour, glassy-white but not translucent when bleached. Zooids elongated hexagonal to polygonal (mean ZL/ZW = 1.79), separated by faint sutures; frontal shield flat to very slightly convex, surface granular throughout, distinct buttresses visible in early ontogenetic zooids separating numerous round areolar pores (30–47) that are arranged in one or two rows, buttresses later levelled by thick frontal calcification, a round to oval spiramen of similar size than areolar pores positioned in zooid centre; vertical walls with numerous basal chambers connecting neighbouring zooids.

Peristome slightly raised distally in early onto-genetic zooids, levelled by secondary calcification during late ontogeny, secondary orifice D-shaped or almost oval, broader than long with a straight proximal margin, widest at about mid-distance.

Avicularia fully developed in only a few zooids, single, positioned between spiramen and orifice, rostrum elongated triangular when well developed, acute to frontal surface and pointing distally, the cystid thus producing a suboral umbo; in most zooids the avicularium is replaced by a more or less oval kenozooid associated with the suboral umbo (length c. 55 μm, width c. 45 μm).

Small interzooidal kenozooids with a round or oval opesia (ø = 40–50 μm) present in some colony parts, positioned at the proximal corner(s) of the zooidal bud, i.e. in the junctions between three zooids.

Gonozooids longer and broader than autozooids, and with a large D-shaped orifice that is much broader than wide.

Ancestrular complex composed of six zooids of similar shape as, but of smaller dimensions than, adult zooids.

Discussion: As most of the previously studied material from the Azores was collected by research vessels using large trawls and rock dredges, which can only be employed in deeper water, information on the archipelago's shallow-subtidal fauna is relatively scarce. Few species have therefore been previously reported from <50m water depth (Wisshak *et al.* 2015; Micael *et al.* 2019, and references therein). As is apparent from the great percentage of species left in open nomenclature or merely conferred to other nominal species in these works, a considerable number of new species await description (e.g. Berning *et al.* 2019).

Mainly owing to the similarly small adventitious avicularia, *Reptadeonella santamariae* sp. nov. is superficially very similar to *R. violacea*, and the question has been raised whether the central Atlantic population represents a non-indigenous species in the Azores (Micael *et al.* 2019: 476). The species has not been recorded from ports during sampling surveys for invasive species (J. Micael, pers. comm. 2019), however, and it also occurs in fairly remote regions, such as the eastern coast of the island of Santa Maria. More importantly, while *R. violacea* is clearly the morphologically most closely related of

Table 2. Morphometric measurements (in μm) of *Reptadeonella santamariae* sp. nov.

Character	Mean	SD	Minimum	Maximum	N
Autozooid length	618	45	537	731	12
Autozooid width	346	39	260	389	12
Orifice length	78	10	61	87	12
Orifice width	113	5	106	125	12
Spiramen length	30	2	28	33	11
Spiramen width	23	3	19	30	11
Gonozooid length	748	–	–	–	1
Gonozooid width	461	–	–	–	1
Gonozooid orifice length	96	–	–	–	1
Gonozooid orifice width	178	–	–	–	1
Avicularium length	110	11	97	125	5
Avicularium width	49	5	44	55	5

SD = standard deviation; N = number of measurements.
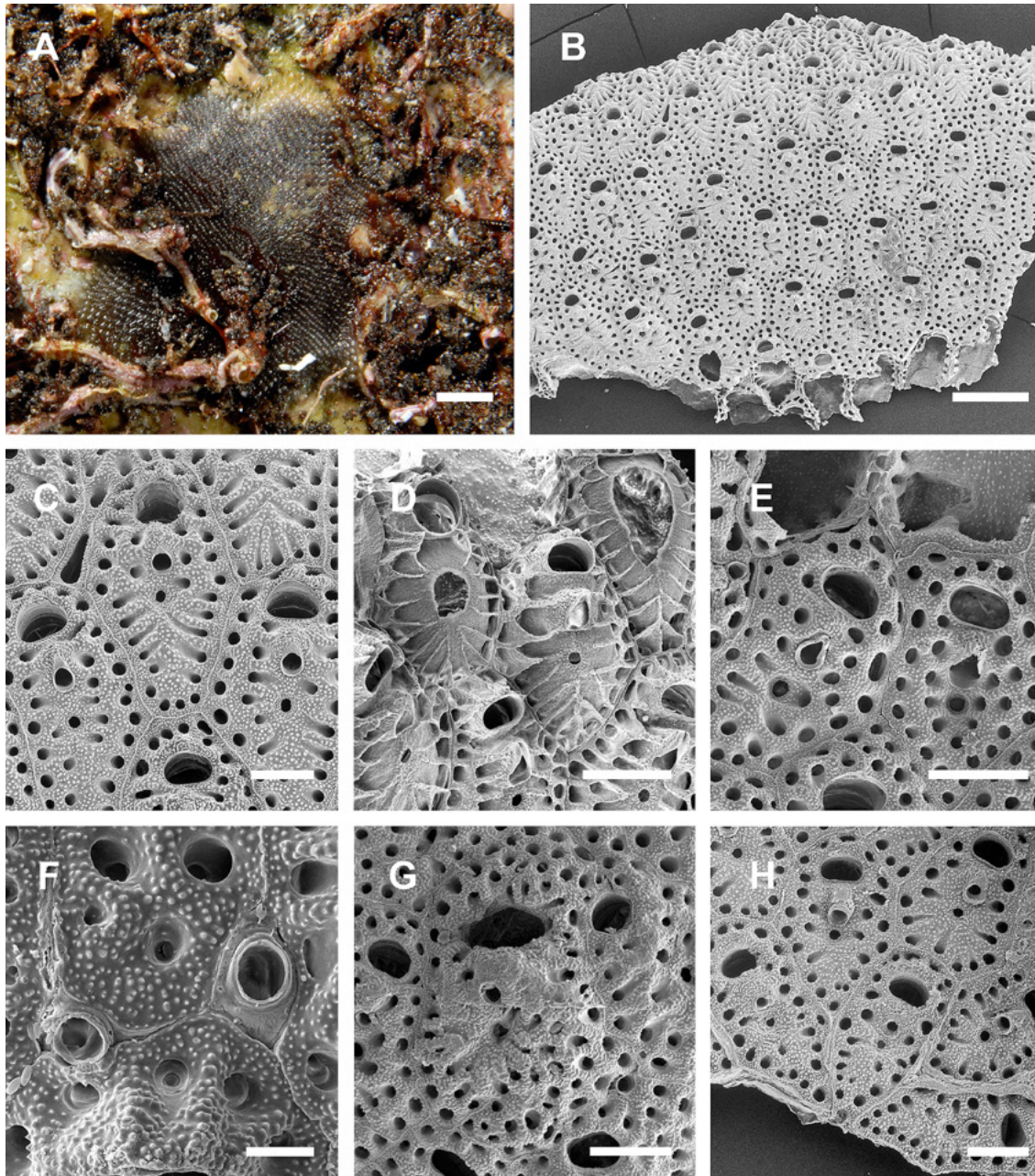
Figure 2. *Reptadeonella santamariae* **sp. nov.,**
A–F, H: paratype, Faial, Azores (SMF 60074), G: holotype, Santa Maria, Azores (DBUA-BRY 001).
(A) Optical image of the paratype colony right after retrieval of the settlement panel
which it encrusts, note the grey to black colour; (B) overview of colony fragment;
(C) close-up of autozooids showing orifices, presumably non-functional avicularia as present in by far most
zooids, and spiramina; (D) early ontogenetic autozooids at the colony margin showing different stages
of frontal shield, avicularium and orifice formation; (E) two fully formed zooids near the colony margin,
the left one with a somewhat malformed avicularium; (F) interzooidal kenozooids produced in junctions
between fully formed zooids; (G) gonozooid, note the presence of an interzooidal kenozooid at the junction
of the gonozooid and the two autozooids to the right; (H) three of the six zooids of the ancestrular complex.
Scale bars: A = 0.25 cm; B = 500 µm; C, H = 150 µm; D, E, G = 200 µm; F = 50 µm.

all Atlantic *Reptadeonella* species (see also Almeida *et al*. 2015), we can show here that the Azorean population is specifically distinct and presumably endemic to the archipelago. Its origin or time of arrival on the islands is unknown, however, as no *Reptadeonella* species was present in the lower Pliocene bryozoan assemblages on the island of Santa Maria (Ávila *et al*. 2015; Rebelo *et al*. 2016).

Reptadeonella hortae shares the grey to black colour (lighter at the colony margin) with *R. zabalai* but differs in having slightly more elongated zooids (ZL/ZW = 1.79 vs. 1.54) and only very small suboral avicularia. Many of these avicularia may actually not be fully developed and functional, the avicularian cystid only forming a small oval opesia instead of a triangular rostrum. The fully formed avicularia are thus very similar to *R. violacea*, while these two species differ in colour and in that the small interzooidal kenozooids are visible even in late ontogenetic zooids in *R. santamariae*. The tubular kenozooids may, however, be absent from large colony regions in the new species. Another difference between *R. santamariae* and *R. violacea* concerns the dimensions of the gonozooids and their orifices compared to autozooids. While in *R. violacea* the gonozooids and orifices are wider but of similar length, in *R. santamariae* they are both distinctly wider and longer, although we must stress that only a single gonozooid was present in the available colonies.

The new species was observed to grow on pebbles, competing with coralline algae, and also encrusted the upper side of a settlement panel (Wisshak *et al*. 2015). Another specimen, recorded by Micael *et al*. (2019) in their study on shallow-water bryozoans, was collected in a grotto on the western slope of the Monte da Guia (Faial Island) between 10 and 15 m depth (J. Micael, pers. comm. 2019).

Distribution: *Reptadeonella santamariae* has so far been reported only from the island of Faial in the central Azores as well as from Santa Maria, the easternmost of the islands, occurring at about 10 to 15 m depth in both regions.

DISCUSSION

Inspection of *Reptadeonella* colonies from the Azores and central Mediterranean Sea, which have hitherto been referred to *R. violacea*, show that these are specifically distinct, differing in several characters from the type species of the genus. The number of *Reptadeonella* species in European waters is therefore doubled from two to four.

Separating *R. violacea* from *R. zabalai* and *R. santamariae*, however, may not be easy and may require SEM studies. In dried material, the distinctive deep purple colour of *R. violacea* may be lost and turns to grey or even black as the two new species. Also, the tubular kenozooids, which are difficult to detect with an optical microscope, as well as gonozooids only occur sporadically in the new species and may be absent from extensive parts of the colony. If only fragments of colonies are available for study, these character states may thus not be detected. Moreover, in some colony regions of *R. zabalai*, small avicularia and frontal kenozooids are produced that are similar in length to those in *R. violacea*, making it again difficult to attribute small fragments of dead colonies to either of the species.

It is therefore necessary to study well-preserved and living material using SEM at best. Since few of the reported *Reptadeonella* colonies from the central and particularly the eastern Mediterranean Sea have been figured or thoroughly described, it is also necessary to revise the material of previous studies in order to separate *R. zabalai* from *R. violacea*, which occur in sympatry in these regions.

REFERENCES

ABDELSALAM, K.M. 2014. Benthic bryozoan fauna from the northern Egyptian coast. *Egyptian Journal of Aquatic Research* **40**, 269–282.

ALMEIDA, A.C.S., SOUZA, F.B.C., SANNER, J. AND VIEIRA, L.M. 2015. Taxonomy of recent Adeonidae (Bryozoa, Cheilostomata) from Brazil, with the description of four new species. *Zootaxa* **4013**(3), 348–368.

ÁVILA, S.P., RAMALHO, R.S., HABERMANN, J., QUARTAU, R., KROH, A., BERNING, B., JOHNSON, M.E., KIRBY, M., ZANON, V., TITSCHACK, J., GOSS, A., REBELO, A.C., MELO, C., MADEIRA, P., CORDEIRO, R., MEIRELES, R., BAGAÇO, L., HIPÓLITO, A., UCHMAN, A., DA SILVA, C.M., CACHÃO, M. AND MADEIRA, J. 2015. Palaeoecology, taphonomy, and preservation of a lower Pliocene shell bed (coquina) from a volcanic oceanic island (Santa Maria Island, Azores). *Palaeogeography, Palaeoclimatology, Palaeoecology* **430**, 57–73.

BERNING, B., TILBROOK, K.J. AND ROSSO, A. 2008. Revision of the north-eastern Atlantic and Mediterranean species of the genera *Herentia* and *Therenia* (Bryozoa: Cheilostomata). *Journal of Natural History* **42**(21–22), 1509–1547.

BERNING, B., ACHILLEOS, K. AND WISSHAK, M. 2019. Revision of the types species of *Metroperiella* (Bryozoa, Cheilostomatida), with the description of two new species. *Journal of Natural History* **53**(3–4), 141–158.

CHIMENZ GUSSO, C., NICOLETTI, L. AND BONDANESE, C. 2014. Briozoi. *Biologia Marina Mediterranea* **20**(Suppl. 1), 1–330.

HAYWARD, P.J. 1974. Studies on the cheilostome bryozoan fauna of the Aegean island of Chios. *Journal of Natural History* **8**, 369–402.

HAYWARD, P.J. AND MCKINNEY, F.K. 2002. Northern Adriatic Bryozoa from the vicinity of Rovinj, Croatia.

Bulletin of the American Museum of Natural History **270**, 1–139.

HAYWARD, P.J. AND RYLAND, J.S. 1999. *Cheilostomatous Bryozoa. Part 2. Hippothooidea – Celleporoidea*. Field Studies Council, Shrewsbury.

LEVINSEN, G.M.R. 1909. *Morphological and Systematic Studies on the Cheilostomatous Bryozoa*. Nationale Forfatteres Forlag, Copenhagen.

MCKINNEY, F.K. 2009. Bryozoan-hydroid symbiosis and a new ichnogenus, *Caupokeras*. *Ichnos* **16**(3), 193–201.

MICAEL, J., TEMPERA, F., BERNING, B., LÓPEZ-FÉ, C.M., OCCHIPINTI-AMBROGI, A. AND COSTA, A.C. 2019. Shallow-water bryozoans from the Azores (central North Atlantic): native vs. non-indigenous species, and a method to evaluate taxonomic uncertainty. *Marine Biodiversity* **49**(1), 469–480.

NOVOSEL, M. AND POŽAR-DOMAC, A. 2001. Checklist of Bryozoa of the eastern Adriatic Sea. *Natura Croatica* **10**(4), 367–421.

NOVOSEL, M., POŽAR-DOMAC, A. AND PASARIC, M. 2004. Diversity and distribution of the Bryozoa along underwater cliffs in the Adriatic Sea with special reference to thermal regime. *Marine Ecology* **25**(2), 155–170.

NOVOSEL, M., HAGEMAN, S.J., MIHANOVIC, H. AND NOVOSEL, A. 2020. Bryodiversity along the Croatian coast of the Adriatic Sea. In: P.N. Wyse Jackson and K. Zágoršek (eds), *Bryozoan Studies 2019*. Prague, Czech Geological Survey, pp. 99–109.

ORR, R.J.S., HAUGEN, M.N., BERNING, B., BOCK, P.E., CUMMING, R., FLORENCE, W., HIROSE, M., DI MARTINO. E., RAMSFJELL, M.H., SANNUM, M.M., SMITH, A.M., VIEIRA, L.M., WAESCHENBACH, A. AND LIOW, L.H. in press. A genome-skimmed phylogeny of a widespread bryozoan family, Adeonidae. *BMC Evolutionary Biology*.

REBELO, A.C., RASSER, M.W., KROH, A., JOHNSON, M.E., RAMALHO, R.S., MELO, C., UCHMAN, A., BERNING, B., SILVA, L., ZANON, V., NETO, A.I., CACHÃO, M. AND ÁVILA, S.P. 2016. Rocking around a volcanic island shelf: Pliocene rhodolith beds from Malbusca, Santa Maria Island (Azores, NE Atlantic). *Facies* **62**(3), 22.

REVERTER-GIL, O., SOUTO, J., NOVOSEL, M. AND TILBROOK, K.J. 2015. Adriatic species of *Schizomavella* (Bryozoa: Cheilostomata). *Journal of Natural History* **50**(5–6), 281–321.

POUYET, S. AND MOISSETTE, P. 1992. Bryozoaires du Pliocène dAltavilla (Sicile-Italie): révision de la

collection Cipolla, nouvelles données, paléoécologie. Palaeontographica Abt. A **223**, 19–101.

SOKOLOVER, N., TAYLOR, P.D. AND ILAN, M. 2016. Bryozoa from the Mediterranena coast of Israel. *Mediterranean Marine Science* **17**(2), 440–458.

WISSHAK, M., BERNING, B., JAKOBSEN, J. AND FREIWALD, A. 2015. Temperate carbonate production: biodiversity of calcareous epiliths from intertidal to bathyal depths (Azores). *Marine Biodiversity* **45**(1), 87–112.

The growth of *Celleporina attenuata* estimated based on the oxygen isotopic compositions and microfocus X-ray CT imaging analysis

Masato Hirose¹*, Aria Ide¹ and Kotaro Shirai²

¹ School of Marine Biosciences, Kitasato University, 1-15-1,
Kitasato, Minami, Sagamihara, Kanagawa 252-0373, Japan [*corresponding author: e-mail: mhirose64@gmail.com]
² Atmosphere and Ocean Research Institute, The University of Tokyo, 5-1-5,
Kashiwanoha, Kashiwa-shi, Chiba 277-8564, Japan

ABSTRACT

A robust erect colony of *Celleporina attenuata* (Ortmann, 1890) has distinct growth bands inside the branch. The growth bands in several branches within a single colony of *C. attenuata* were observed using microfocus X-ray CT, and also a C and O stable isotopic profile through a single branch were analyzed. In the observation with CT, three branches were selected and the linear distances between observed growth bands were measured. The skeletal density of each growth band was also analyzed based on the CT images. At least 11 growth bands were recognized in CT images for each branch; the growth band was formed by increased thickness of the frontal and lateral walls. The linear distance between each growth band was about 4.5 mm; the growth rate was among the three branches. In the isotope analysis, totally 92 samples were collected at intervals of 0.5 mm along the longitudinal axis of the branch using a micro-drilling system. Although some growth bands could not be clearly identified isotopically, most of the growth bands corresponded with the lighter values of δ18O; the results indicate these growth bands were formed during summer and most of them can be regarded as the annual growth periodicity.

INTRODUCTION

As well as corals and foraminiferans, bryozoan carbonate skeletons provide the growth pattern and history of themselves, and also provide information about the past environmental changes. In some foliaceous and branching erect species, bryozoans form periodic check marks on the colony or branch, which are called "growth bands" or "growth checks" (see Key *et al.* 2018). The growth band is generally formed with the thickened skeletal wall of zooids during the period that colony stopping the growth (Pätzold *et al.* 1987), and it is clearly observed with X-ray imaging (Lombardi *et al.* 2006). Growth bands are bracketed by growth checks (Key *et al.* 2018). Most of the previous studies on bryozoan growth bands were based on the flat branches and/or colonies, of such taxa as *Pentapora*, which can be observed without sectioning in most cases (Lombardi et al. 2006; 2008; Knowles *et al.* 2010). Since growth bands showed seasonality in several previous studies (Barnes 1995; O'Dea and Okamura 2000; Key *et al.* 2018), they can be regarded as annual growth indicators which allows estimating colony age and growth rates.

Carbon and oxygen isotopic compositions in biogenic carbonate skeletons are useful for analyzing the growth rate of organisms as well as

past environmental changes. The oxygen isotopic composition ($\delta^{18}O$) shows lower values during the higher temperature and lower salinity of surrounding seawater (Key *et al.* 2018). The carbon isotopic composition ($\delta^{13}C$) shows a lower value as the amount of phytoplankton in food sources are increased (Brey et al. 1999). Furthermore, $\delta^{13}C$ presents a higher value as a result of sexual reproduction in some bryozoans (Bader and Schäfer 2005). Therefore, biogenic carbonate skeletons are a useful indicator of the environment and growth pattern of the organism. Several previous studies estimate the growth rate and/or age of erect bryozoan colonies and environmental changes based on the C and O isotopic compositions of colony skeletons (Pätzold *et al.* 1987; Brey *et al.* 1999; Bader and Schäfer 2005; Smith and Key 2004; Smith *et al.* 2004; O'Dea 2005; Key *et al.* 2008, 2013a, 2013b, 2018; Hirose and Sakai 2019).

Even though, only a few studies measured both the bryozoan growth checks and the isotopic compositions together (Pätzold *et al.*1987; Brey *et al.* 1999; Lombardi *et al.* 2006; 2008; Knowles *et al.* 2010; Key *et al.* 2018). In the first study on the colony of *Pentapora foliacea* Pätzold *et al.* (1987) estimated the age and growth rate of the colony based on the periodic changes of $\delta^{18}O$ and the corresponding growth bands. Another study of *Cellaria incula* from the Antarctic estimated the age of the colony based on the periodic fluctuation of $\delta^{18}O$ and $\delta^{13}C$ between the bifurcated points of the branch (Brey *et al.* 1999). A recent study on *Melicerita chathamensis* Uttley and Bullivant, 1972 clarified that the branch width pattern, the portion and skeletal density of the growth checks determined by X-ray analysis, and the fluctuation pattern of the stable oxygen isotope values corresponded; as a result, the annual growth rate was estimated as 5.5 mm per year (Key *et al.* 2018). Some of the intensive studies on *Pentapora* reconstructed the seasonal changes of seawater temperature based on the isotopic composition, zooid mineralogy, and zooid size (Lombardi *et al.* 2006; 2008; Knowles *et al.* 2010). The study on growth rates and age of

bryozoan colony based on the growth bands and the isotopic compositions, however, have been poorly studied on robust bryozoan colonies and also on the colonies collected from Japanese waters.

Robust colonies of erect bryozoan species *Celleporina attenuata* (Ortmann, 1890) live about 70 m deep at the entrance of Otsuchi Bay, Iwate Prefecture, on the Pacific coast of Tohoku (Hirose *et al.* 2012). The colony of *C. attenuata* has a number of growth checks on its branches (Hirose and Kawamura 2016), and the growth bands correspond with the $\delta^{18}O$ fluctuation pattern (Hirose unpublished data). Otsuchi Bay was damaged by the 2011 Great East Japan Earthquake and tsunami, and the influence of the tsunami on the benthic organisms was studied based on the isotopic compositions of the shell of bivalve *Mercenaria stimpsoni* (Kubota *et al.* 2017; Shirai *et al.* 2018) and *Mytilus galloprovincialis* (Murakami-Sugihara *et al.* 2019). On the other hand, the influence of the tsunami on the benthic organisms in deeper habitats has still been unresolved in detail; therefore, the colony of *C. attenuata* is a potentially useful indicator for the assessment of the impact of the tsunami on the benthic community in the deeper waters (i.e., around 70 m deep). In this study, therefore, we analyzed the growth history of the colony of *C. attenuata* collected from the mouth of Otsuchi Bay based on the observation of growth bands by microfocus X-ray CT system and the isotopic compositions of their skeletal wall. We also attempt to reveal the growth pattern of the colony and uniquely compare the growth rate between different branches within a single colony.

MATERIAL AND METHODS
Collection of the colonies
A robust colony of *Celleporina attenuata* (Fig. 1) was collected by dredge at 67–88 m depth at the mouth of Otsuchi Bay (39°21'56.13"N, 142° 0'0.27"E–39°21'50.45"N, 142° 0'3.30"E), on 27 June 2016 (Fig. 2). The colony is about 6 cm in height and approximately 8 g in the total weight.
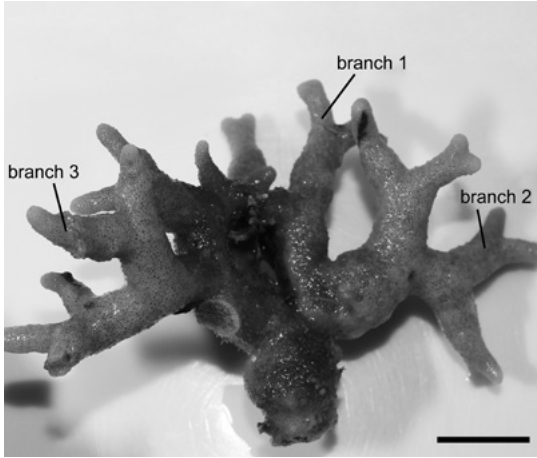
Figure 1. The colony of *Celleporina attenuata* with the branches analyzed in this study. Scale bar = 1 cm.

Observation and analysis of the growth bands

The robust colony of *C. attenuata* (Fig. 1) was observed with a benchtop microfocus X-ray CT system (inspeXio SMX-90CT Plus, SHIMADZU) at 90 kV voltage and 110 µA current, and accurately mapped the position and number of growth checks inside the colony.

Three branches (*branch 1* to *branch 3*) were selected based on the CT images, and an arbitrary cross section image was created for each branch, and the distance between the growth bands in the branch were measured by ImageJ 1.37v software (Image Processing and Analysis in Java, Wayne Rasband, National Institutes of Health, USA: http://rsb.info.nih.gov/ij/). For each measurement,
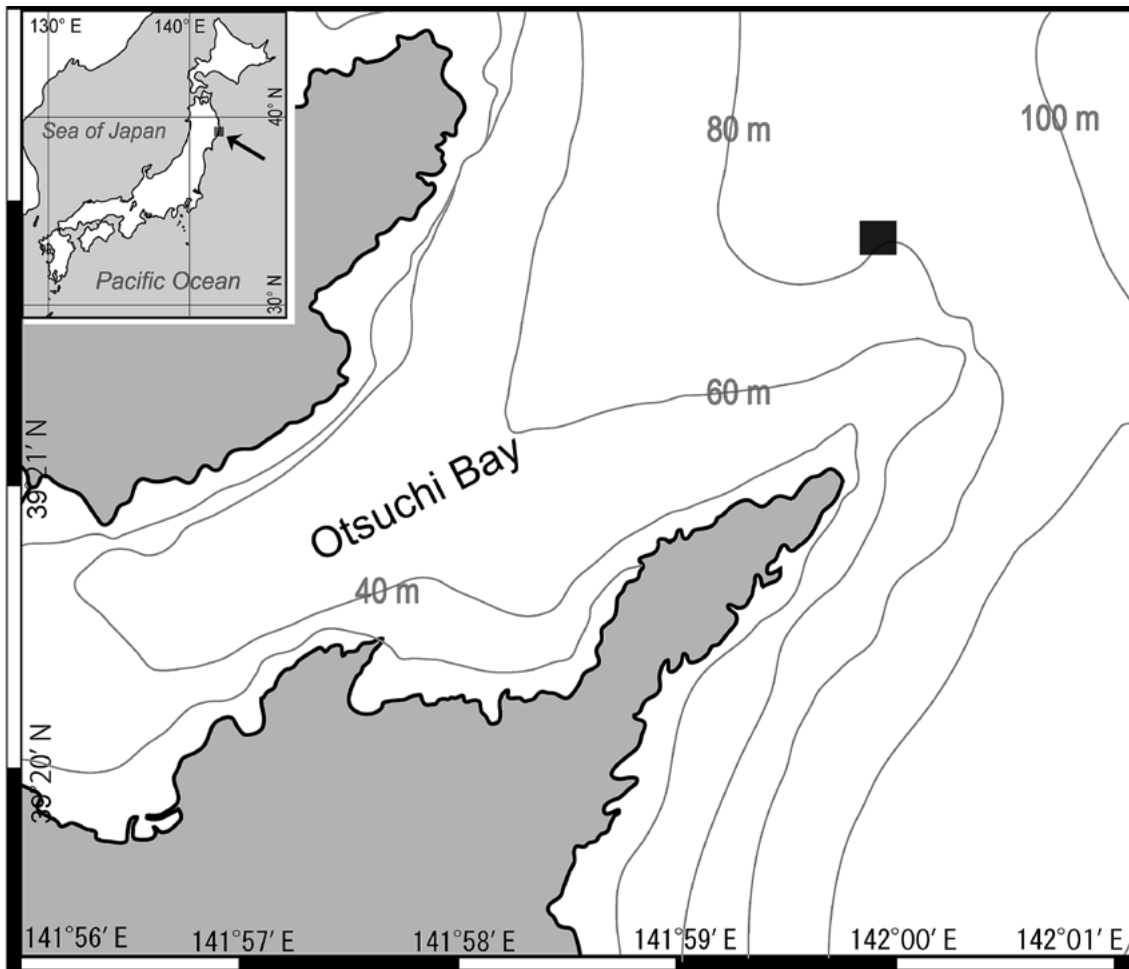
Figure 2. Map showing the localities where the analyzed colony was collected.

three to 11 consecutive images were used, and the length along the branch axis from the tip of the growth band to the tip of the next growth band was measured in each image; the longest length was adopted as the value of the distance between the growth bands.

In addition, the skeletal density of each growth band was quantified based on the pixel value (0 to 255) of the CT images. The pixel value at the tip of the growth band was measured three to 30 times per growth band, and the value with the highest whiteness among them was adopted as the representative value for skeletal density of the growth band. Subsequently, the values were standardized for the comparison among branches. Since the brightness of each image might be slightly different between branches, we selected the growth band at the basal part of the colony that can be observed in all analyzed branches as the reference point. The value of the reference point was set to 0 in each branch and the values of the other growth bands were calculated as the difference from the reference point. Finally, the skeletal density was defined as -35 to -25 at Level 1, -24 to 5 at Level 2, 6 to 35 at Level 3, 36 to 65 at Level 4, and compared between the growth bands and branches.

Collecting and analytical techniques

Based on the result of the observation by the above-mentioned CT images, a single branch which showed clear growth checks without the perforation by a serpulid annelid tube was selected as *Branch 1*. Subsequently, the selected branch was grinded from both sides in the longitudinal direction until the growth band was exposed, and a section of about 1.5 mm thick was obtained. The section was washed with an ultrasonic bath, dried, and attached to a slide glass with an epoxy-based adhesive (Araldite Rapid, Huntsman Japan). The powder samples (each 100–200 μg) for isotope analysis were obtained by drilling the sectioned branch in 1.2 mm deep and 0.5 mm wide using a 0.3 mm diameter micro drill. The powder sampling was carried out at 0.5 mm intervals along the growth axis of branch to obtain a total of 92 layers

of powder sample. The micro drill was cleaned by paper cloth, and the stage and the sample were cleaned by air cleaner every collecting to prevent the inter-sample contamination. In order to precisely assign the position obtaining powder samples to the specific banding pattern of the branch section, a photograph of the branch was taken for every drilling. Powder sample was measured using an isotope ratio mass spectrometer (Delta V plus, Thermo Fisher Scientific), equipped with an automated carbonate reaction device (GasBench II, Thermo Fisher Scientific), installed at the Atmosphere and Ocean Research Institute, the University of Tokyo. Detailed analytical conditions have been reported elsewhere (e.g. Kubota *et al*. 2017). Repeated analysis of the NBS-19 standard yielded an external reproducibility of $\delta^{18}O$ and $\delta^{13}C$ measurements better than 0.15 ‰ and 0.13 ‰, respectively.

RESULTS

Growth bands in the three branches

At least 11 growth bands were observed in the longitudinal section of all branches (*branch 1–3*) as a result of observation by CT (Figs 3, 4). The *Branch 1* (about 4.5 cm in length) revealed 12 growth bands, *Branch 2* (about 4.3 cm in length) 11 growth bands, *Branch 3* (about 4.8 cm in length) with 12 growth bands was perforated by a serpulid annelid tube inside the branch (Fig. 4). *Branch 2* lacked the sixth growth band counting from the end of the branch. The growth band of *Celleporina attenuata* is formed by the thickening of the lateral and frontal wall of the zooecia at the outer margin of the growth band (Fig. 3B).

Isotopic composition of Branch 1

The $\delta^{13}C$ and $\delta^{18}O$ values from *Branch 1* from -4.5‰ to 0.6‰ (average -1.8 ± 1.2‰) and -0.7‰ to 2.0‰ (average 0.9 ± 0.6‰), respectively (Table 1). Among the 12 growth checks observed by CT, nine were consistent with a drop in $\delta^{18}O$ values (Fig. 5). The other three growth bands showed higher $\delta^{18}O$ values and was positioned within increasing
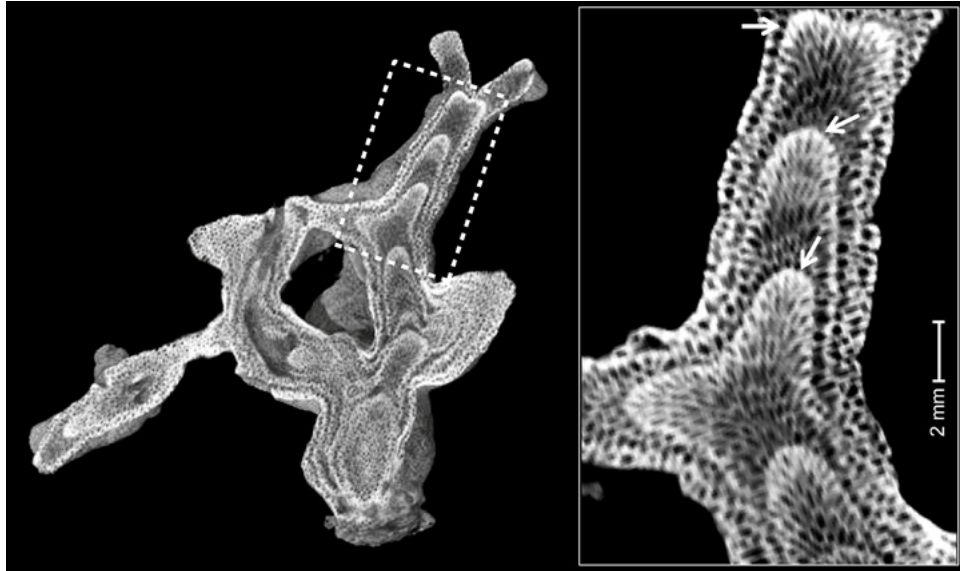
Figure 3. Microfocus X-ray CT image of the examined colony and the enlargement of *Branch 1* shows clear growth bands with thick frontal and lateral walls of zooecia (white arrows).
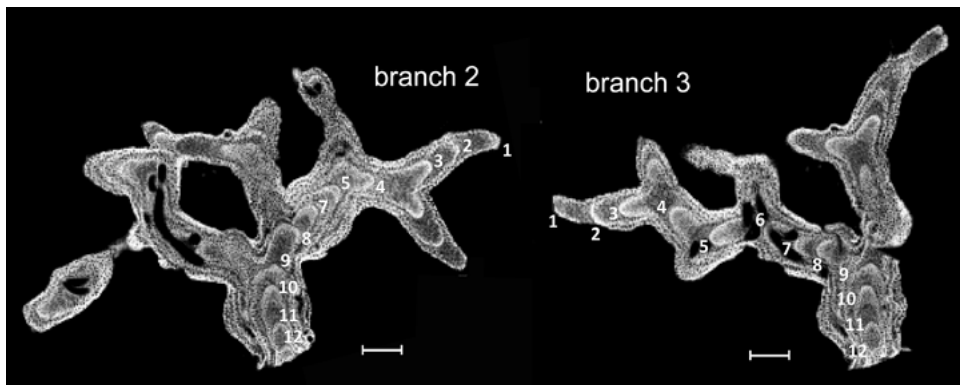
Figure 4. Microfocus X-ray CT images of the examined colony showing *Branch 2* and *Branch 3*. The consecutive numbers from the end of the branch indicated in each branch are corresponding with that in *Branch 1*. The dark area inside the colony is a drilled hole by serpulid polychaeta. Scale bars = 5 mm.

trend in $\delta^{18}O$ values. There were no hidden peaks of lower $\delta^{18}O$ value which did not match the growth bands, in the branch. The growth band which is consistent with the trough of $\delta^{18}O$ shows also lower values in $\delta^{13}C$; five growth bands were consistent with the lower peak of $\delta^{13}C$ values.

The $\delta^{13}C$ and $\delta^{18}O$ values in *Branch 1* showed positive correlations (with the slope of the regression line = 0.39, p = 9.28E-18) (Fig. 6). The part of growth bands consistent with the lower peak of $\delta^{18}O$ also

showed slightly positive correlations (with the slope of the regression line = 0.39, p = 1.07E-13). The part of growth bands inconsistent with the lower peak of $\delta^{18}O$ also shows positive correlations (with the slope of the regression line = 0.36, p = 0.0004).

Distance between the growth bands and the skeletal density

The distance between the growth bands and the skeletal density in each examined branch are

Table 1. Isotopic composition in *Branch 1* shows each analyzed data from the basal part (sample No. 1) to the tip (sample No. 92) of the branch.

Sample No.	δ13C VPDB (‰)	δ18O VPDB (‰)	Sample No.	δ13C VPDB (‰)	δ18O VPDB (‰)	Sample No.	δ13C VPDB (‰)	δ18O VPDB (‰)
1	0.17	1.81	34	−2.83	0.82	67	−1.87	1.08
2	0.12	1.83	35	−0.72	1.45	68	−1.25	1.97
3	0.62	1.39	36	−1.08	1.20	69	−2.16	1.43
4	0.06	1.55	37	−0.26	1.57	70	−1.82	1.12
5	−0.23	1.88	38	−0.81	1.31	71	−1.37	0.94
6	−0.72	1.59	39	−0.54	1.76	72	−2.06	0.65
7	−0.54	1.84	40	−0.82	1.63	73	−2.47	0.06
8	−2.00	0.01	41	−0.32	1.41	74	−0.49	1.50
9	−0.23	0.78	42	−0.46	1.36	75	−0.77	1.49
10	−0.84	0.96	43	−1.04	2.01	76	−0.72	1.57
11	−0.90	1.20	44	−1.42	1.85	77	−0.21	1.47
12	−2.19	0.83	45	−0.61	1.51	78	−0.55	1.30
13	−2.39	1.23	46	−0.73	1.27	79	−1.25	1.05
14	−2.62	0.85	47	−1.32	0.66	80	−1.08	0.91
15	−2.89	0.52	48	−1.17	0.53	81	−1.10	0.68
16	−3.96	-0.37	49	−2.71	0.92	82	−1.39	0.62
17	−3.94	-0.10	50	−2.02	0.88	83	−0.88	0.50
18	−4.52	-0.68	51	−1.06	0.68	84	−1.78	0.69
19	−1.96	0.78	52	−1.04	1.36	85	−1.89	1.07
20	−2.85	0.63	53	−1.94	1.01	86	−2.10	1.09
21	−3.44	0.58	54	−0.83	1.15	87	−2.25	1.14
22	−3.91	0.13	55	−1.52	1.05	88	−2.57	0.90
23	−4.51	-0.56	56	−1.52	1.61	89	−2.76	0.94
24	−4.13	-0.63	57	−2.43	1.15	90	−2.89	0.68
25	−1.07	0.33	58	−2.37	1.36	91	−3.37	0.31
26	−1.65	0.30	59	−2.97	0.56	92	−3.23	0.53
27	−1.88	0.38	60	−2.73	0.58			
28	−1.95	0.66	61	−3.56	0.25			
29	−2.34	0.80	62	−3.12	-0.09	*n*	92	92
30	−2.80	0.59	63	−2.99	-0.31	Min.	**−4.5**	**−0.7**
31	−3.03	0.85	64	−2.84	0.52	Mean	**−1.8**	**0.9**
32	−2.76	1.14	65	−3.09	1.08	Max.	**0.6**	**2.0**
33	−2.52	1.05	66	−1.55	1.97	SD	**1.2**	**0.6**

shown in Table 2. The distance between the 12 growth bands in *Branch 1* were ranged from 2.0 to 6.3 mm (average 4.1 ± 1.5 mm, n = 11). In *Branch 2* and *Branch 3* the distance was ranged from 2.9 to 7.5 mm (average 4.7 ± 1.4 mm, n = 10) and from 2.1 to 7.0 mm (average 4.7 ± 1.6 mm, n = 11) respectively. The distance between two growth bands vary depending

on the year, however, the distances considered to be formed at the same year were almost the same length in all examined branches (Fig. 7).

With regards to the skeletal density, the pixel values in *Branch 1* ranged from 163 to 255, of which five growth bands were classified to level 3 or higher, while the other seven growth bands
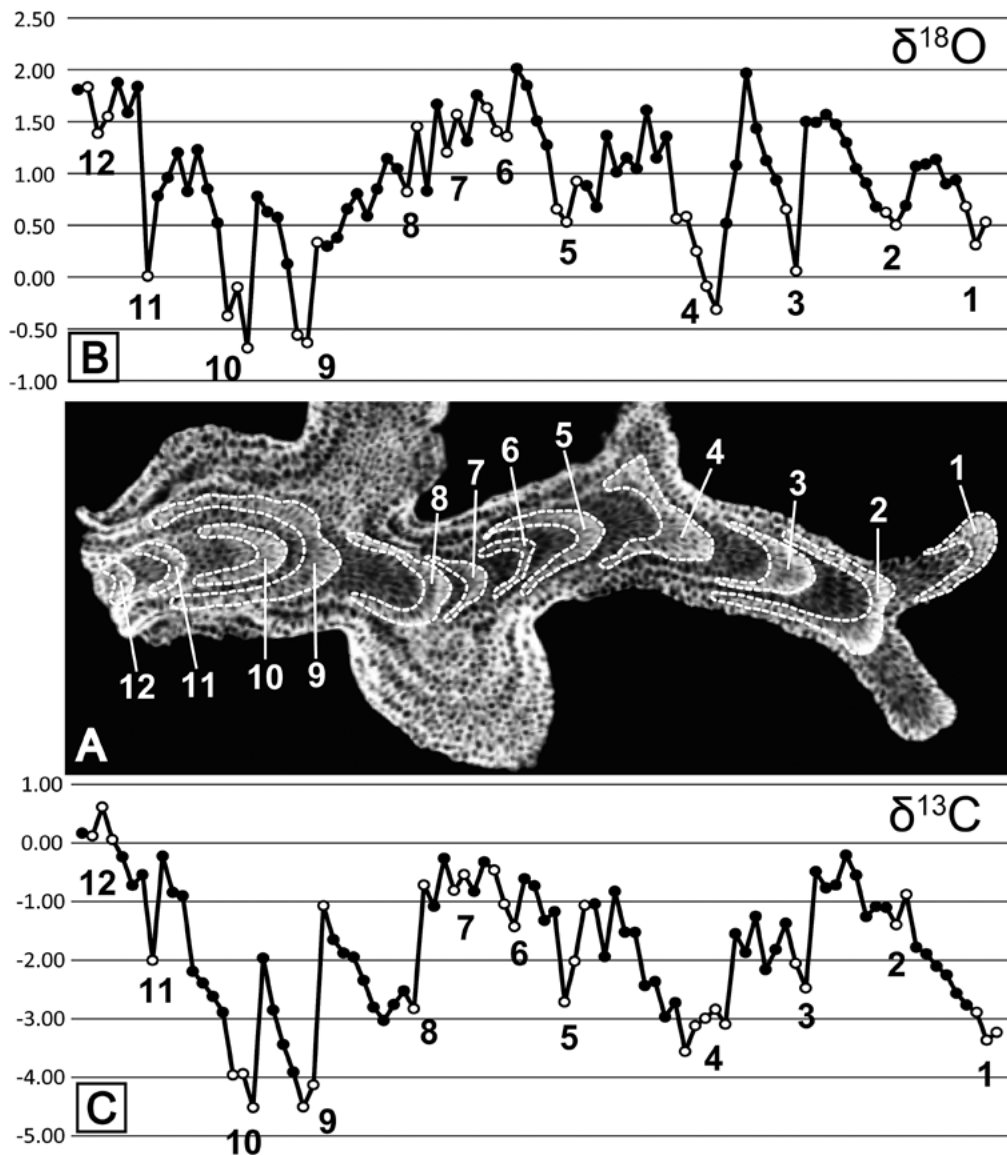
Figure 5. Oxygen and carbon stable isotope profiles along *Branch 1*.
(A) Each growth band is indicated with a dashed white line and numbered consecutively
from the end of the branch. Open circles and the numbers of the isotope profiles indicate each
corresponding growth band (B and C).

$$y = 0.3885x + 1.6305$$
$$R^2 = 0.5607$$
$$p < 0.05$$
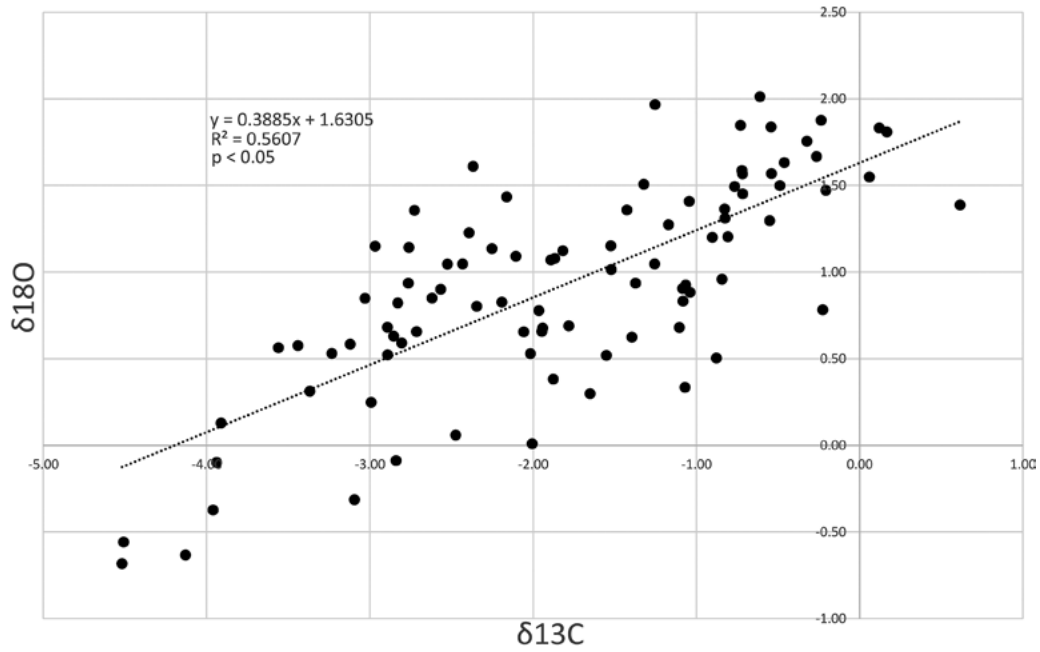
**Figure 6. Oxygen and carbon stable isotope values of the *Branch 1*
showing a strong positive correlation.**
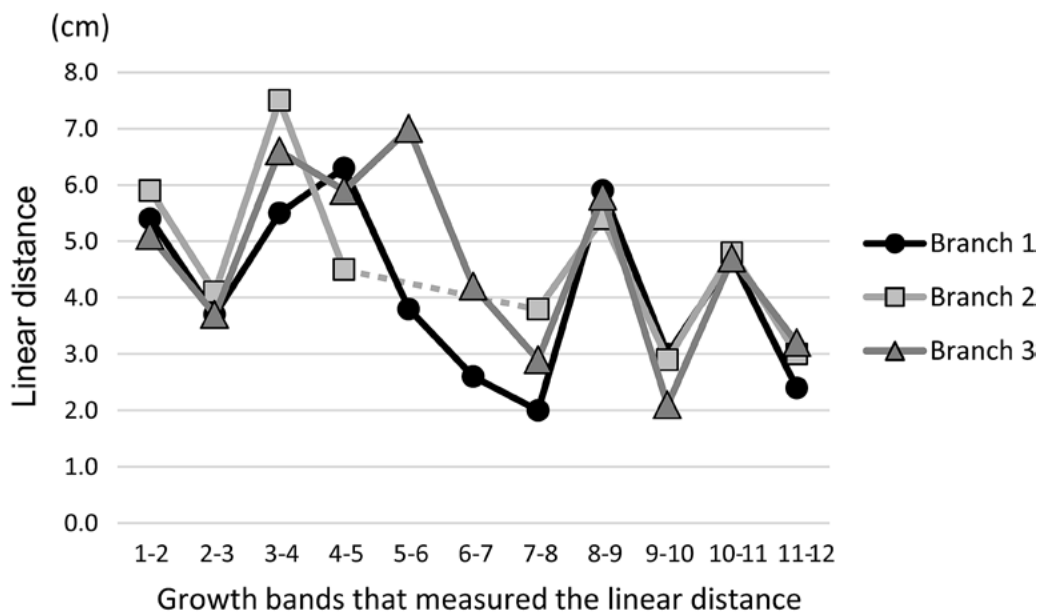
Figure 7. Distance between two growth bands in all examined branches.

Table 2. Distance between the growth bands and the skeletal density in the all examined branches (*Branch 1–3*).

Growth band	Branch 1		Branch 2		Branch 3		
	Level of skeletal density	Linear distance from the adjacent growth band (mm)	Level of skeletal density	Linear distance from the adjacent growth band (mm)	Level of skeletal density	Linear distance from the adjacent growth band (mm)	SD in the linear distance of the three branches
1	3	5.4	3	5.9	2	5.1	0.40
2	4	3.7	4	4.1	4	3.7	0.23
3	3	5.5	4	7.5	4	6.6	1.00
4	3	6.3	4	4.5	4	5.9	0.95
5	2	3.8	4	–	4	7.0	2.26
6	1	2.6	–	–	2	4.2	1.13
7	1	2.0	4	3.8	3	2.9	0.64
8	2	5.9	3	5.4	3	5.8	0.26
9	2	3.0	3	2.9	2	2.1	0.49
10	3	4.7	3	4.8	3	4.7	0.06
11	2	2.4	2	3.0	2	3.2	0.42
12	2	–	4	–	4	–	–
n		11		9		11	
Mean		4.1		4.8		4.7	
Min.		2.0		2.9		2.1	
Max.		6.3		7.5		7.0	
SD		1.5		1.5		1.6	

were classified to lower than level 2 (Table 2). The growth bands without accompanying the lower peak of the $\delta^{18}O$ values tend to show a lower skeletal density than the other growth bands in *Branch 1*. The pixel values in *Branch 2* ranged from 128 to 186, of which 10 growth bands correspond to higher than level 3, whereas another growth band only correspond to lower than level 2. The values in *Branch 3* were ranged from 123 to 196, of which eight growth bands correspond to more than level 3, while the other four growth bands correspond to less than level 2. All examined branches showed a slightly weaker degree of calcification in the growth band at the proximal part of the branch and the distal end of the branch.

DISCUSSION
Growth band formation and the isotopic composition in Celleporina attenuata
The growth bands of the examined colony were found to be formed mainly from the frontal and lateral walls of the zooecia during the growth band formation; most of the growth bands were recognized as broad bands consisting of the almost entire zooid. Both frontal and lateral walls of zooecia in the growth bands showed a slightly thicker wall than the

Table 3. Estimated and actual water temperature (°C) in Otsuchi Bay. Estimated water temperatures were calculated from δ18O values following Kim *et al.*'s (2007) δ18O–temperature relationship.

	Estimated water Temperature	Actual water temperature in Otsuchi Bay
Mean	12.4	13.7
Min.	7.1	6.4
Max.	19.5	19.4
SD	2.9	4.2

zooecia in the other part of the colony; the thickness of zooecial wall in the growth bands and the other part were 0.12–0.23 mm (average 0.17 ± 0.03 mm, n = 10) and 0.11–0.17 mm (average 0.14 ± 0.02 mm, n = 10), respectively.

Significant positive correlation (linear regression, p<0.05) between $\delta^{13}C$ and $\delta^{18}O$ values in the samples from *Branch 1* suggest the influence of a biological vital effect in the examined branch (McConnaughey 1989; McConnaughey *et al.* 1997). The isotopic composition of most of the growth bands on *Branch 1* corresponds with the lower values of $\delta^{18}O$. Although calcium carbonate skeleton formed at higher water temperature and/or lower salinity shows lower $\delta^{18}O$ (e.g. Kim *et al.* 2007), the fluctuation in isotopic composition in the examined colony is thought to reflect the water's temperature rather than the salinity, since the colony of *C. attenuata* examined in this study was collected at about 70 m deep, where the area and depth mainly affected by the Tsugaru Warm Current which has a salinity range from 33.7‰ to 34.2‰ (Hanawa and Mitsudera 1987). The growth bands coincident with the drop in $\delta^{18}O$ values; therefore, it can be regarded as an annual band formed in summer. Furthermore, the water temperature estimated based on the $\delta^{18}O$ values at the growth bands using $\delta^{18}O$-temperature relationship reported by Kim *et al.* (2007) were included within the range of the field

water temperature (Table 3); therefore, the $\delta^{18}O$ values seems to actually reflect the fluctuation of the water temperature. In the preliminary analysis of the colony collected from the same locality in January 2013, the end of branch where the growth band was not observed in the section showed clearly higher $\delta^{18}O$ value (Fig. 8). The result of this preliminary analysis also indicates the active growth of the branch during the winter. Since the nine of twelve growth bands were found to be corresponding to the lower values of $\delta^{18}O$ in *Branch 1*, the examined colony was estimated as at least nine years old. On the $\delta^{13}C$ values of the growth bands, five bands coincided with the peak of $\delta^{13}C$ decline. Fluctuation of $\delta^{13}C$ values was possibly caused by complex environmental and biological factors such as food sources, growth rate, and metabolism.

On the other hand, three of twelve growth bands were found to be not associated with the fluctuation pattern of the $\delta^{18}O$ (named here as "irregular growth band"). Since none of the drop in $\delta^{18}O$ was observed when the "irregular growth bands" were formed, it might be possible to consider that these "irregular growth bands" were not formed during summer. Although there is the possibility that colonies also form a growth band outside summer, it is unlikely that they form three growth bands during the autumn to the next spring and grows more than three times in length compared to the other years. Given that the position where the "irregular growth bands" were observed was located where another branch is radiated, the irregular fluctuation pattern of the $\delta^{18}O$ in this portion is likely attributed from complex nature of skeletal growth and from a deviation of the sampling path from the major growth axis.

Growth rate and skeletal density
At the mean growth rate of the three analyzed branches from the colony of *C. attenuata* was 4.5 ± 1.5 mm (ranged 2.0–7.5 mm) per year while assuming that the growth bands are formed annually. In the comparison between the observed branches,
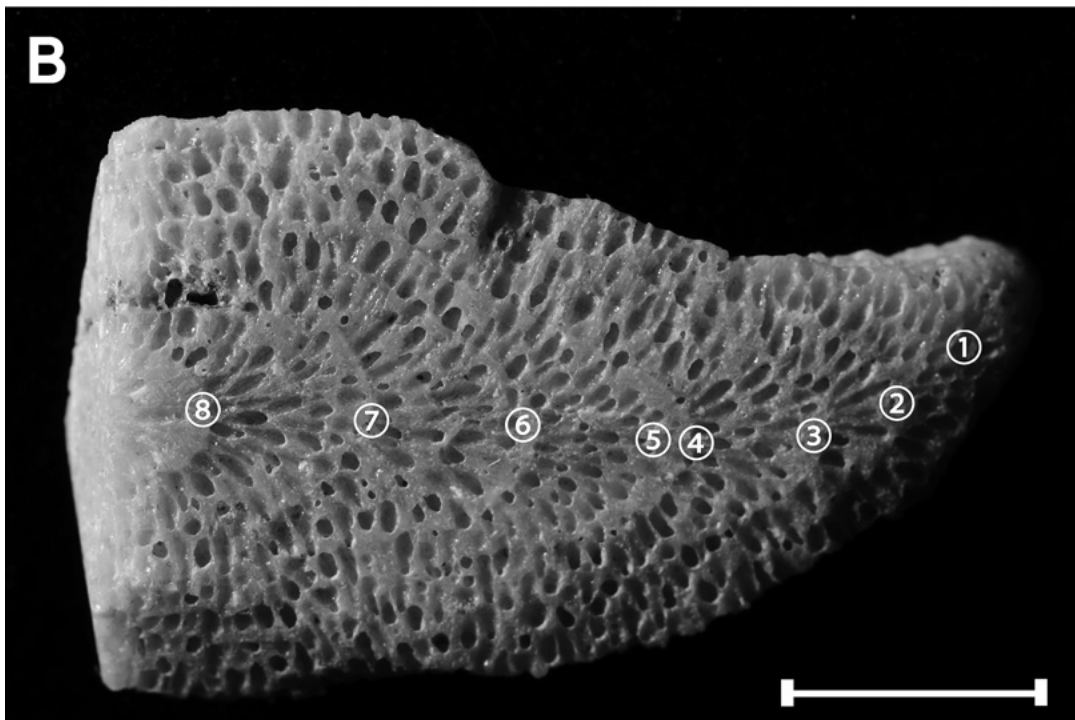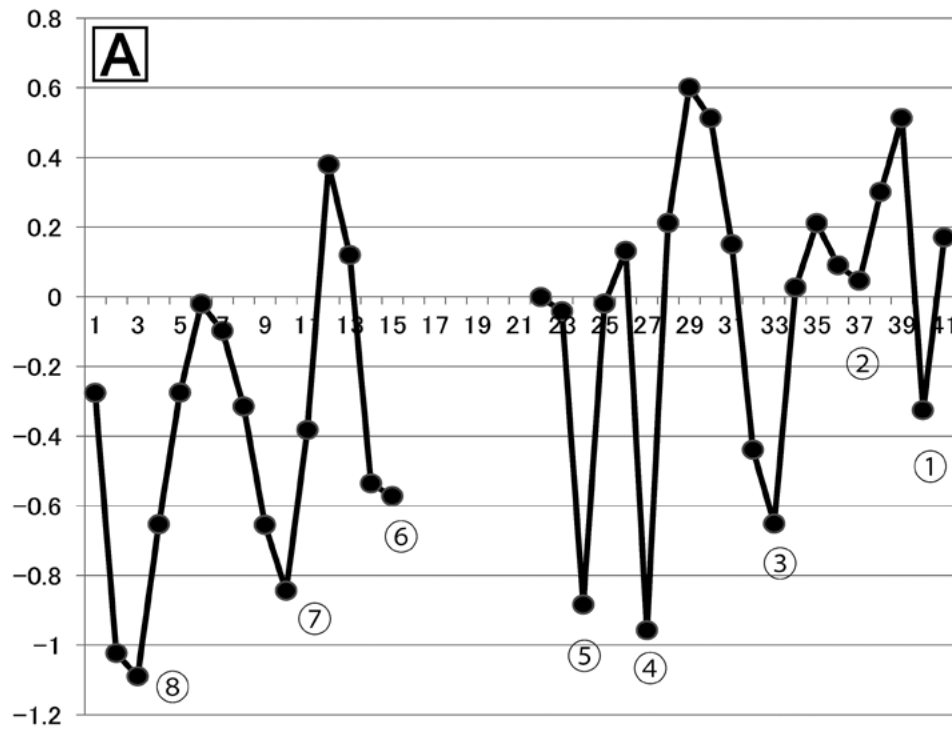
Figure 8. Oxygen stable isotope profile (A) along a branch collected in January 2013 (B) in a preliminary study. Each growth band is numbered consecutivly from the end of the branch. Scale bar = 5 mm.

the distances between the growth bands of the same year tended to be similar in the all observed branches (Table 2); the results suggest that the growth rate of each branch is almost the same within the same year.

The skeletal density tended to weak at the end of the branch in all branches examined in this study; the result indicates the growth band at the end of the branch of the colony collected in June was under construction. On the skeletal density in *Branch 1*, the "irregular growth bands" tended to be weaker than the annual summer growth bands (Fig. 5, Table 2). Some of the annual summer growth bands (e.g. growth band 5 and 9 in *Branch 1*; see Table 2) were however also categorized as lower in the density; therefore, it is difficult to identify whether they were annual rings or not only based on the skeletal density. Although all growth bands showed higher skeletal density in *Branch 2*, the "irregular growth bands" were also considered to be lower in density in different branches of the same colony. Furthermore, *Branch 2* lacks the growth band corresponding to the 6th growth band in *Branch 1*. Since the 6th growth band is an "irregular growth band" with lower density in *Branch 1* and *Branch 3*, it is considered that this growth band may not have been formed in *Branch 2*. Therefore, the formation of "irregular growth bands" may differ depending on the branches even in the same colony. In addition, at the base of the colony, the skeletal density of the growth band varies depending on the direction in the same band (e.g. see 12th growth band in Table 2). The results indicate growth band formation has a directional component to its formation.

More detail analysis of the branch growth rate will enable us to clarify whether growth pattern is consistent among all branches in the same colony or the growth pattern differs depending on the branch. Further study and analysis are needed to clarify whether the factors and mechanism that cause the difference in growth rate are determined by the marine environment or by biological factors of the bryozoan itself.

CONCLUSIONS

Carbon and Oxygen isotope profiles and microfocus X-ray CT imaging revealed that *Celleporina attenuata* in Otsuchi Bay, Japan forms growth band by increasing the thickness of the frontal and lateral walls of zooecia during the summer. The growth bands can be regarded as annual growth indicators. However, some growth bands may not have formed during the summer. Although there are still issues left in considering the growth bands as indicators of the colony age, the observation of the growth bands in several branches by microfocus X-ray CT is a quite useful method for comparing and estimating the growth rate of the branches within a colony. In the colony observed in this study, the distance between the growth bands indicated the growth of the colony was approximately 4.5 mm per year and the growth rate was not very different between branches, whereas the skeletal density of the growth bands showed differences depending on the branch and direction.

ACKNOWLEDGMENTS

REFERENCES

BADER, B. AND SCHÄFER, P. 2005. Impact of environmental seasonality on stable isotope composition of skeletons of the temperate bryozoan *Cellaria sinuosa*. *Palaeogeography, Palaeoclimatology, Palaeoecology* **226**, 58–71.

BREY, T., GERDES, D., GUTT, J., MACKENSEN, A. AND STARMANS, A. 1999. Growth and age of the Antarctic bryozoan *Cellaria incula* on the Weddell Sea shelf. *Antarctic Science* **11**(4), 408–414.

BARNES, D.K.A. 1995. Seasonal and annual growth in erect species of Antarctic bryozoans. *Journal of Experimental Marine Biology and Ecology* **188**(2), 181–198.

HANAWA, K. AND MITSUDERA, H. 1987. Variation of Water System Distribution in the Sanriku Coastal Area. *Journal of the Oceanographical Society of Japan* **42**, 435–446.

HIROSE, M. AND KAWAMURA, T. 2016. Sessile organisms in Otsuchi Bay and Matsushima Bay after the Great East Japan Earthquake and Tsunami. In: K. Kogure, M. Hirose, H. Kitazato and A. Kijima (eds), *Marine ecosystems after Great East Japan Earthquake in 2011. Our knowledge acquired by TEAMS*, Tokai University Press, Kanagawa, pp. 71–72.

HIROSE, M., MAWATARI, S.F. AND SCHOLZ, J. 2012. Distribution and diversity of erect bryozoans along the Pacific coast of Japan. In: A. Ernst, P. Schaefer and J. Scholz (eds), *Bryozoan Studies 2010. Lecture Notes in Earth System Sciences* 143, Heidelberg, Springer, pp. 121–136.

HIROSE, M. AND SAKAI S. 2019. Carbon and oxygen isotopic composition in lepralioid and umbonuloid frontal shields of two adeonid bryozoans from southwestern Japan. In: R. Schmidt, C.M. Reid, D.P. Gordon, G. Walker-Smith, S. Martin and I. Percival (eds) *Bryozoan Studies 2016. Memoirs of the Australasian Association of Palaeontologists*, vol. 52, Melbourne.

KEY, M.M., JR., WYSE JACKSON, P.N., MILLER, K.E. AND PATTERSON, W.P. 2008. A stable isotope test for the origin of fossil brown bodies in trepostome bryozoans from the Ordovician of Estonia. In: S.J. Hageman, M.M. Key, Jr. and J.E. Winston (eds) *Bryozoan Studies 2007. Virginia Museum of Natural History Special Publication* no. 15, Martinsville, pp. 75–84.

KEY, M.M., JR., HOLLENBECK, P.M., O'DEA, A. AND PATTERSON, W.P. 2013a. Stable isotope profiling in modern marine bryozoan colonies across the Isthmus of Panama. *Bulletin of Marine Science* **89**(4), 837–856.

KEY, M.M., JR., ZÁGORŠEK, K. AND PATTERSON, W.P. 2013b. Paleoenvironmental reconstruction of the Early to Middle Miocene Central Paratethys using stable isotopes from bryozoan skeletons. *International Journal of Earth Sciences* **102**(1), 305–318. https://doi.org/10.1007/s00531-012-0786-z

KEY, M.M., JR., ROSSI, R.K., SMITH, A.M., HAGEMAN, S.J. AND PATTERSON, W.P. 2018. Stable isotope profiles of skeletal carbonate validate annually-produced growth checks in the bryozoan *Melicerita chathamensis* from Snares Platform, New Zealand. *Bulletin of Marine Science* **94**(4), 1447–1464.

KIM, S.T., O'NEIL, J.R., HILLAIRE-MARCEL, C. AND MUCCI, A. 2007. Oxygen isotope fractionation between synthetic aragonite and water: Influence of temperature and Mg2+ concentration. *Geochimica et Cosmochimica Acta* **71**, 4704–4715.

KNOWLES, T., LENG, M.J., WILLIAMS, M., TAYLOR, P.D., SLOANE, H.J. AND OKAMURA, B. 2010. Interpreting seawater temperature range using oxygen isotopes and zooid size variation in *Pentapora foliacea* (Bryozoa). *Marine Biology* **157**, 1171–1180.

KUBOTA, K., SHIRAI, K., MURAKAMI-SUGIHARA, N., SEIKE, K., HORI, M. AND TANABE, K. 2017. Annual shell growth pattern of the Stimpson's hard clam *Mercenaria stimpsoni* as revealed by sclerochronological and oxygen stable isotope measurements. *Palaeogeography, Palaeoclimatology, Palaeoecology* **465**, 307–315.

LOMBARDI, C., COCITO, S., HISCOCK, K., OCCHIPINTI-AMBROGI, A., SETTI, M. AND TAYLOR, P.D. 2008. Influence of seawater temperature on growth bands, mineralogy and carbonate production in a bioconstructional bryozoan. *Facies* **54**, 333–342.

LOMBARDI, C., COCITO, S., OCCHIPINTI-AMBROGI, A. AND HISCOCK, K. 2006. The influence of seawater temperature on zooid size and growth rate in *Pentapora fascialis* (Bryozoa: Cheilostomata). *Marine Biology* **149**, 1103–1109.

MCCONNAUGHEY, T.A. 1989. ^{13}C and ^{18}O isotopic disequilibrium in biological carbonates: I. patterns. *Geochimica et Cosmochimica Acta* **53**, 151–162.

MCCONNAUGHEY, T.A., BURDETT, J., WHELAN, J.F. AND PAULL, C.K. 1997. Carbon isotopes in biological carbonates: respiration and photosynthesis. *Geochimica et Cosmochimica Acta* **61**, 611–622.

MURAKAMI-SUGIHARA, N., SHIRAI, K., HORI, M., AMANO, Y., FUKUDA, H., OBATA, H., TANAKA, K., MIZUKAWA, K., SANO, Y., TAKADA, H. AND OGAWA, H. 2019. Mussel shell geochemical analyses reflect coastal environmental changes following the 2011 Tohoku tsunami. *ACS Earth and Space Chemistry* **3**(7), 1346–1352.

O'DEA, A. 2005. Zooid size parallels contemporaneous oxygen isotopes in a large colony of *Pentapora foliacea* (Bryozoa). *Marine Biology* **146**, 1075–1081.

O'DEA, A. AND OKAMURA, B. 2000. Life history and environmental inference through retrospective morphometric analysis of bryozoan:a preliminary study. *Journal of the Marine Biological Association of the United Kingdom* **80**(6), 1127–1128.

PÄTZOLD, J., RISTEDT, H. AND WEFER, G. 1987. Rate of growth and longevity of a large colony of *Pentapora foliacea* (Bryozoa) recorded in their oxygen isotope profiles. *Marine Biology* **96**, 535–538.

SHIRAI, K., KUBOTA, K., MURAKAMI-SUGIHARA, N., SEIKE, K., HAKOZAKI, M. AND TANABE, K. 2018. Stimpson's hard clam *Mercenaria stimpsoni*; a multi-decadal climate recorder for the northwest Pacific coast. *Marine Environmental Research* **133**, 49–56.

SMITH, A.M. AND KEY, M.M., JR. 2004. Controls, variation, and a record of climate change in detailed stable isotope record in a single bryozoan skeleton. *Quaternary Research* **61**, 123–133.

SMITH, A.M., NELSON, C.S., KEY, M.M., JR. AND PATTERSON, W.P. 2004. Stable isotope values in modern bryozoan carbonate from New Zealand and implications of paleoenvironmental interpretation. *New Zealand Journal of Geology & Geophysics* **47**, 809–821.

Estimating colony age from colony size in encrusting cheilostomes

Marcus M. Key, Jr.

Department of Earth Sciences, Dickinson College, Carlisle, PA 17013-2896, USA
[e-mail: key@dickinson.edu]

ABSTRACT

The goal of this study is to develop a method of estimating colony age in encrusting cheilostomes from colony size. This will be useful for estimating colony age of small encrusting epibiotic bryozoans on ephemeral motile host animal substrates (e.g., exoskeletons of crabs that are susceptible to molting). Colony age (i.e., number of days) was modelled from colony size (i.e., number of zooids) from data collected by Xixing *et al.* (2001) on five cheilostome species grown in the laboratory. The growth of each species was measured in two different seasons for a total of 10 growth curves. The curves were best modelled by the following power function: $y = 0.2053x^{2.2663}$ (y = number of zooids, x = number of days, $R^2 = 0.97$). This function was then used to estimate the ages of encrusting epibiotic cheilostome bryozoan colonies from the author's previous studies on extant and extinct epibiotic bryozoans found on ephemeral motile host animal substrates. When using these kinds of predictive growth curves, it is important to stress that bryozoan growth rates are a function of several variables and so an estimated colony age range is recommended rather than simply a single "best guess" age.

INTRODUCTION

Of all research on bryozoan growth rates, encrusting colonies have received the most attention. This is most likely because they are more easily grown in both the laboratory and field and their more two-dimensional nature is more easily measured than other more three-dimensional zoarial morphologies such as erect colonies (Smith 2007, 2014; Smith and Key 2019). This study focuses on growth rates in encrusting bryozoans. Early work on measuring growth rates of encrusting bryozoan colonies began with Lutaud (1961) on the best-documented species, *Membranipora membranacea*. Since then, numerous studies have examined the various factors affecting bryozoan colony growth rates (Table 1).

In studies of encrusting epibiotic bryozoans living on host animals, being able to estimate colony age from colony size would useful for constraining the age of the host. Some motile host animals provide only ephemeral substrates due to skin shedding (e.g., sea snakes: Key *et al.* 1995) or molting of their exoskeleton (e.g., arthropods: Key and Barnes 1999; Key *et al.* 1996a, b, 1999, 2000, 2013, 2017). Knowing colony age would help constrain intermolt duration of the hosts, especially fossil hosts (e.g., Gili *et al.* 1993; Key *et al.* 2010, 2017). Therefore, the goal of this study is to model encrusting cheilostome colony age from colony size as quantified by the number of zooids which can be more easily measured on fossil host exoskeletons.

I follow the terminology of Wahl (1989) and refer to the motile hosts as basibionts (i.e. the host substrate organisms) and the bryozoans as epibionts (i.e. the

Table 1. Known variables that affect encrusting bryozoan colony growth rates.

Variable	Reference(s)
Food availability	Winston 1976; Cancino and Hughes 1987; Hughes 1989; O'Dea and Okamura 1999; Hermansen *et al.* 2001
Competition for food along the margins of neighboring colonies	Buss 1980; McKinney 1992, 1993
Temperature	O'Dea and Okamura 1999; Amui-Vedel *et al.* 2007
Water flow velocity	Hughes and Hughes 1986; Cancino and Hughes 1987; Pratt 2008; Sokolover *et al.* 2018
Availability of substrate space with adjacent colonies competing for space	Stebbing 1973; Yoshioka 1982
Availability of substrate space without adjacent colonies	Winston and Hakansson 1986
Presence of associated fauna	Cocito *et al.* 2000
Relative investment in sexual reproduction vs. asexual colony growth	Harvell and Grosberg 1988; Hughes 1989; Herrera *et al.* 1996
Development of anti-predatorMorphologies	Harvell 1986, 1992; Grünbaum 1997
Genetic variation	Bayer and Todd 1996

sessile organisms attached to the basibiont's outer surface without trophically depending on it). Following the terminology of Taylor and Wilson (2002), I will focus on epibionts as opposed to endosymbionts as the bryozoans are ectosymbionts or episkeletozoans inhabiting the surface of their basibiont host.

MATERIALS AND METHODS

To model growth in encrusting bryozoans, the rich growth rate datasets from Xixing *et al.* (2001) were used. Their tables 14–15, 18–20 list growth rates of five fouling marine cheilostome species raised on artificial substrates in the laboratory (Table 2). They are all exclusively encrusting species except for *Membranipora grandicella* and *Watersipora subtorquata* which can become erect during later astogeny, but these species only exhibited encrusting growth during the study. Xixing *et al.* (2001) report data from two different growth periods in the summer of 1995 (i.e., the slightly cooler months of May–June and the slightly warmer months of July–August) for each species. Small colonies, consisting of ancestrulae, were collected on panels in 2–8 m depth and transported to the laboratory. There were

collected from the mouth of Jiaozhou Bay offshore of Qingdao, China located on the Yellow Sea at ~36°01'N, 120°20'E. The authors tried to mimic the conditions in the coastal waters of Qingdao as far as temperature, salinity, and food availability, but not the presence of predators. During the laboratory experiments, salinity was held constant at 32 ppt. Water temperatures for the May–June experiments ranged from 15 to 24°C, while in July–August they ranged from 24 to 28°C. The bryozoans were fed a diet of $1–2\times10^5$ cells twice per day of unicellular marine microalgae consisting of *Platymonas* sp. 1048, *Isochrysis galbana* 3011, and *Phaeodactylum tricornutum* 2038. The authors reported that other than the effect of predators, the growth rates in the laboratory paralleled those observed on artificial and natural substrates offshore. Epibionts on ephemeral motile basibionts experience almost no predation (Ross 1983). Therefore, Xixing *et al.*'s (2001) growth rates should be generally representative of encrusting epibiont cheilostomes growing in temperate marine environments. The authors report the number of zooids by the number of days of growth (Table 2). The number zooids counted per colony ranges from 391 to 1644 (mean: 744, standard deviation: 325

zooids). The number of days of growth ranges from 30 to 66 (mean: 44, standard deviation: 14 days).

The rate of asexual zooid replication increases with colony size in many bryozoan species (Lutaud 1983; Winston and Jackson 1984; Hughes and Hughes 1986; Lidgard and Jackson 1989). Therefore, the rate of growth in the number of zooids is non-linear. There are five commonly used curves to model such growth: exponential, power, Gompertz, logistic, and Bertalanffy (Kaufmann 1981). The standard graphing practice of Kauffman (1981) was followed with the horizontal (x) axis being time and the vertical (y) axis being size. The best fit curve for each of Xixing *et al.*'s (2001) 10 laboratory experiments was calculated.

RESULTS AND DISCUSSION

The power curve model had the highest R^2 values (mean = 0.97, range: 0.93–0.98, standard deviation = 0.17) for each of the 10 data sets (Fig. 1, Table 2). The equation of a power growth curve is $y = ax^b$. In this study, y = colony size (i.e., the number of zooids), x = time (i.e., the number of days of growth), a = value of the coefficient in the power function (a.k.a., the proportionality constant), and b = value of the exponent (i.e., the power to which x is raised). Combining the data from all five species, the mean growth curve for the cooler late

spring–early summer months (i.e., May–June) is $y = 0.1522x^{2.3490}$, and the mean growth curve for the warmer late summer months (i.e., July–August) is $y = 0.2583x^{2.1836}$ (Fig. 2). The mean growth curves are not significantly different between May–June and July–August (t-Tests, coefficient and exponent in power function, $P = 0.36$ and $P = 0.27$, respectively). Therefore, all 10 curves were combined into the mean growth power curve of $y = 0.2053x^{2.2663}$ (Table 2).

The growth curves of the young colonies in this study lack the early steeply concave up, exponential start and late concave down end of a sigmoidal curve. Young colonies often show the early steeply concave up, exponential start (Winston 1976) whereas some longer lived encrusting bryozoans show a more sigmoidal growth curve (Hayward and Ryland 1975; Kaufmann 1981). The latter are better modelled by a Gompertz growth curve (Kaufmann 1981; Karkach 2006). Xixing *et al.* (2001, p. 785) noted the absence of this classic logarithmic increase in the number of zooids in the youngest part of the colonies, and the experiments were not run long enough to document any later astogenetic slowdown in growth. The species in this study always had a concave up growth curve best modelled by a power curve (Kaufmann 1981). The power function has been previously used to model growth in bryozoans (Hartikainen *et al.* 2014).
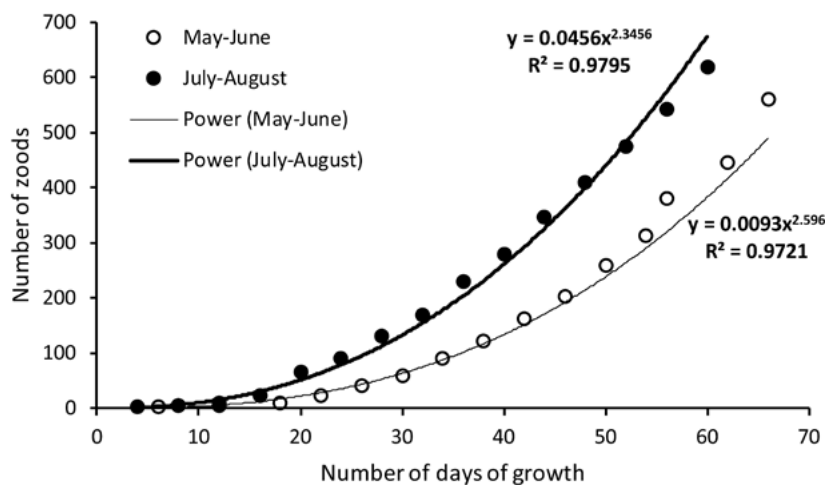
Figure 1. Growth curves for the cheilostome *Watersipora subtorquata*. Data from Xixing *et al.* (2001, table 20).

Table 2. Summary growth rate data of encrusting cheilostome bryozoans grown in the laboratory by Xixing *et al.* (2001).

Table number in Xixing *et al.* (2001)	Species	Growth season	Total number of zooids counted	Total days of growth	Mean number of days between measurements	R² value	Value of coefficient in power function	Value of exponent in power function
14	*Membranipora grandicella*	May-June	660	38	2.4	0.9765	0.0828	2.4255
14	*Membranipora grandicella*	July-August	929	32	2.0	0.9839	0.4999	2.1270
15	*Electra tenella*	May	633	30	2.0	0.9825	0.4625	2.0468
15	*Electra tenella*	July	1644	30	2.0	0.9773	0.2599	2.4721
18	*Schizoporella unicornis*	May-June	649	58	2.9	0.9555	0.0324	2.3412
18	*Schizoporella unicornis*	July-August	656	36	2.1	0.9838	0.2474	2.1258
19	*Cryptosula pallasiana*	May	702	30	2.0	0.9632	0.1740	2.3354
19	*Cryptosula pallasiana*	July-August	391	60	4.0	0.9299	0.2387	1.8476
20	*Watersipora subtorquata*	May-June	560	66	4.4	0.9721	0.0093	2.5960
20	*Watersipora subtorquata*	July-August	618	60	4.0	0.9795	0.0456	2.3456
		Number:	10	10	10	10	10	10
		Minimum:	391	30	2.0	0.9299	0.0093	1.8476
		Mean:	744	44	2.8	0.9704	0.2053	2.2663
		Maximum:	1644	66	4.4	0.9839	0.4999	2.5960
		Standard deviation:	325	14	0.9	0.0161	0.1639	0.2135

Since the goal of this study is to estimate colony age of small encrusting cheilostome colonies on ephemeral hard substrates such as arthropod carapaces, the power curve is the best way to model the growth. Because the ephemeral substrates the basibionts produce do not provide long-lived substrates for bryozoans, I chose to model growth using higher temporal resolution, shorter duration growth studies. For example, Hayward and Ryland (1975, fig. 2) measured growth in *Alcyonidium hirsutum* for almost a year, so they took monthly measurements (i.e., roughly every 30 days). Most ephemeral basibiont substrates do not last that long due to the basibiont molting or shedding. The data from Xixing *et al.* (2001) included up to two months of growth data, but measurements were made on average every three days

(mean = 2.8, range = 2.0–4.4, standard deviation = 0.9 days). For larger/older colonies (e.g., *Alcyonidium hirsutum* in Hayward and Ryland (1975, fig. 2)), a more sigmoidal growth curve (e.g., Gompertz) may be more applicable than a power curve as used here.

To demonstrate the utility of the equations in Table 2, I applied them to previous studies where the number of zooids were reported for colonies encrusting basibionts that produce ephemeral substrates (Table 3). Ideally one would apply the predictive models to the same species as growth rates vary among species (Smith 2007, 2014; Smith and Key 2019), and to species growing in the same location and environmental conditions as growth rates vary in response to different environmental conditions (Table 1). Being this restrictive would be the most conservative approach but would greatly limit its

applicability. When using these equations to estimate colony age, these limitations must be kept in mind. But for the fossil record of small colonies encrusting crab carapaces, it is recommended to use the equations to bracket a range of colony ages to the nearest order of magnitude. Therefore, the equations were herein used to calculate a minimum, mean, and maximum estimated colony age (Table 3). One must also keep in mind that in fossils, colonies may not be completely intact, so some zooids may be missing from the count.

The calculated mean colony ages ranged from 6 to 31 days, depending on the size of the colony (Table 3). The calculated range in colony ages was 4–246 days (i.e., two orders of magnitude variation). This large range is not due as much to variation in growth rate, which are surprisingly constrained (Table 2) but is more due to variation in colony size. Colony size varies greatly depending on the host (Table 3), typically in proportion to host age and intermolt duration (Gili *et al.* 1993).

These colony age estimates also help constrain the duration of the host substrate between shedding or molting events, unless the host species experiences terminal anecdysis. A few crab species do this (i.e., continue to live without molting after reaching sexual reproduction) (Abelló *et al.* 1990; Fernandez-Leborans, 2010). In those cases, minimum colony age is a more accurate way to estimate intermolt duration. Estimating epibiont bryozoan colony age is useful for fossil basibionts where intermolt duration is often impossible to constrain. For example, in trilobites with morphologically distinct developmental stages (e.g., Park and Choi 2011, fig. 4), the number of zooids counted in a colony on a fouled basibiont would indicate the minimum time since the last molt. In the hosts listed in Table 3, the minimum intermolt duration indicated by the minimum colony age varies from 4–14 days, a much more constrained range than 4–246 days. Of course, the estimated intermolt durations should be most accurate if restricting their use to Cenozoic fossil crabs fouled by cheilostomes as indicated in Table 3 as opposed to Paleozoic stenolaemates, for example.

In a microevolutionary fitness sense, the colonies must achieve sexual reproduction before the basibiont molts/sheds in order for the epibiotic relationship to
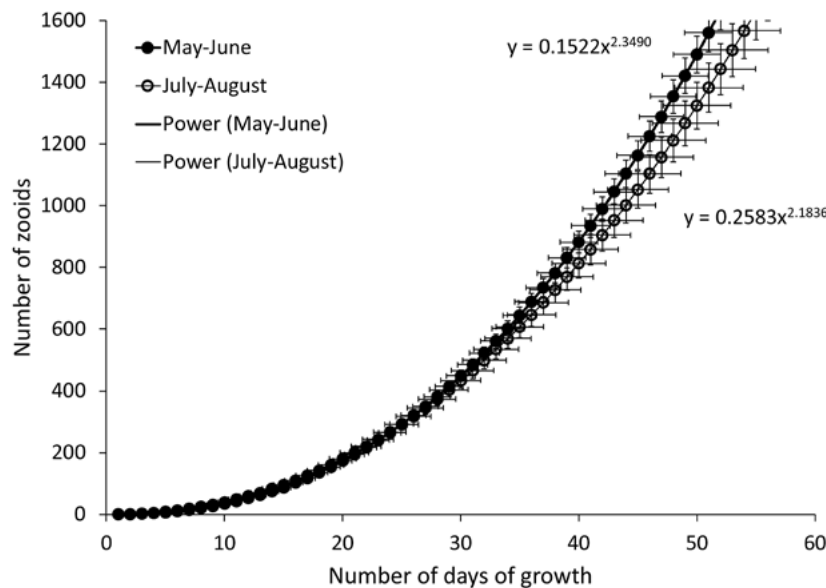
Figure 2. Mean growth curve for the cooler late spring-early summer months (i.e., May-June) and the warmer late summer months (i.e., July-August) averaged from the five cheilostome species in Table 2. Error bars indicate variation among species in each growth period.

Table 3. Estimated ages of encrusting epibiotic cheilostome bryozoan colonies from author's previous studies. Colony ages were calculated from modelled growth curves based on the number of zooids per colony and the minimum, mean, and maximum power functions in Table 2.

Epibiont bryozoan species	Basibiont host species	Source	Geologic age	# of zooids	Colony age (days)		
					Min.	Mean	Max.
Arbopercula (Electra) angulata	*Lapemis hardwickii* (sea snake)	Key *et al.* (1995)	Extant	14-16	4	6-7	52-56
Arbopercula (Electra) angulata	*Enhydrina schistosa* (sea snake)	Key *et al.* (1995)	Extant	19-156	4-9	7-19	62-193
Acanthodesia sp.	*Myra* sp. (crab)	Key *et al.* (2017)	Miocene	22	4	8	67
Indeterminate ascophoran	Indeterminate crab	Key *et al.* (2017)	Miocene	35-243	5-11	10-23	86-246
Thalamoporella sp.	Indeterminate crab	Key *et al.* (2017)	Miocene	504	14	31	365
Acanthodesia sp.	Indeterminate leucosiid crab	Key *et al.* (2017)	Miocene	43	6	11	96

benefit the bryozoan. Unfortunately, age of onset of sexual reproduction in bryozoan colonies is not often recorded in longitudinal studies due to the length of time required. Colony size at sexual maturity in encrusting cheilostome species ranges widely. For example, *Rallocytus ridiculs* reached sexual maturity at only four zooid size, many interstitial species reached sexual maturity by <10 zooids, *Drepanophora* sp. by 30 zooids, *Parasmittina* sp. and *Stylopoma spongites* by 150 zooids, but *Stylopoma* sp. not until it had 4600 zooids (Jackson and Wertheimer, 1985; Winston and Hakansson, 1986; Herrera *et al.* 1996; Grishenko *et al.* 2018). Applying the highest number to the encrusting colonies in Table 3, none ever reached sexual reproduction. Applying the lowest number, all reached sexual reproduction. Applying the mode (i.e., 150 days) most never reached the age of sexual reproduction. Unfortunately, most of the bryozoan species listed in Table 3 do not produce ovicells, which would have provided an independent test of female (though not male) sexual reproduction. For those colonies not reaching sexual maturity, the relationship with their host would be better described as commensalism. For those colonies that were estimated to have lived long enough to reach sexual maturity (e.g., *Thalamoporella* sp. growing on an Eocene crab which lived up to 365 days), the relationship with their host was potentially mutualistic (Key and Schweitzer, 2019).

This study highlights the importance of publishing raw data tables, not just summary statistics or graphs, or at least including supplemental data tables or appendices. You never know how your data could be mined at a later date for another seemingly unrelated study.

REFERENCES

ABELLÓ, P., VILLANUEVA, R. AND GILI, J.M. 1990. Epibiosis in deep-sea crab populations as indicator of biological and behavioural characteristics of the host. *Journal of the Marine Biological Association of the United Kingdom* **70**, 687–695.

AMUI-VEDEL, A.-M., HAYWARD, P.J. AND PORTER, J.S. 2007. Zooid size and growth rate of the bryozoan *Cryptosula pallasiana* Moll in relation to temperature, in culture and in its natural environment. *Journal of Experimental Marine Biology and Ecology* **353**, 1–12.

BAYER, M.M. AND TODD, C.D. 1996. Effect of polypide regression and other parameters on colony growth in the cheilostomate *Electra pilosa* (L.). In: D.P. Gordon, A.M. Smith and J.A. Grant-Mackie (eds), *Bryozoans in Space and Time*. Wellington, National Institute of Water and Atmospheric Research, pp. 29–38.

BUSS, L.W. 1980. Bryozoan overgrowth interactions – the interdependence of competition for space and food. *Nature* **281**, 475–477.

CANCINO, J.M. AND R.N. HUGHES. 1987. The effect of water flow on growth and reproduction of *Celleporella hyalina* (L.) (Bryozoa: Cheilostomata). *Journal of Experimental Marine Biology and Ecology* **112**, 109–130.

COCITO, S., FERDEGHINI, F., MORRI, C. AND BIANCHI C.N. 2000. Patterns of bioconstruction in the cheilostome bryozoan *Schizoporella errata*: the influence of hydrodynamics and associated biota. *Marine Ecology Progress Series* **192**, 153–161.

FERNANDEZ-LEBORANS, G. 2010. Epibiosis in Crustacea: an overview. *Crustaceana* **83**, 549–640.

GILI, J.-M., ABELLÓ, P. AND VILLANUEVA, R. 1993. Epibionts and intermoult duration in the crab *Bathynectes piperitus*. *Marine Ecology Progress Series* **98**, 107–113.

GRISCHENKO, A.V., GORDON, D.P. AND MELNIK, V.P. 2018. Bryozoa (Cyclostomata and Ctenostomata) from polymetallic nodules in the Russian exploration area, Clarion-Clipperton Fracture Zone, eastern Pacific Ocean-taxon novelty and implications of mining. *Zootaxa* **4484**, 1–91.

GRÜNBAUM, D. 1997. Hydromechanical mechanisms of colony organization and cost of defense in an encrusting bryozoan, *Membranipora membranacea*. *Limnology and Oceanography* **42**, 741–752.

HARTIKAINEN, H., HUMPHRIES, S. AND OKAMURA, B. 2014. Form and metabolic scaling in colonial animals. *Journal of Experimental Biology* **217**, 779–786.

HARVELL, C.D. 1986. The ecology and evolution of inducible defenses in a marine bryozoan: cues, costs, and consequences. *American Naturalist* **128**, 810–823.

HARVELL, C.D. 1992. Inducible defenses and allocation shifts in a marine bryozoan. *Ecology* **73**, 1567–1576.

HARVELL, C.D. AND GROSBERG, R.K. 1988. The timing of sexual maturity in clonal animals. *Ecology* **69**, 1855–1864.

HAYWARD, P.J. AND RYLAND, J.S. 1975. Growth, reproduction and larval dispersal in *Alcyonidium hirsutum* (Fleming) and some other Bryozoa. *Pubblicazioni della Stazione Zoologica di Napoli* **39**(suppl. 1), 226–241.

HERMANSEN, P., LARSEN, P.S. AND RIISGARD, H.U. 2001. Colony growth rate of encrusting marine bryozoans (*Electra pilosa* and *Celleporella hyalina*). *Journal of Experimental Marine Biology and Ecology* **263**, 1–23.

HERRERA, A., JACKSON, J.B.C., HUGHES, D.J., JARA, J. AND RAMOS, H. 1996. Life-history variation in three coexisting cheilostome bryozoan species of the genus *Stylopoma* in Panama. *Marine Biology* **126**, 461–469.

HUGHES, D.J. 1989. Variation in reproductive strategy among clones of the bryozoan *Celleporella hyalina*. *Ecological* Monographs **59**, 387–403.

HUGHES, D.J. AND HUGHES, R.N. 1986. Life history variation in *Celleporella hyalina* (Bryozoa). *Proceedings of the Royal Society of London. Series B, Biological Sciences* **228**, 127–132.

JACKSON, J.B.C. AND WERTHEIMER, S. 1985. Patterns of reproduction in five common species of Jamaican reef-associated bryozoans. In: C. Nielsen and G.P. Larwood (eds), *Bryozoa: Ordovician to Recent*. Fredensborg, Olsen and Olsen, pp. 161–168.

KARKACH, A.S. 2006. Trajectories and models of individual growth. *Demographic Research* **15**, 347–400.

KAUFMANN, K.W. 1981. Fitting and using growth curves. *Oecologia* **49**, 293–299.

KEY, M.M., JR. AND BARNES, D.K.A. 1999. Bryozoan colonization of the marine isopod *Glyptonotus antarcticus* at Signy Island, Antarctica. *Polar Biology* **21**, 48–55.

KEY, M.M., JR. AND SCHWEITZER, C.E. 2019. Coevolution of post-Palaeozoic arthropod basibiont diversity and encrusting bryozoan epibiont diversity? *Lethaia* https://doi.org/ 10.1111/let.12350.

KEY, M.M., JR., HYŽNÝ, M., KHOSRAVI, E., HUDÁČKOVÁ, N., ROBIN, N. AND MIRZAIE ATAABADI, M. 2017. Bryozoan epibiosis on fossil crabs: a rare occurrence from the Miocene of Iran. *Palaios* **32**, 491–505.

KEY, M.M., JR., JEFFRIES, W.B. AND VORIS, H.K. 1995. Epizoic bryozoans, sea snakes, and other nektonic substrates. *Bulletin of Marine Science* **56**, 462–474.

KEY, M.M., JR., JEFFRIES, W.B., VORIS, H.K. AND YANG, C.M. 1996a. Epizoic bryozoans and mobile ephemeral host substrata. In: D.P. Gordon, A.M. Smith and J.A. Grant-Mackie (eds), *Bryozoans in Space and Time*. Wellington, National Institute of Water and Atmospheric Research, pp. 157–165.

KEY, M.M., JR., JEFFRIES, W.B., VORIS, H.K. AND YANG, C.M. 1996b. Epizoic bryozoans, horseshoe crabs, and other mobile benthic substrates. *Bulletin of Marine Science* **58**, 368–384.

KEY, M.M., JR., JEFFRIES, W.B., VORIS, H.K. AND YANG, C.M. 2000. Bryozoan fouling pattern on the horseshoe crab *Tachypleus gigas* (Müller) from Singapore. In: A. Herrera Cubilla and J.B.C. Jackson (eds), *Proceedings of the 11th International Bryozoology Association Conference*. Balboa, Smithsonian Tropical Research Institute, pp. 265–271.

KEY, M.M., JR., KNAUFF, J.B. AND BARNES, D.K.A. 2013. Epizoic bryozoans on predatory pycnogonids from the South Orkney Islands, Antarctica: "If you can't beat them, join them". In: A. Ernst, P. Schäfer and J. Scholz (eds), *Bryozoan Studies 2010*. Berlin, Springer-Verlag Lecture Notes in Earth System Sciences **143**, pp. 137–153.

KEY, M.M., JR., SCHUMACHER, G.A., BABCOCK, L.E., FREY, R.C., HEIMBROCK, W.P., FELTON, S.H., COOPER, D.L., GIBSON, W.B., SCHEID, D.G. AND SCHUMACHER, S.A. 2010. Paleoecology of commensal epizoans fouling *Flexicalymene* (Trilobita) from the Upper Ordovician, Cincinnati Arch region, USA. *Journal of Paleontology* **84**, 1121–1134.

KEY, M.M., JR., WINSTON, J.E., VOLPE, J.W., JEFFRIES, W.B. AND VORIS, H.K. 1999. Bryozoan fouling of the blue crab, *Callinectes sapidus*, at Beaufort, North Carolina. *Bulletin of Marine Science* **64**, 513–533.

LIDGARD, S. AND JACKSON, J.B.C. 1989. Growth in encrusting cheilostome bryozoans: I. evolutionary trends. *Paleobiology* **15**, 255–282.

LUTAUD, G. 1961. Contribution à l'étude du bourgeonnement et de la croissance des colonies chez *Membranipora membranacea* (Linné), Bryozoaire Chilostome. *Annales Societe Royale Zoologique de Belgique* **91**, 157–300.

LUTAUD, G. 1983. Autozooid morphogenesis in anascan cheilostomes. In: R.A. Robison (ed), *Treatise on Invertebrate Paleontology. Part G. Bryozoa (revised)*. Boulder and Lawrence, Geological Society of America and University of Kansas Press, pp. 208–237.

MCKINNEY, F.K. 1992. Competitive interactions between related clades: evolutionary implications of overgrowth interactions between encrusting cyclostome and cheilostome bryozoans. *Marine Biology* **114**, 645–652.

MCKINNEY, F.K. 1993. A faster paced world?: contrasts in biovolume and life-process rates in cyclostome (Class Stenolaemata) and cheilostome (Class Gymnolaemata) bryozoans. *Paleobiology* **19**, 335–351.

O'DEA, A. AND OKAMURA, B. 1999. Influence of seasonal variation in temperature, salinity and food availability on module size and colony growth of the estuarine bryozoan *Conopeum seurati*. *Marine Biology* **135**, 581–588.

PARK, T.-Y. AND CHOI, D.K. 2011. Ontogeny of the Furongian (late Cambrian) remopleuridioid trilobite *Haniwa quadrata* Kobayashi 1933 from Korea: implications for trilobite taxonomy. *Geological Magazine* **148**, 288–303.

PRATT, M.C. 2008. Living where the flow is right: How flow affects feeding in bryozoans. *Integrative and Comparative Biology* **48**, 808–822.

ROSS, D.M. 1983. Symbiotic relations. In: D.E. Bliss (ed), *The Biology of Crustacea, Volume 7*. New York, Academic Press, pp. 163–212.

SMITH, A.M. 2007. Age, growth and carbonate production by erect rigid bryozoans in Antarctica. *Palaeogeography, Palaeoclimatology, Palaeoecology* **256**, 86–98.

SMITH, A.M. 2014. Growth and calcification of marine bryozoans in a changing ocean. *Biological Bulletin* **226**, 203–210.

SMITH, A.M. AND KEY, M.M., Jr. 2020. Growth geometry and measurement of growth rates in marine bryozoans: a review. In P.N. Wyse Jackson and K. Zágoršek (eds). *Bryozoan Studies 2019*. Prague, Czech Geological Survey, pp. 137–154.

SOKOLOVER, N., OSTROVSKY, A.N. AND ILAN, M. 2018. *Schizoporella errata* (Bryozoa, Cheilostomata) in the Mediterranean Sea: abundance, growth rate, and reproductive strategy. *Marine Biology Research* **14**, 868–882.

STEBBING, A.R.D. 1973. Competition for space between the epiphytes of *Fucus serratus* L. *Journal of the Marine Biological Association of the United Kingdom* **53**, 247–261.

TAYLOR, P.D. AND WILSON, M.A. 2002. A new terminology for marine organisms inhabiting hard substrates. *Palaios* **17**, 522–525.

WAHL, M. 1989. Marine epibiosis. 1. Fouling and antifouling – some basic aspects. *Marine Ecology Progress Series* **58**, 175–189.

WINSTON, J.E. 1976. Experimental culture of the estuarine ectoproct *Conopeum tennuissimum* from Chesapeake Bay. *Biological Bulletin* **150**, 318–335

WINSTON, J.E. AND HÅKANSSON, E. 1986. The interstitial bryozoan fauna from Capron Shoal, Florida. *American Museum Novitates* **2865**, 1–50.

WINSTON, J.E. AND JACKSON, J.B.C. 1984. Ecology of cryptic coral reef communities. IV. Community development and life histories of encrusting cheilostome Bryozoa. *Journal of Experimental Marine Biology and Ecology* **76**, 1–21.

XIXING, L., XUEMING, Y. AND JIANGHU, M. 2001. *Biology of Marine-Fouling Bryozoans in the Coastal Waters of China*. Beijing, Science Press.

YOSHIOKA, P.M. 1982. Role of planktonic and benthic factors in the population dynamics of the bryozoan *Membranipora membranacea*. *Ecology* **63**, 457–468.

The last known cryptostome bryozoan?
Tebitopora from the Tibetan Triassic

Junye Ma[1]*, Caroline J. Buttler[2] and Paul D. Taylor[3]

[1] State Key Laboratory of Palaeobiology and Stratigraphy, Nanjing Institute of Geology and Palaeontology, Chinese Academy of Sciences (CAS), Nanjing 210008, China.
[*corresponding author jyma@nigpas.ac.cn]
[2] Department of Natural Sciences, Amgueddfa Cymru – National Museum Wales, Cardiff, CF10 3NP, UK
[Caroline.Buttler@museumwales.ac.uk]
[3] Department of Earth Sciences, Natural History Museum, London SW7 5BD, UK
[p.taylor@nhm.ac.uk]

ABSTRACT

Bryozoans of the superorder Palaeostomata dominated Palaeozoic bryozoan faunas but fewer than twenty palaeostomate genera have been recorded in the Triassic and by the end of this period the superorder was extinct. Although species belonging to the palaeostomate order Cryptostomata abound in rocks of Lower Ordovician to Permian age, only one Triassic genus – *Tebitopora* – is known. *Tebitopora* was first described by Hu (1984) from Tibet and has since been recorded in India and New Zealand. It was originally placed in the trepostome family Dyscritellidae but subsequent workers have considered it to be a rhabdomesine cryptostome, generally placing it in the family Nikiforovellidae, which is consistent with the restricted, axial budding locus. We redescribe *Tebitopora* based on Hu's Chinese material of the type species *T. orientalis* and its subjective synonym *T. depressa*. *Tebitopora* is here assigned to the cryptostome family Rhomboporidae, a family we consider to be the senior synonym of Nikiforovellidae. In view of the stratigraphically isolated occurrence of this genus, and the presence of some trepostome-like morphological characters, it is difficult to discount the possibility that *Tebitopora* is a trepostome homeomorph rather than a true cryptostome.

INTRODUCTION

The Palaeozoic–Mesozoic transition was a pivotal time in the evolution of marine bryozoans. Species of the superorder Palaeostomata are the most common bryozoans in the Palaeozoic. However, by the end of the Permian they had been critically decimated. The compilation of Powers and Pachut (2008) listed a mere 73 species of Triassic bryozoans, the majority occurring in the Middle and Late Triassic. No species are known to have survived from the Permian into the Triassic. All but eight Triassic bryozoan species are palaeostomates. The majority are trepostomes and only one cryptostome genus – *Tebitopora* Hu, 1984 – has been recorded in the Triassic. The subsequent end-Triassic extinction event appears to have wiped out all remaining Palaeostomata (Powers and Pachut 2008), and cyclostomes were the only stenolaemates to survive from the Palaeozoic into the Jurassic. However, there are significant morphological differences between Late Palaeozoic and Mesozoic cyclostomes. Along with a disconcerting Early Triassic gap in the fossil record of these stenolaemates (Ernst and Schäfer 2006), this underlines the need for further sampling and research to test the relationship between Palaeozoic and post-Palaeozoic cyclostomes.

Our aim here is to redescribe the last known cryptostome, *Tebitopora*, based on a study of the type material of Hu (1984) in the collections of the Nanjing Institute of Geology and Palaeontology, China (NIGPAS).

TRIASSIC PALAEOSTOMATA

Permian bryozoans were high in diversity, abundance and distributed worldwide (Ross 1995; Gilmour *et al* 1998, Gilmour & Morozova 1999). Some palaeogeographical differences have been recognised, with Boreal Realm faunas shown to have a greater diversity than those from East Gondwana, which in part may be due to a mid-latitude position and nutrient-fed depositional environments (Reid and James 2010). Two Late Permian extinction events have been recognised: one at the end of the Guadalupian, and a second at the very end of the Permian in the Changhsingian (Stanley and Yang 1994). Clapham *et al.* (2009) considered that the end-Guadalupian extinction entailed a gradual rather than a sudden loss of taxa. Bryozoans suffered a massive decline as a result of these extinctions. Notably, all Fenestrata, which had been abundant and diverse throughout the Permian, became extinct (Taylor and Larwood 1988). In the Early Triassic, the only bryozoans that have been identified are seven species placed in three genera of Trepostomata, restricted to the northern hemisphere (Powers and Pachut 2008). Trepostomes went on to diversify in the Late Triassic: seven new genera evolved but none survived into the Jurassic and the last records of the order are from the Rhaetian stage at the end of the Triassic. Three cystoporate taxa have been identified in the Triassic of Italy and Iran (Schäfer and Fois 1987, Schäfer *et al.* 2003), but the bryozoan affinity of at least one of these genera – *Cassianopora* – is doubtful and it may instead be a calcified demosponge (Engeser and Taylor 1989).

TRIASSIC CRYPTOSTOMATA

Cryptostome bryozoans are generally regarded as a typically Palaeozoic order of bryozoans. They are classified into two suborders: Ptilodictyina and Rhabdomesina. Ptilodictyines are most common in the Ordovician and Silurian. Only a few ptilodictyine genera are known from the Devonian and Carboniferous, and just one Permian genus has been described: *Phragmophera* from the Artinskian (Ernst and Nakrem 2007). Although present in the Lower Palaeozoic, rhabdomesines are much more numerous in the Upper Palaeozoic (Keim 1983, table 4), and are common in the Permian. Boardman (1984) noted similarities between some Cretaceous cyclostomes and Palaeozoic cryptostomes, and speculated whether cryptostomes were ancestral to these post-Palaeozoic stenolaemates in contrast to the conventional that they represent homeomorphs resulting from convergent evolution.

No cryptostome genera are known to have crossed the Permian-Triassic boundary and the order is lacking in the documented Lower Triassic fossil record. However, the rhabdomesine cryptostome *Tebitopora* has been identified in the Middle and Upper Triassic. Hu (1984) first described *Tebitopora* from the Middle Triassic (Ladinian) of Tulung, Tibet. He referred two new species to his new genus: the type species, *T. orientalis*, and a second species, *T. depressa*. *Tebitopora* has since been recorded from the Middle Triassic of New Zealand and the Upper Triassic of Tibet and India. All of these localities would have been situated in the southern Gondwanan region during Triassic times (Fig. 1).

SYSTEMATIC PALAEONTOLOGY
Phylum Bryozoa Ehrenberg, 1831
Class Stenolaemata Borg, 1926
Superorder Palaeostomata Ma, Buttler and Taylor, 2014
Order Cryptostomata Vine, 1884
Suborder Rhabdomesina Astrova and Morozova, 1956
Family Rhomboporidae Simpson, 1895

Nikiforovellidae Goryunova, 1975, p. 67.
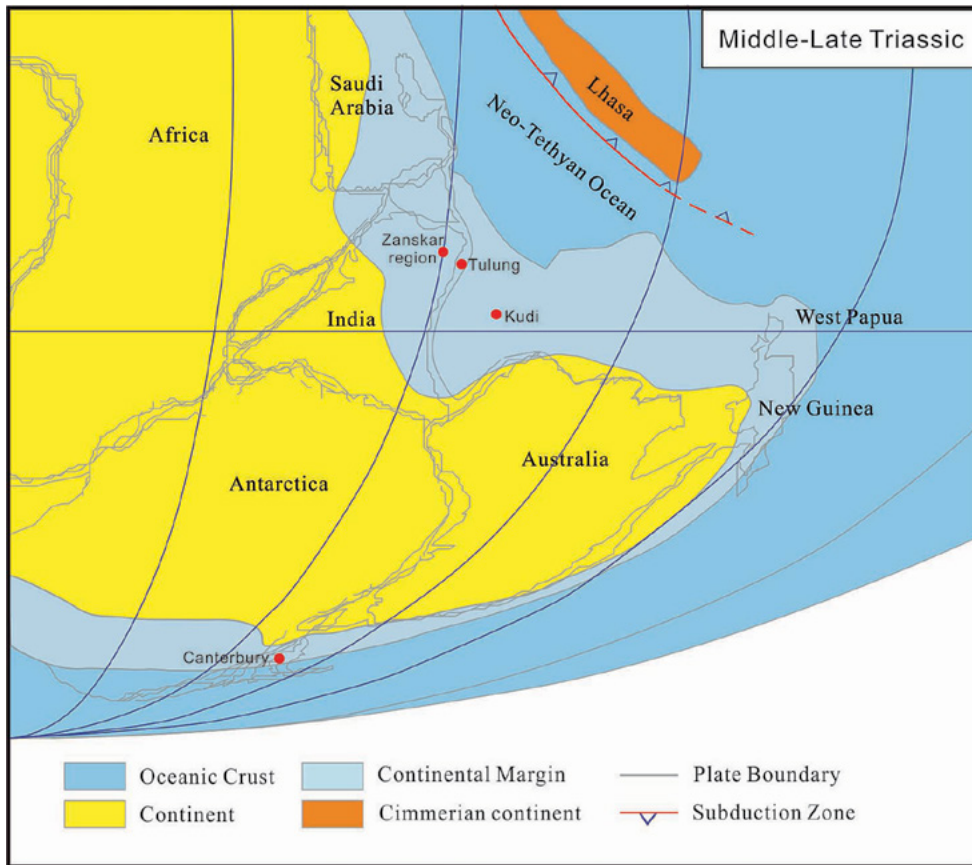
Figure 1. Locations of *Tebitopora* finds plotted on a Triassic palaeogeographical reconstruction (after Cai *et al.* 2016).

Revised diagnosis: Zoaria dendroid, rarely jointed. Branches subcircular in cross section. Apertures arranged rhombically, sometimes irregular; longitudinal ridges sometimes present. Metazooecia may be present. Axial region formed by median axis or planar surface, discontinuous in some species; weakly developed axial zooecia may be present. Zooecial bases attenuated to inflated and flattened in longitudinal profile. Zooecial cross sections polygonal in endozone, hexagonal, subhexagonal to rounded in exozone. Budding may be in a helical pattern. Zooecia diverge from axial region at 20° to 90°; living chambers in exozones oval to subcircular in cross section, oriented 50° – 90° to branch surfaces. Autozooecial length approximately twice to 10 times diameter. Hemisepta usually absent; diaphragms rare to common. Exozonal width one-fifth to four-fifths branch radius in mature stems. Zooecial boundaries narrow, dark; granular and non-laminated material in some areas but can be obscure. Lamellar profiles V-shaped to broadly rounded in exozones. Acanthostyles, aktinotostyles and mural spines may be present (based on Blake 1983a).

Stratigraphical range: Devonian–Triassic.

Remarks: The main stated difference between the families Rhomboporidae and Nikiforovellidae is the absence of paurostyles in Rhomboporidae. In other respects, their morphologies overlap (Blake 1983b). Weighed against the numerous similarities, this difference is minor and we consider the two families to be synonymous, with Rhomboporidae having priority.

Genus *Tebitopora* Hu, 1984

Type species: Tebitopora orientalis Hu, 1984, from the Middle Triassic (Ladinian) of Tulung, Tibet.

Occurrence: Middle Triassic (Ladinian) of Tulung, Tibet; Upper Triassic (Norian), Zozar Formation, Zanskar region, West Himalaya of India; Upper Triassic (Norian), Tarap Formation, Kudi, Dzaghar Chu Valley, South Tibet; Middle Triassic, Otamitan Stage, North Mathias River, Canterbury, New Zealand.

Diagnosis: Colony ramose. Autozooecia bud in spiral pattern from branch axis. Exozone very wide. Autozooecia curve gradually to meet zoarial surface at 90°. Apertures oval in cross section, arranged in rows on zoarial surface. Widely spaced diaphragms present in zooecial tubes. Long acanthostyles extend from centre of colony to edge. Metazooecia rounded in shape, containing sparse diaphragms and completely surrounding autozooecia in exozone.

Remarks: Tebitopora was originally placed by Hu (1984) in the trepostome family Dyscritellidae. However, subsequent workers have unanimously considered it to be a cryptostome (Schäfer and Fois 1987; Sakagami *et al.* 2006; Powers and Pachut 2008). Schäfer and Fois (1987) tentatively assigned it the family Nikiforovellidae due to the presence of budding from a linear central axis, abundant mesozooecia, lack of hemisepta and rare diaphragms. However, these characteristics could also place the genus in the family Rhomboporidae, and critical evaluation of these two families leads us to synonymize Nikiforovellidae with Rhomboporidae and to assign *Tebitopora* to Rhomboporidae.

The abundant metazooecia found in *Tebitopora* recalls the Permian genus *Ogbinopora* from the family Hyphasmoporidae, although this family is characterized by an axial bundle and hemisepta that are lacking in *Tebitopora*. *Tebitopora* also resembles the Carboniferous/Permian genus *Primorella* in

having a linear axis and narrow endozone, but metazooecia are absent in *Primorella*.

The etymology of *Tebitopora* was not stated by Hu (1984) who used this name consistently throughout his paper. It seems very likely to have been derived from Tibet, and the handwritten labels on the thin sections in NIGPAS give the name as '*Tibetopora*'. However, in view of the fact that the spelling *Tebitopora* has been used in several subsequent publications, we retain prevailing usage for the sake of nomenclatural stability.

***Tebitopora orientalis* Hu, 1984**

Tebitopora orientalis Hu, 1984: p. 23, pl. 1, figs 1–8.
Tebitopora depressa Hu, 1984: pp. 23, 24, pl. 1, figs 9–10; pl. 2, figs 1–3.
Tebitopora orientalis Hu, 1984: Schäfer and Fois, 1987: pp. 188, 189, pl. 9, figs 1–5; pl. 10, figs 1, 2.
Tebitopora orientalis Hu, 1984: Schäfer and Grant-Mackie 1994: pp. 40, 41, 42, fig. 42A, B.
Tebitopora orientalis Hu, 1984: Sakagami *et al.*, 2006, p. 18, fig. 10G, H.

Type material: Holotype: Middle Triassic (Ladinian), Tulung, Tibet (Nanjing Institute of Geology and Palaeontology) NIGPA79784.

Description: Colony erect, ramose with cylindrical branches (Fig. 2A), 2.2–3.7 mm in diameter. Autozooecia bud from axis in the centre of the colony in a helical pattern (Fig. 2B, C). Endozonal region very narrow, mean diameter 1.1 mm, the autozooecia curving to meet the colony surface at 90° (Fig. 2D, E,). Apertures oval in cross section, measuring 0.17–0.26 mm longitudinally and 0.12–0.17 mm transversely (Fig. 2F), roughly arranged in rows on the surface, spaced between 0.5-0.7 mm along the branch. Widely spaced thin diaphragms in zooecial tubes, rare in the endozone but slightly more common in the exozone (Fig. 2D). Extremely long acanthostyles extend from centre of colony to edge, 0.03 mm in diameter (Fig. 2G). Autozooecial walls thick in the exozone. Zooecial boundaries
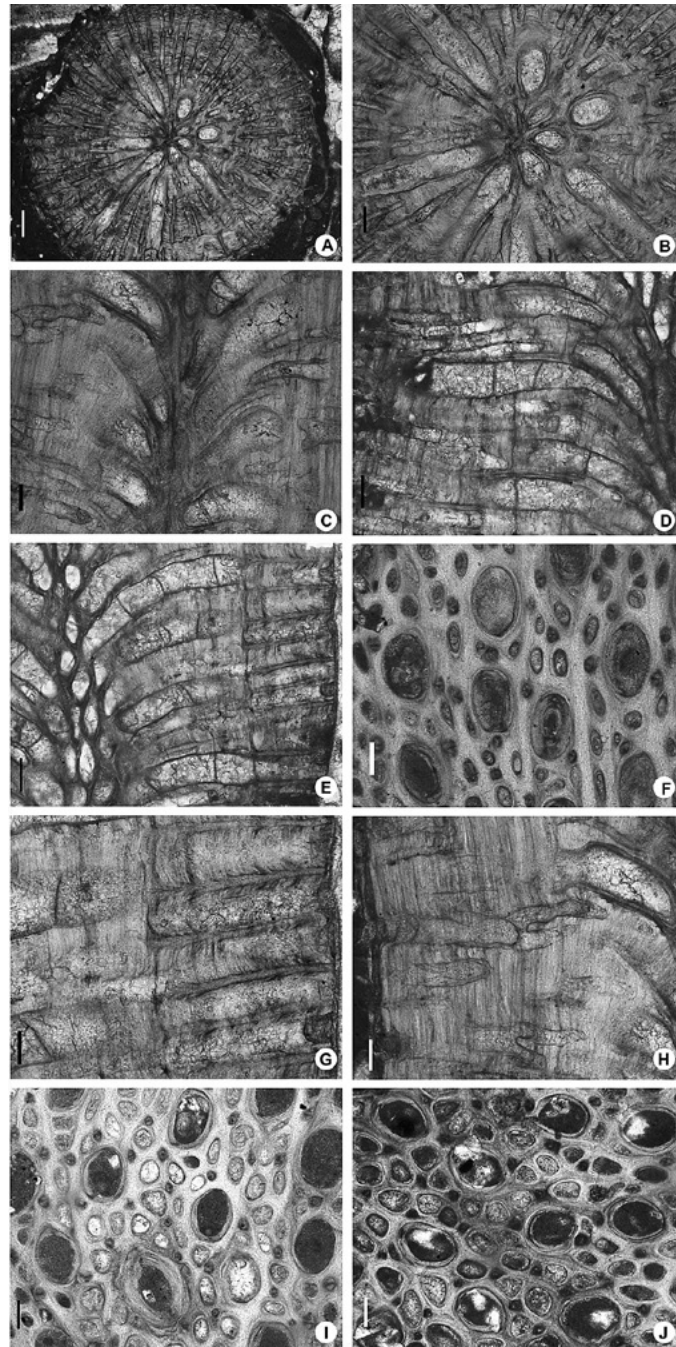
Figure 2. *Tebitopora orientalis*, Middle Triassic (Ladinian), Tulung, Tibet. (A) Cylindrical colony branches with wide exoxone and central axis (NIGPA79784, transverse section), (B) Autozooecia bud from central axis in a spiral fashion (NIGPA79784, transverse section), (C) Narrow endozonal area with central axis (NIGPA79784, longitudinal section), (D) Wide exozonal area region (NIGPA79787, longitudinal section), (E) Widely spaced diaphragms in autozooecia (NIGPA79787, longitudinal section), (F) Oval zooecial apertures, small metazooecia and styles, (NIGPA79784 tangential section), (G) Long acanthostyles extending from centre of colony (NIGPA79787 longitudinal section), (H) Thick exozonal zooecial walls, (NIGPA79784, longitudinal section), (I) Autozooecia lined with cingulum-like material (NIGPA79784, tangential section), (J) Mesozooecia surrounding autozooecia (NIGPA79785, tangential section). Scale bars: A, D, E, = 200 μm; B, C, F, G, H, I, J = 100 μm.

Table 1. Measurements of *Tebitopora orientalis* Hu, 1984. Abbreviations: CW = Colony width;
EXW = exozone width; ENW = enozone width; AD = autozooecial diameter;
AS = aperture spacing along branch; ASD = acanthostyle diameter; MW = metazooecia width.

	Mean (mm)	Range (mm)	Standard deviation	Number of measurements
CW	3.0	2.2–3.7	0.612	5
EXW	1.11	0.73–1.72	0.365	5
ENW	0.95	0.73–1.22	0.163	5
AD	0.15	0.12–0.18	0.016	18
AS	0.60	0.5–0.7	0.063	12
ASD	0.03	0.02–0.04	0.005	65
MW	0.06	0.03–0.07	0.013	75

hard to distinguish (Fig. 2H) but in places appearing broadly merged. Cingulum-like material present in some autozooecial tubes (Fig. 2I). Metazooecia rounded, 0.06 mm in diameter and containing sparse diaphragms; surrounding autozooecia in the exozone (Fig. 2J) and forming patches (maculae) on colony surface where autozooecia are lacking. Aktinotostyles and mural spines absent.

Remarks: Two species of *Tebitipora* were originally described by Hu (1984), *T. orientalis* and *T. depressa*, both from the same locality. *Tebitipora depressa* was described as differing from *T. orientalis* by having a greater number of styles, and a more irregular arrangement of zooecial apertures on the colony surface. However, only one specimen of *T. depressa* is known and the tangential section is deeper than those prepared for *T. orientalis*. The type of *T. depressa* is slightly larger than that of *T. orientalis* but when compared with specimens subsequently described (Schäfer and Fois 1987; Sakagami *et al.* 2006), it falls within the range of variation. Therefore, we place the two species into synonymy.

In tangential sections cingulum-like material is present in some autozooecial tubes of *Tebitopora*. Cingulum is common in Early Palaeozoic trepostome bryozoans (Boardman 2001) but is not normally described in rhabdomesines. Its occurrence in *Tebitopora* can be interpreted as another convergent character to add to those discussed by Blake (1980) between trepostomes and cryptostomes (but see Discussion).

Material of *Tebitopora* from the Upper Triassic (Norian) Tarap Formation of Tibet (Sakagami *et al.* 2006) is similar to Hu's Tibetan specimens. Only oblique transverse sections were illustrated by Sakagami *et al.* (2006) but these show the distinctive thick exozone. Branch diameter is 2.6–3.5 mm, which is within the range of the original specimens described by Hu. No diaphragms were observed, but these are rare and difficult to distinguish in *Tebitopora*. Schäfer and Fois (1987) when describing *T. orientalis* from the Upper Triassic, Early Norian Zozar Formation of Zanskar in India also recognized a radial budding pattern around a central axis as observed in the type specimens from Tulung, Tibet. The specimens described by Schäfer and Grant-Mackie (1994) appear to have smaller and more abundant acanthostyles than the originally described material.

DISCUSSION
The sole Triassic cryptostome *Tebitopora* is distinctive due to its spiral budding pattern and the extremely wide exozone and narrow endozone, unlike cryptostomes known from the Late Permian. *Tebitopora* shares with Triassic trepostomes thick

zooecial walls, not only in the exozone but in the endozone too, as well as a cingulum-like thickening of some walls. This raises the possibility that *Tebitopora* might actually be a trepostome that converged on a rhabdomesine cryptostome morphology, mainly through restriction of zooecial budding to narrow locus in the axis of the ramose branches. Blake (1980) pointed to restricted budding loci as a way of distinguishing cryptostomes from trepostomes. However, he emphasized that this character may not be a panacea as it could have evolved convergently in non-cryptostome clades. Unfortunately, there is a limited range of morphological characters available to test whether *Tebitopora* is a true cryptostome or a trepostome homeomorph of a cryptostome and evaluation of these two options must await a more comprehensive phylogenetic analysis of relevant palaeostomate taxa.

ACKNOWLEDGEMENTS

REFERENCES

ASTROVA, G.G. AND MOROZOVA, I.P. 1956. K sistematike mshanok otryada Cryptostomata. *Doklady Akademii Nauk SSS* **110**, 661–664.

BLAKE, D.B. 1980. Homeomorphy in Paleozoic bryozoans: a search for explanations. *Paleobiology* **6**, 451–465.

BLAKE, D.B. 1983a. Introduction to the suborder Rhabdomesina. In: Robison, R.A. (ed.), *Treatise on Invertebrate Paleontology, Part G, Bryozoa revised, Volume 1*. Boulder and Lawrence, Geological Society of America and University of Kansas, pp. 530–549.

BLAKE, D.B. 1983b. Systematic descriptions for the suborder Rhabdomesina. In: Robison, R.A. (ed.), *Treatise on Invertebrate Paleontology, Part G, Bryozoa revised, Volume 1*. Boulder and Lawrence, Geological Society of America and University of Kansas, pp. 550–592.

BOARDMAN, R.S. 1984. Origin of the Post-Triassic Stenolaemata (Bryozoa): a taxonomic oversight. *Journal of Paleontology* **58**, 19–39.

BOARDMAN, R.S. 2001. The growth and function of skeletal diaphragms in the colony life of Lower Paleozoic Trepostomata (Bryozoa). *Journal of Paleontology* **75**, 225–240.

BORG, F. 1926. Studies on Recent cyclostomatous Bryozoa. *Zoologiska Bidrag från Uppsala* **10**, 181–507.

CAI, F., DING, L., LASKOWSKI, A.K., KAPP, P, WANG, H., XU, Q. AND ZHANG, L. 2016. Late Triassic paleogeographic reconstruction along the Neo–Tethyan Ocean margins, southern Tibet. *Earth and Planetary Science Letters* **435**, 105–114.

CLAPHAM, M.E., SHEN, S. AND BOTTJER, D.J. 2009. The double mass extinction revisited: reassessing the severity, selectivity, and causes of the End-Guadalupian Biotic Crisis (Late Permian) *Paleobiology* **35**, 32–50.

EHRENBERG, C.G. 1831. Symbolae Physicae, seu Icones et descptiones Corporum Naturalium novorum aut minus cognitorum, quae ex itineribus per Libyam, Aegiptum, Nubiam, Dongalaam, Syriam, Arabiam et Habessiniam, studia annis 1820–25, redirent. *Pars Zoologica*, 4, Animalia Evertebrata exclusis Insectis: Berolini, Mittler, 10 pls.

ENGESER, T. AND TAYLOR, P.D. 1989. Supposed Triassic bryozoans in the Klipstein Collection from the Cassian Formation of the Italian Dolomites redescribed as calcified demosponges. *Bulletin of the British Museum (Natural History), Geology Series* **45**, 39–55.

ERNST, A. AND NAKREM, H.A. 2007. Lower Permian Bryozoa from Ellesmere Island (Canada). *Paläontologische Zeitschrift* **81**, 17–28.

ERNST, A. AND SCHÄFER, P. 2006. Palaeozoic vs. post-Palaeozoic Stenolaemata: Phylogenetic relationship or morphological convergence? *Courier Forschungsinstitut Senckenberg* **257**, 49–64.

GILMOUR, E.H. AND MOROZOVA, I.P. 1999: Biogeography of the Late Permian bryozoans. *Paleontologicheskii Zhurnal* **99**, 38–53.

GILMOUR, E.H., MOROZOVA, I.P. AND NEYENS JR, L.M. 1998. Paleobiogeography of Late Permian Bryozoa. *Palaeoworld* **9**, 87–96.

GORYUNOVA R.V. 1975 Permskie mshanki Pamira. *Trudy Paleontologicheskogo instituta Akademii Nauk SSSR* **148**, 128 pp.

HU, Z. 1984. Triassic Bryozoa from Xizan (Tibet) with reference to their biogeographical provincialism in the world. *Acta Palaeontologica Sinica* **23**, 568–577.

KEIM, J.D. 1983. Ranges of Taxa. In: R.A. Robison (ed.), *Treatise on Invertebrate Paleontology,* Part G, *Bryozoa revised.* Boulder and Lawrence, Geological Society of America and University of Kansas, pp. 322–326.

MA, J.-Y., BUTTLER, C.J. AND TAYLOR, P.D., 2014. Cladistic analysis of the 'trepostome' Suborder Esthonioporina and the systematics of Palaeozoic bryozoans. *Studi Trentini di Scienze Naturali* **94**, 153–161.

POWERS, C.M. AND PACHUT, J.F. 2008. Diversity and distribution of Triassic Bryozoans in the aftermath of the end-Permian mass extinction. *Journal of Paleontology* **82**, 362–371.

REID, C.M. AND JAMES, N.P.J. 2010. Permian higher latitude bryozoan biogeography. *Palaeogeography, Palaeoclimatology, Palaeoecology* **298**, 31–41.

ROSS, J.R.P. 1995. Permian Bryozoa. In: P.A. Scholle, T.M. Peryt and D.S. Ulmer-Scholle (eds.), *The Permian of northern Pangea*. New York, Springer, pp. 196–209.

SAKAGAMI, S., SCIUNNACH, D. AND GARZANTI, E. 2006. Late Paleozoic and Triassic bryozoans from the Tethys Himalaya (N India, Nepal and S Tibet). *Facies* **52***, 279–298.

SCHÄFER, P. AND FOIS, E. 1987 Systematics and evolution of Triassic Bryozoa. *Geologica et Palaeontologica* **21**,173–225.

SCHÄFER, P. AND GRANT-MACKIE, J.A. 1994, Triassic Bryozoa from the Murihiku and Torlesse Supergroups, New Zealand, *Memoirs of the Australasian Association of Palaeontologists* **16**, 1–52.

SCHÄFER, P., SENOWBARI-DARYAN, B. ND HAMEDANI, A. 2003. Stenolaemate Bryozoans from the Upper Triassic (Norian-Rhaetian) Nayband Formation, Central Iran.*Facies,* **48**, 135–150.

SIMPSON, G.B. 1897 [1895]. A. Handbook of the Genera of the North American Paleozoic Bryozoa; with an introduction upon the structure of living species, *State Geologist New York, 14th Annual Report*, pp. 403–669.

STANLEY, S.M. AND YANG, X.N. 1994. A double mass extinction at the end of the Paleozoic era. *Science* **266**, 1340–1344.

TAYLOR, P.D. AND LARWOOD, G.P. 1988. Mass extinctions and patterns of bryozoan evolution. In: G.P. Larwood (ed.), *Extinction and Survival in the Fossil Record*. Systematics Association Special Volume **34**, 99–119.

VINE, G.R. 1884. Fourth report of the committee, consisting of Dr. H. C. Sorby and Mr. G. R. Vine, Appointed for the purpose of reporting on fossil Bryozoa. *British Association for the Advancement of Science* **1884**, 161–209.

Bryodiversity along the Croatian coast of the Adriatic Sea

Maja Novosel[1*], Steven J. Hageman[2], Hrvoje Mihanović[3] and Anđelko Novosel[4]

[1] University of Zagreb, Faculty of Science, Department of Biology, Rooseveltov trg 6,
10000 Zagreb, Croatia [*corresponding author: e-mail: maja@biol.pmf.hr]
[2] Department of Geological and Environmental Sciences, Appalachian State University,
Boone, North Carolina 28608, USA
[3] Institute of Oceanography and Fisheries, Šetalište I. Meštrovića 63, 21000 Split, Croatia
[4] Ecological Research Society Paks, Stjepana Vojnovića 19, 10362 Kašina, Croatia

ABSTRACT

Hard-bottom bryozoans along the Croatian coast of the Adriatic Sea were surveyed at 73 localities. Altogether 3,298 colonies have been sampled and 211 bryozoan species were found. From total number of found species, 36% have been found along the entire Croatian Adriatic coast. We analysed species according to their abundance, depth distribution and type of substrate on which they grow. Maximum bryozoan diversity was found on deep escarpments with strong currents. Depth distribution of bryozoans showed division into species that inhabit exposed, e.g. shallower habitats of the infralittoral zone, and those that grow in more shadowed hard substratum of the circalittoral zone. Only 7% of species were found growing non-selectively in both infralittoral and circalittoral zones. Much greater insight to understanding morphology and behaviour of bryozoans will be gained from environments with low diversity but high abundance of each species. In high diversity settings, species richness itself is a more important environmental indicator than colonial morphology of any constituent.

INTRODUCTION

According to its origin and its ecological features, the Adriatic Sea is a part of the Mediterranean Sea, but it displays some distinctive properties. The northern Adriatic is shallow, dominated by the continent and large subterranean freshwater inflow, while the southern part is much deeper, dominated by the open sea and influenced by the warm Mediterranean water (Gamulin-Brida 1974). South-eastward of the line connecting Zadar and Ancona the depth quickly reaches 270 m at the bottom of the second distinctive part (Jabuka Pit). The 170-m deep Palagruža Sill separates the Jabuka Pit from the South Adriatic Pit (the deepest part of the Adriatic, with depths exceeding 1200 m). At the southernmost part the Adriatic the bottom rises and forms the Otranto Strait (780 m) which separates Adriatic from the Ionian Sea. The western and eastern side of the Adriatic also quite differ. The western coast is relatively smooth, with almost no islands and slow depth changes offshore. In contrast, the eastern coastline is very rugged, with numerous islands, islets and rocks, and steep irregular bottom features (Gačić et al 2001).

The Adriatic also represents a major source of the densest water masses in the Eastern Mediterranean – North Adriatic Dense Water (NAdDW), generated in the northern Adriatic during winter cold wind outbreaks (e.g. Vilibić and Supić 2005). It spreads along the western shelf filling the Jabuka Pit and

a part of it overflows the Palagruža Sill and moves towards the southern Adriatic. The Palagruža Sill is also a natural barrier for the saline Levantine Intermediate Water (LIW) originating from the Ionian Sea. It is largely trapped in the South Adriatic Pit, but a part of it is advected in the northern Adriatic along eastern coast. A detailed analysis of Adriatic water masses can be found in Vilibić and Orlić (2002), where the authors concentrate on dense water formation in the South Adriatic.

As for the near-surface currents, generally the flow consists of a cyclonic circulation with north-westerly flow along the eastern coast and south-easterly flow on the western side of the basin. However, this simplified description does not account for spatial details in the circulation and their temporal changes. An overview of the currents and circulation in the Adriatic Sea can be found in Orlić *et al.* (1992).

Although the eastern Adriatic coast is mainly rocky, little is known about the ecology of hard-bottom sessile invertebrates, especially those that are difficult to sample, such as those from benthic communities of underwater escarpments and steep rocky bottoms. Bryozoans are one of the most dominant groups of sessile invertebrates on Adriatic hard bottom habitats (for the history of bryozoan research along the eastern Adriatic coast, see Novosel and Požar-Domac 2001). In places, Bryozoa form dense "meadows" on rocky plateaus swept by strong currents (Novosel 2005), cover large parts of volcanic escarpments (Zavodnik *et al.* 2000) or form giant colonies around freshwater submarine springs (Novosel *et al.* 2005). Today, bryozoans are considered to be good indicators of overall marine biodiversity (Clarke and Lidgard 2000; Rowden *et al.* 2004) and pollution (Ayling 1981; Best and Thorpe 1996; Harmelin and Capo 2002). They are widely distributed geographically (Ryland 1970) and live mainly on a "firm" substrata (McKinney and Jackson 1989). As a part of sessile benthic communities, bryozoans can give us an insight into the state of the marine environment, because they reflect the long-term environmental

conditions (Bader and Schäfer 2005; Berning 2007; Barnes and Griffiths 2008).

The objectives of this study were to: 1) document the distribution and diversity of bryozoan species along the Croatian coast of the Adriatic Sea; 2) identify and compare hard bottom bryozoan assemblages throughout the eastern Adriatic Sea; 3) recognize bryozoan species that may be depth controlled; and 4) identify which bryozoan taxa are the most important for characterizing the observed sampling locality groups and for evaluating their potential as key ecological indicators.

MATERIALS AND METHODS

Sampling was undertaken on 73 localities along the eastern (Croatian) Adriatic coast and grouped into 32 stations (Fig. 1).

Sampled 11 stations in the north Adriatic were: 1 – Novigrad Istra (marina), 2 – Lim Channel, Orlandin and Vrsar islets, 3 – Rovinj (Banjole), 4 – Krk (Marag Cape), 5 – Prvić Island near Senj (Šilo and Stražica capes), 6 – Sveti Juraj (Kola Cape), 7 – Žrnovnica Bay, 8 – Ždralova Cove, 9 – Grmac Cove, 10 – Veliki and Mali Ćutin, 11 – Silba (west Grebeni).

Sampled 16 stations in the central Adriatic were: 12 – Dugi otok (Lopati Cape, Lagnić Islet), 13 – Starigrad Paklenica (vrulja Zečica), 14 – islands Iž, Fulija, Kluda and Kudica, 15 – Dugi otok (Vele stijene), 16 – Kornati (Kamičići, Mana, Mala Sestrica, Veliki and Mali Garmenjak), 17 – Rogoznica (Soline), 18 – Jabuka Shoal, 19 – Jabuka, 20 – Brusnik, 21 – Biševo (southwest coast, Blue Cave, Gatula Cape), 22 – Vis (Komiža Bay), 23 – Drvenik, 24 – Brač (Milna), 25 – Palagruža, 26 – Sušac (Kanula Cape), 27 – Hvar (Kozja Cove).

Sampled 5 stations in the south Adriatic were: 28 – Lastovo (Struga Cape, Skrivena luka, Ubli, Vrhovine), 29 – Pelješac (Podobuće), 30 – Korčula (Lučnjak, capes Ražnjić and Konjska glava, Lumbard), 31 – Mljet (Lenga Cape, Štit, Vanji školj, Velika Priveza, Veliki most, dock), 32 – Dubrovnik (Grebeni).
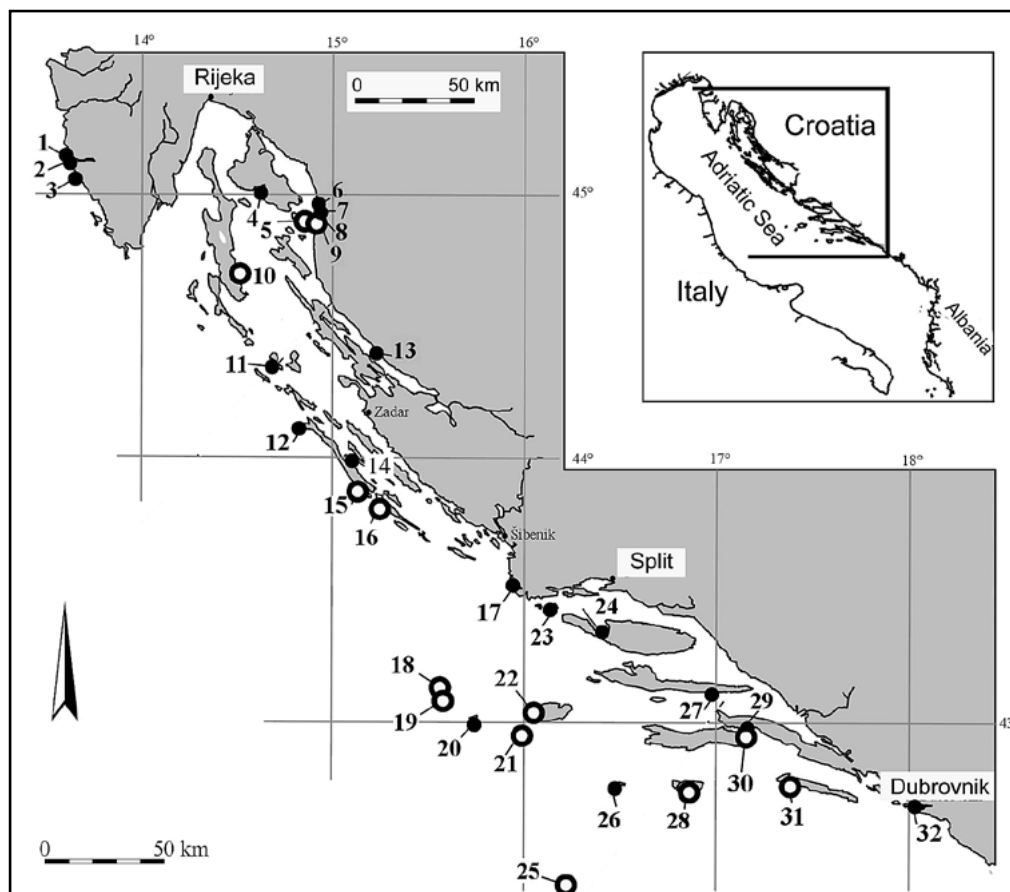
Figure 1. Sampling localities. 1 – Novigrad Istra (marina), 2 – Lim Channel, Orlandin and Vrsar islets,
3 – Rovinj (Banjole), 4 – Krk (Marag Cape), 5 – Prvić Island near Senj (Šilo and Stražica capes),
6 – Sveti Juraj (Kola Cape), 7 – Žrnovnica Bay, 8 – Ždralova Cove, 9 – Grmac Cove,
10 – Veliki and Mali Ćutin, 11 – Silba (west Grebeni), 12 – Dugi otok (Lopati Cape, Lagnić Islet),
13 – Starigrad Paklenica (vrulja Zečica), 14 – islands Iž, Fulija, Kluda and Kudica,
15 – Dugi otok (Vele stijene), 16 – Kornati (Kamičići, Mana, Mala Sestrica,
Veliki and Mali Garmenjak), 17 – Rogoznica (Soline), 18 – Jabuka Shoal,
19 – Jabuka, 20 – Brusnik, 21 – Biševo (southwest coast, Blue Cave, Gatula Cape),
22 – Vis (Komiža Bay), 23 – Drvenik, 24 – Brač (Milna), 25 – Palagruža, 26 – Sušac (Kanula Cape),
27 – Hvar (Kozja Cove), 28 – Lastovo (Struga Cape, Skrivena luka, Ubli, Vrhovine),
29 – Pelješac (Podobuće), 30 – Korčula (Lučnjak, capes Ražnjić and Konjska glava, Lumbard),
31 – Mljet (Lenga Cape, Štit, Vanji školj, Velika Priveza, Veliki most, dock),
32 – Dubrovnik (Grebeni). The thirteen localities with three or more
grid samples are highlighted as larger open circles.

Bryozoans were collected by SCUBA diving between 1997 and 2006, from 40 m depth to the surface at 5 m intervals, within the quadrant frame sized 15x15 cm. Exposed sites were considered those facing the open sea and prone to wave action, whereas sheltered sites are those protected from strong storm swells.

All specimens are catalogued and housed at the Department of Biology, Faculty of Science, University of Zagreb.

A qualitative comparison of lists of bryozoan species with common distributions to the environmental conditions was used to highlight potential proxies between bryozoan species and their environments, and

formulate initial ideas about specific environmental controls over the distribution of certain bryozoan species.

For each environmental parameter (water depth and substrate type), the expected values were derived from the percentage of all occurrences that were reported from each setting. For example, if 60% of all species were observed in shallow water, < 20m and 40% in deeper water, 20–40 m, these values were used as the expected distribution to which the occurrence of individual species were compared. These values highlight major deviations from the overall average bryozoan distribution, and invite further investigation for their significance.

RESULTS

Altogether, 3,298 bryozoan colonies were identified, and 211 bryozoan species were recorded. Of the total number of species found, 75 (36%) were found along the entire coast of the Croatian Adriatic and the most common among them were: *Schizomavella*

(*Schizomavella*) *cornuta*, *Chorizopora brongniartii*, *Adeonella pallasii*, *Mollia patellaria*, *Escharina vulgaris* and *Scrupocellaria scrupea*.

Depth distribution of bryozoans showed separation of species into those that inhabit exposed, e.g. shallower habitats of the infralittoral zone, and those that grew in more shadowed hard substratum of the circalittoral zone (Fig. 2). In general, 18% of bryozoan species only inhabited localities shallower than 20 m depth and 22% of species only inhabited localities deeper than 20 m depth (Table 1). Only 15 species (7%) were found growing non-selectively in both infralittoral and circalittoral zones, and these were: *Bugula gautieri*, *Cellaria fistulosa*, *Celleporina canariensis*, *C. lucida*, *C. pygmaea*, *Epistomia bursaria*, *Onychocella marioni*, *Rosseliana rosselii*, *Schizomavella* (*Schizomavella*) *subsolana*, *Schizoporella cornualis*, *Crisia ramosa*, *Exidmonea coerulea*, *Filicrisia geniculata*, *Frondipora verrucosa* and *Tubulipora aperta*.

Some bryozoans showed high affinity to specific substrate type, e.g. all colonies (25) of *Haplopoma*
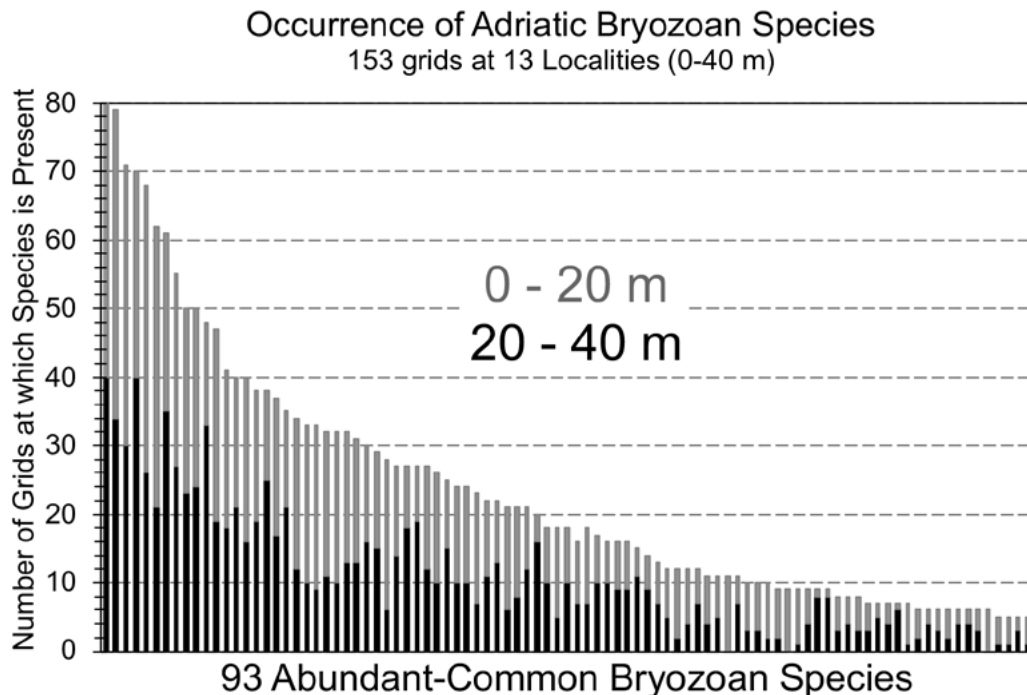
Figure 2. Depth distribution of abundant and common bryozoan species.

Table 1. Twenty bryozoan species with distributions that may be depth controlled.
Each has occurrences at either more than 65% or less than 35% of grids above or below 20 meters water
depth from the 13 localities highlighted in Figure 1 (random expectation of 51.6% and 48.4% based
on all bryozoan species present). The number of grids is out of 153 possible (79 shallow, 74 deep).

Species	Number of Grids total range	0 < 20m	20 < 40m
Shallow		**51.6%**	**Expected**
Beania hirtissima	20	80.0%	20.0%
Calpensia nobilis	15	73.3%	26.7%
Hippopodinella kirchenpaueri	27	70.4%	29.6%
Patinella radiata	48	68.8%	31.3%
Celleporina caliciformis	27	66.7%	33.3%
Schizobrachiella sanguinea	38	65.8%	34.2%
Deep		**48.4%**	**Expected**
Puellina pedunculata	11	0.0%	100.0%
Membraniporella nitida	12	16.7%	83.3%
Schizomavella mamillata	10	20.0%	80.0%
Crassimarginatella maderensis	28	21.4%	78.6%
Smittina cervicornis	33	27.3%	72.7%
Figularia figularis	18	27.8%	72.2%
Aetea sica	21	28.6%	71.4%
Puellina setosa	10	30.0%	70.0%
Rhynchozoon neapolitanum	10	30.0%	70.0%
Puellina hincksi	33	30.3%	69.7%
Rhynchozoon pseudodigitatum	23	30.4%	69.6%
Diplosolen obelia	32	31.3%	68.8%
Schizomavella auriculata	12	33.3%	66.7%
Schizotheca serratimargo	62	33.9%	66.1%
Beania magellanica	32	34.4%	65.6%

impressum were found on uncalcified algae while 99% of all *Adeonella pallasii* colonies (90) grew on rock substrate (Table 2).

DISCUSSION

Among 32 hard bottom localities along the eastern (Croatian) coast of the Adriatic Sea the highest bryodiversity was found on escarpments exposed to the open sea. The upwelling and strong currents on escarpments and steep slopes provide either optimal or at least acceptable environments for most Adriatic bryozoans. Strong currents supply abundant food, oxygen and good larvae distribution. Among the escarpments, the localities Jabuka Islet (19), Jabuka Shoal (19) and Lastovo Island (28) differ significantly, as they are the deepest and most isolated escarpment localities in the Adriatic

Table 2. Occurrence of bryozoan species on specified substrates as a percentage within each species, i.e. in Column 1, 99% of all *Adeonella pallasii* occurrences were on rock substrates, whereas 0% of all *Haplopoma impressum* occurrences were on rock substrates. Expected values were derived from the percentage of all occurrences that were reported from each substrate type. Taxa significantly above (~2x) or below (~0.5x) the expected values are reported. The intent of the table is to draw attention to potential patterns for further investigation, no inferences of statistical significances are made.

(1) Rock Substrate		(2) Uncalcified Algae		(3) Dead Shell	
Adeonella pallasii	99%	*Haplopoma impressum*	100%	*Hippopodinella kirchenpaueri*	67%
Myriapora truncata	96%	*Puellina gattyae*	82%	*Rhynchozoon neapolitanum*	30%
Reteporella grimaldii	91%	*Puellina setosa*	80%	*Schizoporella magnifica*	30%
Smittina cervicornis	91%	*Escharoides coccinea*	79%	*Figularia figularis*	28%
Margaretta cereoides	84%	*Aetea sica*	71%	*Microporella appendiculata*	28%
Schizomavella mamillata	80%	*Chorizopora brongniartii*	71%	*Puellina innominata*	27%
Parasmittina tropica	73%	*Celleporina caliciformis*	70%	*Diplosolen obelia*	22%
Schizotheca serratimargo	71%	*Schizomavella discoidea*	69%	*Gregarinidra gregaria*	19%
Rhynchozoon pseudodigitatum	70%	*Beania mirabilis*	69%	*Callopora dumerilii*	19%
Schizomavella auriculata	67%	*Metroperiella lepralioides*	68%		
		Microporella ciliata	67%	EXPECTED	9%
EXPECTED	37%				
		EXPECTED	35%	*Scrupocellaria scrupea*	3%
Puellina hincksi	18%			*Schizotheca serratimargo*	3%
Puellina innominata	18%	*Rhynchozoon pseudodigitatum*	17%	*Beania magellanica*	3%
Tubulipora liliacea	17%	*Diplosolen obelia*	16%	*Schizobrachiella sanguinea*	3%
Celleporina lucida	17%	*Schizomavella cornuta*	15%	*Margaretta cereoides*	3%
Microporella appendiculata	17%	*Schizoporella dunkeri*	10%	*Myriapora truncata*	2%
Schizomavella discoidea	16%	*Bugula fulva*	8%	*Haplopoma impressum*	0%
Celleporina caliciformis	15%	*Parasmittina tropica*	7%	*Puellina setosa*	0%
Hippopodinella kirchenpaueri	15%	*Schizotheca serratimargo*	6%	*Escharoides coccinea*	0%
Aetea truncata	14%	*Margaretta cereoides*	5%	*Aetea sica*	0%
Escharina vulgaris	13%	*Hippopodinella kirchenpaueri*	4%	*Beania mirabilis*	0%
Beania mirabilis	13%	*Smittina cervicornis*	3%	*Metroperiella lepralioides*	0%
Metroperiella lepralioides	13%	*Myriapora truncata*	2%	*Scrupocellaria reptans*	0%
Patinella radiata	13%	*Adeonella pallasii*	1%	*Scrupocellaria maderensis*	0%
Callopora dumerilii	11%	*Reteporella grimaldii*	0%	*Celleporina lucida*	0%
Chorizopora brongniartii	10%	*Rhynchozoon neapolitanum*	0%	*Hippaliosina depressa*	0%
Microporella ciliata	10%	*Reptadeonella violacea*	0%	*Schizomavella mamillata*	0%
Puellina gattyae	9%			*Smittina cervicornis*	0%
Fenestrulina malusii	9%			*Adeonella pallasii*	0%
Membraniporella nitida	8%			*Reteporella grimaldii*	0%
Haplopoma impressum	0%				

(4) Other Bryozoans		(5) Mixed Substrates		(6) Other Substrate	
Bugula fulva	42%	*Reptadeonella violacea*	29%	*Membraniporella nitida*	25%
Reptadeonella violacea	26%	*Puellina radiata*	27%	*Puellina radiata*	23%
Celleporina lucida	25%	*Puellina innominata*	23%	*Puellina pedunculata*	18%
Savygniella lafontii	23%	*Crassimarginatella maderensis*	21%	*Hippaliosina depressa*	14%
Scrupocellaria reptans	23%	*Hippaliosina depressa*	21%	*Diplosolen obelia*	13%
Crisia occidentalis	22%	*Savygniella lafontii*	20%	*Microporella appendiculata*	11%
Beania magellanica	22%	*Schizomavella cornuta*	20%	*Schizobrachiella sanguinea*	8%
Scrupocellaria delilii	18%			*Savygniella lafontii*	7%
Beania hirtissima	15%	*EXPECTED*	10%	*Fenestrulina malusii*	6%
				Beania mirabilis	6%
EXPECTED	7%	*Celleporina caliciformis*	4%	*Puellina hincksi*	6%
		Schizomavella discoidea	3%	*Scrupocellaria scruposa*	6%
Hippopodinella kirchenpaueri	0%	*Scrupocellaria delilii*	0%		
Rhynchozoon neapolitanum	0%	*Beania mirabilis*	0%	*EXPECTED*	2%
Figularia figularis	0%	*Aetea sica*	0%		
Microporella appendiculata	0%	*Puellina gattyae*	0%		
Gregarinidra gregaria	0%	*Puellina pedunculata*	0%		
Schizoporella dunkeri	0%	*Schizomavella auriculata*	0%		
Puellina gattyae	0%	*Myriapora truncata*	0%		
Puellina pedunculata	0%	*Haplopoma impressum*	0%		
Umbonula ovicellata	0%	*Puellina setosa*	0%		
Membraniporella nitida	0%	*Escharoides coccinea*	0%		
Schizomavella auriculata	0%	*Schizomavella mamillata*	0%		
Mollia circumcincta	0%	*Adeonella pallasii*	0%		
Schizomavella linearis	0%				
Parasmittina tropica	0%				
Platonea stoechas	0%				
Chorizopora brongniartii	0%				
Rhynchozoon pseudodigitatum	0%				
Schizobrachiella sanguinea	0%				
Myriapora truncata	0%				
Haplopoma impressum	0%				
Puellina setosa	0%				
Escharoides coccinea	0%				
Scrupocellaria maderensis	0%				
Schizomavella mamillata	0%				
Smittina cervicornis	0%				
Adeonella pallasii	0%				
Reteporella grimaldii	0%				

(Fig. 1). They are characterized by strong upwelling and large temperature oscillations, especially on Lastovo Island where the first diurnal internal tides were detected in the Adriatic (Novosel *et al.* 2004; Mihanović *et al.* 2006). These localities had the highest number of bryozoan species, namely 116 species were found on Struga escarpment on Lastovo, 110 species on Jabuka Islet and 109 species on Jabuka Shoal (Table 3).

Several localities are sheltered in the north Adriatic: Prvić near Senj (5), Grmac (9) and Ćutin near Cres Island (19) but each is an escarpment with moderate to strong currents. At northern Adriatic stations from the Velebit Channel (7-Žrnovnica, 8-Ždralova and 9-Grmac), benthic organisms are under the influence of numerous submarine freshwater springs, so the conditions are very different from other habitats in the North Adriatic. The salinity and sea temperature are lower than in the other parts of the North Adriatic (Orlić *et al.* 2000; Penzar *et al.* 2001; Novosel *et al.* 2005). Furthermore, submarine springs significantly increase the input of nutrients, oxygen and dissolved carbonates into benthic habitats (Novosel *et al.* 2005). Higher values of dissolved carbonates provide building material for the massive bryozoan colonies which are one of the major producers of biogenic sediments in the temperate seas (Cocito *et al.* 2004; Smith *et al.* 2006; Berning 2007; McKinney 2007). This supports the finding of the largest bryozoan colonies in the Adriatic (up to 150 cm in diameter), namely *Pentapora fascialis*, recorded on the surveyed stations in the Velebit Channel. Beside this, the growth rate of *P. fascialis* colonies in the Velebit Channel is 9.8 cm/yr, which is the fastest growing bryozoan ever reported (Cocito *et al.* 2006).

A post hoc comparison of the locality's physical features (originally defined on species composition alone) correspond to three major environmental parameters – (1) total water depth, (2) degree of thermal variation, and (3) strength of prevailing currents (Table 3).

Localities with low gradient sea floor (typically < 10°), shallow water (< 20m) with moderate to weak thermal variation and moderate to very weak currents

showed very low bryodiversity. This suggests that these are stressful conditions for bryozoans and reflect some of the more tolerant taxa.

The distribution of Adriatic bryozoan species throughout depth categories reveals that some species (20) have selective depth ranges (Table 1) while others are not restricted to any of the water depth categories. Bryozoan species strongly discriminate between the upper 20 m of a setting with a strong current that extends to 60 m relative to the upper 20 m of a setting with a maximum water depth of 20 m and a shallow slope. These results are not surprising, but should raise caution for any palaeoecology study where faunal distributions are used as proxies for water depth.

Under special environmental conditions bryozoan abundance can reach such an acme that bryozoans play a substantial role in carbonate sediment production (Taylor and Allison, 1998). In modern settings these conditions are associated with other heterotrophic skeletal producers such as ahermatypic benthic foraminifera, molluscs, and barnacles in cool water carbonate settings (Nelson 1988; James 1997; Pedley and Carannante 2006).

Settings have informally been called "bryozoan gardens" in regions where significant abundance/volume of bryozoan skeletal crop is associated with high species diversity. Throughout the Phanerozoic, sample localities with 20 to 40 bryozoan species are not uncommon, but those with 100 bryozoan species or more are uncommon, e.g. modern southern Australia (Hageman *et al.* 1995), modern New Zealand (Gordon 1986, 1989), some Miocene facies of Australia (unpublished data), Castle Hayne Eocene of North America (Canu and Bassler 1920). There is interest in what controls the production of these settings because their distribution through the Phanerozoic may be a signal for Global Climate Change (James 1997). However, our understanding of the controls is not clear (Taylor and Allison 1998).

Carbonate accumulation from the high diversity localities does not currently qualify as a factor, partially because it is short lived (Šegota 1988). However, the high diversity may provide insights as to how a bryozoan garden develops.

Table 3. Physical characteristics of 13 localities; see Figure 1 for position of the Sample Localities.
(5 – Prvić, 9 – Grmac, 10 – Veliki and Mali Ćutin, 15 – Dugi otok (Vele stijene), 16 – Kornati, 18 –Jabuka Shoal,
19 – Jabuka, 21 – Biševo, 22 – Vis, 25 – Palagruža, 28 – Lastovo, 30 – Korčula, 31 – Mljet).

Localities	# of species	Slope	Position	water depth	thermal variation	currents
5. Prvić near Senj	76	escarpment	sheltered	< 40 m	moderate	strong
9. Grmac	38	escarpment	sheltered	< 30 m	moderate	strong
10. Cres, Ćutin	43	escarpment	sheltered	< 30 m	moderate	moderate
15. Dugi Otok, Vele stijene	59	escarpment	exposed	< 40 m	moderate	moderate
16. Kornati	53	escarpment	exposed	< 60 m	moderate	moderate
18. Jabuka Shoal	109	escarpment	exposed	< 60 m	extreme	upwelling
19. Jabuka	110	escarpment	exposed	< 60 m	extreme	upwelling
21. Biševo	60	escarpment	exposed	< 40 m	moderate	strong
22. Vis, Komiža Bay	58	45°	exposed	< 30 m	moderate	moderate
25. Palagruža	67	45°	exposed	< 40 m	moderate	strong
28. Lastovo	116	escarpment	exposed	< 60 m	extreme	upwelling
30. Korčula	61	45°	sheltered	< 30 m	moderate	moderate
31. Mljet	66	escarpment	exposed	< 40 m	moderate	strong

In other regions, several studies were made in order to find out which factors influenced bryozoan communities. Mainly, it was depth (Gautier 1961; Hughes and Jackson 1992; Clarke and Lidgard 2000; Rowden, Warwick and Gordon 2004; Kuklinski *et al.* 2005), upwellings (Clarke and Lidgard 2000) or nutrient-rich bottom currents (Hayward and Ryland 1978; López-Gappa 2000; Hughes 2001), substratum (Hayward and Ryland 1978; McKinney and Jackson 1989; Kuklinski *et al.* 2006), temperature (Hayward and Ryland 1978; Kuklinski and Bader 2007) and competition (Barnes and Rothery 1996).

Our analysis provided insights into the ecological factors that control the distribution of bryozoan species in the Croatian Adriatic. Such information could be of further use in predictive models for environmental and palaeoenvironmental assessments based on bryozoan fauna alone and in monitoring environmental conditions (static/changing) over several time scales, as well as in the study of habitat selection at the species scale.

The distribution of bryozoan species in the Adriatic Sea probably depends mainly on the morphology of the Adriatic basin, bottom types, temperature and sea currents. However, future research of hard bottom benthic communities can help in understanding the patterns of biodiversity and environmental conditions in the Adriatic Sea.

REFERENCES

AYLING, A.M. 1981. The role of biological disturbance in temperate subtidal encrusting communities. *Ecology* **62**, 830–847.

BADER, B. AND SCHÄFER, P. 2005. Impact of environmental seasonality on stable isotope composition of skeletons of the temperate bryozoan *Cellaria sinuosa*. *Palaeogeography, Palaeoclimatology, Palaeoecology* **226**, 58–71.

BARNES, D.K.A. AND ROTHERY, P. 1996. Competition in encrusting Antarctic bryozoan assemblages: outcomes, influences and implications. *Journal of Experimental Marine Biology and Ecology* **196**, 267–284.

BARNES, D.K.A. AND GRIFFITHS, H.J. 2008. Biodiversity and biogeography of southern temperate

and polar bryozoans. *Global Ecology and Biogeography* **17**, 84–99.

BERNING, B. 2007. The Mediterranean bryozoan *Myriapora truncata* (Pallas, 1766): a potential indicator of (palaeo-) environmental conditions. *Lethaia* **40**, 221–232.

BEST, M.A. AND THORPE, J.P. 1996. The effects of suspended particulate matter (silt) on the feeding activity of the intertidal ctenostomate bryozoans *Flustrellidra hispida* (Fabricius). In: D.P. Gordon, A.M. Smith and Grant-Mackie, J.A. (eds.) *Bryozoans in Space and Time*, NIWA, Wellington.

CANU, F. AND BASSLER, R.S. 1920. North American Early Tertiary Bryozoa. *Smithsonian Institute United States National Museum Bulletin* **106**, 1–163.

CLARKE, A. AND LIDGARD, S. 2000. Spatial patterns of diversity in the sea: bryozoan species richness in the North Atlantic. *Journal of Animal Ecology* **69**, 799–814.

COCITO, S., NOVOSEL M. AND NOVOSEL, A. 2004. Carbonate bioformations around underwater freshwater springs in the north-eastern Adriatic Sea. *Facies* **50**, 13–17.

COCITO, S., NOVOSEL, M., PASARIĆ, Z. AND KEY, M.M.JR. 2006. Growth of the bryozoan *Pentapora fascialis* (Cheilostomata, Ascophora) around submarine freshwater springs in the Adriatic Sea. *Linzer biologische Beitrage* **38**, 15–24.

GAČIĆ, M., POULAIN, P.M., ZORE-ARMANDA, M. AND BARALE, V. 2001. Overview. In: B. Cushman-Roisin, M. Gačić, P.M. Poulain and Artegiani, A. (eds.), *Physical Oceanography of the Adriatic Sea*, Kluwer Academic Publishers, Dordrecht.

GAMULIN-BRIDA. H. 1974. Biocoenoses benthiques de la mer Adriatique. *Acta Adriatica* **15**, 1–102.

GAUTIER, Y.V. 1961 *Recherches écologiques sur les Bryozoaires Chilostomes en Méditerrannée Occidentale.* PhD thesis, Université d'Aix-Marseille, France.

GORDON, D.P. 1986. The marine fauna of New Zealand: Bryozoa: Gymnolaemata (Ctenostomata and Cheilostomata Anasca) from the western South Island continental shelf and slope. *New Zealand Oceanographic Institute Memoir* **95**, 1–121.

GORDON, D.P. 1989. The marine fauna of New Zealand: Bryozoa: Gymnolaemata (Cheilostomida Ascophorina) from the western South Island continental shelf and slope. *New Zealand Oceanographic Institute Memoir* **97**, 1–158.

HAGEMAN, S.J., BONE, Y., MCGOWRAN, B. AND JAMES, N.P. 1995. Modern bryozoan assemblages and distribution on the cool-water Lacepede Shelf, southern Australian margin. *Australian Journal of Earth Sciences* **42**, 571–580.

HARMELIN, J.G. AND CAPO, S. 2002. Effects of sewage on bryozoan diversity in Mediterranean rocky bottoms.

In: P. N. Wyse Jackson, C.J. Buttler and Spencer Jones, M.E. (eds.) *Bryozoan Studies 2001*, Swets & Zeitlinger, Lisse.

HAYWARD, P.J. AND MCKINNEY, F.K. 2002. Northern Adriatic Bryozoa from the vicinity of Rovinj, Croatia. *Bulletin of the American Museum of Natural History,* 1–139.

HAYWARD, P.J. AND RYLAND, J.S. 1978. Bryozoa from the Bay of Biscay and western approaches. *Journal of the Marine Biological Association of the United Kingdom* **58**, 143–159.

HUGHES, D.J. 2001. Quantitative analysis of a deep-water bryozoan collection from the Hebridean continental slope. *Journal of the Marine Biological Association of the United Kingdom* **81**, 987–993.

HUGHES, D.J. AND JACKSON, J.B.C. 1992. Distribution and abundance of cheilostome bryozoans on the Caribbean reefs of central Panama. *Bulletin of Marine Science* **51**(3), 443–465.

JAMES, N.P. 1997. The cool-water depositional realm. In: N.P. James and Clarke, J.A.D. (eds), *Cool-Water Carbonates. Special publication (Society of Economic Paleontologists and Mineralogists)* **56**, 1–20.

KUKLINSKI, P. AND BADER, B. 2007. Comparison of bryozoan assemblages from two contrasting Arctic shelf regions. *Estuarine, Coastal and Shelf Science* **73**, 835–843.

KUKLINSKI, P., GULLIKSEN, B., LØNNE, O.J. AND WESLAWSKI, J.M. 2005. Composition of bryozoan assemblages related to depth in Svalbard fjords and sounds. *Polar Biology* **28**, 619–630.

KUKLINSKI, P., GULLIKSEN, B., LØNNE, O.J. AND WESLAWSKI, J.M. 2006. Substratum as a structuring influence on assemblages of Arctic bryozoans. *Polar Biology* **29**, 652–661.

LÓPEZ-GAPPA, J. 2000. Species richness of marine Bryozoa in the continental shelf and slope off Argentina (south-west Atlantic). *Diversity and Distributions* **6**, 15–27.

MCKINNEY, F.K. 2007. *The Northern Adriatic ecosystem: deep time in a shallow sea*. New York, Columbia University Press.

MCKINNEY, F.K. AND JACKSON, J.B.C. 1989. *Bryozoan evolution*. Chicago/London, University of Chicago Press.

MIHANOVIĆ, H., ORLIĆ, M. AND PASARIĆ, Z. 2006. Diurnal internal tides detected in the Adriatic. *Annals of Geophysics* **24**, 2773–2780.

NELSON, C.S. 1988. An introductory perspective on non-tropical shelf carbonates. *Sedimentary Geology* **60**, 3–12.

NOVOSEL, M. 2005. Bryozoans of the Adriatic Sea. *Denisia* **16**, 231–246.

NOVOSEL. M., OLUJIĆ, G., COCITO, S. AND POŽAR-DOMAC, A. 2005. Submarine freshwater springs in the Adriatic Sea: a unique habitat for the bryozoan *Pentapora fascialis*. In: H.I. Moyano, J.M. Cancino, J.M. and P.N. Wyse Jackson (eds) *Bryozoan Studies 2004*. Leiden, A.A. Balkema, pp. 215–221.

NOVOSEL, M. AND POŽAR-DOMAC, A. 2001. Checklist of Bryozoa of the Eastern Adriatic Sea. *Natura Croatica* **10**, 367–421.

NOVOSEL, M., POŽAR-DOMAC, A. AND PASARIĆ, M. 2004. Diversity and distribution of the Bryozoa along underwater cliffs in the Adriatic Sea with special reference to thermal regime. *Marine Ecology-Pubblicazioni della Stazione Zoologica di Napoli* 25, 155–170.

ORLIĆ, M., GAČIĆ, M. AND LA VIOLETTE, P.E. 1992. The currents and circulation of the Adriatic Sea. *Oceanologica Acta*, **15/2**, 109–124.

ORLIĆ, M., LEDER, N., PASARIĆ, M. AND SMIRČIĆ, A. 2000. Physical properties and currents recorded during September and October 1998 in the Velebit Channel (East Adriatic). *Periodicum biologorum* **102**, 31–37.

PEDLEY, M. AND CARANNANTE, G. 2006. Cool-water carbonate ramps: a review. *Geological Society of London Special Publication* **255**, 1–9.

PENZAR, B., PENZAR, I. AND ORLIĆ, M. 2001. *Weather and Climate of the Croatian Adriatic*. Zagreb, Biblioteka Geographia Croatica, Dr. Feletar.

ROWDEN, A.A., WARWICK, R.M. AND GORDON, D.P. 2004. Bryozoan biodiversity in the New Zealand region and implications for marine conservation. *Biodiversity and Conservation* **13**, 2695–2721.

RYLAND, J.S. 1970. *Bryozoans*. Hutchinson University Library, London.

SMITH, A.M., KEY, M.M. JR. AND GORDON, D.P. 2006. Skeletal mineralogy of bryozoans: taxonomic and temporal patterns. *Earth-Science Reviews* **78**, 287–306.

ŠEGOTA, T. 1988. *The Climate of the Last Glaciation. Climatology for Geographists*. Zagreb, Školska knjiga.

TAYLOR, P.D. AND ALLISON, P.A. 1998. Bryozoan carbonates through time and space. *Geology* **26**, 459–462.

VILIBIĆ, I. AND ORLIĆ, M. 2002. Adriatic water masses, their rates of formation and transport through the Otranto Strait. *Deep-Sea Research Part I*, **49**, 1321–1340.

VILIBIĆ, I. AND SUPIĆ, N. 2005. Dense water generation on a shelf: the case of the Adriatic Sea. *Ocean Dynamics* **55/5-6**, 403–415.

ZAVODNIK, D., JAKLIN, A., RADOŠEVIĆ, M. AND ZAVODNIK, N. 2000. Distribution of benthos at Jabuka, an islet of volcanic rock (Adriatic Sea). *Periodicum biologorum* **102**, 157–167.

Skeletal mineralogy patterns of Bryozoa from the Aleutian Islands in the context of revealing a global pattern in bryozoan skeletal mineralogy

Anna Piwoni-Piórewicz[1]*, Małgorzata Krzemińska[1], Anna Iglikowska[1], Najorka Jens[3] and Piotr Kukliński[1,2]

[1]Institute of Oceanology Polish Academy of Sciences, Powstańcow Warszawy 55, 81-712, Sopot, Poland
[*corresponding author: e-mail: apiwoni@iopan.pl]
[2]Department of Life Sciences, Natural History Museum, Cromwell Road, London SW7 5BD, United Kingdom
[3]Imaging and Analysis Centre, Natural History Museum, Cromwell Road, London SW7 5BD, United Kingdom

ABSTRACT

In many areas of the world ocean bryozoans are important carbonate producers. Evidence suggests that in colder high-latitude marine environments most bryozoan species precipitate in most cases low-magnesium calcite (≤ 4 mol% $MgCO_3$) carbonate skeletons, while secretion of aragonite and high-magnesium calcite (≥ 12 mol% $MgCO_3$) is largely restricted to warmer low-latitude waters. Although such a pattern seems to exist, it is not robustly confirmed by empirical data. This study explores the mineralogical composition of bryozoans along the Aleutian Islands to examine the mineralogical variability of skeletons precipitated in the transition zone between temperate and Arctic areas. The mineralogical investigation of 120 bryozoan samples from the Aleutian Islands indicates that 117 skeletons are built of calcite and three of mixed calcite and aragonite layers with magnesium content in calcite ranging from 2.2 to 8.0 mol% $MgCO_3$. The mineralogical profile of Aleutian bryozoans is consistent with the increasing solubility of aragonite and high-magnesium calcite with decreasing water temperature. A high variability of Mg content in calcite within and among species is most likely caused by species-specific physiological features. In a global context, this study confirms the latitudinal pattern in bryozoan mineralogy and indicates environment as an important factor controlling the calcification process.

INTRODUCTION

Many marine organisms produce calcium carbonate hard parts in the form of shells and skeletons with specific properties. They can precipitate two polymorphic forms of calcium carbonate, aragonite and calcite. Most shells and skeletons are purely calcite or purely aragonitic or may contain both aragonite and calcite in separate layers (Lowenstam 1981; Lowenstam and Weiner 1989; Mann 2001). The calcification process includes a broad spectrum of factors controlling precipitation. Although the type of mineral composition in organisms is mainly biologically and genetically controlled (Watabe and Wilbur 1960; Addadi and Weiner 1992; Belcher *et al*. 1996, Dove 2010, Tambutté *et al*. 2012), environmental physical-chemical factors (e.g. temperature, salinity) also affect its properties (Dodd 1965; Lorens and Bender 1980; Bourgoin 1990; Pitts and Wallace 1994; Klein *et al*. 1996a, 1996b). In biologically-controlled mineralization, the organism steers the process of crystal nucleation and growth independently from environmental

conditions. Biogenic minerals develop on the organic matrix under specific biological conditions (e.g. growth rate, sex, age) and genetic control. In contrast, environmentally-controlled mineralization is dependent on surrounding conditions, mainly temperature, pH and salinity (Lowenstam and Weiner 1989, Smith *et al*. 1998, 2006; Kuklinski and Taylor 2009; Taylor *et al*. 2009, 2014, 2016; Krzeminska *et al*. 2016). Thus, sequentially formed biogenic calcium carbonate layers record the growth history and environmental conditions in which the organism calcified (Fuge *et al*. 1993; Klein *et al*. 1996a, 1996b; Stecher *et al*. 1996; Swart and Grottoli 2003; Strasser *et al*. 2008).

Aragonite, being denser and harder than calcite (Chen *et al*. 2012) is thermodynamically more expensive to build and more soluble, especially in cold water (Anderson and Crerer 1993). Calcite is stable and least soluble in cold water, but it is brittle. Adding Mg to calcite increases its solubility (Morse *et al*. 2007; Nehrke 2007; Gebauer and Cölfen 2011; Radha and Navrotsky 2013). A recent study found $CaCO_3$ polymorph selection might be temperature-dependent, with a pronounced trend in the proportion of aragonite and bimineralic skeletons, as well as $MgCO_3$ content in calcite, showing a latitudinal increase into the warmer waters (Cohen and Branch 1992; Smith *et al*. 1998, 2006; Kuklinski and Taylor 2009; Taylor *et al*. 2009, 2014, 2016; Ramajo *et al*. 2015, Taylor *et al*. 2016, Krzeminska *et al*. 2016).

The focus of this investigation is the skeletal mineralogy of sub-arctic bryozoans. They are good model taxa for tracking changes in biomineralogy. They are colonial sessile invertebrates, occurring in a wide range of marine and freshwater habitats (stones, algae, sediments), depths (Figuerola *et al*. 2012) and latitudes (Smith *et al*. 2006; Kuklinski and Taylor 2009). The majority of these colonial invertebrates use calcium carbonate to build the external skeletons (Taylor *et al*. 2014). Carbonate composition of bryozoan skeletons is highly variable due to their ability to precipitate calcite, aragonite, or both minerals (Smith *et al*. 2006; Taylor *et al*. 2014).

The species and genera with the highest degree of variability in mineralogy have great potential for interpretation of environmental and paleoenvironmental conditions. Yet, environmentally-related variations cannot be robustly reconstructed without a clear understanding of the factors driving the mineralogical variability present within the bryozoans. Previous mineralogical studies covered a small proportion of living bryozoans. The research on bryozoan mineralogy was conducted most intensively in the temperate zone, e.g., New Zealand (Smith *et al*. 1998; Steger *et al*. 2005; Smith *et al*. 2010), the Mediterranean (Poluzzi and Sartori 1975; Lombardi *et al*. 2011), Chile (Smith and Clark 2010) and Scottish waters (Loxton *et al*. 2018); but also in tropical Malaysia (Taylor *et al*. 2016); Arctic, e.g., Svalbard (Kuklinski and Taylor 2009) and Antarctic (Loxton *et al*. 2012; Loxton *et al*. 2014; Taylor *et al*. 2009; Krzeminska *et al*. 2016).

The Aleutian Islands are located between 51° and 55° N latitude, which places them both on the northern boundary of the temperate zone and in the southern Arctic region (Fig. 1). The water temperature around the Aleutians has year-round variability ranging from about 0 to 13°C (NOAA, 2019). Such conditions act as very good model area to examine the mineralogical variability of skeletons precipitated by bryozoans in the transition zone between the temperate and arctic zones. Investigations of bryozoans from this region are scanty, and especially the investigations focusing on bryozoan skeletal mineralogy that are absent. Therefore, the aim of this study is to analyse the skeletal mineralogy of bryozoans from the Aleutian Islands. The new data from this region will help us to understand the global patterns of bryozoan mineralogy.

MATERIALS AND METHODS
Study area
The Aleutian Islands are a 2260 km long chain of almost 70 islands belonging to both USA and Russia. They extend between Alaska, Siberia and southern edge of the Bering Sea, forming

a permeable boundary between the North Pacific and the Bering Sea. The two investigated islands, Amchitka (51°32'N, 178°59'E) and Adak (51°47'N, 176°38'W), are located on the western border of the eastern hemisphere near 180 degrees longitude (Fig. 1). The surrounding shelf is narrow, and water depth increases rapidly off the shelf. The climate of the islands is oceanic. Summer weather is much cooler than Southeast Alaska region, but the winter temperature is nearly the same, shaping the annual surface water temperature between 0 and 10°C (Coyle and Pinchuk 2005, Ladd 2005, NOAA, 2019).

The collection and processing of samples

The collection of bryozoans was conducted in July 2011 around Amchitka and Adak by SCUBA divers at depths down to 20 m. Samples were preserved in 75% ethanol.

The mineralogical analysis was based on both well and weakly calcified forms of encrusting and erect species. Bryozoans from the natural environment are often abundantly covered with overgrowing flora and fauna. These epibionts can potentially introduce contamination into sample with their own mineralogy, thus each bryozoan colony was examined under a stereo microscope in order to remove unwanted organisms. Afterwards, samples were identified under a stereo microscope to the lowest possible taxonomic level. The bryozoan biodiversity of the Aleutian Islands is still incomplete (Kuklinski *et al.* 2015), therefore individuals were classified to the family and genus or species rank. Specimens that could not be classified were marked as sp. 2 – sp. 13. From all individuals 5-10 mm (depending on the colony size) of the colony edge was ground into powder using an agate pestle and mortar, and subjected

Figure 1. Map of the study area, Aleutian Islands. The study area, marked by black dots, includes two islands: Amchitka (51°32'N, 178°59'E) and Adak (51°47'N, 176°38'W).

to mineralogical analyses to evaluate the calcite and aragonite content (wt%), as well as content of magnesium calcite (mol% MgCO$_3$).

Data for the illustrating the geographical variability of MgCO$_3$ in bryozoan skeletons were obtained from the literature (Loxton *et al*. 2018; Krzeminska *et al*. 2016; Smith *et al*. 1998; Kuklinski and Taylor 2009; Borisenko and Gontar 1991; Poluzzi and Sartori 1975; Smith and Clark 2010; Taylor *et al*. 2016) and this study.

Mineralogical analysis

Mineralogical analyses were carried out at the Imaging and Analysis Centre of the Natural History Museum in London (in a similar procedure as reported in Piwoni-Piorewicz *et al*. 2017; Loxton *et al*. 2018; Krzeminska *et al*. 2016; Smith *et al*. 1998; Kuklinski and Taylor 2009). Powdered samples were placed on circular quartz discs (zero-background holders) and analysed using an Enraf-Nonius PDS 120 X-ray diffractometer. The XRD system is equipped with a primary monochromator (germanium 111) and an INEL 120º curved position sensitive detector (PSD). The X-ray tube (cobalt) was operated at 40 kV and 35 mA and pure Co Kα_1 radiation was selected using slits settings of 0.14 x 5 mm after the monochromator. The 2Theta linearity of the PSD was calibrated with Y$_2$O$_3$ as external standard. Furthermore, an internal standard (NaCl) was added to the samples to correct for sample displacement.

Diffractograms were collected in asymmetric flat-plate reflection geometry without angular movement of tube, sample and detector position. The tilting angle between the incoming monochromatic beam and the sample holder was kept constant at ~6º. The measurements were usually 15 min long and samples were rotated during the analysis to increase the number of crystallites in the X-ray beam.

The amount of the CaCO$_3$ polymorph was determined by fitting whole-pattern intensities of standard patterns, generated from 100% aragonite (BM 53533) and 100% calcite (ground Iceland Spar), to the sample patterns. The error associated with this method was estimated to be within ± 3%.

The position of the d104 peak was measured to calculate the Mg content (expressed as mol% MgCO$_3$) in calcite using equation (1):

$$mol\%MgCO_3 = \frac{d_{104}^{calcite} - d_{104}^{Mg-calcite\,(sample)}}{d_{104}^{calcite} - d_{104}^{magnesite}} \quad (1)$$

with d104 values for calcite and magnesite taken from NBS standards (reference codes [5-586] and [8-479] in PDF-2 database from ICDD). A linear relationship exists between d104 and mol% MgCO$_3$ in calcite in the range between 0 and 20 mol% (e.g. Mackenzie *et al*. 1983, Bischoff *et al*. 1983) and compositions of all calcites in this study fall into this range. Peak assignment and fitting was performed using the Highscore software (Panalytical).

Data analysis

The statistical testing was conducted to evaluate the differences between mol% MgCO$_3$ in calcite of globally sampled bryozoans. The data were not normally distributed (Shapiro-Wilk test), therefore the differences were tested by one-way Kruskal-Wallis nonparametric ANOVA and post-hoc Dunn's test (*p*-value = 0.05). Statistical computing and graphical visualizations were performed in RStudio software.

RESULTS

Among all analysed specimens (n = 120, 46 different taxa), 90 individuals were assigned to at least family taxonomic level (16 families), and 30 individuals were unidentified and classified as 12 unknown species (Appendix 1).

The mineralogical investigation of 120 bryozoan skeletal samples from the Aleutian Islands indicated all taxa to be built of calcite, while three skeletons of coexisting calcite and aragonite. The only one bimineralic species was *Parasmittina* sp. Among the three analyzed samples, calcite was the dominant form, while aragonite occupied 15.8 ± 0.5 wt% (Appendix 1).

Due to small colony sizes of two taxa, *Hippothoa hyalina* (n = 2) and *Hippothoa* sp. (n = 1), they were excluded from measurement of $MgCO_3$ in calcite and further analysis was conducted for the remaining 117 individuals. The content of $MgCO_3$ was on average 5.1 ± 1.6 mol% (2.2 to 7.4 mol% $MgCO_3$). The skeletons were mostly precipitated as intermediate magnesium calcite (IMC, 69% of skeletons, n = 81) with mean 6.0 ± 1.0 mol% $MgCO_3$, whereas the remaining 31% (n = 36) as low magnesium calcite (LMC) with mean 3.1 ± 0.6 mol% $MgCO_3$ (Appendix 1). *Tricellaria* cf. *ternata* was found to have the smallest content of $MgCO_3$ (2.2 mol% $MgCO_3$, n = 1), whereas the highest values were detected in *Parasmittina* cf. *jeffreysi* (7.9 mol% $MgCO_3$, n = 1) with highest value. The highest variability of mol% $MgCO_3$ was found in *Tricellaria* cf. *ternata* (3.5 ± 2.5 mol% $MgCO_3$, n = 5) and *Dendrobeania* sp. 1 (6.1 ± 2.4 mol% $MgCO_3$, n = 5) (Fig. 2).

Bryozoans from 14 families secreted on average IMC, whereas LMC was found in two families (Myriaporidae, Candidae). The lowest mean content of mol% $MgCO_3$ was found in family Myriaporidae (3.4 ± 0.9 mol% $MgCO_3$, n = 8) and the highest in Hippoporidridae (7.0 ± 0.5 mol% $MgCO_3$, n = 2). Family Candidae was the most variable in terms of mol% $MgCO_3$ (3.5 ± 2.5 mol% $MgCO_3$, n = 5). However, this variability results from one outlying sample with elevated $MgCO_3 = 7.9$ mol%. High variability was found likewise within Bugulidae family (5.3 ± 2.3 mol% $MgCO_3$, n = 9), and here samples were distributed between 2.9 and 8.0 mol% $MgCO_3$ (Appendix 1, Table 1).

The bryozoans from Arctic, Antarctic and Aleutian Islands were dominantly calcitic. (Fig. 3). A Kruskal-Wallis test (H = 82.873, $p < 0.01$) revealed significant variability of mol% $MgCO_3$ in skeletons from the polar and temperate zones (Fig. 4). A post-hoc Dunn's test for all regions showed no significant differences in mol% $MgCO_3$ in calcite between Arctic and Antarctic ($p = 0.14$), and distinguished them from most regions of temperate zone, except no differences between Aleutians and Antarctic ($p = 1.00$). Within temperate zone, the differences were found between

the Mediterranean Sea and Aleutian Islands ($p < 0.01$), Scotland ($p < 0.01$) and New Zealand ($p < 0.01$), as well as between Scotland and Aleutian Islands ($p = 0.03$) (Table 2). The highest content of mol% $MgCO_3$ was calculated for bryozoans from Mediterranean Sea (IMC = 7.7 ± 2.0 mol% $MgCO_3$, n = 81), while the lowest from Arctic (LMC = 4.0 ± 2.2 mol% $MgCO_3$, n = 149) (Appendix 1, Fig. 4).

DISCUSSION

The study of skeletal mineralogy of bryozoans from the Aleutian Islands: Amchitka and Adak revealed this assemblage as predominantly built of intermediate Mg calcite (5.1 ± 1.6 mol%, n = 117, Fig. 2). Of the 120 studied samples, three varied mineralogically, being a mixture of calcite and aragonite. Such mineralogy appears to be shaped by water temperature to avoid the corrosion of aragonite and high Mg calcite in cold waters (Taylor and Reid 1990; Cohen and Branch 1992; Kuklinski and Taylor 2009; Loxton *et al.* 2012; Ramajo *et al.* 2015; Krzeminska *et al.* 2016). Lombardi *et al.* (2008) examined winter and summer growth bands from bimineralic *Pentapora* sampled in the three localities characterized by the same thermal regime (min T = 9.1°C) and revealed a higher calcite content in the winter (mean 32 – 42 wt%) than in the summer (mean 22 – 29 wt%) growth bands. The Aleutian Islands belong to the oceanic sub-polar region with moderately cold winters and cool summers (Troll 1965). A longer winter than summer season and the warm Alaskan Stream shape the surface water temperature with yearly variation from about 0 to 10°C with mean about 5°C (Reed and Stabeno 1994; Coyle and Pinchuk 2005; Ladd 2005; NOAA 2019). Such environmental conditions, most likely, contributed to the dominance of intermediate $MgCO_3$ level within the Aleutian bryozoan population (Fig. 2). Intermediate Mg content in bryozoan skeletons has been mainly reported in previous publications investigating the mineralogy of bryozoans from temperate waters. The main environmental controlling factor usually discussed
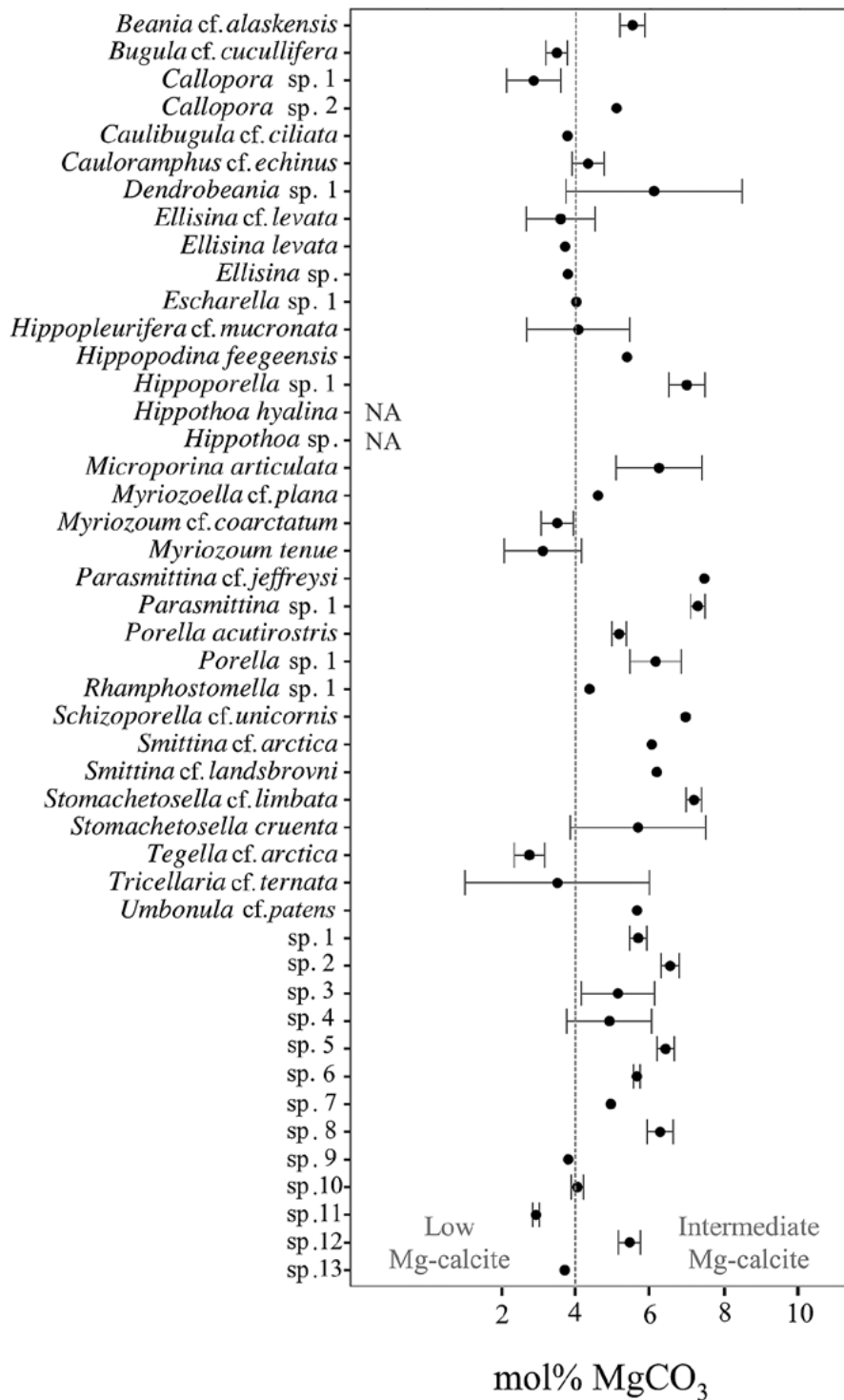
Figure 2. Distribution of means (black dots) and ± 1 standard deviations (whiskers) of magnesium level in calcite (mol% MgCO₃) among studied bryozoan taxa from the Aleutian Islands. The dotted line separates samples consisted of low magnesium calcite (< 4 mol%) and intermediate magnesium calcite (4 – 12 mol%), NA – not available.
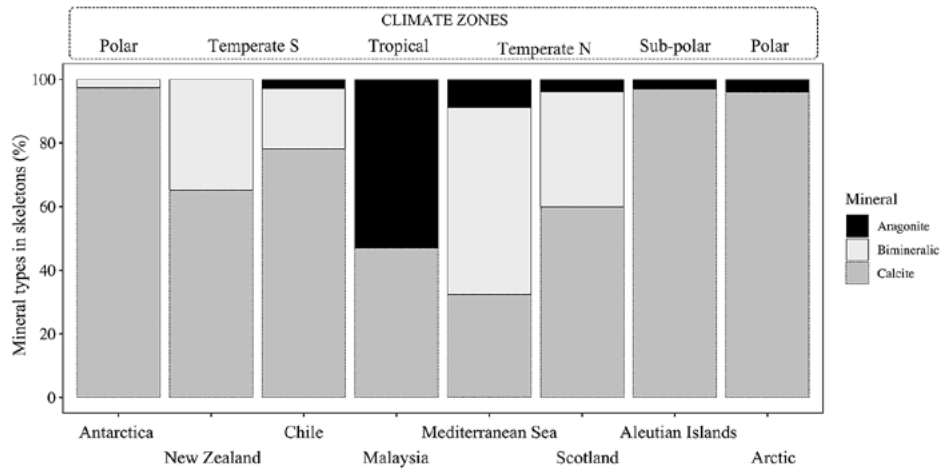
Figure 3. Global latitudinal distribution of mineral type (calcite, aragonite or bimineralic) within skeletons of bryozoans based on data extracted from literature (see methodology) and from this study (Aleutian Islands), N = North, S = South.

was temperature that positively drives the $MgCO_3$ level in skeletons (Lombardi *et al.* 2006, 2008; Barnes *et al.* 2006, 2007; Smith 2007, Smith and Clark 2010; Loxton *at al.* 2018). Nevertheless, other environmental parameters, e.g. food availability, variability in seawater $CaCO_3$ saturation state, as well as biological features may act in combination with temperature to determine the bryozoan mineralogy. The $CaCO_3$ saturation state decreases with decreasing temperature and along depth gradient (Orr *et al.* 2005;

Table 1. The mean magnesium level in calcite (mol% $MgCO_3$) among studied bryozoan families from the Aleutian Islands.

Family	N	Mean mol% $MgCO_3$	±1SD
Myriaporidae	8	3.4	0.9
Candidae	5	3.5	2.5
Romancheinidae	4	4.1	1.1
Umbonulidae	2	5.0	0.9
Calloporidae	17	5.1	0.0
Bugulidae	9	5.3	2.3
Hippopodinidae	1	5.4	0.0
Beaniidae	4	5.5	0.3
Reteporellidae	5	5.7	0.2
Bryocryptellidae	8	5.9	0.7
Microporidae	10	6.2	1.2
Stomachetosellidae	5	6.6	1.2
Smittinidae	6	6.9	0.6
Schizoporellidae	1	6.9	0.0
Hippoporidridae	2	7.0	0.5
Hippothoidae	3	*NA*	*NA*

Andersson *et al.* 2008; Fabry *et al.* 2009). Lower CO_3^{2-} concentration in cold waters favours carbonate deposits as calcite with low Mg level both kinetically and thermodynamically (Mackenzie *et al.* 1983). Furthermore, as calcite is less energetically costly than aragonite to precipitate (Ramajo *et al.* 2015), a relatively low metabolic rate of cold-water organisms (Andersson *et al.* 2008) might support the dominance of intermediate-Mg calcite in skeletons from the sub-polar region of Aleutian Islands.

The analysis of mol% $MgCO_3$ in calcite within Aleutian bryozoans revealed a compositional variability within families (Table 3) and species (Fig. 2), affected by the same environmental parameters. The $MgCO_3$ content varied from 2.2 to 7.9 mol% with mean 5.1 ± 1.6 mol%. The intraspecific differences from a single location were previously found in bryozoans and were believed to result from biologically controlled processes (Smith *et al.* 1998; Smith 2006, Krzeminska *et al.* 2016). Each collected individual could be at a different level of astogenetical

development, had a slightly different growth rate or could be in a different reproduction phase. These biological processes might lead to physiological regulations over Mg incorporation into calcite and could be reflected in mol% $MgCO_3$ variability in skeletons of individuals both on species or family level (Magdans and Gies 2004). Loxton *et al.* (2018) likewise revealed mineralogical variability of Scottish bryozoans and concluded a combined reflection of physiology and phylogeny, as well as seasonal environmental conditions of Scotland's waters.

The global latitudinal distribution of the mineral type (calcite, aragonite or bimineralic) and mol% $MgCO_3$ content among bryozoans occurring in Aleutian Islands combined with literature data (Loxton *et al.* 2018; Krzeminska *et al.* 2016; Smith *et al.* 1998; Kuklinski and Taylor 2009; Borisenko and Gontar 1991; Poluzzi and Sartori 1975; Smith and Clark 2010; Taylor *et al.* 2016) is most likely due to the different temperature regimes in selected localities (Figs. 4 and 5). The mineralogy of Aleutian

Figure 4. Global latitudinal distribution of mean mol% $MgCO_3 \pm 1$ standard deviation (whiskers) in calcite among bryozoans based on data extracted from literature and from this study (Aleutian Islands). The dotted line separates samples consisting of low magnesium calcite (< 4 mol% $MgCO_3$) and intermediate magnesium calcite (4–12 mol% $MgCO_3$), N = North, S = South
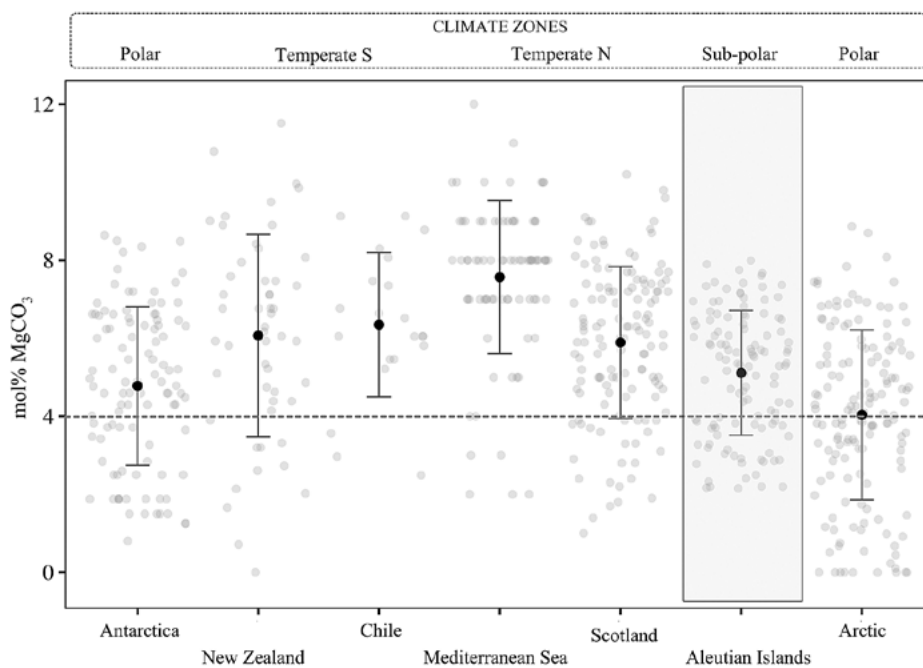
Table 2. Pairwise comparison (post-hoc Dunn's test, p = 0.05) of mol% MgCO$_3$ in skeletons of bryozoans from different regions of the World Ocean based on data extracted from literature (see methodology) and from this study (Aleutian Islands).

Region	p
Mediterranean Sea – Arctic	< 0.01
Antarctic – Mediterranean Sea	< 0.01
Mediterranean Sea – Aleutian Islands	< 0.01
Scotland – Arctic	< 0.01
Mediterranean Sea – Scotland	< 0.01
New Zealand – Arctic	< 0.01
Chile – Arctic	< 0.01
New Zealand – Mediterranean Sea	< 0.01
Antarctic – Scotland	< 0.01
Antarctic – New Zealand	0.01
Aleutian Islands – Arctic	0.01
Antarctic – Chile	0.03
Scotland – Aleutian Islands	0.03
New Zealand – Aleutian Islands	0.06
Chile – Aleutian Islands	0.08
Antarctic – Arctic	0.14
Chile – Mediterranean Sea	0.14
New Zealand – Scotland	0.71
New Zealand – Chile	1.00
Chile – Scotland	1.00
Antarctic – Aleutian Islands	1.00

specimens reflects the transition area between temperate zone and Arctic region. The skeletons of Aleutian bryozoans are most reminiscent of the Arctic and Antarctic populations (Fig. 3), which seems to be a consequence of thermal conditions prevailing in the studied area (Fig. 1). The visualized mineralogical pattern indicates these three cold-water regions as almost entirely favourable to the production of calcite. A low content of aragonite was found in four Arctic bryozoan species: *Lepralioides nordlandica* (8.2–10.4 wt%), *Pachyegis princeps* (7.2–17.4 wt%), and

Raymondica bella (11.8–12.9 wt%), *Parasmittina trispinosa* (10.6 wt%, Kuklinski and Taylor 2009), and one Antarctic species: *Isosecuriflustra angusta* (11–33 wt%, Loxton *et al.* 2012). However, *I. angusta* examined by Krzeminska *et al.* (2016) turned out to be fully calcitic. This mineralogical difference was suggested to be a result of genetic isolation between eastern (Loxton *et al.* 2012) and western (Krzeminska *et al.* 2016) Antarctic populations or possibly cryptic speciation. *Parasmittina* sp. 1 (n = 3) was the only one Aleutian taxa found to secrete bimineralic skeletons (15.3–16.3 wt% of aragonite). Simultaneously, *Parasmittina* cf. *jeffreysi* (n = 1) contained pure calcite (Appendix 1). The aragonite/calcite ratio within this genus varied greatly. Kuklinski and Taylor (2009) examined three samples of *Parasmittina trispinosa* in the Arctic and one likewise was bimineralic with 10.6 wt% of aragonite, while two were calcitic. Species of *Parasmittina*, a cosmopolitan genus, have the ability to precipitate both calcite and aragonite in different proportions, and were found to be fully aragonitic in tropics (Taylor *et al.* 2016). Comparisons between the mineralogy of bryozoans along a temperature gradient have corroborated this phenomenon and shown some widely distributed genera to precipitate aragonite towards lower latitudes and higher temperatures. *Schizoporella unicornis* was found to produce more calcite in higher latitudes than in warmer, low-latitude waters (Lowenstam, 1954; Rucker and Carver 1969). Lombardi *et al.* (2008) studied the bimineralic *Pentapora* and likewise found higher content of aragonite in a population from the warmer waters of Mediterranean than in Atlantic. However, Smith *et al.* (1998) revealed no temperature effect on the mineralogy of bryozoans covering a wide range of latitudes (25–52°S) around New Zealand. Furthermore, *Foveolaria cyclops* showed a reverse trend with more aragonite deposited at higher latitudes. This was probably due to a biologically mediated change in precipitation or a kind of genetic differentiation.

The analysis of the latitudinal MgCO$_3$ content shows that polar regions do not differ in mol%

MgCO$_3$ contained in bryozoan skeletons ($p = 0.14$). Furthermore, there were no differences between Antarctic and sub-polar Aleutian Islands ($p = 1$). Close location of Aleutian Islands and Arctic did not allow to avoid the divergence in MgCO$_3$ level between relevant populations. The Arctic fauna predominantly consists of species with Pacific and Atlantic origin that colonized the Arctic Ocean after the last glacial maximum (Dunton 1992). The content of MgCO$_3$ in skeletons shows adaptation to the coldest polar environment by incorporating the lowest level of Mg into calcite (Fig. 4) as suggested by Loxton *et al*. (2018). Furthermore, the narrow connection throughout the Bering Strait potentially could lead to genetic isolation. Globally, Mg incorporation had an increasing tendency towards higher temperatures with a maximum in the warmest Mediterranean Sea (IMC = 7.67 ± 1.96, Fig. 4). The sub-arctic population had a lower MgCO$_3$ content than the Scottish one from higher latitude ($p = 0.03$). A latitudinal trend in MgCO$_3$ deposition has previously been found in comparisons among Arctic, temperate and tropical bryozoans (Kuklinski and Taylor 2009; Figuerola *et al*. 2015, Lombardi *et al*. 2008; Loxton *et al*. 2012) as well as among representatives of foraminifera (Lea *et al*. 1999; Nürnberg *et al*. 1996), coccoliths (Ra *et al*. 2010) or molluscs (Vander Putten *et al*. 2000; Gillikin *et al*. 2005). The data presenting skeletal MgCO$_3$ in a latitudinal order supported variability between specimens within populations (Fig. 4). Therefore, as discussed above, the biological regulation without a doubt determines the mineralogical properties of skeletons (Magdans and Gies 2004; Loxton *et al*. 2014; Smith 2014).

CONCLUSIONS

The Aleutian bryozoans precipitate mostly monomineral skeletons composed of calcite with a MgCO$_3$ content variing from 2.2 to 7.9 mol%. Such mineralogy makes Aleutian population a part of the global trend of calcite increase with a decrease of MgCO$_3$ content towards colder water. The differences in mol% MgCO$_3$ content within

species and populations are likely to be biologically determined. Temperature, which controls numerous water parameters and physiological processes, is most likely the strongest driver of the mineralogical variability.

This study suggests that biological regulation affects the mineralogical properties of bryozoan skeleton; yet globally does not dominate over temperature dependence during calcification. Even if temperature does not change the species-specific mineralogy, it can selectively affect species occurrence. On this basis, we suggest that bryozoans provide a promising indicator of paleo-temperature, yet still require a robust understanding of the factors driving the species-specific mineralogical course.

ACKNOWLEDGEMENTS

REFERENCES

ADDADI, L. AND WEINER, S. 1992. Control and design principles in biological mineralization. *Angewandte Chemie International Edition* **31**, 153–169.

ANDERSON, G.M. AND CRERER, D.A. 1993. Standard state thermodynamic properties of selected minerals and other compounds. In: G.M. Anderson and D.A. Crerer (eds.), *Thermodynamics in geochemistry: the equilibrium model*. New York, Oxford University Press, pp. 547−552.

ANDERSSON, A.J., MACKENZIE, F.T. AND BATES, N.R. 2008. Life on the margin: implications of ocean acidification on Mg-calcite, high latitude and cold-water marine calcifiers. *Marine Ecology Progress Series* **373**, 265–273.

BARNES, D.K.A. AND CONLAN, K.E. 2007. Disturbance, colonization and development of Antarctic benthic communities. *Philosophical Transactions of the Royal Society, Series B* **362**, 11–38.

BARNES, D.K.A., HODGSON, D.A., CONVEY, P., ALLEN, C.S. AND CLARKE, A. 2006. Incursion and excursion of Antarctic biota: past, present and future. *Global Ecology and Biogeography* **15**, 121–142.

BELCHER, A.M., WU, X.H., CHRISTENSEN, R.J., HANSMA, P.K., STUCKY, G.D. AND MORSE, D.E.

1996. Control of crystal phase switching and orientation by soluble mollusc-shell proteins. *Nature* **381**, 56–58.

BISCHOFF W.D., BISHOP F.C., MACKENZIE F.T. (1983) Biogenically produced magnesian calcite, inhomogeneities in chemical and physical-properties comparison with synthetic phases. American Mineralogist 68: 1183−1188

BORISENKO, Y.N. AND GONTAR, V. 1991. Biogeochemistry of skeletons of coldwater Bryozoa. *Biologiya Morya* **1**, 80−90.

BOURGOIN, B.P. 1990. *Mytilus edulis* shell as a bioindicator of lead pollution: considerations on bioavailability and variability. *Marine ecology progress series. Oldendorf* **61**(3), 253–262.

CHEN, P.Y., MCKITTRICK, J. AND MEYERS, M.A. 2012. Biological materials: functional adaptations and bioinspired designs. *Progress in Materials Science* **57**, 1492–1704.

COHEN, A.L. AND BRANCH, G.M. 1992. Environmentally controlled variation in the structure and mineralogy of *Patella granularis* shells from the coast of southern Africa: implications for palaeotemperature assessments. *Palaeogeography, Palaeoclimatology, Palaeoecology* **91**, 49−57.

COYLE, K.O. AND PINCHUK, A.I. 2005. Seasonal cross-shelf distribution of major zooplankton taxa on the northern Gulf of Alaska shelf relative to water mass properties, species depth preferences and vertical migration behavior. *Deep Sea Research Part II: Topical Studies in Oceanography* **52.1-2**: 217-245.

DODD, J.R. 1965. Environmental control of strontium and magnesium in *Mytilus. Geochimica et Cosmochimica Acta* **29**, 385–398.

DOVE, P.M. 2010. The rise of skeletal biominerals. *Elements* **6**, 37–42.

DUNTON K. 1992. Arctic biogeography: the paradox of the marine benthic fauna and flora. *Trends in Ecology & Evolution* **7**, 183–189.

FABRY, V.J., MCCLINTOCK, J.B., MATHIS, J.T. AND GREBMEIER, J.M. 2009. Ocean acidification at high latitudes: the bellwether. *Oceanography* **22**, 160–171.

FIGUEROLA, B., MONLEÓN-GETINO, T., BALLESTEROS, M. AND AVILA, C. 2012. Spatial patterns and diversity of bryozoan communities from the Southern Ocean: South Shetland Islands, Bouvet Island and Eastern Weddell Sea. *Systematics and Biodiversity* **10**(1), 109–123.

FIGUEROLA, B., KUKLIŃSKI, P. AND TAYLOR, P.D. 2015. Depth patterns in Antarctic bryozoan skeletal Mg-calcite: can they provide an analogue for future environmental changes? *Marine Ecology Progress Series* **540**, 109–120.

FUGE, R., PALMER, T.J., PEARCE, N.J.G. AND PERKINS, W.T. 1993. Minor and trace element chemistry of modern shells: a laser ablation inductively coupled plasma spectrometry study. *Applied Geochemistry* **2**, 111–116.

GEBAUER, D. AND CÖLFEN, H. 2011. Prenucleation clusters and non-classical nucleation, *Nano Today* **6**, 564–584.

GILLIKIN, D.P., LORRAIN, A., NAVEZ, J., TAYLOR, J.W., KEPPENS, E., BAEYENS, W. AND DEHAIRS, F. 2005. Strong biological controls on Sr/Ca ratios in aragonitic marine bivalve shells. *Geochemistry, Geophysics, Geosystems* **6**, Q05009.

KLEIN, R.T., LOHMANN, K.C. AND THAYER, C.W. 1996a. Sr/Ca and ^{13}C/^{12}C ratios in skeletal calcite of *Mytilus trossulus*: covariation with metabolic rate, salinity, and carbon isotopic composition of seawater. *Geochimica et Cosmochimica Acta* **60**, 4207–4221.

KLEIN, R.T., LOHMANN, K.C. AND THAYER, C.W. 1996b. Bivalve skeletons record sea-surface temperatures and ^{18}O via Mg/Ca and ^{18}O/^{16}O ratios. *Geology* **24**, 415–418.

KRZEMINSKA, M., KUKLINSKI, P., NAJORKA, J. AND IGLIKOWSKA, A. 2016. Skeletal mineralogy patterns of Antarctic Bryozoa. *The Journal of Geology* **124**(3), 411–422.

KUKLINSKI, P., GRISCHENKO, A.V. AND JEWETT, S.C. 2015. Two new species of the cheilostome bryozoan *Cheilopora* from the Aleutian Islands. *Zootaxa* **3963**(3), 434–442.

KUKLINSKI, P. AND TAYLOR, P.D. 2009. Mineralogy of Arctic bryozoan skeletons in a global context. *Facies* **55**, 489–500.

LADD, C., HUNT JR., G.L., MORDY, C.W., SALO, S.A. AND STABENO, P.J., 2005. Marine environment of the Eastern and Central Aleutian Islands. *Fisheries Oceanography* **14**, 22–38.

LEA, D.W., MASHIOTTA, T.A. AND SPERO, H.J. 1999. Controls on magnesium and strontium uptake in planktonic foraminifera determined by live culturing. *Geochimica et Cosmochimica Acta* **63**, 2369−2379.

LOMBARDI, C., COCITO, S., HISCOCK, K., OCCHIPINTI-AMBROGI, A., SETTI, M. AND TAYLOR, P.D. 2008. Influence of seawater temperature on growth bands, mineralogy and carbonate production in a bioconstructional bryozoan. *Facies* **54**, 333–342.

LOMBARDI, C., COCITO, S., OCCHIPINTI-AMBROGI, A. AND HISCOCK, K. 2006. The influence of seawater temperature on zooid size and growth rate in *Pentapora fascialis* (Bryozoa: Cheilostomata). *Marine Biology* **149**, 1103–1109.

LOMBARDI, C., RODOLFO-METALPA, R., COCITO, S., GAMBI, M.C. AND TAYLOR, P.D. 2011. Structural and geochemical alterations in the Mg calcite bryozoan *Myriapora truncata* under elevated seawater pCO$_2$

BRYOZOAN STUDIES 2019

simulating ocean acidification. *Marine Ecology* **32**, 211–221.

LORENS, R. AND BENDER, M. 1980. The impact of solution chemistry on *Mytilus edulis* calcite and aragonite. *Geochimica et Cosmochimica Acta* **44**, 1265–1278.

LOWENSTAM, H.A. 1954. Environmental Relations of Modification Compositions of Certain Carbonate Secreting Marine Invertebrates. *Proceedings of the National Academy of Sciences USA* **40**(1), 39–48.

LOWENSTAM, H.A. 1981. Minerals formed by organisms. *Science* **211**, 1126–1131.

LOWENSTAM, H.A. AND WEINER, S. 1989. *On biomineralization*. New York, Oxford University Press.

LOXTON, J., KUKLINSKI, P., BARNES, D.K.A., NAJORKA, J., SPENCER JONES, M. AND PORTER, J. 2014. Variability of Mg-calcite in Antarctic bryozoan skeletons across spatial scales. *Marine Ecology Progress Series* **507**, 169–180.

LOXTON, J., KUKLINSKI, P., MAIR, J.M., SPENCER JONES, M. AND PORTER, J. 2012. Patterns of magnesium-calcite distribution in the skeleton of some polar bryozoan species. *Lecture Notes in Earth System Sciences* **143**, 169–185.

LOXTON, J., JONES, M.S., NAJORKA, J., SMITH, A.M. AND PORTER, J.S. 2018. Skeletal carbonate mineralogy of Scottish bryozoans. *PloS one* **13**(6), e0197533.

MACKENZIE, F., BISCHOFF, W., BISHOP, F., LOIJENS, M., SCHOONMAKER, J. AND WOLLAST, R. 1983. Magnesian calcites: Low-temperature occurrence, solubility and solid-solution behavior. *Reviews in Mineralogy and Geochemistry* **11**, 97–144.

MAGDANS, U. AND GIES, H. 2004. Single crystal structure analysis of sea urchin spine calcites: systematic investigations of the Ca/Mg distribution as a function of habitat of the sea urchin and the sample location in the spine. *European Journal of Mineralogy* **16**, 261–268.

MANN, S. 2001. *Biomineralization: Principles and Concepts in Bioinorganic Materials Chemistry*. New York, Oxford University Press.

MORSE, J.W., ARVIDSON, R.S. AND LÜTTGE, A. 2007. Calcium carbonate formation and dissolution. *Chemical reviews* **107**(2), 342–81.

NEHRKE, G., REICHART, G.J., VAN CAPPELLEN, P., MEILE, C. AND BIJMA, J. 2007. Dependence of calcite growth rate and Sr partitioning on solution stoichiometry: non-Kossel crystal growth. *Geochimica and Cosmochimica Acta* **71**(9), 2240–2249.

NOAA, National Centers for Environmental Information, https://www.nodc.noaa.gov/dsdt/cwtg/alaska.html, 14.06.2019.

NÜRNBERG, D., BIJMA, J. AND HEMLEBEN, C. 1996. Assessing the reliability of magnesium in foraminiferal calcite as a proxy for water mass temperatures. *Geochimica and Cosmochimica Acta* **60**, 803−814.

ORR, J.C., FABRY, V.J., AUMONT, O., BOPP, L., DONEY, S.C., FEELY, R.A., GNANADESIKAN, A., GRUBER, N., ISHIDA, A., JOOS, F., KEY, R.M., LINDSAY, K., MAIER-REIMER, E., MATEAR, R.J., MONFRAY, P., MOUCHET, A., NAJJAR, R.G., PLATTNER, G.-K., RODGERS, K.B., SABINE, C.L., SARMIENTO, J.L., SCHLITZER, R., SLATER, R.D., TOTTERDELL, I.J., WEIRIG, M.-F., YAMANAKA, Y. AND YOOL, A. 2005. Anthropogenic ocean acidification over the twenty-first century and its impact on calcifying organisms. *Nature* **437**, 681–686.

PITTS, L.C. AND WALLACE, G.T. 1994. Lead deposition in the shell of the bivalve, *Mya arenaria*: an indicator of dissolved lead in seawater. *Estuarine, Coastal and Shelf Science* **39**, 93–104.

PIWONI-PIÓREWICZ, A., KUKLINSKI, P., STREKOPYTOV, S., HUMPHREYS-WILLIAMS, E., NAJORKA, J. AND IGLIKOWSKA, A. 2017. Size effect on the mineralogy and chemistry of *Mytilus trossulus* shells from the southern Baltic Sea: implications for environmental monitoring. *Environmental Monitoring and Assessment* **189**(4), 197.

POLUZZI, A. AND SARTORI, R., 1975. Report on the carbonate mineralogy of Bryozoa. *Documents des Laboratoires de Geologie de la Faculte des Sciences de Lyon, Hors Serie* **3**, 193–210.

RA, K., KITAGAWA, H. AND SHIRAIWA, Y. 2010. Mg isotopes and Mg/Ca values of coccoliths from cultured specimens of the species *Emiliania huxleyi* and *Gephyrocapsa oceanica*. *Marine Micropaleontology* **77**: 119−124.

RADHA, A.V. AND NAVROTSKY, A. 2013. Thermodynamics of carbonates. *Reviews in Mineralogy and Geochemistry* **77**, 73–121.

RAMAJO, L., RODRIGUEZ-NAVARRO, A., DUARTE, C.M., LARDIES, M.A. AND LAGOS N.A. 2015. Shifts in shell mineralogy and metabolism of *Concholepas concholepas* juveniles along the Chilean coast. *Marine Freshwater Research* **66**, 1147–1157.

REED, R. AND STABENO, P., 1994. Flow along and across the Aleutian Ridge. *Journal of Marine Research* **52**, 639–648.

RUCKER, J.B. AND CARVER, R.E. 1969. A survey of the carbonate mineralogy of cheilostome Bryozoa. *Journal of Paleontology* **43** 791–799.

SMITH, A.M. 2007. Age, growth and carbonate production by erect rigid bryozoans in Antarctica. *Palaeogeography, Palaeoclimatology, Palaeoecology* **256**, 86–98.

SMITH, A.M. 2014. Growth and calcification of marine bryozoans in a changing ocean. *The Biological Bulletin* **226**, 203–210.

SMITH, A.M. AND CLARK, D.E. 2010. Skeletal carbonate mineralogy of bryozoans from Chile: an independent check of phylogenetic patterns. *Palaios* **25**, 229–233.

SMITH, A.M. AND GIRVAN, E. 2010. Understanding a bimineralic bryozoan: skeletal structure and carbonate mineralogy of *Odontoniella cyclops* (Foveolariidae: Cheilostomata: Bryozoa) in New Zealand. *Palaeogeography, Palaeoclimatology, Palaeoecology* **289**, 113–122.

SMITH, A.M., KEY, M.M. JR. AND GORDON, D.P. 2006. Skeletal mineralogy of bryozoans: Taxonomic and temporal patterns. *Earth-Science Reviews* **78**, 287–306.

SMITH, A.M., NELSON, C.S. AND SPENCER, H.G. 1998. Skeletal carbonate mineralogy of New Zealand bryozoans. *Marine Geology* **151**, 27–46.

STECHER, H.A., KRANTZ, D.E., LORD, C.J., LUTHER, G.W. AND BOCK, K.W. 1996. Profiles of strontium and barium in *Mercenaria mercenaria* and *Spisula solidissima* shells. *Geochimica et Cosmochimica Acta* **60**, 3445–3456.

STEGER, K.K. AND SMITH, A.M. 2005. Carbonate mineralogy of free-living bryozoans (Bryozoa: Otionellidae), Otago Shelf, southern New Zealand. *Palaeogeography, Palaeoclimatology, Palaeoecology* **218** 195–203.

STRASSER, C.A., MULLINEAUX, L.S. AND WALTHER, B.D. 2008. Growth rate and age effects on *Mya arenaria* shell chemistry: Implications for biogeochemical studies. *Journal of Experimental Marine Biology and Ecology* **355**, 153–163.

SWART, P.K. AND GROTTOLI, A. 2003. Proxy indicators of climate in coral skeletons: a perspective. *Coral Reefs* **22**, 313–315.

TAMBUTTÉ, S., HOLCOMB, M., FERRIER-PAGÈS, C., REYNAUD, S., TAMBUTTÉ, É., ZOCCOLA, D. AND ALLEMAND, D. 2012. Coral biomineralization: from the gene to the environment. *Journal of Experimental Marine Biology and Ecology* **408**, 58–78.

TAYLOR, J.D. AND REID, D.G. 1990. Shell microstructure and mineralogy of the Littorinidae: ecological and evolutionary significance. *Hydrobiologia* **193**, 199–215.

TAYLOR, P.D., JAMES, N., BONE, Y., KUKLINSKI, P. AND KYSER, K.T. 2009. Evolving mineralogy of cheilostome bryozoans. *Palaios* **24**, 440–452.

TAYLOR, P.D., LOMBARDI, C. AND COCITO, S. 2014. Biomineralization in bryozoans: present, past and future. *Biological Reviews* **90**(4), 1118–1150.

TAYLOR, P.D., TAN S.H.A., KUDRYAVSTEV, A.B. AND SCHOPF, J.W. 2016. Carbonate mineralogy of a tropical bryozoan biota and its vulnerability to ocean acidification. *Marine Biology Research* **12**(7), 776–780.

TROLL, C. 1965. Seasonal climates of the earth. In: *Weltkarten zur Klimakunde/World Maps of Climatology*. Springer, Berlin, Heidelberg, pp. 19–25.

VANDER PUTTEN, E., DEHAIRS, F., KEPPENS, E. AND BAEYENS, W. 2000. High resolution distribution of trace elements in the calcite shell layer of modern *Mytilus edulis*: environmental and biological controls. *Geochimica et Cosmochimica Acta* **64**, 997–1011.

WATABE, N. AND WILBUR, K.M. 1960. Influence of the organic matrix on crystal type in molluscs. *Nature* **188**, 334.

Apendix 1. The list of investigated taxa from Aleutian Islands and mineralogical characteristics of skeletons (NA = not analysed).

Family	Species	% calcite	mol% MgCO^3	Family	Species	% calcite	mol% MgCO^3
Beaniidae	*Beania* cf. *alaskensis*	100	5.2	Myriaporidae	*Myriozoum* cf. *coarctatum*	100	3.2
Beaniidae	*Beania* cf. *alaskensis*	100	5.3	Myriaporidae	*Myriozoum* cf. *coarctatum*	100	3.8
Beaniidae	*Beania* cf. *alaskensis*	100	5.7	Myriaporidae	*Myriozoum tenue*	100	2.2
Beaniidae	*Beania* cf. *alaskensis*	100	5.9	Myriaporidae	*Myriozoum tenue*	100	2.2
Bryocryptellidae	*Porella acutirostris*	100	5.0	Myriaporidae	*Myriozoum tenue*	100	3.0
Bryocryptellidae	*Porella acutirostris*	100	5.3	Myriaporidae	*Myriozoum tenue*	100	3.5
Bryocryptellidae	*Porella* sp. 1	100	5.3	Myriaporidae	*Myriozoum tenue*	100	4.7
Bryocryptellidae	*Porella* sp. 1	100	5.5	Reteporellidae	sp. 1	100	5.8
Bryocryptellidae	*Porella* sp. 1	100	6.1	Reteporellidae	sp. 1	100	5.3
Bryocryptellidae	*Porella* sp. 1	100	6.3	Reteporellidae	sp. 1	100	5.7
Bryocryptellidae	*Porella* sp. 1	100	6.7	Reteporellidae	sp. 1	100	5.7
Bryocryptellidae	*Porella* sp. 1	100	7.0	Reteporellidae	sp. 1	100	5.9
Bugulidae	*Bugula* cf. *cucullifera*	100	3.3	Romancheinidae	*Escharella* sp. 1	100	4.0
Bugulidae	*Bugula* cf. *cucullifera*	100	3.7	Romancheinidae	*Hippopleurifera* cf. *mucronata*	100	3.1
Bugulidae	*Caulibugula* cf. *ciliata*	100	3.8	Romancheinidae	*Hippopleurifera* cf. *mucronata*	100	3.5
Bugulidae	*Dendrobeania* sp. 1	100	2.9	Romancheinidae	*Hippopleurifera* cf. *mucronata*	100	5.6
Bugulidae	*Dendrobeania* sp. 1	100	3.3	Schizoporellidae	*Schizoporella* cf. *unicornis*	100	6.9
Bugulidae	*Dendrobeania* sp. 1	100	7.2	Smittinidae	*Parasmittina* cf. *jeffreysi*	100	7.4
Bugulidae	*Dendrobeania* sp. 1	100	7.6	Smittinidae	*Parasmittina* sp. 1	84.7	7.1
Bugulidae	*Dendrobeania* sp. 1	100	7.7	Smittinidae	*Parasmittina* sp. 1	84.1	7.3
Bugulidae	*Dendrobeania* sp. 1	100	8.0	Smittinidae	*Parasmittina* sp. 1	83.7	7.4
Calloporidae	*Cauloramphus* cf. *echinus*	100	3.9	Smittinidae	*Smittina* cf. *arctica*	100	6.0
Calloporidae	*Cauloramphus* cf. *echinus*	100	4.3	Smittinidae	*Smittina* cf. *landsbrovni*	100	6.2
Calloporidae	*Cauloramphus* cf. *echinus*	100	4.8	Stomachetosellidae	*Stomachetosella* cf. *limbata*	100	7.0
Calloporidae	*Ellisina* cf. *levata*	100	2.8	Stomachetosellidae	*Stomachetosella* cf. *limbata*	100	7.2
Calloporidae	*Ellisina* cf. *levata*	100	2.9	Stomachetosellidae	*Stomachetosella* cf. *limbata*	100	7.4
Calloporidae	*Ellisina* cf. *levata*	100	4.0	Stomachetosellidae	*Stomachetosella cruenta*	100	4.4
Calloporidae	*Ellisina* cf. *levata*	100	4.7	Stomachetosellidae	*Stomachetosella cruenta*	100	7.0
Calloporidae	*Ellisina levata*	100	3.7	Umbonulidae	*Rhamphostomella* sp. 1	100	4.4
Calloporidae	*Ellisina* sp.	100	3.8	Umbonulidae	*Umbonula* cf. *patens*	100	5.6
Calloporidae	*Tegella* cf. *arctica*	100	2.3	Unknown species	sp. 2	100	6.2
Calloporidae	*Tegella* cf. *arctica*	100	2.8	Unknown species	sp. 2	100	6.5
Calloporidae	*Tegella* cf. *arctica*	100	3.1	Unknown species	sp. 2	100	6.5
Calloporidae	*Callopora* sp. 1	100	2.2	Unknown species	sp. 2	100	6.6
Calloporidae	*Callopora* sp. 1	100	2.5	Unknown species	sp. 2	100	6.8
Calloporidae	*Callopora* sp. 1	100	2.9	Unknown species	sp. 3	100	4.4
Calloporidae	*Callopora* sp. 1	100	3.9	Unknown species	sp. 3	100	5.8
Calloporidae	*Callopora* sp. 2	100	5.1	Unknown species	sp. 4	100	4.1
Candidae	*Tricellaria* cf. *ternata*	100	2.2	Unknown species	sp. 4	100	5.7
Candidae	*Tricellaria* cf. *ternata*	100	2.2	Unknown species	sp. 5	100	6.2
Candidae	*Tricellaria* cf. *ternata*	100	2.4	Unknown species	sp. 5	100	6.6
Candidae	*Tricellaria* cf. *ternata*	100	2.8	Unknown species	sp. 6	100	5.6
Candidae	*Tricellaria* cf. *ternata*	100	7.9	Unknown species	sp. 6	100	5.7
Hippopodinidae	*Hippopodina feegeensis*	100	5.4	Unknown species	sp. 7	100	4.9
Hippoporidridae	*Hippoporella* sp. 1	100	6.6	Unknown species	sp. 8	100	5.9
Hippoporidridae	*Hippoporella* sp. 1	100	7.3	Unknown species	sp. 8	100	6.5
Hippothoidae	*Hippothoa hyalina*	100	NA	Unknown species	sp. 8	100	6.5
Hippothoidae	*Hippothoa hyalina*	100	NA	Unknown species	sp. 9	100	3.8
Hippothoidae	*Hippothoa* sp.	100	NA	Unknown species	sp. 10	100	3.9
Microporidae	*Microporina articulata*	100	3.8	Unknown species	sp. 10	100	4.2
Microporidae	*Microporina articulata*	100	4.8	Unknown species	sp. 11	100	2.9
Microporidae	*Microporina articulata*	100	6.1	Unknown species	sp. 11	100	3.0
Microporidae	*Microporina articulata*	100	6.1	Unknown species	sp. 12	100	5.0
Microporidae	*Microporina articulata*	100	6.4	Unknown species	sp. 12	100	5.1
Microporidae	*Microporina articulata*	100	6.5	Unknown species	sp. 12	100	5.4
Microporidae	*Microporina articulata*	100	6.6	Unknown species	sp. 12	100	5.5
Microporidae	*Microporina articulata*	100	7.0	Unknown species	sp. 12	100	5.5
Microporidae	*Microporina articulata*	100	7.3	Unknown species	sp. 12	100	5.7
Microporidae	*Microporina articulata*	100	7.8	Unknown species	sp. 12	100	5.8
Myriaporidae	*Myriozoella cf. plana*	100	4.6	Unknown species	sp. 13	100	3.7

Turbicellepora incrassata and Corallium rubrum: unexpected relationships in a coralligenous habitat from NW Sardinia, Mediterranean Sea

Antonietta Rosso[1]*, Jean-Georges Harmelin[2], Rossana Sanfilippo[1] and Francesco Sciuto[1]

[1] Dipartimento di Scienze Biologiche, Geologiche e Ambientali, Università di Catania, Corso Italia, 57, Catania I-95129, Italy [*corresponding author: e-mail: rosso@unict.it]
[2] GIS Posidonie & M.I.O., OSU Pytheas, Aix-Marseille University, Station marine d'Endoume, Marseille 13007, France

ABSTRACT

The examination of a coarse bioclastic sample collected at about 80 m depth off NW Sardinia, at the base of an underwater cliff colonised by a coralligenous community allowed the opportunity to record for the first time, mutual interactions between the large erect cheilostome *Turbicellepora incrassata* (Lamarck, 1816) [= *T. avicularis* (Hincks, 1860)] and the octocoral *Corallium rubrum* (Linnaeus, 1758). An assemblage of bryozoans coexisting with these species consisted of celleporids and multilaminar encrusters belonging to 40 species. The celleporid *T. incrassata* dominated in volume in this assemblage, forming branched colonies about 15 cm high. In the examined sample, *T. incrassata* is intimately associated with *C. rubrum*: most collected bryozoan branches develop on the coral axial skeleton, but the red coral itself can also overgrow *T. incrassata*. Bryozoan colonisation happens on exposed portions of the coral skeleton sometimes when the coral was still attached to the rock. In most instances, however, the occurrence of soft tissue (coenenchyme) and sclerites of red coral below or alternating with layers of *Turbicellepora* zooids indicates that the two species can overgrow each other. Other bryozoan species also interact with red coral, colonizing exposed parts of the coral skeleton, and, being sometimes overgrown by *C. rubrum*.

INTRODUCTION

Known as precious coral, the red coral *Corallium rubrum* (Linnaeus, 1758) is an Alcyonacean octocoral endemic to the Mediterranean Sea and Atlantic areas nearby the Gibraltar Strait. It thrives in poorly-lit or dark habitats from shallow depths in submarine caves (Laborel and Vacelet 1961) to deeper sites along rocky cliffs and overhangs in the coralligenous habitat where it plays a significant role as an engineer species (e.g. Cattaneo-Vietti and Cicogna 1993). The deepest records are from about 1000 m in the Sicily Straits (Taviani *et al*. 2010; Knittweis *et al.* 2016), where it coexists with cold-water corals [*Desmophyllum dianthus* (Esper, 1794), *Madrepora oculata* Linnaeus, 1758]. *C. rubrum* is a long-lived, slow-growing species (Garrabou and Harmelin, 2002). Following active harvesting during centuries and overexploitation (Cattaneo-Vietti *et al*. 2016, and references therein), this species is presently partly protected in Sardinia and its exploitation regulated (e.g. Cau *et al*. 2016). *C. rubrum* has white polyps with eight tentacles immersed in a coenenchyme

covering a red mineralised carbonate skeleton, which is repeatedly branched and arborescent, sculptured with longitudinal ridges, furrows and small protuberances. Small sclerites dispersed in the coenenchyme add rigidity to the latter.

Turbicellepora incrassata (Lamarck, 1816), a heavily mineralised Atlanto-Mediterranean celleporid bryozoan, is typically associated with gorgonians in the coralligenous habitat (Fig. 1) (Gautier 1959, 1962; Hayward and McKinney 2002; Chimenz Gusso *et al*. 2014). Colonies are pale orange to greenish (when colonized by micro-algae), celleporiform when young, forming mounds or nodules with small, and stout, irregularly ramified branches ('vinculariiform'), up to 20 cm in size when fully developed. Branches are cylindrical with conical ends and their surface is somewhat irregular owing to frontal budding of convex zooids.

Co-occurrence and interactions between *T. incrassata* and *C. rubrum* had never been reported. Even relationships between the red coral and bryozoans in general have so far been scarcely considered in published works, except for single minor mentions (e.g. Harmelin 1984; Giannini *et al*. 2003; Casas-Güell *et al*. 2016). However, more data may exist in the grey-literature, such as the fouling of dead *C. rubrum* colonies by 19 bryozoan species at

Monaco (rocky wall, 23-30 m depth, Harmelin 2003, unpublished report). This colonization likely occurred after mass mortality of red coral in shallow-water sites affected by abnormal warming during late summer 1999 (Garrabou *et al*. 2001).

The association between large-sized bryozoans and gorgonians is more commonly observed and reported. Bare portions of the gorgonian colonies offer a 'filiform' substratum around which colonizers can attain a 3D development. Epibiosis on erect slender substrata is an effective strategy to elevate from the bottom boundary layer, largely exploited nowadays as in the geological past (e.g. Di Martino and Taylor, 2014). In the Mediterranean, available data, refer especially to monitoring of gorgonacean populations (also including *C. rubrum*) after mortality events following long-lasting sea temperature raise, and consequently remark as bryozoans settle on exposed skeletons after decay of living tissues (Harmelin 1984; Harmelin and Marinopoulos 1994; Garrabou *et al*. 2001; Linares *et al*. 2005; Gili *et al*. 2014). Competition between bryozoans and small scleractinian corals is a natural phenomenon common in the same habitat as *C. rubrum.* Encrusting bryozoans colonise the thecal portion bounding the calice of corallites during periods of coral growth stasis, and can afterwards be covered by coral
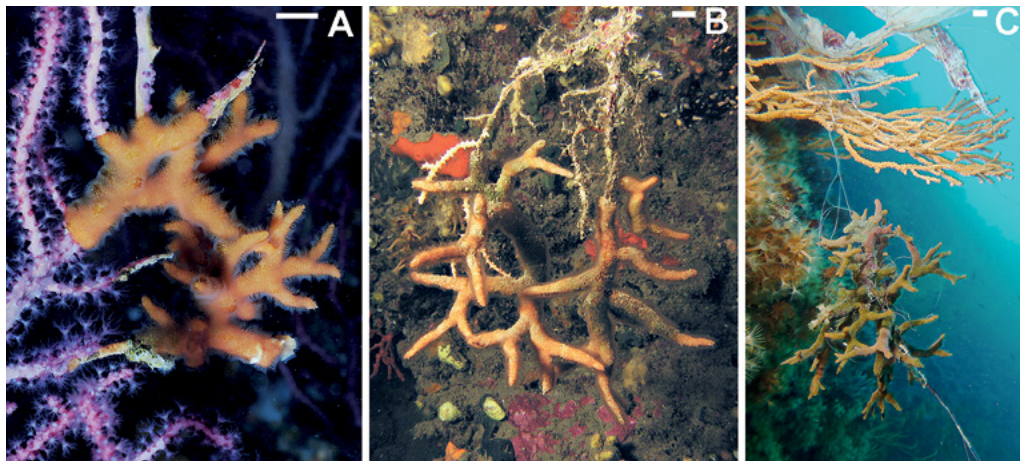

**Figure 1. Underwater images of *Turbicellepora incrassata*. (A) Associated with the gorgonian *Paramuricea*.
(B) A partly fouled colony on *Eunicella*. (C) Large colony on a fishing line.
Largest colony branches about 1 cm in diameter in all images.**

tissues and skeleton layers after polyp recovery (Harmelin 1990).

The present paper aims at describing and discussing: 1. Bryozoan assemblages associated with *C. rubrum*; 2. Relationships between *C. rubrum* and *T. incrassata*; 3. Occasional relationships between *C. rubrum* and further bryozoan species with small encrusting colonies; 4. The role of *T. incrassata* in the assemblage and 5. The taxonomic status of *T. incrassata*, a species often reported as *T. avicularis,* supporting the maintenance of the senior synonym.

MATERIAL AND METHODS

Examined material originates from a single sample of coarse bioclastic fragments (about 1.2 litres in volume), collected off Alghero, NW Sardinia (approximately 40°25'N and 8°11'E). Sampling was performed in September 2002 with the collecting devices of the ROV PLUTO 1000, at the base of a low steep underwater cliff, at 80 metres depth. Deep-water red coral populations are known in the area and ROV surveys carried out in 2007 reported colonies growing in patches on 1-5 m high boulders surrounded by detritic bottoms (Cannas *et al.* 2010; Follesa *et al.* 2013). Large-sized coral colonies having a basal diameter exceeding 1 cm and reaching 15-20 cm in height were abundant, representing more than 30% (Follesa *et al.* 2013). These authors also reported some associated taxa, including scleractinian corals, molluscs, brachiopods and a few bryozoan species, namely *Myriapora truncata* (Pallas, 1766), *Cellepora pumicosa* (Pallas, 1766), *Reteporella grimaldii* (Jullien, 1903) [as *R. septentrionalis* (Harmer, 1903)], and *Patinella radiata* (Audouin, 1826) [as *Lichenopora radiata* (Audouin and Savigny, 1816)].

The sample was washed and examined preliminarily for bryozoan species in the Palaeoecological Laboratory of the Dipartimento di Scienze Biologiche, Geologiche e Ambientali (DSBGA) of the University of Catania. In view of the abundance of red coral fragments, material was afterwards examined in order to identify the relationships between bryozoans and the red coral. Low magnification photographs were taken with a Zeiss Discovery V8A stereomicroscope equipped with an Axiovision acquisition system. High magnification images were obtained using back-scattered electrons on selected specimens examined uncoated under a low vacuum Scanning Electron Microscope at the Microscopical Laboratory of the DSBGA. Material is housed in the Paleontological Museum of the University of Catania (PMC), under the collection code PMC.I.H.2002. Sardinia red coral Rosso Collection.

RESULTS

Collected material largely consisted of biogenic fragments (about 75%) and subordinate pieces of biogenic concretions and heavily bioeroded limestone substratum. Most fragments are large-sized (usually larger than 1 cm) and sharp-edged. A large percentage (about 40%) of biogenic pieces consisted of living bryozoan fragments showing chitinous mandibles/opercula and soft tissue inside zooids. Colony branches of *Turbicellepora incrassata,* up to 7-8 cm long and 2 cm in maximum diameter, dominated. A large proportion of these branches presented a core occupied by broken skeleton of the red coral *Corallium rubrum*. Red coral fragments were also encrusted by membraniporiform multi-layered and celleporifom bryozoans. Other taxa included solitary scleractinians (mostly *Leptosammia pruvoti* Lacaze-Duthiers, 1897), serpulids [mostly *Serpula vermicularis* Linnaeus, 1767 and *Spirobranchus lima* (Grube, 1862), and subordinate *Spirobranchus triqueter* (Linnaeus, 1758), *Hydroides* spp., *Serpula lobiancoi* Rioja, 1917], spirorbids, large-sized vermetid gastropods, sparse specimens of the brachiopod *Novocrania anomala* (O.F. Müller, 1776), boring and byssate bivalves, and the encrusting foraminifer *Miniacina miniacea* (Pallas, 1766).

Associated bryozoans

In total, 40 bryozoan species were recognised (Tab. 1) in the sample (35 cheilostomatids and 5 cyclostomatids). Among them, 30 species

Table 1. Systematic list of bryozoan species associated with *Turbicellepora incrassata* and *Corallium rubrum* from NW Sardinia. *: < 10 specimens; **: 11-30 specimens; ***: > 30 specimens.

	total number of species	Living fragments/ colonies	Dead fragments/ colonies
Bryozoa	**40**		
Cyclostomatida	**5**		
Diplosolen obelius (Johnston, 1838)			*
Plagioecia patina Lamarck, 1816			*
? *Annectocyma major* (Johnston, 1847)			*
? *Filifascigera* sp.		? *	*
Lichenoporidae sp.		? *	**
Cheilostomatida	**35**		
Aetea sp.			*
Callopora dumerilii pouilleti (Alder, 1857)		*	*
Corbulella maderensis (Waters, 1898)		**	*
Crassimarginatella crassimarginata (Hincks, 1880)		*	*
Ellisina gautieri Fernández Pulpeiro & Reverter Gil, 1993		*	
Gregarinidra gregaria (Heller, 1867)		*	*
Beania magellanica (Busk, 1852)		*	
Candidae sp. und.		*	
Onychocella marioni (Jullien, 1881)		*	*
Cribrilaria radiata (Moll, 1803)		**	*
Cribrilaria venusta Canu & Bassler, 1925			*
Cribrilaria sp.		*	*
Chorizopora brongniartii (Audouin, 1826)		*	
Trypostega cf. *venusta* (Norman, 1864)		*	*
Escharoides mamillata (Wood, 1844)			*
Prenantia cheilostoma (Manzoni, 1869)			*
Prenantia ligulata (Manzoni, 1870)		*	*
Smittoidea reticulata (MacGillivray, 1842)		*	*
Schizomavella (*Calvetomavella*) *discoidea* (Busk, 1859)			*
Schizomavella (*Schizomavella*) *asymetrica* (Calvet, 1927)		*	*
Schizomavella (*Schizomavella*) *cornuta* (Heller, 1867)		**	*
Schizomavella (*Schizomavella*) *linearis* (Hassall, 1841)		**	*
Schizomavella (*Schizomavella*) *mamillata* (Hincks, 1880)		*	
Escharina dutertrei protecta Zabala, Maluquer & Harmelin, 1993		*	
Escharina vulgaris (Moll, 1803)		*	*
Herentia hyndmanni (Johnston, 1847)		*	
Fenestrulina sp.		*	*
Microporella appendiculata (Heller, 1867)		**	*
Celleporina caminata (Waters, 1879)		**	**
Turbicellepora avicularis (Hincks, 1860)		***	**
Turbicellepora coronopusoida (Calvet, 1931)			*
Reteporella sp.			*
Rhynchozoon spp.		*	*
Schizotheca fissa (Busk, 1856)		*	*
Stephanollona armata (Hincks, 1861)		**	*

were present with living colonies/fragments, and the majority of them (23) also included dead representatives. By contrast, ten species exclusively occurred with dead specimens. *Turbicellepora incrassata* was the most abundant species, represented by large fragments (see below), accounting for more than 80% of the estimated volume. *Celleporina caminata* (Waters, 1879) was also common with numerous hemispherical, dome-shaped to stout- and poorly branched colonies, up to 2 cm high, (often) detached from their substratum or colonising *C. rubrum* branches and limestone debris. Colonies of *Schizomavella* spp. were relatively abundant, largely represented by *S. cornuta* (Heller, 1867) and *S. linearis* (Hassall, 1841), and subordinately by *S. asymetrica* (Calvet, 1927) and *S. mamillata* (Hincks, 1880). All these species exhibited multi-laminar encrusting colonies, up to a dozen square centimetres in size. Among other, less abundant, components of the bryozoan assemblage were *Corbulella maderensis* (Waters, 1898), *Microporella appendiculata* (Heller, 1867), and *Cribrilaria radiata* (Moll, 1803), followed by *Crassimarginatella crassimarginata* (Hincks, 1880), *Onychocella marioni* (Jullien, 1882*), Smittoidea reticulata* MacGillivray, 1842, *Escharina vulgaris* (Moll, 1803) and *Stephanollona armata* (Hincks, 1862). Lichenoporids were the only common cyclostomes.

Relationships between Corallium rubrum *and* Turbicellepora incrassata *and other bryozoans*

The collected fragments of *Turbicellepora incrassata* were parts of slender-to-stout branched colonies. Some of these fragments (up to one cm in diameter) were distal tapering branches without internal substratum, increasing in diameter through frontal budding. However, the majority of branch fragments revealed a core consisting of broken skeleton of *Corallium rubrum*, with typical longitudinal ridges (Figs 2, 3E, 4A, C, E) their red colour contrasting with the whitish bryozoan skeleton. Furthermore, several broken branches showed a central tubular cavity

roughly reproducing the morphology of *C. rubrum* axial skeleton (Fig. 2A, arrowed). In most cases, the red coral fragments were partially to heavily bioeroded and/or coated with a thin whitish-brownish layer of carbonate precipitation. However, some coral tips presented still preserved soft tissues or showed evidences of coenenchyme remains with sclerites (Figs 2B-C, G-H, 3, 4). These latter are typically 60-90 µm long, with 6-9 symmetrically arranged *c.* 20 µm long protuberances, each consisting of clumps of cone-like crystal (cf. Grillo *et al.* 1993) (Fig. 4D). In a few fragments, soft tissues are missing, but slit-like spaces occur separating the red coral skeleton from the basal wall of *T. incrassata* colonies (Fig. 2B-C). Some fragments showed *C. rubrum* basal expansions, which encrust the colony surface of *T. incrassata,* sometimes covering living zooids (Figs 2G-I, 3A-C). Finally, some fragments showed the subsequent superimposition of thin red coral layers and bryozoan colonies (Figs 2G-J, 3A-C). In a few instances, laminar expansions of *C. rubrum* outgrow other bryozoan species but leaving uncovered openings (Figs 4E-G).

DISCUSSION
Turbicellepora incrassata
vs Turbicellepora avicularis

The most abundant bryozoan found in the examined assemblage is common in NW Mediterranean and is one of the rare bryozoans named by sport-divers ('Turbicellépore cornu', André *et al.* 2014). In the scientific literature, this species is usually reported as *Turbicellepora avicularis* (Hincks, 1860) although it is a junior synonym of *Cellepora incrassata* Lamarck (1816), as already noted by d'Hondt (1994). This synonymy has been currently questioned/unaccepted (see Rosso *et al.* 2010) in conformity with the Article 23.9 of the International Code of Zoological Nomenclature (Zoological Code; ICZN 1999) concerning the 'Reversion of Precedence'. It has been confirmed, however, by the recent digitalization of the Lamarck's types (1816) at the Muséum national d'Histoire Naturelle de Paris
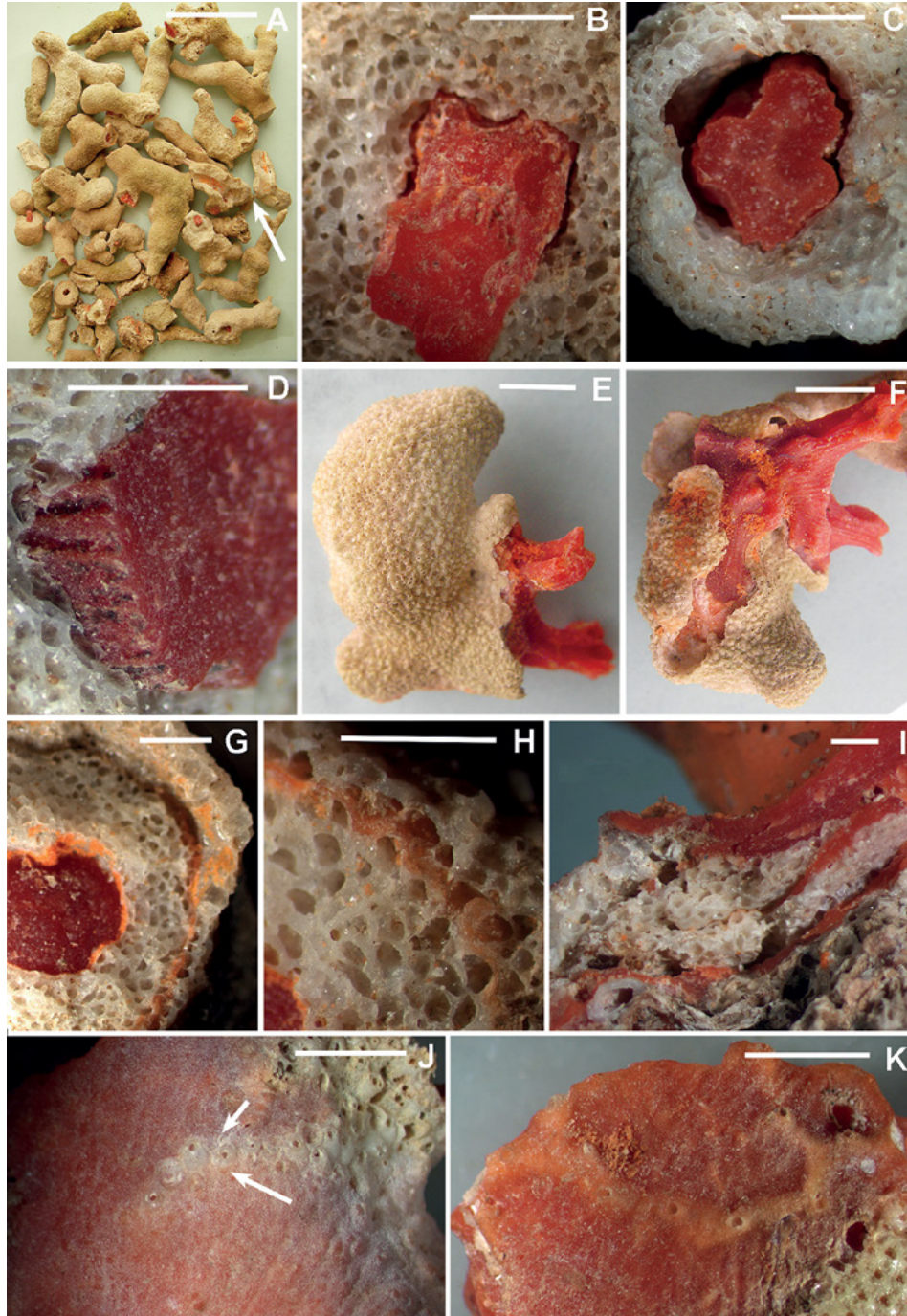
Figure 2. (A) Large colony branches of *Turbicellepora incrassata* growing on *Corallium rubrum* skeleton (red coloured). (B–C) Branch cross-sections: fissures between the coral skeleton and the bryozoan colony point to the first occurrence of coral tissues and/or soft-bodied organisms. (D) *T. incrassata* adhering to coral skeleton pointing to colonisation of exposed skeleton. (E–F) Views of *T. incrassata* encrusting a coral fragment with growing tips in the opposite direction. (G-I) Repeated superimpositions of *T. incrassata* and *C. rubrum*. (J) Intergrowth of *C. rubrum* and *Turbicellepora coronopusoida* (Calvet, 1931). Zooids left uncovered can ensure survivorship of the colony. (K) *C. rubrum* covering a tubuliporine cyclostome, leaving the tube orifices free. Scale bars: A: 5 cm; B–D, G-I: 1 mm; E–F: 5 mm; J-K: 2 mm.
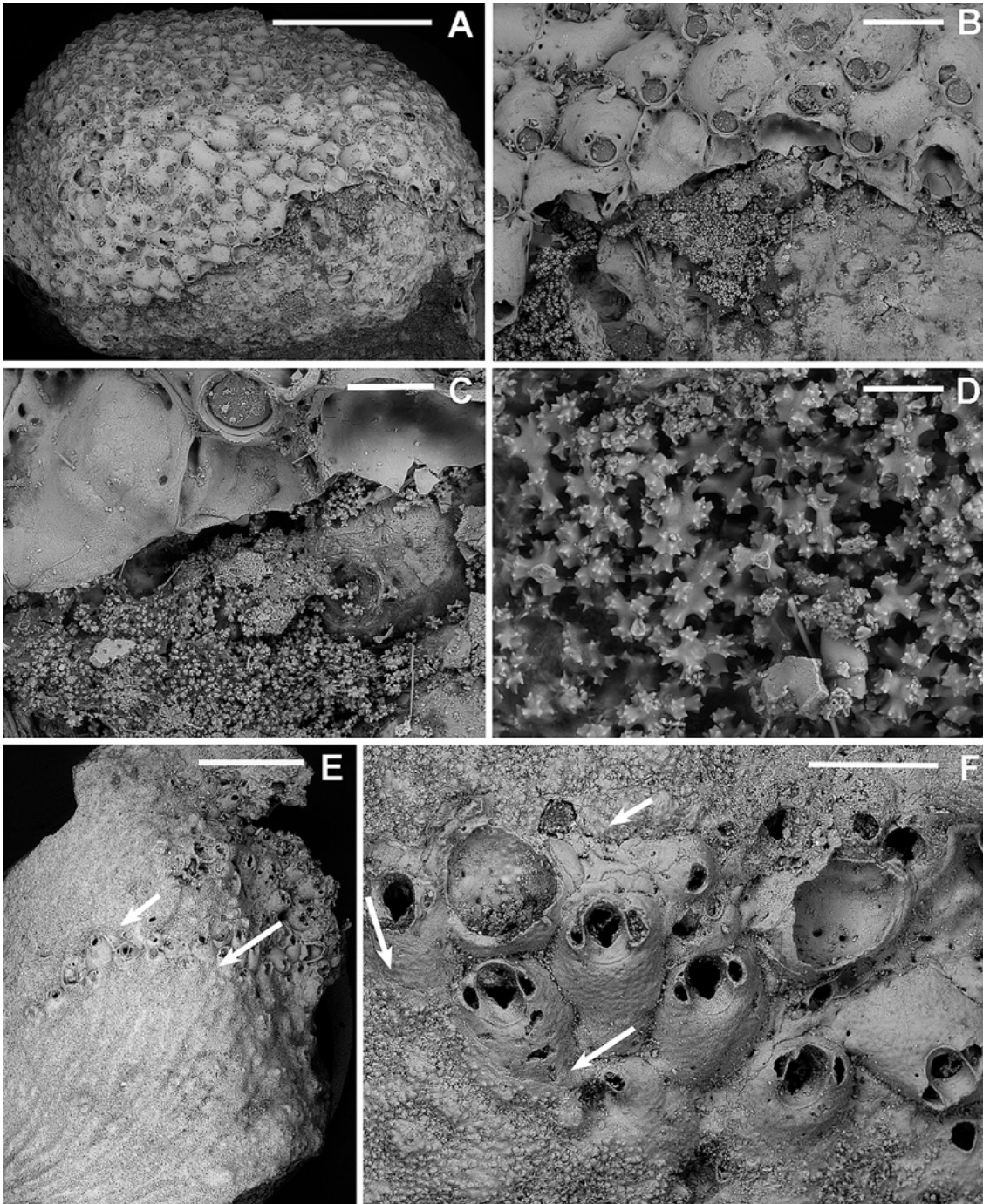
Figure 3. (A-C) General view (A) and enlargements (B and C)
of the superimposition of *T. incrassata* on *C. rubrum*.
The presence of coenenchyme is indicated by soft tissue still enveloping
sclerites diagnostic of the species. (D) Close-up of *C. rubrum* sclerites.
(E-F) SEM view and details of Figure 2J showing zooids
of *T. coronopusoida* overgrowing (short arrows)
and overgrown (long arrows) by the coral.
Scale bars: A–B, F: 500 mm; C 200 mm; D: 50 mm; E: 2 mm.
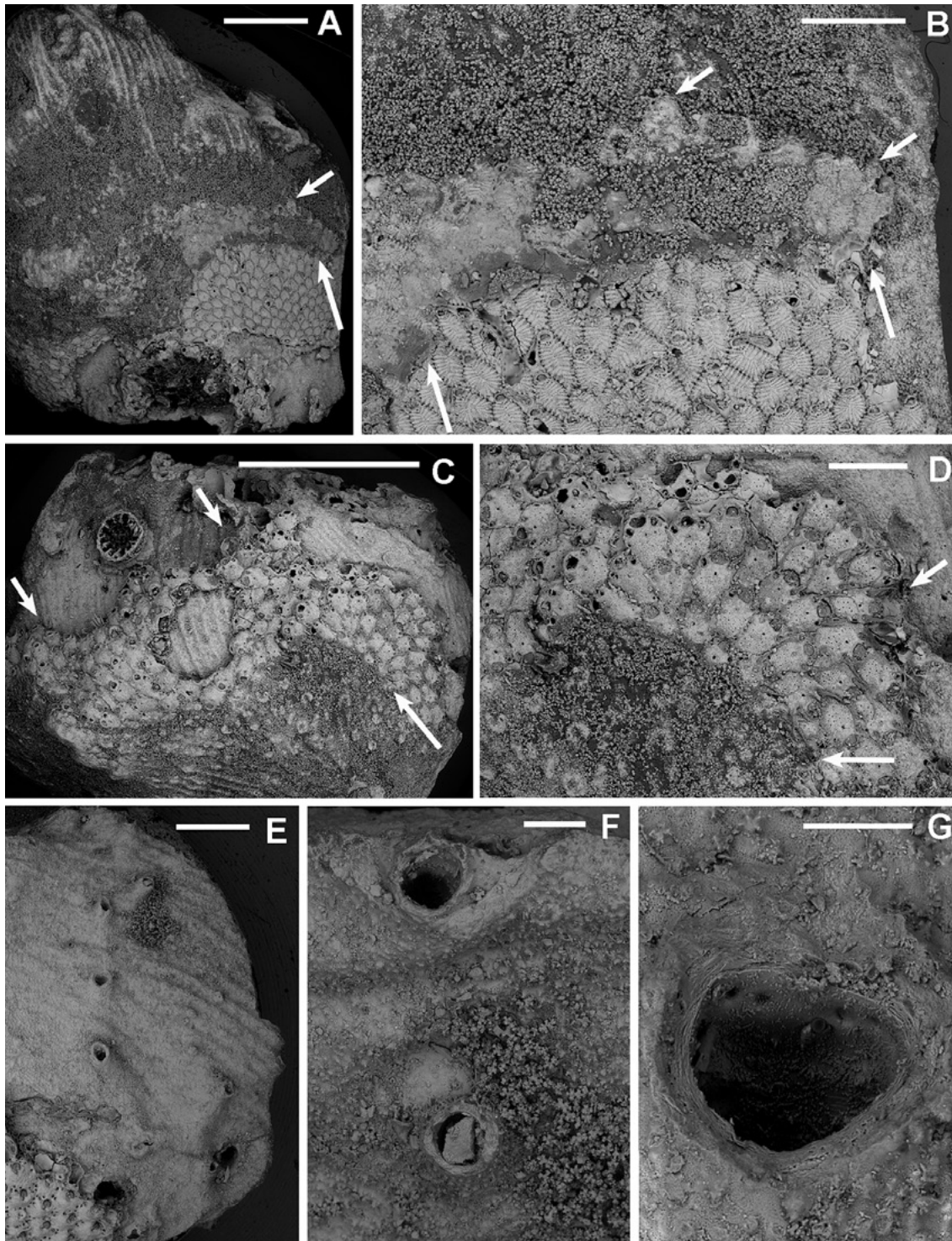
Figure 4. (A-B) General view and close-up of *Cribrilaria radiata* (Moll, 1803) growing on (short arrow) and overgrown by (long arrow) *C. rubrum*. **(C–D)** General view and close-up of *Microporella appendiculata* growing on (short arrow) and overgrown by (long arrow) *C. rubrum*. **(E–G)** SEM view and details of Figure 2K showing the tubuliporine tubes surrounded by the coral. Scale bars: A, C: 5 mm; B, D, E: 1 mm; F: 200 mm; G: 100 mm.

(program RECOLNAT – ANR-11-INBS-0004 – https://science.mnhn.fr/all/list?originalCollection = Coll.+Lamarck) that provided pictures of the type material at high resolution. Embracing ideas by Dubois (2010), we here choose, and suggest the use of the subjective senior synonym *T. incrassata*.

Bryozoan assemblage and habitat

All species found in the sampled bryozoan assemblage are known to be widely distributed in mid-to-outer shelf environments of the Mediterranean Sea. Most of them [among which the abundant *C. maderensis*, *C. crassimarginata*, *S. (S.) linearis*, *S. (S.) mamillata*, *E. vulgaris* and *M. appendiculata*] are usually associated with coralligenous habitat (Gautier 1962; Laubier 1966; Harmelin 1976; 2017; Rosso and Sanfilippo 2009). Some species, such as *Escharina dutertrei protecta* Zabala, Maluquer and Harmelin, 1993 and *Herentia hyndmanni* (Johnston, 1847), have typically been recorded from relatively deep shelf sites and the upper slope (Zabala *et al.* 1993; Berning *et al.* 2008; Mastrototaro *et al.* 2010; Rosso *et al.* 2014). Conversely, *T. incrassata* is usually reported from water depths shallower than 60 m (Gautier 1962; Harmelin 1976; 2017; Hayward and McKinney 2002; Chimenz Gusso *et al.* 2014). This species thrives in coralligenous and precoralligenous habitats (Harmelin 1976; 2017), where it often occurs as an epibiont on axes of large-sized gorgonians (Moissette and Pouyet 1991; André *et al.* 2014; Gatti *et al.* 2015; Harmelin 2017; online underwater images on the Doris web page). Young colonies of *T. incrassata*, less than 2 cm high, were collected on erect stems of *Flabellia petiolata* (Turra) Nizamuddin from a deep coralligenous bottom (86-113 m) in the Sicily Straits (Di Geronimo *et al.* 1993). *T. incrassata* was so far never recorded as being intimately associated with *C. rubrum* (see section *Corallium rubrum-Turbicellepora incrassata relationships*). The occurrence of large-sized living colony branches of *T. incrassata* on dead or partly alive branches of *C. rubrum*, attests that the two species thrived together on deep coralligenous walls from NW Sardinia. The dimensions of branches of *T. incrassata* in the studied sample allow inferring large (up to 15-20 cm) colony sizes, possibly larger than colonies of red coral from the same site. These large sizes point not only to conditions suitable for the species (including the occurrence of near-bottom currents providing oxygen and food) but also to good quality of the environment, because this species is highly sensitive to pollution (Harmelin and Capo 2002). Owing to its repeatedly branched, large-sized colonies, *T. incrassata* may play an important role in promoting habitat complexity. Indeed, *T. incrassata* branch surfaces offer colonisable space for small encrusting and erect bryozoans and other biota, especially when and where zooids become senescent.

Corallium rubrum-Turbicellepora incrassata *relationships*

This sample allowed us to state not only that *Corallium rubrum* and *Turbicellepora incrassata* lived together (see section *Bryozoan assemblage and habitat*) but also that they were strictly associated and established relationships with each other. *T. incrassata* (and, very subordinately, other bryozoans) could have colonised limestone clasts and some worn red coral fragments after they accumulated on the bottom surface at the base of the underwater cliff. This is indicated by: (1) *Turbicellepora* colonies that cover only one side of some coral branches and (2) complete or partial encrustation of broken surfaces of some coral fragments. Most *T. incrassata* colonies, however, possibly colonised *C. rubrum* when the coral was still attached to its substratum. This idea is supported by the branched morphology of the bryozoan colonies, which are usually sleeve-shaped around red coral branches and exhibit functional zooids on their surfaces. Close adhesion of some colonies of *T. incrassata* to the red coral skeleton indicates that colonisation occurred when the coral was dead or that at least the particular encrusted skeletal portion was exposed. Colonisation of exposed axial skeletons of Mediterranean gorgonians (mostly belonging to *Paramuricea* and *Eunicella*) and antipatarians [(*Leiopathes glaberrima* (Esper, 1788)], by large-

sized bryozoans (and by other epibionts/sclerobionts including *T. incrassata*) is a common phenomenon (e.g. Weinberg and Weinberg 1979; Linares *et al.* 2005; Garrabou *et al.* 2009; Angiolillo and Canese 2018). These papers record encrustations that are usually restricted to the stems and branches where gorgonian skeletons are naked owing to colony senescence and mostly to local damage produced in relation to environmental stress and partial or total mortality of colonies connected with exceptionally high sea temperature during summer (e.g. Linares *et al.* 2005). In particular, Garrabou *et al.* (2001) and Harmelin (2003) reported encrustations of bryozoan colonies on bare skeletons of *C. rubrum* in populations of the French Mediterranean coast and Monaco, which were affected by partial mortality in 1999. Harmelin and Marinopoulos (1994) and Gili *et al.* (2014) remarked that epibiosis of benthic organisms, including bryozoans, on gorgonians could be promoted/enhanced by the removal of soft tissues following abrasion produced by several factors, including fishing lines. Linares *et al.* (2005) also suggested that the growth extent of epibiont cover could be considered as an indicator of time elapsed from the injury event.

Literature records largely come from underwater observations. Therefore, close documentation of relationships between species is missing. Data acquired from the examination of NW Sardinia fragments, clearly indicate that *T. incrassata* is able to grow on bare portions of the red coral skeleton and also on coral tissue. Indeed, in some instances the abfrontal walls of zooids from the basal layer of *T. incrassata* colonies are separated from the enveloped red coral fragments by fissures measuring from hundreds of microns to about one millimetre. These fissures often result from the decay of the coral tissues which became "immured" following the bryozoan encrustation. This is indicated by reddish tissue remains and/or clusters of sclerites diagnostic of *C. rubrum* (cf. sclerite description in Grillo *et al.* 1993) which occur within several fissures. However, the simple occurrence of a thin layer of coenenchyme including sclerites does not

unequivocally indicate that red coral branches were healthy when overgrown, and that they possessed functional polyps that were never observed in the available material.

The occurrence of some *C. rubrum* basal colony expansions encrusting the surface of *T. incrassata* indicated that this species also served as substratum for *C. rubrum*. Some of these coral colonies reached large sizes on the cliff wall, as pointed out by the size of some broken branches (about one cm in diameter). Finally, subsequent superimpositions of thin layers of *C. rubrum* and *T. incrassata* skeletons indicate that these species can actively overgrow each other, possibly competing for space and/or to elevate from the colonised rocky wall to intercept local current flow carrying oxygen and food. However, it is sometimes difficult to ascertain if covering represents an overgrowth, i.e. an interaction between living colonies, and hence a real competition, or a mere superimposition, i.e. a colonisation after death of the encrusted specimens/colony. In the former hypothesis, it could be remarked that overgrowth, if occurring at the base of the coral colony could be relatively insignificant for the latter, whose basal expansions usually lack feeding polyps. Conversely, it seems substantially dangerous for the bryozoan, at least locally, because zooids occur on the whole exposed surface of colonies and usually become sealed and hidden beneath coral skeleton, when overgrown.

CONCLUSIONS

Accumulation of a large quantity of fragments in the sampled site, at the base of a cliff indicate that it was colonised by a possibly dense population of red coral in agreement with direct observations in the area (Cannas *et al.* 2010; Follesa *et al.* 2013). Natural breakage and downfall of detached colonies is possible, but only marginally, i.e. produced by borers or a strong physical disturbance. Indeed, the occurrence of unworn, sharp-edged small fragments could point to human impact in relation to red coral harvesting activity that has been intense in Sardinia

before the issuing of restrictive regulations in 2006 and 2008 (Cannas *et al.* 2010).

Examined fragments pointed to the co-occurrence of *C. rubrum* and *T. incrassata* in deep coralligenous habitats and allowed to describe for the first time relationships between these two species, including their competition for space. The two species seem to have the ability to overgrow each other, with final stages sometimes including the complete coating of some coral growing tips and consequently partial death of the impacted red coral branches. However, the competition with the bryozoan did not presumably prevent the red coral colonies in the area to reach large sizes. Furthermore, with colonies usually reaching two decimetres in size*, T incrassata*, like *C. rubrum*, acts as an engineer species in deep coralligenous habitats, increasing the spatial complexity and providing colonisable elevated surfaces for further species.

ACKNOWLEDGEMENTS

REFERENCES

ANDRÉ, F., COROLLA, J.P., LANZA, B. AND ROCHEFORT, G. 2014. *Bryozoaires d'Europe. Les carnets du plongeur*. Editions Neptune Plongée, Gargas, Fr., 255 pp.

ANGIOLILLO, M. AND CANESE, S. 2018. Deep gorgonians and corals from the Mediterranean Sea. IntechOpen. http://dx.doi.org/10.5772/intechopen.69686

BERNING, B., TILBROOK, K.J. AND ROSSO, A. 2008. Revision of the north-eastern Atlantic and Mediterranean species of the genera *Herentia* and *Therenia* (Bryozoa: Cheilostomata). *Journal of Natural History*, **42** (21–22), 1509–1547.

CANNAS, R., CAOCCI, F., FOLLESA, M.C., GRAZIOLI, E., PEDONI, C., PESCI, P., SACCO, F. AND CAU, A. 2010. Multidisciplinary data on the status of red coral (*Corallium rubrum*) resource in Sardinian seas (central western Mediterranean). In: E. Bussoletti, D. Cottingham, A. Bruckner, G. Roberts and R. Sandulli (eds), *Proceedings of the International Workshop on Red Coral Science, Management, and Trade: Lessons from the Mediterranean.* NOAA Technical Memorandum CRCP-13, pp. 40–57.

CASAS-GÜELL, E., CEBRIAN, E., GARRABOU, J., LEDOUX, J.-B., LINARES, C. AND TEIXIDÓ, N. 2016. Structure and biodiversity of coralligenous assemblages dominated by the precious red coral *Corallium rubrum* over broad spatial scales. *Scientific Reports* **6**,36535. DOI: 10.1038/srep36535

CATTANEO-VIETTI, R. AND CICOGNA, F. (eds) 1993. *Il corallo rosso in Mediterraneo: Arte, Storia e Scienza, Red Coral in the Mediterranean Sea: Art, History and Science.* Rome, Ministero delle Risorse Agricole, Alimentari e Forestali, 263 pp.

CATTANEO-VIETTI, R., BO, M. CANNAS, R., CAU, A., FOLLESA, C., MELIADÒ, E., RUSSO, G.F., SANDULLI, R., SANTANGELO, G. AND BAVESTRELLO, G. 2016. An overexploited Italian treasure: past and present distribution and exploitation of the precious red coral *Corallium rubrum* (L., 1758) (Cnidaria: Anthozoa). *Italian Journal of Zoology* **83**(4): 443–455.

CAU, A., BRAMANTI, L., CANNAS, R., FOLLESA, M.C., ANGIOLILLO, M., CANESE S., BO, M., CUCCU, D. AND GUIZIEN K. 2016. Habitat constraints and selfthinning shape Mediterranean red coral deep population structure: implications for conservation practice. *Scientific Reports* **6**, 23322, DOI: 10.1038/srep23322

CHIMENZ GUSSO, C., NICOLETTI, L. AND BONDANESE, C. 2014. Briozoi. *Biologia Marina Mediterranea*, 20 (Suppl. 1), 1–336.

DI GERONIMO, I., ROSSO, A. AND SANFILIPPO, R. 1993. The *Corallium rubrum* fossiliferous banks off Sciacca (Strait of Sicily). In: R. Cattaneo-Vietti and F. Cicogna (eds), *Il corallo rosso in Mediterraneo: Arte, Storia e Scienza, Red Coral in the Mediterranean Sea: Art, History and Science.* Rome, Ministero delle Risorse Agricole, Alimentari e Forestali, pp. 75–107.

DI MARTINO, E. AND TAYLOR, P.D. 2014. A brief review of seagrass associated bryozoans, Recent and fossil. In: Bryozoan Studies 2013, Rosso A., Wyse Jackson, P.N. and Porter, J. (eds). Proceedings of the 16th IBA Conference, 2013 Catania, Italy. *Studi Trentini di Scienze Naturali*, **94**, 79–94.

Doris web page. http://doris.ffessm.fr/Especes/Turbicellepore-cornu4 (accessed on 3.5.2019)

DUBOIS, A. 2010. Zoological nomenclature in the century of extinctions: priority *vs.* 'usage'. *Organisms Diversity & Evolution*, 10:259–274, doi 10.1007/s13127-010-0021-3

FOLLESA, M.C., CANNAS, R., CAU, A., PEDONI, C., PESCI, P. AND CAU, A. 2013. Deep-water red coral from the island of Sardinia (north-western Mediterranean): A local example of sustainable management. *Marine and Freshwater Research* **64**, 706–715.

GARRABOU, J. AND HARMELIN, J.-G. 2002. A 20-year study of life history traits of a harvested long-lived temperate coral in NW Mediterranean: insights into conservation and management needs. *Journal of Animal Ecology* **71**, 966–978.

GARRABOU, J., PEREZ, T., SARTORETTO, S. AND HARMELIN, J.-G. 2001. Mass mortality event in red coral *Corallium rubrum* populations in the Provence region (France, NW Mediterranean). *Marine Ecology Progress Series* **217**, 263–272.

GARRABOU, J., COMA, R., BENSOUSSAN, N., BALLY, M., CHEVALDONNÉ, P., CIGLIANOS, M., DIAZ, D., HARMELIN, J.-G., GAMBI, M.C., KERSTING D.K., LEDOUX, J.B., LEJEUSNE, C., LINARES, C. MARSCHAL, C., PÉREZ, T., RIBES, M., ROMANO, J.C., SERRANO, E., TEIXIDO, N., TORRENTS, O., ZABALA, M., ZUBERER, F. AND CERRANO, C. 2009. Mass mortality in Northwestern Mediterranean rocky benthic communities: effects of the 2003 heat wave. *Global Change Biology* **15**, 1090–1103.

GATTI, G., BIANCHI, C.N., PARRAVICINI V., ROVERE, A., PEIRANO, A., MONTEFALCONE, M., MASSA, F. AND MORRI, C. 2015. Ecological Change, Sliding Baselines and the Importance of Historical Data: Lessons from Combing Observational and Quantitative Data on a Temperate Reef Over 70 Years. *PLoS ONE* **10**(2): e0118581. doi:10.1371/journal.pone.0118581

GAUTIER, Y.V. 1959. Essai d'étude quantitative sur les bryozoaires d'un fond coralligène à gorgones. *Recueil des Travaux de la Station Marine d'Endoume* **26**(16), 137–142.

GAUTIER, Y.V. 1962. Recherches écologiques sur les Bryozoaires chilostomes en Méditerranée occidentale. *Recueil des Travaux de la Station Marine d'Endoume* **38**(24), 1–434.

GIANNINI F., GILI J.-M. AND SANTANGELO G. 2003. Relationship between the spatial distribution of red coral *Corallium rubrum* and coexisting suspension feeders at Medas Islands Marine Protected Area (Spain). *Italian Journal of Zoology*, **70**, 233–239.

GILI, J-M., SARDÁ, R., MADURELL, T. AND ROSSI, S. 2014. Zoobenthos. In: S. Goffredo and Z. Dubinsky (eds), *The Mediterranean Sea: Its history and present challenges*, Springer Science, pp. 213–236.

GRILLO, M.-C., GOLDBERG, V.M. AND ALLEMAND, D. 1993. Skeleton and sclerite formation in the precious red coral *Corallium rubrum*. *Marine Biology* **117**, 119–128.

HARMELIN, J.-G. 1976. Le sous-ordre des Tubuliporina (Bryozoaires Cyclostomes) en Méditerranée. Écologie et systématique. *Mémoires de l'Institut Océanographique* **10**, 1–326.

HARMELIN, J.-G. 1984. Biologie du corail rouge. Paramètres de populations, croissance et mortalité naturelle. Etat des connaissances en France. Report of the GFMC consultation on red coral resources of the western Mediterranean and their rational exploitation. *FAO Fishery Reports* **306**, 99–103.

HARMELIN, J.-G. 1990. Interactions between small sciaphilous scleractinians and epizoans in the northern Mediterranean, with particular reference to bryozoans. *Marine Ecology* **11**, 351–364.

HARMELIN, J.-G. 2003. *Etude de faisabilité: Réhabilitation du tombant coralligène des Spélugues et colonisation des nouveaux ouvrages portuaires. I – Peuplements du tombant coralligène et des nouvelles structures immergées: situation en 2003.* Principauté de Monaco, Rapport COM-GIS Posidonie & AMPN, Direction de l'Environnement, de l'Urbanisme et de la Construction, 69 pp.

HARMELIN, J.-G. 2017. Bryozoan facies in the coralligenous community: two assemblages with contrasting features at Port-Cros Archipelago (Port-Cros National Park, France, Mediterranean). *Scientific Reports Port-Cros national Park* **31**, 105–123.

HARMELIN, J.-G. AND CAPO, S. 2002. Effects of sewage on bryozoan diversity in Mediterranean rocky bottoms. In: P.N. Wyse Jackson, C.J. Buttler, and M.E. Spencer Jones (eds) *Bryozoan Studies 2001, Proceedings of the twelfth International Bryozoology Association Conference.* Lisse, A.A. Balkema, pp.151–158.

HARMELIN, J.-G. AND MARINOPOULOS, J. 1994. Population structure and partial mortality of the gorgonian *Paramuricea clavata* (Risso) in the north-western Mediterranean (France, Port-Cros Island). *Marine Life* **4**(1), 5–13.

HAYWARD, P.J. AND MCKINNEY, F.K. 2002. Northern Adriatic Bryozoa from the vicinity of Rovinj, Croatia. *Bulletin of the American Museum of Natural History* **270**, 1–139.

ICZN, 1999. International code of zoological nomenclature (4th ed.). London: International Trust for Zoological Nomenclature.

KNITTWEIS, L., AGUILAR, P., ALVAREZ, H., BORG, J.A., GARCIA, S. AND SCHEMBRI, F.J. 2016. New depth record of the precious red coral *Corallium rubrum* for the Mediterranean. *Rapports et Procès-Verbaux de la Commission internationale pour l'Exploitation de la Mer Méditerranée* **41**: 467.

LABOREL, J. AND VACELET, J. 1961. Répartition bionomique du *Corallium rubrum* Lamarck dans les grottes et les falaises sous-marines. *Rapports et Procès-Verbaux*

de la Commission internationale pour l'Exploitation de la Mer Méditerranée, **16**, 2, 465–469.

LAUBIER, L. 1966. Le coralligène des Albères: monographie biocénotique. *Annales de l'Institut Océanographique, Monaco* **43**, 137–316.

LINARES, C., COMA, R., DIAZ, D., ZABALA, M., BERNAT HEREU, B. AND DANTART, L. 2005. Immediate and delayed effects of a mass mortality event on gorgonian population dynamics and benthic community structure in the NW Mediterranean Sea. *Marine Ecology Progress Series* **305**, 127–137.

MASTROTOTARO, F., D'ONGHIA, G., CORRIERO, G., MATARRESE, A., MAIORANO, P., PANETTA, P., GHERARDI, M., LONGO, C., ROSSO, A., SCIUTO, F., SANFILIPPO, R., GRAVILI, C., BOERO, F, TAVIANI, M., TURSI, A. 2010. Biodiversity of the white coral bank off Cape Santa Maria di Leuca (Mediterranean Sea): An update. *Deep Sea Research II* **57**(5-6), 412–430.

MOISSETTE, P. AND POUYET, S. 1991. Bryozoan masses in the Miocene-Pliocene and Holocene of France, North Africa, and the Mediterranean. In: F.P. Bigey (ed.), Bryozoaires actuels and fossils. Bryozoa living and fossil. *Bulletin de la Societé de Sciences Naturelle de l'Ouest France, Memoires* HS **1**, Nantes (France), 1991, 271–279.

ROSSO, A., CHIMENZ GUSSO, C. AND BALDUZZI, A. 2010. Bryozoa. In: G. Relini (ed.), Checklist of the flora and fauna in Italian seas (parte II). *Biologia Marina Mediterranea* **17** (suppl.), 589–615.

ROSSO, A. AND SANFILIPPO, R. 2009. The contribution of bryozoans and serpuloideans to coralligenous concretions from SE Sicily. In: *UNEP-MAP-RAC/SPA, Proceedings of the First Symposium on the Coralligenous and other calcareous bio-concretions of the Mediterranean Sea* (15–16 January, 2009), Tabarka, 123–128.

ROSSO, A., SANFILIPPO, R. AND SCIUTO, F. 2014. Open shelf soft bottom bryozoan communities from the Ciclopi Marine Protected Area (E Sicily, Mediterranean). In: A. Rosso, P.N. Wyse Jackson and J. Porter (eds). Bryozoan Studies 2013. Proceedings of the 16th Conference of the International Bryozoological Association, Catania. *Studi Trentini di Scienze Naturali* **94**, 195–207.

TAVIANI, M., FREIWALD, A., BEUCK, L., ANGELETTI, L., REMIA, A., VERTINO, A., DIMECH, M., AND SCHEMBRI, P.J. 2010. The deepest known occurrence of the precious red coral *Corallium rubrum* (L. 1758) in the Mediterranean Sea. In: E. Bussoletti, D. Cottingham, A. Bruckner, G. Roberts and R. Sandulli (eds), *Proceedings of the International Workshop on Red Coral Science, Management, and Trade: Lessons from the Mediterranean.* Silver Spring, MD, NOAA Technical Memorandum CRCP-13, 87–93.

WEINBERG, S. AND WEINBERG, F. 1979. The life cycle of a gorgonian: *Eunicella singularis* (Esper, 1794). *Bijdragen tot de Dierkunde* **48**(2), 127–140.

ZABALA, M., MALUQUER, P. AND HARMELIN, J.-G. 1993. Epibiotic Bryozoans on deep-water scleractinian corals from the Catalonia slope (western Mediterranean, Spain, France). *Scientia Marina* **57**, 65–78.

Growth geometry and measurement of growth rates in marine bryozoans: a review

Abigail M. Smith[1]* and Marcus M. Key, Jr.[2]

[1] Department of Marine Science, University of Otago, P.O. Box 56, Dunedin 9054, New Zealand
[*corresponding author: email: abby.smith@otago.ac.nz]
[2] Department of Earth Sciences, Dickinson College, P.O. Box 1773, Carlisle, PA 17013-2896, USA

ABSTRACT

The relationship between age and size in colonial marine organisms is problematic. While growth of individual units may be measured fairly easily, the growth of colonies can be variable, complex, and difficult to measure. We need this information in order to manage and protect ecosystems, acquire bioactive compounds, and understand the history of environmental change. Bryozoan colonial growth forms, determined by the pattern of sequential addition of zooids or modules, enhance feeding, colony integration, strength, and/or gamete/larval dispersal. Colony age varies from three months to 86 years. Growth and development, including both addition of zooids and extrazooidal calcification, can be linear, two-dimensional across an area, or three-dimensional. In waters with seasonal variation in physico-chemical parameters, bryozoans may exhibit a growth-check, like an annual "tree-ring", showing interannual variation. Growth in other bryozoans are measured using chemical markers (stable isotopes), direct observation, or by inference. Growth rates appear to be dependent on the method of measurement. Calcification rate (in g $CaCO_3$/y) offers a way to compare growth among different growth forms. If the weight of carbonate per zooid is fairly consistent, it can be directly related to the number of zooids/time. Careful consideration of methods for measuring and reporting growth rate in bryozoans will ensure they are robust and comparable.

INTRODUCTION

Bryozoans are lophophorate aquatic invertebrates which typically form colonies by iterative addition of modular clones (zooids). Freshwater species are uncalcified; the majority of marine species are calcified, so that there is an extensive fossil record of marine bryozoan colonies. When calcified colonies grow large, they can provide benthic structures which enhance biodiversity by provision of sheltered habitat. Agencies who wish to manage or protect these productive habitats need to understand the longevity and stability of these structures. But how are size and age related in colonial organisms? We do not automatically know the age of a large bryozoan colony. While growth rate of zooids may be relatively easily measured, the growth rates of colonies can be highly variable, difficult to measure, and complex. Yet without this information, it is difficult to manage or protect ecosystems based on bryozoan colonies, or to grow them for bioactive compounds, or to understand the carbonate record held in them. After several decades of struggling with growth rates in bryozoans, the authors here review and discuss the following issues in bryozoans: zoarial

growth form, maximum size, age, growth (increase in size), and measurements of growth rate (increase in size over time).

SHAPE OF A BRYOZOAN

The individual zooids that make up bryozoan colonies are fairly simple boxes or tubes, with more or less ornamentation. Normal feeding zooids (autozooids) are sometimes aided by zooids who specialise in support, cleaning, or reproduction (heterozooids). Together with extrazooidal carbonate, they make up the colony. Bryozoan colony growth form is thus determined by the pattern of addition of zooids, the same way that the shape of a knitted garment is determined by the addition of stitches.

Most bryozoan colonies start out as a spot (sexually-produced ancestrula). Then the first zooid buds from the ancestrula, but it is the one after the first budding that makes the pattern (Fig. 1). In simple iterative growth, new modules are added sequentially, often in some regular arrangement (Hageman 2003). Zooids can be added in a line, or at the tips of branches, or along an edge, on the substrate or lifting erect off it. This kind of growth results in a small number of simple growth forms, from runners and trees to sheets and mounds (Nelson *et al.* 1988; Smith 1995). Combinations of these simple primary modules can form more complex colonies with secondary structural design units (composed of the primary modules) (Hageman *et al.* 1998; Hageman 2003).

Theoretically, a modular colony could take almost any form, but, in reality, bryozoan colonies tend to occur in a few basic forms, some of which have evolved repeatedly in different clades (McKinney and Jackson 1989). They achieve: access to food particles in the water, integration of the colony (connections between zooids), strength and resistance to water flow/predation, reduction of interaction with other species, competitive advantage, and capacity to distribute larvae into the water (McKinney and Jackson 1989). Bryozoan colonial growth form nomenclature tries to capture this variation, with varying degrees of success.

Early on, bryozoan colonial growth forms were often given names that referred to an exemplar taxon, usually a genus (e.g., Stach 1936; Lagaaij and Gautier 1965). So, a bryozoan that grew an erect flexible leafy colony like that of the genus *Flustra* was referred to as flustriform. This archetypal system was summarised by Schopf (1969). As noted by Hageman *et al.* (1998), each category was made up of a combination of characteristics, with no systemic recognition of shared or common characters. It was cumbersome, difficult for non-specialists, and although there were a great number of categories (with different systems for cheilostomes and cyclostomes), they failed in aggregate to describe all the variety in bryozoan colonial forms.

In the 1980s and 1990s, carbonate sedimentologists who wanted to categorise bryozoans without excessive investment in species identification developed a hierarchical classification system, where a few characteristics were combined to make a simple code to describe overall colonial shape (Nelson *et al.* 1988, revised and expanded by Bone and James 1993; Smith 1995). Colonies were described as erect, encrusting, or free-living; then subdivided into various shapes (e.g., branching, articulated, rooted). These categories were rather broad-brush and took no account of "rampant convergent evolution" (Taylor and James 2013, p. 1186), or of the different ecological roles played by different shapes. An alternative, using a classification based on the ecological function of growth forms (e.g., McKinney and Jackson 1989) was inadequately supported by genuine ecological understanding of bryozoan ecology on different scales (Hageman *et al.* 1998).

Hageman *et al.* (1998) reviewed all this and developed an "Analytical Bryozoan Growth Habit Classification", in which they characterised bryozoan colonial forms using eco-morphological categories: orientation, attachment to substrate, construction, arrangement of zooecial series, arrangement of frontal surfaces, secondary skeletal thickening, structural units and their dimensions, frequency and dimensions of bifurcation, and connections between structural units, along with substrate type. These twelve fundamental

characters provided a complex but comprehensive and systematic method of describing the great diversity of bryozoan colony forms. Hageman revisited this classification in his 2003 review of colonial growth in diverse bryozoan taxa.

It is relevant to note that cyclostomes zooids are tubes, where cheilostome zooids (usually) make more-or-less rectangular boxes. These modules combine differently, but often make remarkably similar growth forms (Fig. 2).

Since Stach (1936), researchers have been enthusiastic about using colonial growth form as an indicator of (paleo)environment (reviewed by Smith 1995; Hageman *et al.* 1997). Despite the appealing notion that different growth forms must be adapted to different environments, and the development of a standardized and statistically robust method (Hageman *et al.* 1997), rigorous investigations

have often failed to show robust correlations with depth, water speed, or temperature (e.g., Liuzzi *et al.* 2018). Certain broad general trends can be observed, for example: that fragile small colonies are probably not representative of strong hydraulic energy. That is not to say that bryozoans do not have potential as environmental indicators; there are, for example, assemblages that are strongly related to habitat (e.g., Wood and Probert 2013), as well as useful environmental geochemical signals in their skeletal carbonate (e.g., Key *et al.* 2018).

SIZE OF A BRYOZOAN

Individual zooids in marine bryozoans are tiny, usually 0.1 to 1 mm across. In a given species, zooid size range is characteristic and sometimes diagnostic. However, at least some species of bryozoans grow
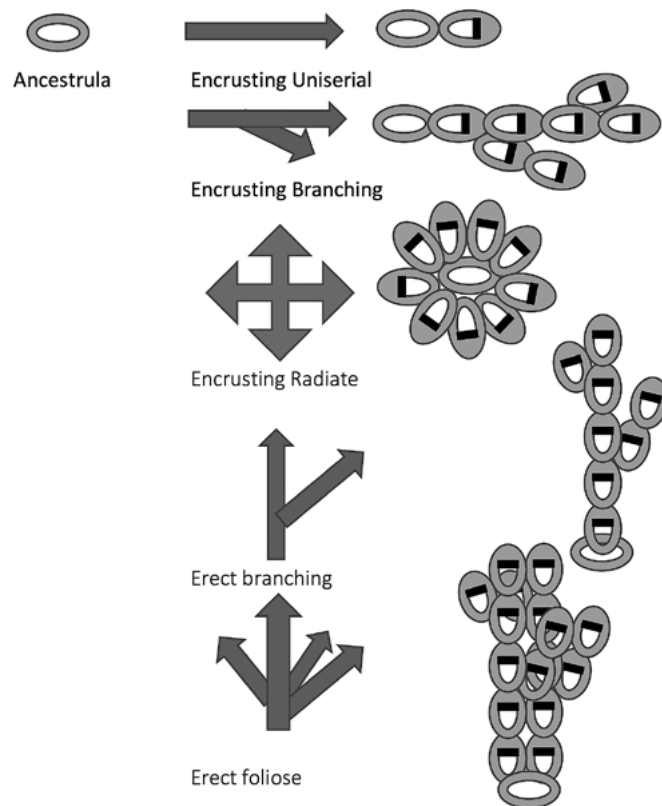

Figure 1. Iterative growth in bryozoans: many ways to combine individual zooids. Multi-laminar and other complex forms are made by iterating these multi-zooid modules.

larger zooids in cooler waters/seasons (see review in Amui-Vedel *et al.* 2007), which has been used as an environmental indicator (e.g., McClelland *et al.* 2014). Zooid size and arrangement are generally held to be optimal for feeding currents (see, e.g., Ryland and Warner 1986).

Size of bryozoan colonies within a species, unlike that of its zooids, varies greatly. A colony becomes mature (sexually reproductive) once it has enough zooids to support embryo production (Nekliudova *et al.* 2019), usually 30-130 zooids, but embryos have been reported in species ranging from 3 to 2700 zooids (Jackson and Wertheimer 1985). A bryozoan "spot" colony can be viable at only a few mm², but equally, at the other end of the spectrum, one encrusting bryozoan (*Einhornia crustulenta*) can cover 8290 mm² (Kuklinski *et al.*

2013). Large erect bryozoans today are generally 10-30 cm tall but Cocito *et al.* (2006) reported modern *Pentapora* colonies in the Adriatic that reached 1 m in height; there are fossil bryozoans that appear to reach a similar size (Cuffey and Fine 2006).

Colony size has been measured in many ways: linear extent (height, width, thickness, diameter), area, volume, and number of zooids. The most natural measurement depends on the colony form. In fact, each main colony form has an obvious method of measuring it (Table 1). Thus, size in one-dimensional colonies is measured in length, whereas sheet-like colonies are sometimes measured in area (or in extension of diameter for flat nearly-circular colonies). Lumpier multilaminar three-dimensional colonies could be measured in volume, but in fact generally are not measured at all, due
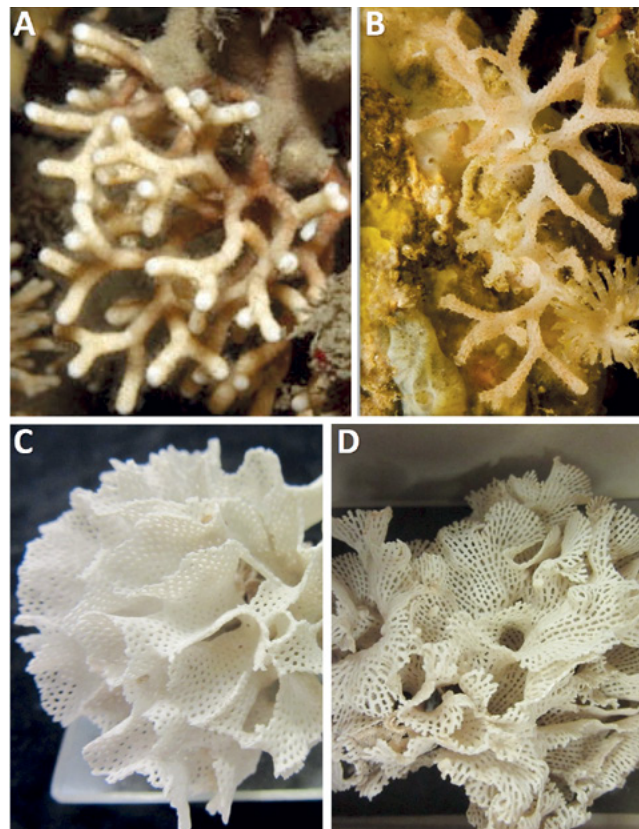

Figure 2. Convergent growth forms from different clades of bryozoans.
(A) *Diaperoecia* sp. (stenolaemate cyclostome); **(B)** *Galeopsis porcellanicus* (gymnolaemate cheilostome);
(C) *Hippellozoon novaezelandiae* (gymnolaemate cheilostome); **(D)** *Hornera foliacea* (stenolaemate cyclostome).

to the challenges presented by their shape (but see Sokolover *et al.* 2018).

Sometimes researchers add to their measurements the spatial density of zooids (i.e., number of zooids/mm^2). In general, this measurement appears to limit counts to autozooids, and it is worthwhile considering whether or not heterozooids deserve counting in this context. There is also a lack of comparability between cheilostome box-like zooids and stenolaemate tube-like zooids.

Because of these different measurement schemes, comparisons of size among growth forms has been problematic and has required researchers to make unit conversions. For example, one could assume constant branch thickness in order to convert branch length to volume. Smith and Nelson (1994) managed this issue by measuring size in terms of weight of skeletal carbonate– which is independent of growth form.

AGE OF A BRYOZOAN

What are life and death to a bryozoan? New individual zooids begin budded at the edge of a colony (often at the "growing edge" or "growth tip" but sometimes frontally on top of old zooids). As the growing edge moves away, the zooids mature, sometimes reproduce sexually, and grow old. They can produce a brown body and then regenerate, they can produce extrazooidal thickening, they can die, and the chamber become empty, or they can bud frontally and essentially overgrow themselves (Ryland 1976). Life history is complex in bryozoans; age of a single bryozoan zooid is not well constrained. It could be important, though, for example, in studies where measuring zooids of the same generation is necessary, such as in age-growth-climate correlations (e.g., Key *et al.* 2018).

On a different scale, the colony's lifespan is the time from metamorphosis of the larva into the ancestrula to the time the last zooid dies, and the colony ceases to function. Some colonies die from an event, like being eaten or crushed or buried. Theoretically, of course, a bryozoan colony is potentially immortal (McKinney and Jackson 1989). Even in a simple encrusting colony, however, age is not necessarily related to size if fission and/or partial mortality have occurred (Jackson and Winston 1981). Most large erect species, on the other hand, appear to have a "normal maximum size," possibly mediated by the mechanics of water flow and skeletal support.

Age in the context of a bryozoan colony is thus how long the colony has been functioning, specifically, time from metamorphosis of the larva into the ancestrula to time of death/collection. There are annuals and perennials among bryozoan colonies. An adult colony can die of old age after three months (e.g., as winter arrives) or last as much as 50 years (*Melicerita obliqua* in the Weddell Sea, Antarctica; Brey *et al.* 1998); *Celleporaria fusca* in the Gulf of Aqaba (Sobich, 1996) holds the longevity record of 86 years. A range of about 90 to over 30,000 days means that age of bryozoan colonies, of different species and in different environments, can vary over four orders of magnitude. Having said that, most large erect heavily-calcified marine specimens that have been studied are about 10-30 years old (Smith 2014).
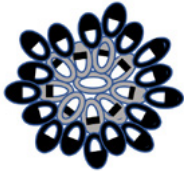
BRYOZOAN COLONY GROWTH

Growth is the increase in occupation of space. In bryozoans, there are different kinds of growth: 1. growth and development of the individual zooid (ontogeny), generally a short-lived and small-scale process; 2. growth and development of the colony by addition of zooids (which we call primary astogeny) which can be on the order of months or years or decades (Lidgard and Jackson 1989); and 3. growth of the colony by extrazooidal calcification (which we could call secondary astogeny) adding strengthening material that is not part of a zooid, also over the life of the colony.

In terms of measuring colony growth, there are only a few categories (Table 1). In general, growth can occur around the edges of a colony (radial growth) or be limited to one or two directions (linear growth), including, in frontal budding, up into the water column. The dimensionality of growth determines the dimensions that must be measured to encapsulate growth. Units of growth rate vary

Table 1. Three categories of geometry in bryozoan colonies, with relevant ways to measure size and growth.

Dimensions	New zooids added	Illustration (ancestrula empty, new growth in black)	Colonial growth form nomenclature	Comment	Growth increment measured over time
1 dimension (length)	In a line at the tip of the colony		Encrusting Uniserial Runners		Length Number of zooids (1 zooid in illustration)
	At the growing tip of each branch		Encrusting multiserial Branching runners Erect branching (all kinds) Erect flexible articulated	Each branch can be one zooid wide, or bilaminar, or a circle of zooids around a central core or even more complex Bifurcation angle and rotation around the branch axis allow branches to grow without running into each other	Additive length increase (= sum of all the new branch lengths) Number of zooids (3 zooids in illustration)
2 dimensions (area)	All along the edge, but flat on the substrate		Encrusting unilaminar Spots, circles Free-Living Caps	Sheets are usually circular unless they run into something or growth is not consistent around the edge (e.g. "belt" shaped colonies) Caps are curved versions	Increase in area, calculated for a circle of radius R Increase in area, calculated as length x width if roughly rectangular Number of zooids (17 zooids in illustration)
	Along the growing edge, away from substrate		Erect foliose Erect fenestrate Rooted sabres Conescharallinids	Can be unilaminar or bilaminar Fenestrate is really just a sheet with holes in it Sabres are leaves that aren't very wide	Height Area = width of growing edge x height Number of zooids (5 zooids in illustration)
3 dimensions (volume)	Along the edge and on the surface		Encrusting multilaminar Mounds and nodules Spheres	Highly variable This is difficult to generalise Self-overgrowth is typical in this group, and can be very irregular	Volume of a sphere: $4/3\pi r^3$ Or a disc/cylinder: $H\,\pi r^2$ Or a prism: H x W x L Number of zooids (6 zooids in illustration)

across the range of size and time, and possibly over the development of the colony. The most commonly used are: zooids added, linear increase (height, length, radius), and increase in area over time.

Bryozoans in cold waters sometimes stop growing, or slow down, during winter (Smith & Key, 2004). If calcification continues while linear extension does not, a thickened skeletal band, or growth check appears in the skeleton. While most growth checks occur in polar colonies, reflecting a lack of food availability

in winter (Brey *et al.* 1998; Smith 2007), temperate species can also slow their growth in the cold months, leaving a thickened layer as an annual marker (e.g., *Melicerita chathamensis*, Smith and Lawton 2010, Key *et al.* 2018), or just a gap in the record (*Adeonellopsis* sp., Smith *et al.* 2001, Smith and Key 2004).

A few colonial growth forms appear to have determinate growth, that is, they stop growing when they reach an optimal size (as some free-living forms do; Winston and Håkansson 1989), or they may shed

layers that are heavily fouled (Winston and Håkansson 1989). Some colonies, such as *Membranipora*, grow along with their macro-algal substrate (Winston and Hayward 2012). Others, such as *Pentapora*, seem as if they could grow forever (Cocito *et al.* 2004).

Growth has consequences – some biological activities do not happen until a colony reaches a critical size. For example, the onset and frequency of reproductive ovicells and degenerative brown bodies can be related to the overall size of the colony (or not, see Hayward and Ryland 1975). Some colonies may exert control over their shape as they grow, for example, by dropping unnecessary branches.

BRYOZOAN COLONIAL GROWTH RATES

As with the measurement of size, growth rates in various forms are also measured in different ways. A radial encrusting colony is generally measured in terms of increase in diameter or area. A branching colony, on the other hand, might be measured in terms of increased height, or the sum of branch lengths or even the number of branches. Smith's (2014) summary of growth rate measurements of bryozoan colonies (updated in Appendix Table) shows a range of units and approaches in reporting growth rates, including cm/y, mm²/y, zooids per month, specific growth rate, and doubling rate. These various measurements are difficult to compare against each other and make it nearly impossible to reach any conclusions about the range of normal growth rates in bryozoans.

Growth rate can translate, in most marine bryozoans, into calcification rate. Specimens can be weighed before and after, or the newly-added skeletal material can be separated and weighed (e.g., Smith *et al.* 2001), or the proportion of volume that is calcified (% calcimass) can be applied to the volume of the newly added colony. Calcification rate (in mg $CaCO_3$/y) offers a way to compare growth rate among different colonial forms which expand in different ways. If the carbonate per zooid is fairly constant (and it might be in a clonal organism, see Smith *et al.* 2001), it can be directly calculated from zooids/

time; conversely, measured calcification rates can be allocated to zooid number in order to determine mg $CaCO_3$ per zooid (Reid 2014). Although technically bryozoans should be bleached or ashed to remove organic material (ash-free dry weight) in order to calculate calcimass, in reality $CaCO_3$ is much heavier than dried organics and, at least among robustly calcified bryozoans, dry weight is not much different (Barnes *et al.* 2011)

Less intuitive growth measures (per Amui-Vedel *et al.* 2007) have been trialled, including: Specific Growth Rate $r = \ln(N/N_0)/t$ where $N_0 =$ initial zooid number; $N =$ final zooid number, $t =$ time (days) elapsed, which ranges from 0.1 to 0.3; and doubling time $t_2 = 0.693/r$ in days, where $r =$ radius.

Smith (2014) collated measured growth rates for 44 bryozoan species from the literature, and we have updated that table (by including additional references), resulting in measured growth rates for 84 bryozoan species (Appendix Table). The most commonly used measure of growth rate was linear extension, either as colony height or radius. We standardised these measures to mm/y (even though many species do not grow all year long); rates ranged from 0.1 to 1400 mm/y (mean 87 mm/y; standard deviation 245 mm/y; N = 54). Another common growth rate measure was increase in area; again, we standardised to annual growth in mm²/y. Colonial growth rate by area ranged from 44 to 193,235 mm²/y (mean 20,998 mm²/y; SD 43,897 mm²/y; N = 19). Calcification rate ranged from 9 to 23,700 mg $CaCO_3$/y (mean 1499 mg $CaCO_3$/y; SD 5247 mg $CaCO_3$/y; N = 20). All three measures of growth rate (Table 2) suggest either that growth rate varies among species by four orders of magnitude, or that growth rates measured by different researchers using different methods cannot be compared. In either case, the data do not lead to any useful generalisation about bryozoan colonial growth rates.

INFLUENCE OF METHODS ON RESULTS

It may be that there is so much variation in measured bryozoan colony growth rates because of the variety of methods that are used. To consider this possibility, we

Table 2. Summary of data comprising 88 measurements of colony growth from 81 species of bryozoan (based on Appendix Table).

	Maximum observed height or radius (mm)	Maximum observed area (mm²)	Maximum known age (y)	Growth rate extension (mm/y)	Increase in area (mm²/y)	Calcimass (% that is skeleton) (wt%)	Calcification rate (mg CaCO$_3$/y)	Calcification per zooid (mg CaCO$_3$/zz)
Min	2	97	0.1	0.1	44	0.4	9	0.1
Mean	114	4229	13	87	20988	85	1499	0.5
Max	1000	23400	86	1400	193235	230	23700	1.0
Range	998	23303	86	1400	193191	230	23691	1
StdDev	196	6288	16	245	43897	92	5247	0.4
N	28	20	42	54	19	4	20	3

have separated methods into seven categories (Table 3). Growth rate in bryozoan colonies can be measured by direct observation (in the laboratory or in the field), mark-and-recapture (both chemical and physical marks can be used) or by inference/proxy. Each of these methods has its strengths and weaknesses.

Direct Observation

Direct observation of growth rate can occur either in the sea (usually using settling plates) or in the lab. Settling plates that are simply empty substrate placed in the sea (e.g., Skerman 1958) provide only a minimum growth rate (as researchers don't know when each colony settled). On the other hand, early growth when colonies are just starting out can be the most rapid growth of the colony's life (Ryland 1976). Different substrates, flow rates, orientations, light regimes, and water depths may affect growth rate (e.g., Edmondson and Ingram 1939). And, of course, there is an element of random chance: researchers only catch the species that settle, which may be random or skewed towards first-colonising weedy r-selected species.

To overcome some of those difficulties, some researchers have settled larvae on glass slides, then grown them in the sea or in the laboratory (e.g., Jebram and Rummert 1978; Kitamura and Hirayama 1984). Others have mounted a piece of adult colony on a substrate (e.g., Sokolover et al. 2018). While this strategy ensures that the exact time of growth

is known, it still measures the earliest, most rapid growth of a colony, as it first spreads out.

Culturing bryozoans in the laboratory provides more environmental control, but it is notoriously difficult, particularly for large robustly-calcified species. Environmental variations, such as temperature (Amui-Vedel et al. 2007) or current speeds (Sokolover et al. 2018), can promote or retard growth. It appears that genetic variation in growth rates may also be considerable (Bayer and Todd 1996). Diet and feeding regime also affect growth rate (Winston 1976; Jebram and Rummert 1978). Lab culture of bryozoans is often over short time periods (e.g., 42 days in Winston 1976), possibly because bryozoans do not grow well in captivity. If conditions are suboptimal, growing bryozoans in culture may underestimate growth rate (see e.g., Smith et al. 2019).

Mark and Recapture

Mark-and-recapture techniques are well known in biology and have been applied to bryozoans as well as whales (e.g., Urian et al. 2015). Here an adult bryozoan colony is marked mechanically or chemically, and its size recorded. Then it is left in its natural habitat to grow. After time elapses, researchers revisit the colony and re-record its size. The bryozoan is photographed before and after marking (e.g., Okamura and Partridge 1999), or the bryozoan is immersed in a chemical marker dye such as calcein (Smith et al. 2019) and

Table 3. Methods used for the measurement of bryozoan colony growth.

	In the ocean (*in vivo*)	In the lab (*in vitro*)	In dead specimens (*post-mortem*)
Direct Observation	A. Settling plate placed empty in the sea, collecting whatever settles B. Seeding a substrate, then returning it to the sea to grow	C. Seeding a substrate, then growing it in the lab	
Mark and Recapture	D. Marking colonies either with chemicals or tags, returning to the field, re-collecting or photographing after a time	E. Marking colonies with chemicals or tags, growing in the lab, then collecting or photographing them	
Inference			F. Counting annual growth checks or generations of ovicells G. Using chemical signals (such as stable isotopes) to track seasonal variations in environment

then recovered and the unmarked skeleton measured (e.g., Smith *et al.* 2001). These techniques have the advantage that growth is of adult colonies, beyond the initial flush of growth, and that growth is occurring in the natural habitat. It is not uncommon, however, to lose colonies or be unable to relocate them, not least because tagging itself can increase colony vulnerability to currents and waves.

Inference/Proxy

Direct observation and mark-and-recapture techniques measure growth over a short period of time. A better way to determine age and growth over the life of the whole colony is to utilize signals, physical and/ or chemical, that indicate periods of time (like tree rings). For example, cross-time colony samples of oxygen isotope concentrations form a record of sea-water temperature and consequently document the passing of seasons (e.g., Pätzold *et al.* 1987; Bader and Schaefer 2005; Key *et al.* 2013, 2018). Colonies with measurable growth checks also allow annual growth to be measured from the annual bands of thicker skeleton that can be detected by x-rays or even just visually (e.g., Barnes 1995; Smith 2007). Using growth checks and isotopes simultaneously allows validation of the annual nature of the signal (Key *et al.* 2018).

Growth checks can lead to underestimation of the overall average growth rate (calculated as a simple size/time) (Key *et al.* 2018). Antarctic bryozoans grow at the same approximate rate as their temperate counterparts, but only for the few months of summer. So, a colony of the same size would be much older than its temperate or tropical cousin.

Comparison of Methodologies

We collated measured growth rates collected using all seven of these methods (see Table 4), grouped them according to method of measurement, and calculated basic descriptive statistics on them, to see if measurement method influences growth rate measured. In every case where there was a range, we chose the maximum growth rate. While there are very unequal sample numbers among methods, and the data were not designed for this test, nevertheless Table 4 shows that long-term measurements of growth over the life of the colony (annual growth checks and chemical proxies for growth) give much lower numbers than those which measure growth rate over periods of days to weeks. Settling plates *de novo* measure the fastest growth rates, which makes sense as they attract early settlers who grow fast to carve out space early.

Table 4. The influence of measurement technique on measured growth rate.

Method of measuring growth rate	Number of species measured this way	Linear extension (mm/y)				Increase in Area (mm²/y)				Calcification Rate (mg CaCO₃/y)			
		Min	Max	Mean	Std Dev	Min	Max	Mean	Std Dev	Min	Max	Mean	Std Dev
A Settling Plates *in vivo, de novo*	38	1	1400	136	331	665	193235	30203	53183	220	736	478	258
B Substrate seeded, *in vivo*	2			220	0			73	0			730	0
C Substrate seeded, in lab	6			438	0	52	7300	3461	3327			48	0
D Mark and Recapture *in vivo*	4	7	730	368	362	44	37595	18820	18776			23700	0
E Mark and Recapture in lab	5	0	1	1	1								
F Annual growth checks (morphological)	23	1	36	9	8					9	1593	270	451
G Chemical proxies for annual growth	4	8	40	19	13			222	0	160	230	195	35
All Methods	81	0	1400	88	245	44	193235	20211	42853	9	23700	1467	5116

CONCLUSIONS

It is a little disappointing to have summarised data from dozens of papers and species and not to be able to answer the question: "How fast do bryozoan colonies grow?" Until we have a standardized methodology, we will be unable to do more than cite whichever paper is most relevant to our own species and growth form. Furthermore, it is currently impossible to compare growth rates among bryozoans, especially among those with different growth forms.

A study should be designed in which bryozoans of both encrusting and erect branching growth forms are cultured in the laboratory, grown at sea, and observed in the wild. *Post-mortem* analysis of oxygen isotopes or growth checks should also be carried out. The use of different techniques over the same season(s) in the same species should reduce variability and allow for selection of the best methods for ascertaining bryozoan growth rates.

In the meantime, we suggest that growth rate studies in bryozoans avoid methods that measure only the first flush of rapid growth or rely on culture in the laboratory. Mark-and-recapture is effective over a short time, but the best picture of growth and growth rate in a bryozoan colony is achieved by the interpretation of physical or chemical annual markers, when present. In addition, we recommend that characterisations of growth in well-calcifieid bryozoans (whether linear, areal, or in number of zooids) include also the weight of the skeleton, so that calcification rate can be calculated. Calcification rate has real potential, among well-calcified bryozoans, to be a unit comparable among growth forms.

ACKNOWLEDGEMENTS

REFERENCES

(includes references found in Appendix Table)

AMUI-VEDEL A.-M., HAYWARD, P.J. AND PORTER, J.S. 2007. Zooid size and growth rate of the bryozoan *Cryptosula pallasiana* Moll in relation to temperature, in culture and in its natural environment. *Journal of Experimental Marine Biology and Ecology 353*, 1–12.

BADER, B. 2000. Life cycle, growth rate and carbonate production of *Cellaria sinuosa*. In: A. Herrera Cubilla and J.B.C. Jackson (eds), *Proceedings of the 11th International Bryozoology Association Conference*. Balboa, Smithsonian Tropical Research Institute, pp. 136–144

BADER, B. AND P. SCHÄFER. 2004. Skeletal morphogenesis and growth check lines in the Antarctic bryozoan *Melicerita obliqua*. *Journal of Natural History* **38**, 2901–2922.

BADER, B. AND P. SCHÄFER. 2005. Impact of environmental seasonality on stable isotope composition of skeletons of the temperate bryozoan *Cellaria sinuosa*. *Palaeogeography Palaeoclimatology Palaeoecolog.* **226**, 58–71.

BARNES, D.K.A. 1995. Seasonal and annual growth in erect species of Antarctic bryozoans. *Journal of Experimental Marine Biology and Ecology.* **188**, 181–198.

BARNES, D.K.A., WEBB, K.E. AND LINSE, K. 2007. Growth rate and its variability in erect Antarctic bryozoans. *Polar Biology* **30**, 1069–1081.

BARNES, D.K.A., KUKLINSKI, P., JACKSON, J.A., KEEL, G.W., MORLEY, S.A. AND WINSTON, J.A. 2011. Scott's collections help reveal accelerating marine life growth in Antarctica. *Current Biology* **21**, R147–R148.

BAYER, M.M. AND TODD, C.D. 1996. Effect of polypide regression and other parameters on colony growth in the cheilostomate *Electra pilosa* (L.). In: D.P. Gordon, A.M. Smith and J.A. Grant-Mackie (eds), *Bryozoans in Space and Time. Proceedings of the 10th International Bryozoology Conference*. Wellington, Wilson and Horton, pp. 29–45.

BAYER, M.M., CORMACK, R.M., AND TODD, C.D. 1994. Influence of food concentration on polypide regression in the marine bryozoan *Electra pilosa* (L.) (Bryozoa: Cheilostomata). *Journal of Experimental Marine Biology and Ecology* **178**, 35–50.

BONE, Y. 1991. Population explosion of the bryozoan *Membranipora aciculata* in the Coorong Lagoon in late 1989. *Australian Journal of Earth Sciences* **38**, 121–123.

BONE Y. AND JAMES N.P. 1993. Bryozoans as carbonate sediment producers on the cool-water Lacepede shelf, southern Australia. *Sedimentary Geology* **86**, 247–271.

BREY, T., GUTT, J., MACKENSEN, A. AND STARMANS, A. 1998. Growth and productivity of the high Antarctic bryozoan *Melicerita obliqua*. *Marine Biology* **132**, 327–333.

BREY, T., GERDES, D., GUTT, J., MACKENSEN, A. AND STARMANS, A. 1999. Growth and age of the Antarctic bryozoan *Cellaria incula* on the Weddell Sea shelf. *Antarctic Science* **11**, 408–414.

COCITO, S. AND FERDEGHINI, F. 2001. Carbonate standing stock and carbonate production of the bryozoan *Pentapora fascialis* in the north-western Mediterranean. *Facies* **45**, 25–30.

COCITO S., NOVOSEL M. AND NOVOSEL A. 2004. Carbonate bioformations around underwater freshwater springs in the northeastern Adriatic Sea. *Facies* **50,** 13–17.

COCINO, S., NOVOSEL M., PASARI´C, Z. AND KEY, M.M. JR. 2006. Growth of the bryozoan *Pentapora fascialis* (Cheilostomata, Ascophora) around submarine freshwater springs in the Adriatic Sea. *Linzer Biologische Beitr*äge **38**, 15–24.

CUFFEY, R.J. AND FINE, R.L. 2006. Reassembled trepostomes and the search for the largest bryozoan colonies. *International Bryozoology Association Bulletin* **2**, 13–15.

ECKMAN, J.E. AND DUGGINS, D.O., 1993. Effects of flow speed on growth of benthic suspension feeders. *Biological Bulletin* **185**, 28–41.

EDMONDSON, C.H. AND INGRAM, W.M. 1939. Fouling organisms in Hawaii. *Occasional Papers of Bernice P Bishop Museum, Honolulu Hawaii* **XIV**, 251–300.

FORTUNATO, H., SCHÄFER, P. AND BLASCHEK, H. 2013. Growth rates, age determination, and calcification levels in *Flustra foliacea* (L.) (Bryozoa: Cheilostomata): preliminary assessment. In: A. Ernst, P. Schäfer and J. Scholz (eds) *Bryozoan Studies 2010, Lecture Notes in Earth System Sciences* **143**, 59–74.

GERACI, S. AND RELINI, G. 1970. Osservazioni sistematico-ecologiche sui briozoi del fouling Portuale di Genova. *Bollettino dei Musei e degli Istituti Biologici del'Universitadi Genova* **38**, 103–139.

HAGEMAN, S.J. 2003. Complexity generated by iteration of hierarchical modules in Bryozoa. *Integrative and Comparative Biology* **43**, 87–98.

HAGEMAN, S.J., BOCK, P.E., BONE, Y., AND MCGOWRAN, B. 1998. Bryozoan Growth Habits: Classification and Analysis. *Journal of Paleontology* **72**, 418–436.

HAGEMAN, S.J., BONE, Y., MCGOWRAN, B. AND JAMES, N.P. 1997. Bryozoan colonial growth forms as paleoenvironmental indicators: Evaluation of methodology. *Palaios* **12**, 406–419.

HAYWARD P.J. AND HARVEY, P.H. 1974. Growth and mortality of the bryozoan *Alcyonidium hirsutum* (Fleming) on *Fucus serratus* L. *Journal of the Marine Biological Association of the UK* **54**, 677–684.

HAYWARD, P.J. AND RYLAND, J.S. 1975. Growth, reproduction and larval dispersal in *Alcyonidium hirsutum* (Fleming) and some other Bryozoa. VIII European Marine Biology Symposium. *Pubblicazioni della Stazione Zoologica de Napoli* **39** Suppl: 226–241.

HERMANSEN, P., LARSEN, P.S. AND RIISGÅRD H.U. 2001. Colony growth rate of encrusting marine bryozoans (*Electra pilosa* and *Celleporella hyalina*). *Journal of Experimental Marine Biology and Ecology* **263**, 1–23.

HUNTER E. AND HUGHES, R.N. 1993. Effects of diet on life-history parameters of the marine bryozoan *Celleporella hyalina* (L.). *Journal of Experimental Marine Biology and Ecology* **167**, 163–177.

JACKSON J.B.C. AND WERTHEIMER S.P. 1985. Patterns of reproduction in five common species of Jamaican reef-associated bryozoans. In: C. Nielsen and G.P. Larwood (eds), *Bryozoa: Ordovician to Recent*. Fredensborg, Olsen and Olsen, pp. 161–168.

JACKSON, J.B.C. AND J.E. WINSTON. 1981. Modular growth and longevity in bryozoans. In: G.P. Larwood and C. Nielson (eds), *Recent and Fossil Bryozoa*. Fredensborg, Olsen and Olsen, pp. 121–126.

JEBRAM, D. AND RUMMERT, H.-D. 1978. Influences of different diets on growth and forms of *Conopeum seurati* (CANU) (Bryozoa, Cheilostomata). *Zoologische Jahrbücher Abteilun für Systematik, Geographie, und Biologie der Teire* **105**, 502–514.

KAHLE, J., LIEBEZEIT, G. AND GERDES, G. 2003. Growth aspects of *Flustra foliacea* (Bryozoa, Cheilostomata) in laboratory culture. *Hydrobiology* **503**, 237–244.

KEY, M.M., JR., HOLLENBECK, P.M., O'DEA, A. AND PATTERSON, W.P. 2013. Stable isotope profiling in modern marine bryozoan colonies across the Isthmus of Panama. *Bulletin of Marine Science* **89**, 837–856.

KEY, M.M., JR., ROSSI, R.K., SMITH, A.M., HAGEMAN, S.J. AND PATTERSON, W.P. 2018. Stable isotope profiles of skeletal carbonate validate annually-produced growth checks in the bryozoan *Melicerita chathamensis* from Snares Platform, New Zealand. *Bulletin of Marine Science* **94**, 1447–1464.

KITAMURA, H. AND HIRAYAMA, K. 1984. Growth of the bryozoan *Bugula neritina* in the sea at various water temperatures. *Bulletin of the Japanese Society of Scientific Fisheries* **50**, 1–5.

KUKLINSKI, P. AND P.D. TAYLOR. 2006. Unique life history strategy in a successful Arctic bryozoan, *Harmeria scutulata*. *Journal of the Marine Biological Association of the UK* **86**, 1305–1314.

KUKLINSKI, P., SOKOLOWSKI, A., ZIOLKOWSKA, M., BALAZY, P., NOVOSEL, M. AND BARNES, D.K.A. 2013. Growth rate of selected sheet-encrusting bryozoan colonies along a latitudinal transect: preliminary results. In: A. Ernst, P. Schäfer and J. Scholz (eds) *Bryozoan Studies 2010*, A. *Lecture Notes in Earth System Sciences* **143**, pp. 155–167

LAGAAIJ, R. AND GAUTIER, Y.V. 1965. Bryozoan assemblages from marine sediments of the Rhone delta, France. *Micropaleontology* **11**, 39–58.

LIDGARD, S. AND JACKSON, J.B.C. 1989. Growth in encrusting cheilostome bryozoans: I. Evolutionary trends. *Paleobiology* **15**, 255–282.

LIUZZI, M.G., LÓPEZ-GAPPA J. AND SALGADO, L. 2018. Bryozoa from the continental shelf off Tierra del Fuego (Argentina): Species richness, colonial growth-forms, and their relationship with water depth. *Estuarine, Coastal and Shelf Science* **214**, 48–56.

LOMBARDI, C., COCITO, S., HISCOCK, K., OCCHIPINTI-AMBROGI, A., SETTI, M. AND TAYLOR, P.D. 2008. Influence of seawater temperature on growth bands, mineralogy and carbonate production in a bioconstructional bryozoan. *Facies* **54**, 333–342.

MCCLELLAND, H.L.O., TAYLOR, P.D., O'DEA, A. AND OKAMURA, B. 2014. Revising and refining the bryozoan zs-MART seasonality proxy. *Palaeogeography, Palaeoclimatology, Palaeoecology* **410**, 412–420.

MCKINNEY F.K. AND JACKSON, J.B.C. 1989. *Bryozoan Evolution.* Boston, Unwin-Hyman, Boston.

MENON, N.R. 1975. Observations on growth of *Flustra foliacea* (Bryozoa) from Helgoland waters. *Helgoländer wiss Meeresunter*s **27**, 263–267.

MENON, N.R. AND NAIR, N.B. 1972. The growth rates of four species of intertidal bryozoans in Cochin backwaters. *Proceedings Indian National Science Academy* **38**, 397–402.

NELSON, C.S., HYDEN, F.M., KEANE, S.L., LEASK, W.L. AND GORDON, D.P. 1988. Application of bryozoan zoarial growth form studies in facies analysis of non-tropical carbonate deposits in New Zealand. *Sedimentary Geology* **60**, 301–322.

NEKLIUDOVA U.A., SHUNKINA K.V., GRISHANKOV A.V., VARFOLOMEEVA M.N., GRANOVITCH A.I. AND OSTROVSKY A.N. 2019. Colonies as dynamic systems: reconstructing the life history of *Cribrilina annulata* (Bryozoa) on two algal substrates. *Journal of the Marine Biological Association of the United Kingdom* **99,** 1–15.

O'DEA, A. AND OKAMURA, B. 2000. Cheilostome bryozoans as indicators of seasonality in the Neogene epicontinental seas of Western Europe. In: A. Herrera-Cubilla and J.B.C. Jackson (eds.), *Proceedings of the 11th International Bryozoology Association Conference.* Balboa, Smithsonian Tropical Research Institute, pp. 74–86.

OKAMURA, B. AND PARTRIDGE, J.C. 1999. Suspension feeding adaptations to extreme flow environments in a marine bryozoan. *Biological Bulletin* **196**, 205–215.

PÄTZOLD, J., RISTEDT H, AND WEFER G. 1987. Rate of growth and longevity of a large colony of *Pentapora foliacea* (Bryozoa) recorded in their oxygen isotope profiles. *Marine Biology* **96**, 535–538.

REID CM. 2014. Growth and calcification rates in polar bryozoans from the Permian of Tasmania, Australia. In:

A. Rosso, P.N. Wyse Jackson and J. Porter (eds) *Bryozoan Studies 2013*, Proceedings of the 16th International Bryozoology Association Conference, Catania, Sicily, *Studi Trentini di Scienze Naturali* **94**, 189–197.

RYLAND, J.S. 1976. Physiology and ecology of marine bryozoans. *Advances in Marine Biology* **14**, 285–443.

RYLAND, J.S. AND WARNER, G.F. 1986. Growth and form in modular animals: ideas on the size and arrangement of zooids. *Philosophical Transactions of the Royal Society of London* B. **313**, 53–76.

SAUNDERS, M. AND METAXAS, A. 2009. Effects of temperature, size, and food on the growth of *Membranipora membranacea* in laboratory and field studies. *Marine Biology* **156**, 2267–2276.

SCHOPF, T.J.M. 1969. Paleoecology of ectoprocts (bryozoans). *Journal of Paleontology* **43**, 234–244.

SKERMAN, T.M. 1958. Marine fouling at the port of Lyttelton. *New Zealand Journal of Science* **1**, 224–257.

SMITH, A.M. 1995. Palaeoenvironmental interpretation using bryozoans: a review. In: D. Bosence and P. Allison (eds), *Marine Palaeoenvironmental Analysis from Fossils. Geological Society Special Publication* **83**, 231–243.

SMITH, A.M. 2007. Age, growth and carbonate production by erect rigid bryozoans in Antarctica. *Palaeogeography, Palaeoclimatology, Palaeoecology* **256**, 86–98.

SMITH, A.M. 2014. Growth and calcification of marine bryozoans in a change ocean. *Biological Bulletin* **226**, 203–210.

SMITH, A.M. AND KEY, M.M., JR. 2004. Controls, variation and a record of climate change in detailed stable isotope record in a single bryozoan skeleton. *Quaternary Research* **61**, 123–133.

SMITH, A.M., KEY, M.M., JR. AND WOOD, A.C.L. 2019. Culturing large erect shelf bryozoans: skeletal growth measured using calcein staining in culture. In: R. Schmidt, C.M. Reid, D.P. Gordon, G. Walker-Smith, S. Martin and I. Percival (eds), *Bryozoan Studies 2016.* Proceedings of the Seventeenth International Bryozoology Association Conference, 10-15 April 2016, Melbourne, Australia. *Memoirs of the Australasian Association of Palaeontologists* **52**, 131–138.

SMITH, A.M. AND LAWTON, E.I. 2010. Growing up in the temperate zone: age, growth, calcification and carbonate mineralogy of *Melicerita chathamensis* (Bryozoa) in southern New Zealand. *Palaeogeography, Palaeoclimatology, Palaeoecology* **298**, 271–277.

SMITH, A.M. AND NELSON, C.S. 1994. Calcification rates of rapidly colonising bryozoans in Hauraki Gulf, northern New Zealand. *New Zealand Journal of Marine and Freshwater Research* **28**, 227–234.

SMITH, A.M., STEWART, B., KEY, M.M., JR. AND JAMET, C.M. 2001. Growth and carbonate production by *Adeonellopsis* (Bryozoa: Cheilostomata) in Doubtful Sound,

New Zealand. *Palaeogeography, Palaeoclimatology, Palaeoecology* **175**, 201–210.

SOBICH, A. 1996. Analyse von stabilen Isotopen und Wachstumsstrukturen der Bryozoe *Celleporaria fusca* zur Rekonstruktion der Umweltbedingungen im nördlichen Golf von Aqaba. Diplomarbeit (Thesis), University of Bremen, 64 pp.

SOKOLOVER N., OSTROVSKY A.N. AND ILAN, M. 2018. *Schizoporella errata* (Bryozoa, Cheilostomata) in the Mediterranean Sea: abundance, growth rate, and reproductive strategy, *Marine Biology Research*, DOI: 10.1080/17451000.2018.1526385

STACH, L.W. 1935. Growth variation in Bryozoa Cheilostomata. *The Annals and Magazine of Natural History* **16**, ser 10, 645–647.

STEBBING, A.R.D. 1971. Growth of *Flustra foliacea* (Bryozoa). *Marine Biology* **9**, 267–272.

TAYLOR, P.D. AND JAMES, N.P. 2013. Secular changes in colony-forms and bryozoan carbonate sediments through geological history. *Sedimentology* **60**, 1184–1212.

TAYLOR, P.D. AND E. VOIGT. 1999. An unusually large cyclostome bryozoan (*Pennipora anomalopora*) from the Upper Cretaceous of Maastricht. *Bulletin de L'Institute Royal des Sciences Naturelle de Belgique Sciences de la Terre* **69**, 165–171.

URIAN, K., GORGONE, A., READ, A., BALMER, B., WELLS, R. S., BERGGREN, P., DURBAN, J., EGUCHI, T., RAYMENT, W., AND HAMMOND, P. S. (2015). Recommendations for photo-identification methods used in capture-recapture models with cetaceans. *Marine Mammal Science*, **31,** 298–321

WASS, R.E., VAIL, L.L. AND BOARDMAN, R.S. 1981. Early growth of Bryozoa at Lizard Island, Great Barrier Reef. In: G.P. Larwood and C. Nielsen (eds), *Recent and Fossil Bryozoa*, Fredensborg, Olsen and Olsen, 299–303.

WINSTON, J.E. 1976. Experimental culture of the estuarine ectoproct *Conopeum tenuissimum* from Chesapeake Bay. *Biological Bulletin* **150**, 318–335.

WINSTON, J.E. 1983. Patterns of growth, reproduction and mortality in bryozoans from the Ross Sea, Antarctica. *Bulletin of Marine Science* **33**, 688–702.

WINSTON J.E. AND HÅKANSSON, E. 1989. Molting by *Cupuladria doma*, a free-living bryozoan. *Bulletin of Marine Science* **44**, 1152–1158.

WINSTON, J.E. AND HAYWARD, P.J. 2012. The marine bryozoans of the northeast coast of the United States: Maine to Virginia. *Virginia Museum of Natural History Memoir* **11**, 1–180.

WOOD, A.C.L. AND PROBERT, P.K. 2013. Bryozoan-dominated benthos of Otago shelf, New Zealand: its associated fauna, environmental setting and anthropogenic threats. *Journal of the Royal Society of New Zealand* **43**, 231–249.

Appendix Table: Summary of published literature on size, age, growth and calcification in 83 species of bryozoans.

Species	Location	Growth form	Reported growth rate	Max observed size (height or radius in mm)	Max observed area (in mm²)	Max age (y)	Growth rate (extension in mm/y)	Growth rate (area in mm²/y)	Calcimass (wt% skeleton)	Calcification rate (mg CaCO₃/y)	Calcification per zooid (mg CaCO₃/zz)	Method	Method Code (Table 4)	Sources
Adeonellopsis sp.	Doubtful Sound, Otago Shelf NZ	Erect rigid branching	6.9 mm/y branch length, 24g CaCO₃/y	300		20	6.9			23700	0.13	Calcein marked in vivo	D	Smith et al., 2001
Adeonellopsis sp.	Otago shelf, New Zealand	Erect rigid branching	1 mm/y				1					Calcein marked in culture	E	Smith et al., 2019
Alcyonidium hirsutum	South Wales, UK	Encrusting unilaminar	up to 100 mm² in 160 days		100	0.4		44				Observation in vivo	D	Hayward & Ryland, 1975
Alderina arabianensis	Cochin, India	Encrusting unilaminar	1964-3020 mm²/mo in spring		3020			36240				Settling plates	A	Menon & Nair 1972
Alloeflustra tenuis	Signy Is	Erect flexible branching	max age 26 y, 63mg ash free dry wt/y			26				63		Annual growth checks	F	Barnes, 1995
Arachnopusia inchoata	Ryder Bay, Antarctica	Encrusting	mean increase 100 mm²/y on artificial panels, n = 10; up to 0.4 mm/d radial extension in summer	2.8			5.6					Settling plates	A	Bowden et al., 2006
Bugula neritina	Kaneohe Bay, Hawaii	Erect flexible branching	3 inches in 3 mo, 65mm height in 156 days				152					Settling plates	A	Edmondson & Ingram 1939
Bugula neritina	Nagasaki, Japan	Erect flexible branching	270 zooids, 28mg, in 14 days							730		Larvae seeded then in vivo	B	Kitamura & Hirayama 1984
Bugula sp. (aff. *neritina*)	Lyttleton, NZ	Erect flexible articulated	7cm in 2 mo	70		0.2	420					Settling plates	A	Skerman 1958
Caberea zelandica	Lyttleton, NZ	Erect flexible articulated	1-3 cm in 6 mo	30		0.5	60					Settling plates	A	Skerman 1958
Callopora dumerilii	Adriatic Sea	Encrusting unilaminar	52-210 mm2 in 18 mo (mean = 131, n=2)				5.5					Settling plates	A	Kuklinski et al., 2013
Cellaria incula	Weddell Sea	Erect flexible articulated	one branch/y, 8 mm/y, max age 14 y	100		14	8					Stable isotope profiles	G	Brey et al., 1999
Cellaria sinuosa	English Channel	Erect flexible articulated	max age 1.5-2 y, growth 32-40 mm/y, 12-57 g/m²/y			2	40			160		Stable isotope profiles	G	Bader, 2000; Bader & Schaefer, 2005
Cellarinella foveolata	Ross Sea	erect branching, flexible base	max size 6cm, 12 internodes (assumed annual)	60		12	5					Annual growth checks	F	Winston, 1983
Cellarinella margueritae	Ross Sea, Weddell Sea	erect branching, flexible base	max size 5.6cm, max 10 internodes; 3.4 mm/y, 24mg CaCO₃/y	56		15	4.4			24		Annual growth checks	F	Winston, 1983; Barnes et al. 2007
Cellarinella njegovanae	Ross Sea	erect branching, flexible base	max size 8cm, max 18 internodes	80		18	4.4					Annual growth checks	F	Winston, 1983
Cellarinella nodulata	Ross Sea, Weddell Sea	erect branching, flexible base	1.3 to 5.6. mm/y, 5-33 mg/y, max age 18 y, max size 4.8 am, max 11 internodes; 5.2 mm/y, 55mg CaCO₃/y	48		18	5.6			55		Annual growth checks	F	Winston, 1983; Smith, 2007; Barnes et al., 2007
Cellarinella mutti	Ross Sea	erect branching, flexible base	1.0 to 7.1 mm/y, 3-57 mg/y, max age 14 y, max size 5.7cm, max 11 internodes, 3.9 mm/y, 30 mg CaCO₃/y	57		14	7.1			57		Annual growth checks	F	Winston, 1983; Barnes et al., 1995; Smith, 2007; Barnes et al., 2011
Cellarinella rogickae	Weddell Sea	erect branching, flexible base	4.6 mm/y, 45mg CaCO₃/y			15	4.6			45		Annual growth checks	F	Barnes et al., 2007
Cellarinella rossi	Ross Sea	erect branching, flexible base	max size 6.0 cm, max 14 internodes	60		14	4.3					Annual growth checks	F	Winston, 1983
Cellarinella roydsi	Antarctica	erect branching, flexible base	7 yrs age			7						Annual growth checks	F	Ryland 1976
Cellarinella sp. M	Ross Sea	erect branching, flexible base	max age 20 y, 5.4 mm/y			20	5.4					Annual growth checks	F	Winston, 1983

Species	Location	Growth form	Notes								Method		Reference
Cellarinella watersi	Signy Is, Weddell Sea	erect branching, flexible base	max age 9 y, max ht 5cm, 4.1 mm/y, 176mg CaCO₃/y	50		11	4.1			176	Annual growth checks	F	Barnes, 1995; Barnes et al., 2007
Celleporaria fusca	Gulf of Aqaba	multilaminar	max age 86 y, avg growth 750μ/y, up to 6.5cm tall	65		86	0.75				Growth checks, isotopes	F	Sobich, 1996
Celleporella hyalina	Wales, UK	Encrusting unilaminar	from 1 to 40 mm²/56 days; from 6 to 591 zooids/56 days (depending on diet)					260			Culture	C	Hunter & Hughes 1993 and many others
Chaperiopsis protecta	Ryder Bay, Antarctica	Encrusting	mean increase 50 mm²/y on artificial panels, n = 20; up to 0.3 mm/day radial extension in summer	2			4				Settling plates	A	Bowden et al., 2006
Cinctipora elegans	Otago shelf, New Zealand	Erect rigid branching	1.15 mm/y				1.15				Calcein marked in culture	E	Smith et al 2019
Conopeum seurati	Kiel Canal, Germany	Encrusting unilaminar	up to about 800 zooids in 25-31 days								Lab Culture	C	Jebram & Rummert, 1978
Conopeum tenuissimum	Chesapeake Bay USA	Encrusting unilaminar	up to 1629 zooids and 8 generations in 42 days			0.12					Culture	C	Winston 1976
Cribrilina annulata	Spitsbergen	Encrusting unilaminar	53 to 88 mm² in 4 y (n = 4)				1.3				Settling plates	A	Kuklinski et al., 2013
Cribrilina annulata	Kandalaksha Bay, White Sea	Encrusting unilaminar	mean max of 155 zooids in July; radius of about 3 mm (measured off photo), max age 17 mo	3		1.5					Ovicell generations	F	Nekliudova et al., 2019
Crisia sp.		Erect flexible branching	180x100 mm in 34 days		18 000			193 235			Settling plates	A	Paul 1942 reported in Menon & Nair
Cryptosula pallasiana	Swansea UK	Encrusting unilaminar	14°C: 100 zooids in 4 weeks; 18C: 300 zooids in 4 weeks								Settling plates	A	Amui-Vedel et al, 2007
Cryptosula pallasiana	Lyttleton, NZ	Encrusting unilaminar	12 cm² in 6 mo		1200	0.5		2400			Settling plates	A	Skerman 1958
Cupuladria exfragminis	Gulf of Panama	Encrusting unilaminar	GP1: 16.8 mm diameter, 0.23 g in 1.0 y; GP2: 16.6mm diameter, 0.31 g in 1.5 y; GP3: 15.6mm diameter, 0.20 g in 2.5 y	8.4	222	2.5	8.4	222	230	230	Stable isotope profiles	G	Key et al., 2013
Diploselen cf obelia	Adriatic Sea	Encrusting unilaminar	82-98 mm² in 18 mo (mean = 92, n = 3)				3.7				Settling plates	A	Kuklinski et al., 2013
Diplosolen arctica	Spitsbergen	Encrusting unilaminar	81 to 234 mm² in 2 y				4.3				Settling plates	A	Kuklinski et al., 2013
Disporella gordoni	Hauraki Gulf, NZ	Encrusting multilaminar	736mg CaCO₃ in one year			1				736	Settling plates	A	Smith & Nelson, 1994
Drepanophora tuberculatum	Rio Bueno Harbour, Jamaica	Encrusting unilaminar	median colony area = 0.6 cm²; smallest reproductive colony = 0.1 cm²; max colony area 1.4 cm²		140								Jackson & Wertheimer, 1985
Einhornia crustulenta	Baltic Sea	Encrusting unilaminar	2376 to 8290 mm² in 8 mo (mean = 4951, n = 4)				77.1				Settling plates	A	Kuklinski et al., 2013
Electra bengalensis	Cochin, India	Encrusting unilaminar	2213-2828 mm²/mo in spring		2828			33936			Settling plates	A	Menon & Nair 1972
Electra crustulenta	Cochin, India	Encrusting unilaminar	314-707 mm²/mo (june-Jan)		707			8484			Settling plates	A	Menon & Nair 1972
Electra pilosa	Scotland, Wales, UK	Encrusting unilaminar	311-1758 mm² in 103 d, lifespan >2 y, 2-15 mm²/14 days; 15-100 zz/14 days			> 2y		1102-6230			Culture	C	Bayer et al., 1994; Bayer & Todd 1996; Hermansen et al., 2001

Summary of published literature on size, age, growth and calcification in 83 species of bryozoans (continuation).

Species	Location	Growth form	Reported growth rate	Max observed size (height or radius in mm)	Max observed area (in mm²)	Max age (y)	Growth rate (extension in mm/y)	Growth rate (area in mm²/y)	Calcimass (wt% skeleton)	Calcification rate (mg CaCO₃/y)	Calcification per zooid (mg CaCO₃/zz)	Method	Method Code (Table 4)	Sources
Encrusting bryozoans (18 spp.)	Hauraki Gulf, NZ	Encrusting, mostly unilaminar	25 to 220 mg CaCO₃ in one year			1				220		Settling plates	A	Smith & Nelson, 1994
Escharella immersa	Norwegian Sea	Encrusting unilaminar	137 to 175 mm² in 3 y (n = 4)				2.5					Settling plates	A	Kuklinski et al., 2013
Escharoides angela	Lyttleton, NZ	Encrusting unilaminar	4 cm² in 20 mo		400	1.7		665				Settling plates	A	Skerman 1958
Fenestrulina rugula	Ryder Bay, Antarctica	Encrusting	mean increase 50 mm²/y on artificial panels, n = 50; up to 0.3 mm/day radial extension in summer	2			4					Settling plates	A	Bowden et al., 2006
Figularia sp.	Otago shelf, New Zealand	Encrusting unilaminar	1.38 mm/y				1.38					Calcein marked in culture	E	Smith et al, 2019
Flustra foliacea	North Sea	Erect flexible branching	1-13 mm² area of front of branches in 92 days, 80-248 zz in 92 days, 3-12 mg in 92 days		97	3		52		48		Lab Culture	C	Kahle et al., 2003
Flustra foliacea	Wales, North Sea, Baltic Sea, Helgoland, Scotland	Erect flexible branching	12 y age, 15 mm/y, 25 – 220 mg CaCO₃/y, ht of 7.93 cm in 8 y, annual growth rates up to 2.65 cm/y			12	10 to 26			about 850		Annual growth checks	F	Stebbing, 1971; Menon 1975; O'Dea & Okamura 2000; Fortunato et al., 2013
Harmeria scutulata	Arctic	Encrusting unilaminar	max diameter of 5.1 mm, less than a year's growth	5.1			2.5					Settling plates	A	Kuklinski & Taylor, 2006
Hornera foliacea	Otago shelf, New Zealand	Erect rigid fenestrate	0.05 mm/y				0.05					Calcein marked in culture	E	Smith et al., 2019
Hornera robusta	Otago shelf, New Zealand	Erect rigid branching	0.05 mm/y				0.05					Calcein marked in culture	E	Smith et al., 2019
Melicerita chathamensis	Snares Platform, S New Zealand	Blade with flexible base	max size 4 cm, 9 segments, 1.3 to 13.7 mm/y, 9 mg CaCO₃/y	40		9	13.7			9		Annual growth checks	F	Smith & Lawton, 2010
Melicerita obliqua	Weddell Sea, Ross Sea	Blade with flexible base	max size 6.6cm, max 22 segments, 4.9 mm/y; 34 mg CaCO₃/y, max age 32	200		50	8.1			34		Annual growth checks	F	Winston, 1983; Brey et al., 1998; Bader & Schaefer, 2004; Barnes et al., 2007
Membranipora aciculata	Coorong Lagoon, S Australia	Encrusting unilaminar	2 mm/day, max diameter 6cm	30			730					Observation in vivo	D	Bone 1991
Membranipora membranacea	Nova Scotia & Washington State	Encrusting unilaminar	0.1 to 1.2 mm/day linear extension				438					Lab Culture	C	Saunders & Metaxas 2009
Membranipora membranacea	Friday Harbour, Washington, USA	Encrusting unilaminar	19 days in pipes with different flows: growth rates from 5 to 20 mm²/day					7300				Larvae seeded then in vitro	C	Eckman & Duggins 1993
Membranipora membranacea	Lough Hyne, Ireland	Encrusting unilaminar	10 days, added 800-900 mm² mean, 1400 mm² max, mean growth rate 86-103 mm²/d					37595				Mark and photograph in situ	D	Okamura & Partridge 1999
Membranipora nitida	Norvegian Sea	Encrusting unilaminar	92 mm² in 4 y				1.4					Settling plates	A	Kuklinski et al., 2013

Species	Location	Growth form	Measurements							Method		Reference
Membranipora sp.		Encrusting unilaminar	41x40mm in 34 days		1640			17605		Settling plates	A	Paul 1942 reported in Menon & Nair 1972
Membranipora sp.	Visakhapatnam Harbour	Encrusting unilaminar	50x50mm in 30 days		2500			30415		Settling plates	A	Ganapati et al 1958 reported in Menon & Nair 1972
Menipea sp.	Lyttleton, NZ	Erect flexible articulated	8-10mm	10						Settling plates	A	Skerman 1958
Microporella arctica	Norwegian Sea	Encrusting unilaminar	109 to 139 mm² in 3 y (n = 4); 89 to 192 mm² in 4 y				2.2			Settling plates	A	Kuklinski et al., 2013
Microporella sp.	Lizard Island, Queensland, Australia	Encrusting unilaminar	5 mm diameter in 3 months	2.5		0.25	10			Settling plates	A	Wass et al., 1981
Nematoflustra flagellata	Signy Is	Erect flexible branching	max age 26 y			26				Annual growth checks	F	Barnes, 1995
Parasmittina sp.	Rio Bueno Harbour, Jamaica	Encrusting unilaminar	median colony area = 5 cm², smallest reproductive colony = 0.4 cm², max colony area 46 cm²		4600							Jackson & Wertheimer, 1985
Patinella sp.	Norwegian Sea	Encrusting unilaminar	8 to 89 mm² in 2y, 44.6 in 4 y				1.3			Settling plates	A	Kuklinski et al., 2013
Pennipora anomalopora	Upper Cretaceous, Maastricht, Netherlands	Erect branching	one large fossil colony with dark bands 3 mm apart	105		35	2.9			Annual growth checks	F	Taylor & Voigt, 1999
Pentapora fascialis	UK, NW Europe, Mediterranean	Erect rigid branching	max size 42 cm tall, 82 cm diameter, 358 to 1214 g/ m²/y, 3.6 cm/y, max skeletal mass 35-1098g. Up to 1m tall, 3 cm/y	1000		11	36		97	Annual growth checks	F	Cocito & Ferdeghini, 2001; Lombardi et al. 2006
Pentapora foliacea	Irish Sea	Erect rigid branching	60 mm in 3 yrs			3	20			Stable isotope profiles	G	Pätzold et al., 1987
Pentapora spp.	Plymouth and Italian Mediterranean	Erect rigid branching	6-7 mm in winter; 12-21 mm in summer; 125 to 889 g/m²/y, largest branch length 232mm	116						Annual growth checks	F	Lombardi et al., 2008
Peullina hincksi	Adriatic Sea	Encrusting unilaminar	100 mm² in 18 mo				3.8			Settling plates	A	Kuklinski et al., 2013
Reptadeonella 'plagiopora'	Rio Bueno Harbour, Jamaica	Encrusting unilaminar	median colony area = 27 cm², smallest reproductive colony = 8 cm², max colony area 234 cm²		23400							Jackson & Wertheimer, 1985
Schizoporella cochinensis	Cochin, India	Encrusting multilaminar	122-260 mm²/mo in spring		260			3120		Settling plates	A	Menon & Nair 1972
Schizoporella errata	Israeli coast of Mediterranean, Ligurian Sea	Encrusting multilaminar	0.73 cm²/day; mean max 37 cm² after 6 weeks; 5.5 cm diam after 3 mo		3700		220	73		Seeding	B	Geraci & Relini 1970; Sokolover et al 2018
Schizoporella sanguinensis		Encrusting multilaminar	30,000 zooids in 5 mo							Settling plates	A	Friedle 1952, reported in Menon & Nair
Schizoporella unicornis	Kaneohe Bay, Hawaii	Encrusting unilaminar	1 mm/d in diameter; 50-70mm in diameater after 3 mo; 132mm after 60 d				803			Settling plates	A	Edmondson & Ingram 1939
Steginoporella sp. nov.	Rio Bueno Harbour, Jamaica	Encrusting unilaminar	median colony area = 55 cm², smallest reproductive colony = 22 cm², max colony area 114 cm²		11400							Jackson & Wertheimer, 1985

Summary of published literature on size, age, growth and calcification in 83 species of bryozoans (continuation).

Species	Location	Growth form	Reported growth rate	Max observed size (height or radius in mm)	Max observed area (in mm²)	Max age (y)	Growth rate (extension in mm/y)	Growth rate (area in mm²/y)	Calcimass (wt% skeleton)	Calcification rate (mg CaCO₃/y)	Calcification per zooid (mg CaCO₃/zz)	Method	Method Code (Table 4)	Sources
Stenopora spiculata	Permian of Maria Island, Tasmania, Australia	Erect branching	8.2 to 16 mm/y, max age 25 y, 12% calcimass, 528mg CaCO₃/y, 0.19 mg/zooid			25	16		12	528	0.19	Annual growth checks	F	Reid, 2019
Stenopora tasmaniensis	Permian of Maria Island, Tasmania, Australia	Erect foliose	35 cm tall, 50 cm wide bilamellar, 12.5mm thick. 28 y old, 6mm/y, 1593 mg CaCO₃/y, 1.03 mg/zooid	350		28	6		38	1593	1.03	Annual growth checks	F	Reid, 2014
Stomhyselosaria watersi	Weddell Sea	erect branching, flexible base	4.5 mm/y, 46 mg CaCO₃/y, 11-15 y max age			15	4.5			46		Annual growth checks	F	Barnes et al., 2007
Stylopoma spongites	Rio Bueno Harbour, Jamaica	Encrusting unilaminar	median colony area = 16 cm², smallest reproductive colony = 4 cm², max colony area 91 cm²		9100									Jackson & Wertheimer, 1985
Swanomia belgica	Ross Sea	erect branching, flexible base	0.6 to 9.7 mm/y, 1-27 mg/y, max age 23 y			23	9.7			27		Annual growth checks	F	Smith, 2007
Tegella arctica	Spitsbergen	Encrusting unilaminar	276 to 495 mm² in 3 y (n = 5)				4.2					Settling plates	A	Kuklinski et al., 2013
Thalamoporella sp.	Lizard Island, Queensland, Australia	Encrusting unilaminar	4.5x1.5 cm in 3 months		675	0.25		2700				Settling plates	A	Wass et al. 1981
Valdemuniella vldemunita	Port Hacking, NSW, Australia	Encrusting unilaminar	Six colonies, 148 to 584 mm² after 9 weeks		584	0.17		3435				Settling plates	A	Wass & Vail 1978
Vittaticella sp	Lizard Island, Queensland, Australia	Erect flexible articulated	4cm wide, 3.5 cm tall in 3 months	350		0.25	1400					Settling plates	A	Wass et al., 1981
Zoobotryon pellucidus	Kaneohe Bay, Hawaii	Erect flexible branching	5mm in 56 days				33					Settling plates	A	Edmondson & Ingram 1939

	Max observed size (height or radius in mm)	Max observed area (in mm²)	Max age (y)	Growth rate (extension in mm/y)	Growth rate (area in mm²/y)	Calcimass (wt% skeleton)	Calcification rate (mg CaCO₃/y)	Calcification per zooid (mg CaCO₃/zz)
Mean	114	4229	13	87	20988	85	1499	0.45
Min	2	97	0.12	0.05	44	0.38	9	0.13
Max	1000	23400	86	1400	193235	230	23700	1.03
Range	998	23303	85.88	1399.95	193191	229.62	23691	0.9
StdDev	196	6288	16	245	43897	92	5247	0.41
N	28	20	42	54	19	4	20	3

List above = 89
duplicates = 5
So N species = 84

Coral-bryozoan associations through the fossil record: glimpses of a rare interaction?

Juan Luis Suárez Andrés[1]*, Consuelo Sendino[2] and Mark A. Wilson[3]

[1] SONINGEO, S.L. Avenida La Cerrada, 10. 39600 Maliaño,
Spain [*corresponding author: e-mail: juanl_suarez@yahoo.es]
[2] Natural History Museum, Cromwell Road, South Kensington, SW7 5BD, London, UK
[3] Department of Earth Sciences, The College of Wooster, Wooster, OH 44691, USA

ABSTRACT

The purpose of this paper is to document patterns of coral-bryozoan associations through the fossil record. A recently discovered rugosan-bryozoan symbiotic intergrowth from the Lower Devonian of Spain is compared with previously reported associations between bryozoans and corals from the Upper Ordovician of Estonia and the USA, and from the Neogene of Western Europe. Cases are exceptional and scattered throughout the fossil record. Available data suggest that some degree of specificity was common and that there is no evidence of negative effects for the partners. Corals allegedly benefitted from a stable substrate and food supply from the bryozoan feeding currents, while the latter received additional protection against predators. The associations originated by settlement of coral larvae on living bryozoan colonies that bioclaustrated (bryoimmured) the growing infester, and were facultative for both partners even for the Neogene *Culicia-Celleporaria* association, in which the coral rarely occurs apart from the bryozoan. This case shows high integration between partners in contrast with the Palaeozoic associations, particularly those in the Ordovician. It is not possible to determine which factors caused coral-bryozoan associations to be extremely rare, but anti-biofouling mechanisms may have played a role in preventing larval settlement on living bryozoan colonies.

INTRODUCTION

Bryozoans are present in the fossil record since the Ordovician, being a widespread, occasionally abundant component of fossil faunas. This fact, along with their modular nature, provides good scope for studies regarding the palaeoecology and palaeobiology of the group. Nevertheless, possibly one of the most interesting subjects within this field, which is the development of symbiotic associations with other organisms, remains largely unknown. It is difficult to assess the occurrence and nature of fossil associations, and mutualism cannot be fully demonstrated (Cadée and McKinney 1994). Skeletal remains are the only available specimens for study and few data can be reasonably deducted from them, which is, of course, a major hampering factor. Besides, it is well known that the fossil record is not only incomplete in the representation of lifeforms, but also strongly discontinuous in terms of chronological record.

Studies focused on symbiosis in fossil bryozoans have been carried out mostly in the last three decades, with a seemingly increasing interest during the last one. Palmer and Wilson (1988) were the first to report a peculiar case of pseudoborings from the Ordovician of the USA as a case of symbiosis between trepostome bryozoans and a soft-bodied infester; the authors introduced the term 'bioclaustration' and named the tubular structure

Catellocaula, treating it as a new ichnogenus. Later, Suárez Andrés (1999), McKinney (2009) and Suárez Andrés (2014) described a bioclaustration structure present in fenestrate bryozoans, which was interpreted as the result of interaction between the bryozoan host and a soft-bodied symbiont, possibly a hydroid. Ernst *et al.* (2014) introduced a new species of the ichnogenus *Chaetosalpinx* developed in a new genus of Devonian bryozoans from Germany. Much attention has been paid to the symbiotic associations present in the Upper Ordovician successions of Estonia (Vinn and Wilson 2015; Vinn *et al.* 2016; 2017; 2018a; b; c; 2019). Wilson *et al.* (2019) defined the term 'bryoimmuration' to stress the important role of bryozoans involved in bioimmuration in the preservation of aragonitic faunas.

Symbiotic associations between bryozoans and corals are known only from the Late Ordovician of Estonia and the USA, and from the Neogene of Western Europe, while Sendino *et al.* (2019) reported a case from the Early Devonian of Spain. Elias (1982) and MacAuley and Elias (1990) described intergrowth between rugose corals and unidentified bryozoans from the latest Ordovician of the USA. Several cases of bioclaustration and symbiosis in bryozoans have been reported recently from the Ordovician of Estonia (Vinn *et al.* 2014; 2018a); specifically, Vinn *et al.* (2016; 2017; 2018c) have described intergrowths between encrusting bryozoans and rugose corals.

Cadée and McKinney (1994) carried out a detailed study on the association between the bryozoan *Celleporaria palmata* (Michelin, 1847) and the scleractinian coral *Culicia parasitica* (Michelin, 1847) from the Neogene of Western Europe. This case has been known since the 19th century (Michelin 1847 p. 325), but the nature of the association had only been subject to brief analyses (Buge 1952; 1957; Pouyet 1978; Darrell and Taylor 1993; Taylor 2015).

The study of material sampled during 2017 from the Devonian outcrop of Arnao, along with specimens belonging to the collections of the University of Oviedo, has led to the identification of an association between cystoporate bryozoans and rugose corals (Sendino *et al.* 2019). The present paper discusses the similarities and differences of this case as compared to the previously described Ordovician and Neogene coral-bryozoan associations.

GEOLOGICAL SETTING

The geographical and geological settings of the Ordovician associations have been described in detail by Elias (1982), MacAuley and Elias (1990), Vinn *et al.* (2016; 2017; 2018) and that of the Neogene case by Cadée and McKinney (1994 and references therein), and will not be repeated here. The Devonian specimens interpreted as representatives of a rugose-coral-bryozoan association (Sendino *et al.* 2019) were collected at an outcrop of the Aguión Formation between La Vela Cape and the western end of Arnao Beach (Fig. 1), close to the locality of Arnao (Asturias, NW Spain). This outcrop is due to an old quarry in which a strongly tectonized Devonian succession is in thrust contact with a Stephanian (Carboniferous) coal-bearing series. García-Alcalde (1992) carried out a detailed stratigraphic and structural study of this area; an updated scheme of the Cantabrian Zone, the tectonostratigraphic unit in which it is included, was presented by Fernández-Martínez (2015). The Devonian beds exposed in this outcrop of Arnao represent an incomplete section of the Upper Emsian (Lower Devonian) Aguión Formation, comprising crinoidal and reefal limestones, grey shales and red and green marls, differentiated by Arbizu *et al.* (1993) as informal units. The palaeontological content of the Aguión Formation includes a very abundant and diverse benthic fauna including rugose and tabulate corals, brachiopods, echinoderms, and bryozoans as the most common groups. The faunal composition of the Aguión Formation at Arnao was briefly summarized by Suárez Andrés *et al.* (2015). The specimens collected by the senior author of this paper in 2017, as well as those housed at the Department of Geology, University

of Oviedo, were derived from the red and green marls subunit (Arbizu *et al.* 1993), which is a 24 m thick succession dominated by highly fossiliferous marls with sparse red to yellowish limestones. Crinoids, bryozoans and brachiopods are the most abundant components of these beds; the bryozoan fauna is extraordinarily rich and diverse, including representatives of very unusual fenestrate growth forms (Suárez Andrés and McKinney 2010; Suárez Andrés and Wyse Jackson 2014).

MATERIAL AND METHODS

Ordovician coral-bryozoan associations from Estonia and the USA were studied on the basis of existing literature and additional images taken by Gennadi Baranov (Tallin University of Technology) and provided by Olev Vinn (University of Tartu) for the Estonian cases, and Mark Florence and Kathy A.

Hollis (Smithsonian Institution, Washington, DC). The Neogene association between *Celleporaria palmata* and *Culicia* was analysed through previous studies and direct observation of specimens housed at the Natural History Museum (NHM), London.

The description of the Devonian coral-bryozoan association is based on 12 specimens from the Emsian Aguión Formation at Arnao, Asturias (NW Spain). Three specimens are housed at the Department of Geology, University of Oviedo (Accession numbers: DGO 12902, DGO 12903, DGO 13408). Nine more specimens were collected at the outcrop in 2017 under the terms of permits granted by national and regional institutions and will be deposited at the Museo de la Mina de Arnao (Accession numbers: MMAGE0032, MMAGE0033, MMAGE0036, MMAGE0037, MMAGE0038, MMAGE0048, MMAGE0049, MMAGE0051, MMAGE0052). The following criteria were applied in order to sample exclusively
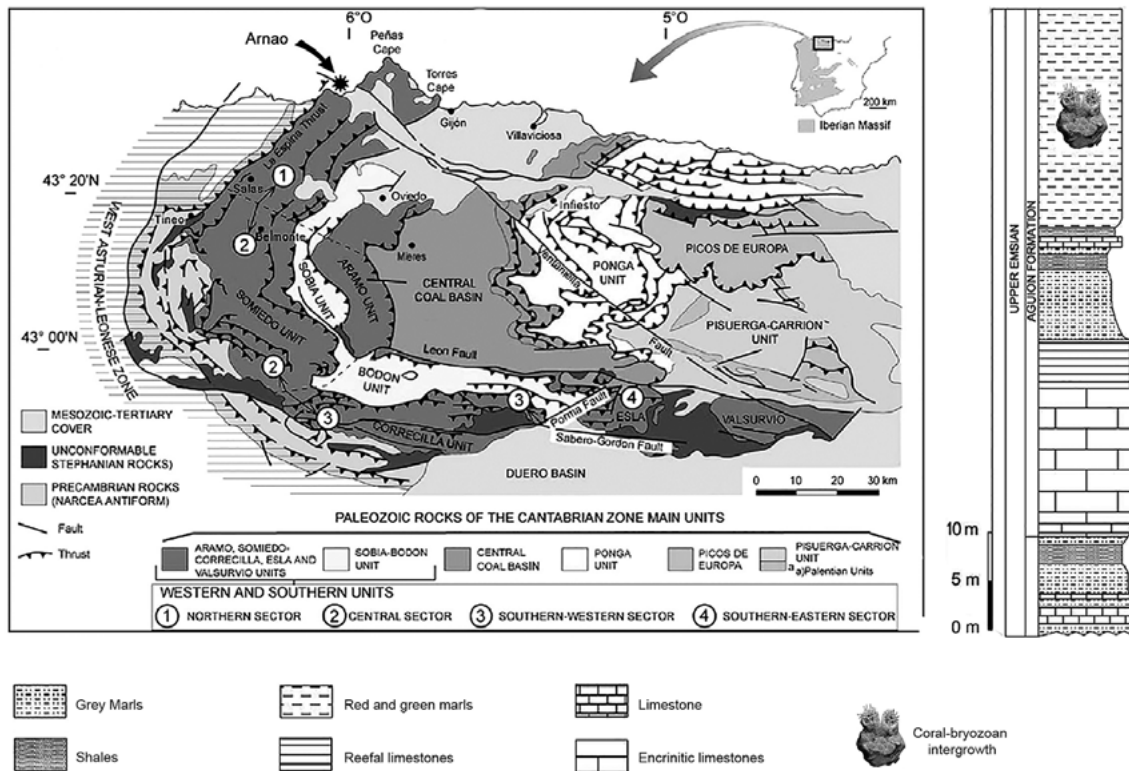

Figure 1. Location and geological scheme of the Arnao outcrop with stratigraphic section of the Lower Devonian Aguión Formation, modified after Pérez-Estaún *et al.* (2004) and Arbizu *et al.* (1993).

material representing symbiotic interaction between rugose corals and bryozoans: i) Overgrowth of rugose corals by bryozoans is extensive and embraces most or all of the surface of the epitheca, but not the calyx, therefore it can be interpreted that the coral was alive during encrustation. ii) The general growth direction of the bryozoan colony roughly parallels that of the encrusted rugose coral. iii) Initial stages of the association are interpreted as such only if the rugose coral is attached to the surface of the bryozoan colony and there is evidence of interaction, i.e. commencement of encrustation of the coral by the bryozoan, so it can be stated that the latter was a living substrate.

Specimens from the Arnao outcrop may preserve superficial structures but are strongly recrystallized, partial dolomitization being also present, so some internal characters and microstructural details are usually obscured or vanished. Acetate peels and polished sections were prepared from seven specimens, while the rest have been preserved uncut to show surface characters.

PREVIOUSLY REPORTED CASES
Ordovician associations

Ordovician coral-bryozoan associations were first reported by Elias (1982) and MacAuley and Elias (1990) from the latest Ordovician of the USA, but these works were strictly focused on rugose corals. The rugose coral *Streptelasma divaricans* (Nicholson, 1875) is an epifaunal species present in low energy carbonate and shaly facies of the Richmond Group in the Cincinnati Arch region; 68% of 59 specimens preserved attached to their substrate grew on encrusting or branching bryozoans. Coral larvae must have settled rather frequently on living bryozoan colonies, as indicated by subsequent overgrowth by the host and less commonly by abnormal growth of septa possibly due to host-infester interaction (Elias 1982, p. 23). The author did not provide identification or descriptions of bryozoan hosts. *S. divaricans* is a small coral largely represented by solitary specimens less than 20 mm

long. Elias (1982) cited previous studies suggesting that *S. divaricans* attached on brachiopods could have taken advantage of feeding currents generated by the latter but no comments were made on the possible interaction with living bryozoan hosts. Bryozoans were the most common substrate according to the data provided by the author. It seems likely that *S. divaricans* not only benefited from attachment on stable, rigid elements, but also from their colony-wide feeding currents.

MacAuley and Elias (1990) described the rugosan species *Streptelasma* sp. A from the Late Ordovician Noix Limestone, Missouri. This unit represents a shallow, high energy carbonate deposit. According to the authors, *Streptelasma* sp. A is based on three tiny epizoic specimens less than 3 mm in diameter, bioclaustrated by a single, unidentified bryozoan colony (Fig. 2A). Observation of photographs of thin sections provided by the Smithsonian Institution allowed for the recognition of zooecial characters that place the bryozoan host within the cystoporates. Corals initially grew subparallel and subsequently perpendicular to the bryozoan colony surface, and the calyxes are not regularly spaced. No observations regarding interaction between the rugose corals and their living substrate were reported by the authors, except that the bryozoan host eventually grew around the corallites.

Three cases of rugose coral-bryozoan intergrowth have been described from the Katian (Late Ordovician) of Estonia. Vinn *et al.* (2016) reported two roughly discoidal bryozoan colonies from the marly limestones of the Kõrgessaare Formation, Hiiumaa Island, embedding up to 13 rugosan endosymbionts that show different stages of growth and embedment. The calyxes of some corals are flush with the bryozoan colony surface. These specimens belong to the collection of the Institute of Geology, Tallinn University of Technology (GIT), from the type locality of this unit, which is composed of 113 bryozoan colonies and 320 rugosans. Both bryozoan colonies have been identified as the cystoporate *Ceramopora intercellata* Bassler, 1911 and the rugose corals as *Lambelasma* sp. and *Bodophyllum* sp. (Fig.

2B); other genera of corals and bryozoans are also represented in the collection. The components of this association also occur independently, and the relationship between them has been interpreted as an accidental, facultative mutualistic symbiosis on the basis of the lack of malformations in the bryozoan hosts (Vinn *et al.* 2016).

Vinn *et al.* (2017) described a single colony of the hemispherical trepostome bryozoan *Stigmatella massalis* Bassler, 1911 from the Katian argillaceous limestones and marls of the Hirmuse Formation, intergrown *syn vivo* with two large specimens of the rugose coral *Lambelasma* sp. The authors remark on the uniqueness of such intergrowth within a collection of hundreds of bryozoan specimens. This association occurred earlier in the Katian than the one reported by Vinn *et al.* (2016); the diameter of the coral calyxes is more than half the diameter of the bryozoan colony, and their embedment is only partial. Despite the large size of the corals, there is no evident malformation or damage caused to the host. Vinn *et al.* (2017, p. 148) suggested that this intergrowth was accidental, the corals growing on the bryozoan as a non-specific substrate, and that the lack of similar cases among the abundant specimens studied might have been due to the occurrence of anti-biofouling agents in bryozoan colonies.

Vinn *et al.* (2018c) reported the earliest known coral-bryozoan association from the early Katian Vasalemma Formation of northern Estonia. This unit is composed of biodetrital limestones with intercalated reef bodies. Only one specimen within a collection of about 300 bryozoan colonies was found to host rugose coral symbionts. The bryozoan colony has been assigned to the trepostome species *Orbignyella germana* Bassler, 1911 and the two symbiotic rugosans to *Lambelasma carinatum* Weyer, 1993. The corals are different in size, the largest being 13.5 mm wide at the calyx; the bryozoan colony is 22 mm in diameter. Encrustation of the symbionts by the host is complete, the calyxes of both corals are even with the bryozoan surface. The morphology of the coralla and the growth features of the bryozoan colony, as observed in thin sections,

clearly support *syn vivo* intergrowth. The association was characterized by the authors as accidental, as the previous cases reported from Estonia.

Neogene association

An association represented by specimens of the scleractinian genus *Culicia* bioclaustrated by the bryozoan *Celleporaria palmata* is known to occur in the Miocene and Pliocene of NW Europe, the Mediterranean and N Africa (Cadée and McKinney 1994; Chaix and Cahuzac 2005). This association is highly specific and facultative but occurrence of *Culicia parasitica* corals alone is exceptional (Chaix and Cauzac 2005). According to Cadée and McKinney (1994), bryozoan colonies reach similar sizes either with or without associated corals but the former show less or no maculae, corals being roughly similar in diameter and spacing to maculae in non-infested bryozoan colonies. A single bryozoan colony may be a host to several coral individuals; growth of host and infester was balanced and corallites are flush with the bryozoan colony surface. The association clearly benefitted the corals mostly by providing a stable substrate and food supply; it is not so clear if it was also beneficial for the bryozoan hosts, but the potential negative effects were probably weak, as deduced from the comparative study of symbiotic and non-symbiotic colonies of *Celleporaria* (Cadée and McKinney 1994).

Other associations might have occurred during the Neogene, but have not been described. Di Martino and Taylor (2014, 2015) reported a diverse bryofauna from the Miocene of Kalimantan, Indonesia, in which several species grew on corals; the authors focused on taxonomy and did not assess any possible interaction between bryozoans and their substrates.

DEVONIAN RUGOSE CORAL-CYSTOPORATE BRYOZOAN ASSOCIATION

Sendino *et al.* (2019) first reported the occurrence of rugose corals intergrown with bryozoans from the Emsian (Lower Devonian) of Asturias, NW

Spain. The association has been described and interpreted (Sendino *et al.* 2019). The host bryozoans correspond to species of the cystoporate genera *Altshedata* Morozova, 1959 and *Fistuliporidra* Simpson, 1897; the bioclaustrated corals cannot be identified due to the simplified internal structures (Fig. 2C; Berkowski, May, Schroeder, pers. comm.), which might be a consequence of symbiotic growth (Berkowski, pers. comm.). Twelve specimens of bryozoans hosting symbiotic rugosans have been found in a single outcrop; six can be assigned to *Altshedata* and six to *Fistuliporidra*. The association is facultative for both bryozoan genera. Despite the abundance of benthic fauna (other bryozoans, brachiopods, crinoids, tabulate corals), the rugose corals have not been observed isolated from their hosts. The morphology of symbiotic colonies may be massive or branching. The size and distribution of rugose corals is neither regular nor similar to those of normal maculae of bryozoan colonies. A few specimens represent initial stages of the association in which immature corals attached to living bryozoan colonies show a recumbent morphology and are only partially bryoimmured by their host (Fig. 2D, MMAGE0037, MMAGE0038; Sendino *et al.* 2019). Most specimens show full encrustation of the epithecae and calyxes flush with the bryozoan colony surface (Fig. 2E). Corals must have benefitted from a steady substrate in a muddy, soft-bottom environment, and from mud clearing and food supply provided by the zooid-generated feeding currents. The bryozoan hosts may have gained protection against predators as well as a suitable substrate to reach higher tiers in turn. Nevertheless, it cannot be stated that the coral symbionts improved fitness of their hosts.

DISCUSSION

Cadée and McKinney (1994) stated in their description of a Neogene coral-bryozoan association that "conspicuous, preferential association between two species in the fossil record is often difficult to interpret. The type of association depends upon the net costs and benefits to the individuals of the species involved, but such effects are best determined as an increase or decrease in fitness, which cannot be determined – and only rarely confidently inferred – from fossils". Upon acceptance of the limitations imposed by the fossil record and particularly by the studied material, similarities and differences among the reported coral-bryozoan associations extracted from compared analyses allow for some interpretation.

One of the similarities among the associations is the mode of development of the intergrowth: coral larvae attached to the surface of a living bryozoan colony that bryoimmured the growing infesters; a single bryozoan colony may host several corals and calyxes may be elevated over the bryozoan surface or flush (Fig. 2B, D-F). Individual symbiotic corals occasionally died and the host overgrew their calyxes *post mortem*.

The interpretation of benefits and negative effects for hosts and infesters is also very similar for all described associations. Hypothetically, benefits for the corals include a stable substrate, additional protection of corallites and food supply by means of the feeding currents generated by the bryozoans. The only evident negative effect for the coral would be being overgrown by the host, but this is not such if it occurred only over dead corallites. The bryozoan hosts would benefit from the protection provided by the stinging cells of the corals and perhaps reaching higher tiers over the sediment surface; the space occupied by the corals on the bryozoan surface has been interpreted as a factor inducing either beneficial or negative effects (Cadée and McKinney 1994). Berkowski and Zapalski (2018) described cystiphyllid corals from the Silurian of Gotland that settled on living colonies of the tabulate *Halysites* and killed the surrounding polyps to expand. Bryozoan colonies that hosted coral symbionts encrusted their epithecae without suffering any damage that could be evidenced by abnormal growth of their skeleton.

Specificity is possibly a common factor for fossil coral-bryozoan associations, but impossible
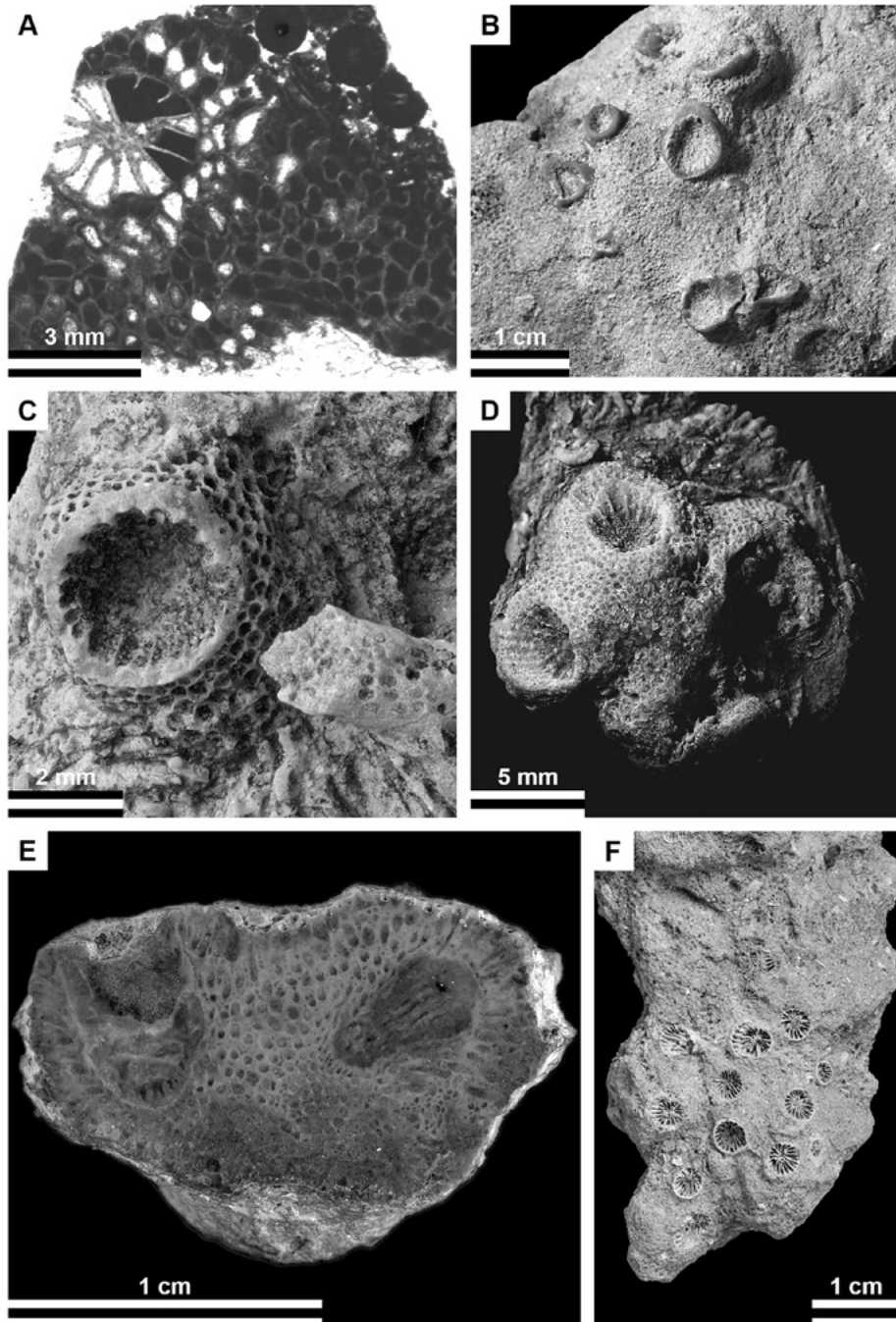
Figure 2. (A) Rugose coral *Streptelasma* sp. A bioclaustrated by a cystoporate bryozoan. USNM-PAL-423412. Gamachian (Uppermost Ordovician), Noix Limestone, NE Missouri, USA. (B) *Ceramopora intercellata* colony with multiple partially embedded rugosans Bodophyllum sp. GIT 666-22. Katian (Upper Ordovician), Kõrgessaare Formation,Hiiumaa Island, NW Estonia. (C) Rugose coral-*Fistuliporidra* sp. MMAGE0051. Emsian (Lower Devonian), Aguión Formation. Arnao, Asturias, NW Spain. (D) Rugose coral-*Fistuliporidra* sp. DGO 12902. Emsian (Lower Devonian), Aguión Formation. Arnao, Asturias, NW Spain. (E) Rugose coral-*Fistuliporidra* sp. MMAGE0033. Emsian (Lower Devonian), Aguión Formation. Arnao, Asturias, NW Spain. (F) *Culicia-Celleporaria palmata* association. NHMUK PI BZ 8774-011. Lower Pliocene, Coralline Crag, Ramsholt Member, Suffolk, UK.

to assess with our present knowledge, because factors such as scarcity and preservation of specimens as well as few taxonomic data prevent confident evaluation. A high specificity has been clearly stated only for the *Culicia parasitica-Cellepora palmata* case (Cadée and McKinney 1994); the Ordovician associations described from Estonia have been identified at the species level for bryozoans and at least at the genus level for corals, but two of the three associations are represented by a single specimen. Nevertheless, the rugosan *Lambelasma* Weyer, 1973 has been identified in all specimens. Bryozoan taxonomy of Ordovician coral-bryozoan intergrowths from the USA reported by Elias (1982) and MacAuley and Elias (1990) is not known, but in all cases the rugosan symbiont belong to the genus *Streptelasma* Hall, 1847. The Devonian coral-bryozoan association from Spain is host-specific; the rugose corals cannot be identified due to the short development of diagnostic characters, and the bryozoans have been assigned to two genera. The symbiont corals have only been observed in intergrowth with *Fistuliporidra* and *Altshedata* within a rich assemblage of diverse bryozoans and other organisms, so it can be assumed that the association was specific, though possibly not at the species level.

Beyond the systematic position of the components, perhaps the most striking difference among the fossil coral-bryozoan associations is the apparent frequency of specimens. Most Ordovician cases are represented by one or very few specimens, except for *Streptelasma divaricans*, which preferred living bryozoans to other substrates (Elias 1982). It cannot be stated that the Devonian association represents an obliged symbiosis, but the number of specimens and host specificity seem to indicate that it was infrequent but not accidental. *Culicia parasitica* has long been considered as a strict symbiont of *Celleporaria palmata* present in Neogene deposits of several countries in Europe and only recent works reported rare occurrences of this species alone (Chaix and Cahuzac 2005). This association also shows a remarkably higher degree of integration/

organization between symbiont and host than the Palaeozoic ones.

Despite the interpreted mutual benefits, coral-bryozoan associations are extremely scarce in the fossil record, commonly facultative and with a low degree of integration of symbiont corals in the functional morphology of their bryozoan hosts. The causes for this scarcity can only be speculated, but the ability of bryozoans to defend from encrustation must have played a significant role. Palaeozoic bryozoans are supposed to have developed colony-wide currents similar to those generated by living forms (Banta *et al.* 1974); in the absence of other mechanical or chemical defences, these currents may have prevented settlement of coral larvae by driving them off the colonies with exhalent flow. Laboratory studies demonstrated that bryozoan feeding currents are capable of cleaning sediment from the colony surface (Cook 1977); Taylor (1979) suggested that this ability would be particularly valuable for colonies living in low-energy environments such as those representing the Palaeozoic associations discussed herein. Palaeozoic bryozoans may have also possessed chemical defences that could have deterred fouling; such ability is known to occur in living bryozoans, and the presence of metabolites active in antifouling has been proved to be common among Antarctic species (Figuerola *et al.* 2014). Several authors reported the negative influence of bryozoan colonies in coral recruitment in Recent assemblages from the Central Pacific (Elmer 2016; Elmer *et al.* 2016), the Great Barrier Reef (Dunstan and Johnson 1998) and the Red Sea (Glassom *et al.* 2004).

Recent faunas also show that some species are not sensitive to antifouling mechanisms of bryozoans; Lombardi and Schiaparelli (2018) reported tannaid crustaceans symbiotic with an Antarctic bryozoan host with active antifouling and antipredatory metabolites. The hydroid family Zancleidae embraces three genera and 42 species, most of which live exclusively as symbionts of other organisms; all the species of *Zanclella* and *Halocoryne* as well as some of *Zanclea* are host-specific and symbiotic with encrusting bryozoans (Maggioni *et al.* 2018). The bryozoan hosts

bryoimmure the hydroids, which become a defensive resource. Osman and Haugsness (1981) reported that colonies of *Celleporaria brunea* bearing *Zanclea* were more successful in overgrowth interactions and deterring predation than colonies without symbiont hydroids. Bock and Cook (2004, p. 137, figs. 1D, 2F) reported and figured an association from Australia in which rooted colonies of *Conescharellina* host minute solitary corals, which in most cases grow on the antapical surface of the conical colonies. The authors concluded that the balanced growth of both organisms might be mutually advantageous and that the settlement of corals was probably controlled by the size and distribution of avicularia.

Thus, it can be speculated that the coral-bryozoan intergrowths found in the fossil record may have been propitiated by the tolerance of specific infesters to the antifouling mechanisms of their hosts, which in many cases allowed for accidental interactions only, but exceptionally gave rise to well-developed, highly specific symbiosis. The *Culicia-Celleporaria* intergrowth (Fig. 1F) is not the only case of bryozoans developing a well-stablished association with a bioclaustrated macrosymbiont in the fossil record: Palmer and Wilson (1988) first described Ordovician bryozoans hosting a soft-bodied symbiont. During the Devonian, five fenestrate bryozoan genera developed bioclaustration structures attributed to a symbiont, possibly a hydroid (Suárez Andrés 2014). The association was facultative for the bryozoan hosts. Symbiotic specimens occur in the Devonian of Belgium, Germany and Spain, and similar structures were reported in a Carboniferous fenestrate species from the USA, indicating that this association was neither local nor exceptional.

CONCLUSIONS

Despite corals and bryozoans being common, widespread components of benthic faunas, their intergrowths are rare in the fossil record. Cases have only been reported from Ordovician, Devonian and Neogene strata.

Intergrowths developed by settlement of coral larvae on living bryozoan colonies that bryoimmured the infesters as they grew. Alleged benefits for hosts and infesters are similar in all cases and there is no unequivocal evidence of damage to the partners.

Most Palaeozoic associations are accidental and represented by very few specimens. Only in the Neogene *Culicia-Celleporaria* association do the coral symbionts show a high integration with their bryozoan hosts. All reported associations are facultative for the bryozoans, and also for corals in the Ordovician intergrowths. Coral symbionts are not known to occur isolated in the Devonian case, and *Culicia parasitica* very rarely occurred alone.

Scarcity of intergrowth cases between bryozoans and bioclaustrated symbionts in the fossil record may be due to antifouling mechanisms preventing or hampering settlement and growth of epibionts on living bryozoan colonies. Coral-bryozoan associations were possibly propitiated by specific infesters overcoming the defences of their hosts.

University), Andreas May (independent, Germany) and Stefan Schröder (Universität zu Köln, retired) for their comments on rugose coral taxonomy, and Philip Bock (Museum Victoria, Melbourne) for highlighting the Recent scleractinian-*Conescharellina* associations from Australia. Hans Arne Nakrem (Natural History Museum, Oslo), Patrick N. Wyse Jackson (Trinity College, Dublin) and Kamil Zagorsek (Technical University, Liberec) are gratefully acknowledged for their constructive reviews which improved the manuscript.

REFERENCES

ARBIZU, M., ÁLVAREZ-NAVA, H., MÉNDEZ-BEDIA, I. AND GARCÍA-LÓPEZ, S. 1993. Las comunidades bióticas de las "Capas con *Trybliocrinus*" (Devónico Inferior) en la Plataforma de Arnao (Asturias, Noroeste de España). *Revista Española de Paleontología*, nº extr., 71–77.

BANTA, W.C., MCKINNEY, F.K. AND ZIMMER, R.L. 1974. Bryozoan monticules: excurrent water outlets? *Science* **185**, 783–784.

BASSLER, R.S. 1911. The early Paleozoic Bryozoa of the Baltic provinces. *Bulletin of the United States National Museum* **77**, 382 pp.

BERKOWSKI, B. AND ZAPALSKI, M.K. 2018. Large dwellers of the Silurian *Halysites* biostrome: rhizosessile life strategies of cystiphyllid rugose corals from the Llandovery of Gotland. *Lethaia* **51**, 581–595.

BOCK, P.E. AND COOK, P.L. 2004. A review of Australian Conescharellinidae (Bryozoa; Cheilostomata). *Memoirs of Museum Victoria* **61**(2), 135–182.

BUGE, E. 1952. Bryozoaires. In: J. Piveteau (ed.), *Traité de Paléontologie* **1**, 688–749.

BUGE, E. 1957. Les bryozoaires du Néogène de l'Ouest de la France. *Mémoires du Muséum National d'Histoire Naturelle (N.S.)* **6**, 1–435.

CADÉE, G.C. AND MCKINNEY, F. K. 1994. A coral-bryozoan association from the Neogene of northwestern Europe. *Lethaia* **27**, 59–66.

CHAIX, C. AND CAHUZAC, B. 2005. Le genre *Culicia* (Scléractiniaire): systématique, écologie et biogéographie au Cénozoïque. *Eclogae Geologicae Helvetiae* **98**, 169–187.

COOK, P.L. 1977. Colony-wide water currents in living Bryozoa. *Cahiers de Biologie Marine* **18**, 31–47.

DARRELL, J. G. AND TAYLOR, P.D. 1993. Macrosymbiosis in corals: a review of fossil and potentially fossilizable examples. *Courier Forschungsinstitut Senckenberg* **164**, 185–198.

DI MARTINO, E. AND TAYLOR, P.D. 2014. Miocene Bryozoa from East Kalimantan, Indonesia. Part I: Cyclostomata and 'Anascan' Cheilostomata. *Scripta Geologica* **146**, 17–126.

DI MARTINO, E. AND TAYLOR, P.D. 2015. Miocene Bryozoa from East Kalimantan, Indonesia. Part II: Cyclostomata and 'Ascophoran' Cheilostomata. *Scripta Geologica* **148**, 1–142.

DUNSTAN, P.K. AND JOHNSON, C.R. 1998. Spatio-temporal variation in coral recruitment at different scales on Heron Reef, southern Great Barrier Reef. *Coral Reefs* **17**, 71–81.

ELIAS, R.J. 1982. Latest Ordovician solitary rugose corals of eastern North America. *Bulletins of American Paleontology* **81**, 116 pp.

ELMER, F. 2016. *Factors affecting coral recruitment and calcium carbonate accretion rates on a Central Pacific coral reef.* Unpublished PhD thesis, Victoria University of Wellington/Te Whare Wānanga o te Ūpoko o te Ika a Māui, 225 pp.

ELMER, F., ROGERS, J.S., DUNBAR, R.B., MONISMITH, S.G., BELL, J.J. AND GARDNER, P.A. 2016. Influence of localised currents, benthic community cover and composition on coral recruitment: integrating field-based observations and physical oceanographic modelling. *Proceedings of the 13th International Coral Reef Symposium*, Honolulu, pp. 101–142.

ERNST. A., TAYLOR, P.D. AND BOHATY, J. 2014. A new Middle Devonian cystoporate bryozoan from Germany containing a new symbiont bioclaustration. *Acta Palaeontologica Polonica* **59,** 173 –183.

FERNÁNDEZ MARTÍNEZ, E. 2015. Palaeozoic from the Cantabrian Zone. In: S. Zamora (coord.), J.J. Álvaro, M. Arbizu, J. Colmenar, J. Esteve, E. Fernández-Martínez, L.P. Fernández, J.C. Gutiérrez-Marco, J.L. Suárez-Andrés, E. Villas and J. Waters. *Field Trip: Palaeozoic Echinoderms from Northern Spain*. In: S. Zamora and I. Rábano (eds), *Progress in Echinoderm Palaeobiology. Cuadernos del Museo Geominero*, **19**. Madrid, Instituto Geológico y Minero de España, pp. 247–248.

FIGUEROLA, B., NÚÑEZ-PONS, L., MONLEÓN-GETINO, T. AND AVILA, C. 2014. Chemo-ecological interactions in Antarctic bryozoans. *Polar Biology* **37**, 1017–1030.

GARCÍA-ALCALDE, J.L. 1992. El Devónico de Santa María del Mar (Castrillón, Asturias, España). *Revista Española de Paleontología* **7**, 53–79.

GLASSOM, D., ZAKAI, D. AND CHADWICK-FURMAN, N.E. 2004. Coral recruitment: a spatio-temporal analysis along the coastline of Eilat, northern Red Sea. *Marine Biology* **144**, 641–651.

HALL, J. 1847. *Palaeontology of New York, I: Containing descriptions of the organic remains of the Lower Division of the New York System (Equivalent to the Lower Silurian rocks of Europe).* Albany, New York, 1–338.

LOMBARDI, C. AND SCHIAPARELLI, S. 2018. Life hanging on a bryozoan: an example of symbiosis from Antarctica. *Proceedings of the 15th Larwood Meeting, 6 – 8 June 2018, Amgueddfa Cymru–National Museum Wales, Cardiff.*

MACAULEY, R.J. AND ELIAS, R.J. 1990. Latest Ordovician to earliest Silurian solitary rugose corals of the east-central United States. *Bulletins of American Paleontology* **98**, 82 pp.

MCKINNEY, F.K. 2009. Bryozoan-hydroid symbiosis and a new ichnogenus, *Caupokeras. Ichnos* **16**, 193–201.

MAGGIONI, D., ARRIGONI, R., GALLI, P., BERUMEN, M.L., SEVESO, D. AND MONTANO, S. 2018. Polyphyly of the genus *Zanclea* and family Zancleidae (Hydrozoa, Capitata) revealed by the integrative analysis of two bryozoan-associated species. *Contributions to Zoology* **87(2)**, 87–104.

MICHELIN, H. 1847. *Iconographie Zoophytologique.* Paris, Bertrand, 348 pp.

MOROZOVA, I.P. 1959. New genus of the Family Fistuliporidae in Devonian in Kuznets Basin. *Trudy Paleontologicheskogo Instituta Akademii Nauk SSSR* **2**, 79–81.

NICHOLSON, H.A. 1875. Description of the corals of the Silurian and Devonian Systems. *Ohio Geological Survey Report* **2**, 181–242.

OSMAN, R.W. AND HAUGSNESS, J.A. 1981. Mutualism among sessile invertebrates. *Science* **211**, 846–848.

PALMER, T.J. AND WILSON, M.A. 1988. Parasitism of Ordovician bryozoans and the origin of pseudoborings. *Palaeontology* **31**, 939–949.

POUYET, S. 1978. L'association bryozoaires-cnidaires. *Réunion Annuelle des Sciences de la Terre*, París, **6**, 319.

PÉREZ-ESTAÚN, A., BEA, F., BASTIDA, F., MARCOS, A., MARTÍNEZ-CATALÁN, J.R., MARTÍNEZ-POYATOS, D., ARENAS, F., DÍAZ-GARCÍA, F., AZOR, A., SIMANCAS, J.F. AND GONZÁLEZ-LODEIRO, F. 2004. La cordillera Varisca Europea. El Macizo Ibérico. In: J.A. Vera (ed), *Geología de España*. Madrid, Sociedad Geológica de España-Instituto Geológico y Minero de España, pp. 19–230.

SENDINO, C., SUÁREZ ANDRÉS, J.L. AND WILSON, M.A. 2019. A rugose coral – bryozoan association from the Lower Devonian of NW Spain. *Palaeogeography, Palaeoclimatology, Palaeoecology* **530**, 271-280.

SIMPSON, G.B. 1897. A handbook of the genera of North American Paleozoic Bryozoa; with an introduction upon the structure of living species. *State Geologist of New York 14th Annual Report (1895)*, 403–669.

SUÁREZ ANDRÉS, J.L. 1999. Parasitismo en briozoos devónicos de la Zona Cantábrica. *Temas Geológico-Mineros ITGE* **26**, 647–650.

SUÁREZ ANDRÉS, J.L. 2014. Bioclaustration in Devonian fenestrate bryozoans. The ichnogenus *Caupokeras* McKinney, 2009. *Spanish Journal of Palaeontology* **29**, 5–14.

SUÁREZ ANDRÉS, J.L. AND MCKINNEY, F.K. 2010. Revision of the Devonian fenestrate bryozoan genera *Cyclopelta* Bornemann, 1884 and *Pseudoisotrypa* Prantl, 1932, with description of a rare growth habit. *Revista Española de Paleontología* **25**, 123–138.

SUÁREZ ANDRÉS, J.L. AND WYSE JACKSON, P.N. 2014. *Ernstipora mackinneyi*, a new unique fenestrate bryozoan genus and species with an encrusting growth habit from the Emsian (Devonian) of NW Spain. *Neues Jahrbuch für Geologie und Paläontologie – Abhhanlungen* **271**, 229–242.

SUÁREZ ANDRÉS, J.L, ARBIZU, M., WATERS, J. AND ZAMORA, S. 2015. Devonian echinoderms from Arnao (Asturias): clay vs. hard-ground pelmatozoan communities. In: S. Zamora, S. (coord.), J.J. Álvaro, M. Arbizu, J. Colmenar, J. Esteve, E. Fernández-Martínez, L.P. Fernández, J.C. Gutiérrez-Marco, J.L. Suárez-Andrés, E. Villas and J. Waters. *Field Trip: Palaeozoic Echinoderms from Northern Spain*. In: S. Zamora and I. Rábano (eds.), *Progress in Echinoderm Palaeobiology. Cuadernos del Museo Geominero* **19**. Madrid, Instituto Geológico y Minero de España, pp. 273–288.

TAYLOR, P.D. 1979. The inference of extrazooidal feeding currents in fossil bryozoan colonies. *Lethaia* **12**, 47–56.

TAYLOR, P.D. 2015. Differentiating parasitism and other interactions on fossilized colonial organisms. *Advances in Parasitology* **90**, 329–347.

VINN, O., ERNST, A. AND TOOM, U. 2016. Earliest symbiotic rugosans in cystoporate bryozoan *Ceramopora intercellata* Bassler, 1911 from the Late Ordovician of Estonia (Baltica). *Palaeogeography, Palaeoclimatology, Palaeoecology* **461**, 140–144.

VINN, O., ERNST, A. AND TOOM, U. 2017. Rare rugosan-bryozoan intergrowth from the Upper Ordovician of Estonia. *Carnets de Geologie* **17(7)**, 145–151.

VINN, O., ERNST, A. AND TOOM, U. 2018a. Symbiosis of cornulitids and bryozoans in the Late Ordovician of Estonia. *Palaios* **33**, 290–295.

VINN, O., ERNST, A. AND TOOM, U. 2018b. Bioclaustrations in Upper Ordovician bryozoans from northern Estonia. *Neues Jahrbuch für Geologie und Paläontologie – Abhhanlungen* **289**, 113–121.

VINN, O., ERNST, A., WILSON, M.A. AND TOOM, U. 2019. Symbiosis of conulariids with trepostome bryozoans in the Upper Ordovician of Estonia (Baltica). *Palaeogeography, Palaeoclimatology, Palaeoecology* **528**. DOI 10.1016/j.palaeo.2019.01.018

VINN, O., TOOM, U. AND ERNST, A. 2018c. Intergrowth of *Orbignyella germana* Bassler, 1911 (Bryozoa) and *Lambelasma carinatum* Weyer, 1993 (Rugosa) in the pelmatozoan-bryozoan-receptaculitid reefs from the Late Ordovician of Estonia. *Palaeontologia electronica* 1–8.

VINN, O. AND WILSON, M.A. 2015. Symbiotic interactions in the Ordovician of Baltica. *Palaeogeography, Palaeo-climatology, Palaeoecology* **436**, 58–63.

VINN, O., WILSON, M.A., MOTUS, M.A. AND TOOM, U. 2014. The earliest bryozoan parasite: Middle Ordovician (Darriwilian) of Osmussaar Island, Estonia.

Palaeogeography, Palaeoclimatology, Palaeoecology **414**, 129–132.

WEYER, D. 1973. Über den Ursprung der Calostylidae Zittel 1879 (Anthozoa Rugosa, Ordoviz-Silur). *Freiberger Forschingsheft C* **282**, 23–87.

WEYER, D. 1993. *Lambelasma carinatum*, eine neue Rugose Koralle aus dem Mittel-Ordoviz von Estland. *Abhandlungen und Berichte für Naturkunde* **16**, 70–77.

WILSON, M.A., BUTTLER, C.D. AND TAYLOR, P.D. 2019. Bryozoans as taphonomic engineers, with examples from the Upper Ordovician (Katian) of Midwestern North America. *Lethaia* **52**, 403–409.

Bryozoans from the late Jurassic–early Cretaceous Štramberk Limestone of the Czech Republic

Paul D. Taylor[1]*, Petr Skupien[2] and Kamil Zágoršek[3]

[1] Department of Earth Sciences, Natural History Museum, London SW7 5BD, UK; p.taylor@nhm.ac.uk

[2] Department of Geological Engineering, VSB-Technical University of Ostrava, 17. listopadu 15, Czech Republic; petr.skupien@vsb.cz

[3] Department of Geography, Technical University of Liberec, Studentská 2, CZ-461 17 Liberec, Czech Republic; kamil.zagorsek@gmail.com

ABSTRACT

Bryozoans are rare in the latest Jurassic and earliest Cretaceous, making it difficult to evaluate the impact on the phylum of the minor mass extinction event at the Jurassic-Cretaceous boundary. The most diverse bryozoan biota described from the Tithonian stage of the late Jurassic is from the Portland Beds of southern England and comprises six cyclostome and one cheilostome species, whereas only one bryozoan species has ever been formally described from the succeeding Berriasian stage of the Cretaceous. Therefore, the bryozoan fauna of the Štramberk Limestone, an allochthonous unit of latest Jurassic– earliest Cretaceous age, has particular importance. Bryozoans have never been formally described from this peri-reefal talus deposit outcropping in the Carpathian Outer Flysch. New research on historical material mostly in the Naturhistorisches Museum, Vienna, along with recent field collections, has revealed the presence of at least 8 cyclostome species. While the exact age of the historical material is unknown, bryozoans have been collected *in-situ* from the Early Berriasian part of the Štramberk Limestone at the Kotouč Quarry. Mediocre surface preservation hinders detailed description. However, a new species of the distinctive cyclostome *Reptoclausa* is described here as *Reptoclausa stramberkensis* sp. nov. The new genus *Rugosopora* (type species

Berenicea enstonensis Pitt and Thomas) is introduced for cyclostomes of the '*Berenicea*' type with regular transverse ribs on the colony surface.

INTRODUCTION

The fossil record of bryozoans in the latest Jurassic and earliest Cretaceous is extremely poor. Although the end of the Jurassic period marked a minor mass extinction (Hallam 1986; Hallam and Wignall 1997; Ruban 2006; Tennant *et al.* 2017), its impact – if any – on bryozoans is unclear. Little is known about the survival of Jurassic bryozoan taxa into the Cretaceous, or the origination of new taxa in the earliest Cretaceous.

The bryozoan biota of the Jurassic was reviewed by Taylor and Ernst (2008). Jurassic bryozoans are patchily distributed in time and space, with the majority of species known from the Middle Jurassic of northwestern Europe. After diversifying in the Middle Jurassic, bryozoans seemingly decreased in diversity during the Late Jurassic before radiating again in the Early Cretaceous. The occurrence of Lazarus genera that are present in the Middle Jurassic and the Early Cretaceous but unrecorded in the Late Jurassic, shows that the low diversity of bryozoans in the Late Jurassic is at least in part due to gaps in the fossil record. An apparent easterly shift in the post-Bathonian of the

carbonate-rich facies belt hosting the most diverse bryozoan assemblages from western Europe to eastern Europe (Viskova 2009), where fewer exposures are available and the bryozoan faunas have been less intensively studied, could also contribute to the Late Jurassic diversity dip. However, it is difficult to avoid the conclusion that bryozoans were indeed depauperate and relatively rare in the Late Jurassic as carbonate facies seemingly favourable to bryozoans are widespread in the Oxfordian and Kimmeridgian in many parts of western Europe. The rarity of bryozoans seems to have persisted from the Late Jurassic into the earliest Cretaceous. Berriasian bryozoans are very uncommon: only one species, a bioimmured ctenostome, has been formally described from this stage (Todd *et al.* 1997), although Walter (1997) recorded the occurrence of 16 cyclostome species in the Late Berriasian of southern France. In contrast, the succeeding Valanginian stage saw the return of richer bryozoan faunas, especially in southern Europe (e.g., Walter 1972).

The only Tithonian bryozoan fauna to have been described comprehensively comes from the Portland Beds of southern England (Taylor 1981). This fauna consists of five cyclostome and one cheilostome species, to which one additional cyclostome was recorded by Riley and Thomas (1987). Multilamellar colonies of one of the cyclostomes constructed small reefs (Fürsich *et al.* 1994). The bryozoan fauna of the Portland Beds is especially notable in containing the first accepted species of a Jurassic cheilostome bryozoan, *Pyriporopsis portlandensis* Pohowsky, 1973. Although since superseded by *P. pohowskyi* Taylor, 1994 from the Oxfordian/Kimmeridgian of the Yemen as the oldest known cheilostome, *P. portlandensis* remains remarkable for its abundance on shelly substrates in some parts of the Portland Limestone Formation.

While the Tithonian Portland Limestone represents a marginal marine deposit containing a rather low diversity of invertebrate fossils (see Townson 1975), the roughly contemporaneous Štramberk Limestone of the Czech Republic has yielded a spectacular diversity of invertebrate fossils. Over 1000 species

have been described from this limestone (Vašíček and Skupien 2005), with molluscs, brachiopods and corals being particularly common. The presence of bryozoans in the Štramberk Limestone was mentioned by Remes (1902), who listed seven species. In addition, Housa and Nekvasilova (1987) noted in a palaeoecological paper the presence of bryozoans encrusting corals and rudists from an isolated boulder of Štramberk Limestone, while Hoffmann *et al.* (2017) mentioned the occurrence of bryozoans in their paper on microencrusters, microbial frameworks and synsedimentary cements. However, the Štramberk bryozoan fauna has never been formally described. Our aim here is to describe the most abundant bryozoan in the Štramberk fauna – *Reptoclausa stramberkensis* sp. nov. – and to offer tentative identifications of the other, typically poorly preserved species present in this deposit.

GEOLOGICAL SETTING

The study area is located in the Outer Flysch Carpathians and comprises Late Jurassic to Early Miocene strata, folded and thrusted to the present position during the Middle Miocene. Deep-sea turbidite sediments prevail, but large blocks of peri-reefal and platform carbonates incorporated in the nappe structures are also present (Picha et al. 2006).

The Štramberk Limestone consists of limestone megablocks, breccias and conglomerates in the immediate vicinity of Štramberk (Fig. 1). It is exposed in several historical quarries, including Castle Hill, Kotouč, the Municipal Quarry and Horní Skalka. Kotouč is the only quarry still in operation. The limestone is a peri-reefal deposit formed during the Late Jurassic–earliest Cretaceous on the Baška-Inwald Ridge of the Peritethys, part of the North European Platform. It represents reef talus rather than the reef itself, as shown by the presence of a deeper-water, open-marine fauna (calpionellids, ammonites) and characteristic microfacies. Abundant bioclasts from coral-*Diceras* reefs, including blocks with corals in growth position, are present.

Partial destruction of the limestone through

platform collapse during the Early Cretaceous produced block accumulations within the Silesian Basin. During the Alpine orogenesis in the Miocene, the block accumulations became a part of the Silesian Nappe (Unit) and, more precisely, the Baška Sub-unit characterised by the influence of reefs as a source area.

The main studied field section is situated on the 5th level in the middle part of the Kotouč Quarry (GPS 49°35'1.3"N, 18°6'59.6"E). The section consists of stratified limestones with an average direction strike of 205° and dip of 75°, presumed to be overturned. Boundaries between individual beds are fuzzy. The occurrence of ammonite shells on bedding planes provides additional information on bedding. The limestones are coarsely to finely detritic and, less frequently, micritic.

Section B (locality 10 of Vašíček and Skupien 2016) is 17.6 m thick and has been subdivided into 22 beds with thicknesses of between 28 cm and 140 cm. The rich fauna includes corals, bivalves, gastropods, crabs, bryozoans, belemnites and ammonites. At the base of Section B (bed B22), *Pseudosubplanites grandis, P. lorioli* and *Mazenoticeras* sp. were found.
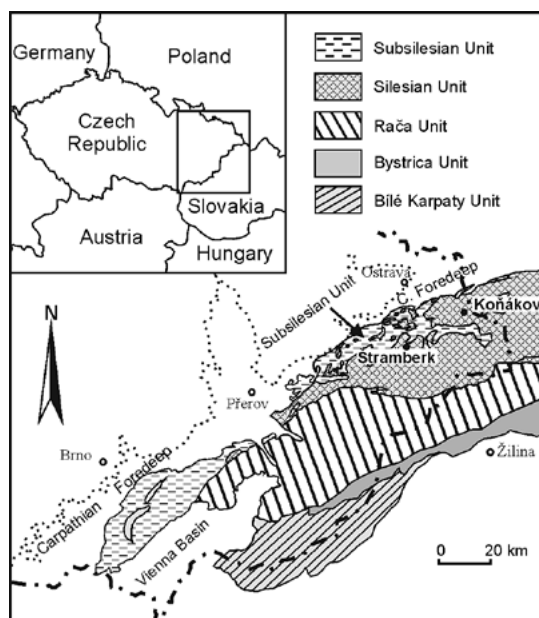

Figure 1. Tectonic map of the Outer Western Carpathian area of the Czech Republic (after Skupien and Smaržová 2011).

The number of collected specimens of *P. grandis* increased up the section. The ammonite-rich Section B can be dated to the upper part of the Early Berriasian based on the presence of *P. grandis* (Berriasella Jacobi Zone: Vašíček *et al.* 2018).

Historical material in museum collections, of which that of the Naturhistorisches Museum, Vienna (NHMV) is the most important to have been studied, seldom includes detailed stratigraphical information, and it is impossible to know whether the bryozoans present came from the Jurassic or the Cretaceous part of the Štramberk Limestone. Other studied material is in the Natural History Museum, London (NHMUK) and the Novy Jicin Museum, Czech Republic (NJM).

Bryozoan preservation and abundance

The preservation of the Štramberk bryozoans varies from moderate to poor. The most pristine Štramberk bryozoans exhibit adequate preservation of apertures and frontal walls to allow generic identification. However, even in the best specimens, the pseudopores, which have proved to be of considerable utility in cyclostome species determination (Zatoń and Taylor 2009), are either not visible or severely corroded. At the other end of the spectrum, the poorest Štramberk bryozoans are scarcely even recognizable as bryozoans – they are often corroded, obscured by diagenetic cement, or represented only by cement casts (steinkerns) of the zooidal chambers. Scanning electron microscope images are invariably disappointing.

The near-ubiquity of smeared shell surfaces – 'micro-slickensides' – raises the possibility of extensive, post-depositional loss of encrusting bryozoans, possibly in association with the tectonic displacement of the Štramberk Limestone. Additionally, some of the undersides of colonial corals that are important substrates for Štramberk bryozoans do not represent original external surfaces as adhering to them are the casts of sponge borings, showing that a bored layer of coral skeleton must have been lost, and with it any encrusting bryozoans. Nevertheless, two lines of evidence imply that bryozoans may in fact have been relatively uncommon. First, inspection of several hundred specimens of brachiopods in the NHMV,

including many of large size and with relatively pristine surface preservation, failed to reveal any encrusting bryozoans. Elsewhere in the Mesozoic brachiopods constitute one of the commonest substrates for bryozoan encrustation (e.g., Brookfield 1973). Secondly, the rarity of bryozoans on the surfaces of mollusc steinkerns is in marked contrast to the Tithonian Portland Limestone of England where undersides of colonies that encrusted the insides of dissolved aragonitic bivalve and gastropod shells are commonly visible. Štramberk mollusc steinkerns seldom reveal bryozoans (cf. Fig. 2), even though these internal surfaces would have been relatively protected from the micro-slickensiding that is believed to have affected the external surfaces of Štramberk fossils, and probably did not suffer the loss of surface layers inferred above for some of the corals. In contrast, the undersides of serpulid and tubeworms are commonly visible on Štramberk steinkerns, demonstrating that shell interiors (mostly of gastropods and ammonites) were routinely colonized by sclerobionts other than bryozoans.

Some pre-depositional loss of encrusting bryozoans and other sclerobionts may have occurred additionally through bioerosion: a few Štramberk bivalve shells (e.g., NHMV 1910-0005-0030) are covered with *Gnathichnus pentax*, the stellate grooves produced by echinoids grazing the shell surface. However, such traces are uncommon and are unlikely to have significantly impacted the preservation of bryozoans in the Štramberk Limestone.

SYSTEMATICS
Order Cyclostomata Busk, 1852
Suborder Tubuliporina Milne Edwards, 1838
Family Stomatoporidae Pergens and Meunier, 1886
Genus *Stomatopora* Bronn, 1825

Type species: *Alecto dichotoma* Lamouroux, 1821, Jurassic, Bathonian, Calvados, France.

Remarks: Problems concerning the systematics of this genus have been discussed elsewhere (e.g., Hara and Taylor 2009) and will not be repeated here. Only one Štramberk specimen with unequivocal examples of *Stomatopora* has been seen. This is a steinkern of a gastropod labelled as *Pseudomelania* in the NHMV collection showing the undersides of two species of *Stomatopora* that encrusted the interior of the final whorl of the shell which was subsequently exfoliated from the cemented infilling sediment. This kind of preservation precludes species determination, especially in the absence of early astogenetic stages showing the ancestrula and the primary zone of astogenetic change.

***Stomatopora* sp. 1**
Fig. 2A

Material: NHMV PDT-S-0001, Tithonian or Berriasian, Štramberk Limestone (undifferentiated), Štramberk.

Description: Colony encrusting, strictly uniserial. Branches ramify at bifurcation angles of *c.* 40–120°, two or three zooids in each internode between successive ramifications. Septa rounded V-shaped, short. Zooids measuring approximately 0.67–0.83 mm long by 0.33 mm in maximum width.

Remarks: Visible only from the underside, this colony shares the same substrate as *Stomatopora* sp. 2, as well as a pauciserial cyclostome which may perhaps be an immature colony of *Reptoclausa stramberkensis*.

***Stomatopora* sp. 2**
Fig. 2A

Material: NHMV PDT-S-0001, Tithonian or Berriasian, Štramberk Limestone (undifferentiated), Štramberk.

Description: Colony encrusting, apparently pseudouniserial with long proximal parts of daughter zooids running alongside parent zooids before coming to occupy the median part of the branch. Branches ramify at bifurcation angles of *c.* 60–180°, one to at least five zooids in each internode between
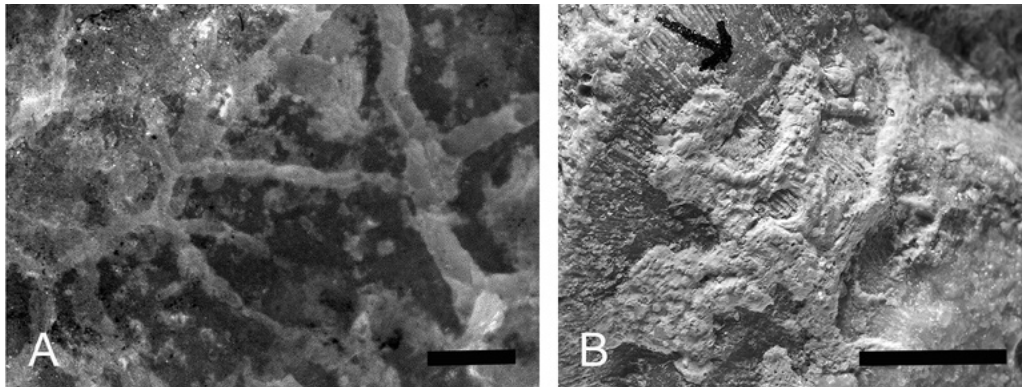
Figure 2. Photographic images of bryozoans from the Štramberk Limestone. (A) *Stomatopora* **spp., undersides of Stomatopora sp. 1 (right) and** *Stomatopora* **sp. 2 (left), the latter with smaller zooids, visible on a gastropod steinkern; NHMV PDT-S-0001, Štramberk Limestone, Štramberk; (B)** *Oncousoecia* **sp., indicated by ink arrow, encrusting a coral; NHMUK BZ8885, Early Berriasian, Štramberk Limestone, Section B, Bed 22, Kotouč Quarry, Štramberk. Scale bars: A = 1 mm; B = 5 mm.**

successive bifurcations. Septa rounded V-shaped, long. Zooids measuring about 0.46–62 mm long by 0.15–0.21 mm in maximum width.

Remarks: Preserved in exactly the same way as *Stomatopora* sp. 1, this species has a more gracile construction, with typically longer internodes and smaller, more slender zooids. The septa, which are less clearly visible than in *Stomatopora* sp. 1, suggest that the zooids have long proximal parts extending alongside the proximal neighbours.

Family Oncousoeciidae Canu, 1918
Genus *Oncousoecia* Canu, 1918

Oncousoecia **sp.**
Figs 2B, 3

Material: NHMUK BZ8885, Early Berriasian, Štramberk Limestone, Section B, Bed 22, Kotouč Quarry, Štramberk.

Description: Colony encrusting a coral, pluriserial. Branches bifurcating, of low profile, about 0.8–2.1 mm wide, broadest at bifurcations, with 4–6 rows of zooids across the branch width. Autozooids *c*. 0.6 mm long by 0.25 mm wide, frontal wall slightly convex distally; aperture circular, about 0.12 mm in diameter. Gonozooid

longitudinally ovoidal, *c*. 1.1 mm long by 0.8 mm wide; ooeciopore terminal, about the same width as an autozooidal aperture but slightly shorter in length.

Remarks: Revised by Taylor and Zatoń (2008), the type species of *Oncousoecia* is Recent but species attributed to this genus of ribbon-like encrusting cyclostomes are common in the Jurassic
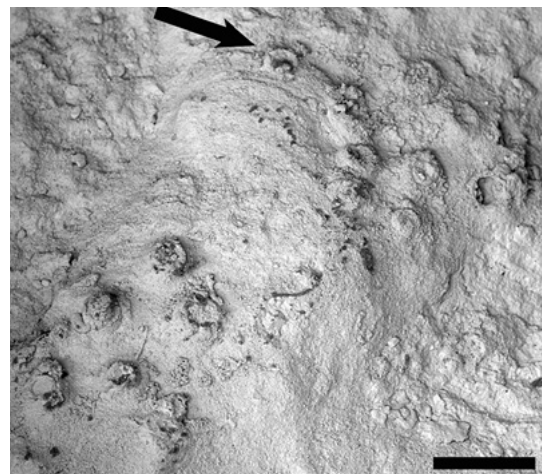

Figure 3. Scanning electron micrograph of fertile *Oncousoecia* sp. with ooeciopore arrowed; NHMUK BZ8885, Early Berriasian, Štramberk Limestone, Section B, Bed 22, Kotouč Quarry, Štramberk. Scale bar = 500 μm.

and Cretaceous. The single colony found in the Štramberk Limestone, although fertile, is partly obscured by sediment and too poorly preserved to allow a meaningful comparison with named species from the Jurassic and Cretaceous.

Family Multisparsidae Bassler, 1935
Genus *Reptoclausa* d'Orbigny, 1853
***Reptoclausa stramberkensis* sp. nov.**
Figs 4–5

Etymology: Named for the type locality Štramberk.

Material examined: Holotype: NHM D54157, Štramberk Limestone, Kotouč Quarry, sector E4, 3rd level, Štramberk, Czech Republic, collected by M. Sandy *c*. 1984. Paratype: NJM PL 2152, Štramberk Limestone, Kotouč Quarry, Štramberk, Czech Republic.

Diagnosis: *Reptoclausa* with new autozooidal ridges originating through intercalation, ridge bifurcation and anastomosis lacking; autozooids short, measuring about 0.37–0.47 mm long by 0.25–0.30 mm wide on ridge crests.

Description: Colony encrusting, multiserial, in early astogeny apparently consisting of a long oligoserial branch from which a ridged multiserial sheet develops laterally, the ridges occupied by autozooids and the intervening furrows by kenozooids (Figs 4, 5A). New ridges are intercalated as the colony increases in diameter; ridge bifurcations and anastomoses are lacking. Crest-to-crest distances between ridges 1.7–4.2 mm, with about 5–8 rows of zooids across each ridge. Colony up to at least 37 mm in diameter, with individual ridges 30 mm or more in length (Fig. 4). Growing edge lobate (Fig. 5B), the convex lobes corresponding to the autozooidal ridges.

Autozooids short, measuring 0.37–0.47 mm long by 0.25–0.30 mm wide close to ridge crests but decreasing in size towards kenozooidal furrows, typically 6-sided rhomboidal in frontal outline with thick boundary walls. Apertures large relative to
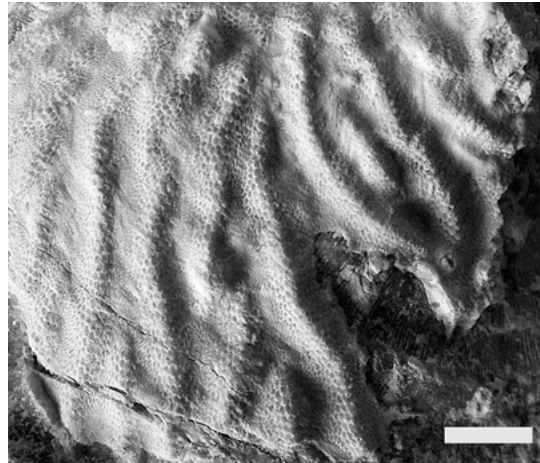

Figure 4. Photographic image of a large colony of *Reptoclausa stramberkensis* sp. nov. Colony growth direction is from top to bottom in this view. Paratype, NJM PL 2152, Štramberk Limestone, Kotouč Quarry, Štramberk. Scale bar = 5 mm.

frontal wall, subcircular, about 0.13 mm in diameter. Apertural rims thick but not prolonged to form a peristome.

Kenozooids more elongate than autozooids, varying in size according to position, those closer to ridges being appreciably larger than those at the middle of the furrows; axes diverging at low angles from ridges with opposing sets of kenozooids flanking adjacent ridges converging along furrow midlines.

Gonozooids rare, two corroded examples observed. Located medially on autozooidal ridges, simple, longitudinally elongate, ooeciopores not preserved.

Remarks: This new species can be compared with two Jurassic and two Cretaceous species. The oldest – *R. porcata* Taylor, 1980 from the Aalenian of Gloucestershire, England – differs in having a bifurcating pattern of autozooidal ridges. The Polish Kimmeridgian species *R. radwanskii* Hara and Taylor, 2009, has elongate autozooids, contrasting with the squat, rhomboidal autozooids of the new species.

In *R. neocomiensis* d'Orbigny, 1853 from the Valanginian of France, the autozooidal ridges are lozenge-shaped, forming 'islands' surrounded
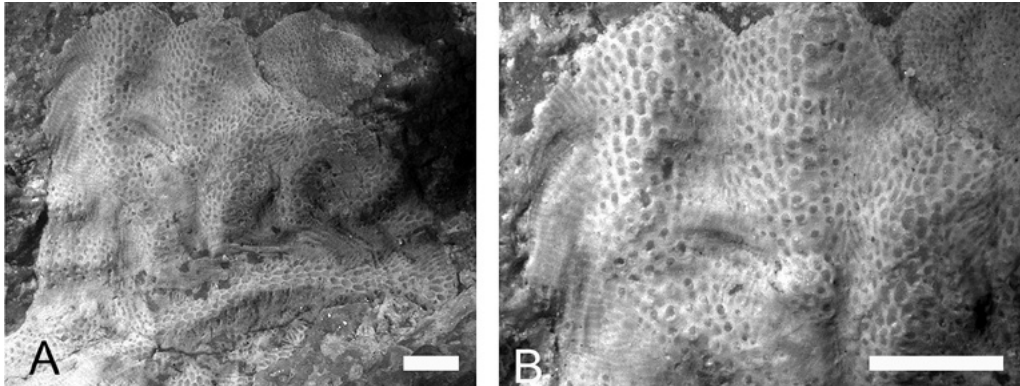
Figure 5. Photographic images of *Reptoclausa stramberkensis* **sp. nov., holotype, NHMUK D54147, Štramberk Limestone, Štramberk , Czech Republic. (A) colony showing ridges formed by autozooids separated by furrows containing kenozooids; (B) detail of three autozooidal ridges and lobate growing edge. Scale bars = 2 mm.**

on all sides by kenozooids. The Aptian species *R. hagenowi* (Sharpe, 1854), revised by Pitt and Taylor (1990), from the Aptian Faringdon Sponge Gravel of Oxfordshire, England, more closely resembles *R. stramberkensis* in the patterning of autozooids and kenozooids. However, the autozooidal ridges in this species are more sinuous and discontinuous.

Early astogenetic stages of *Reptoclausa stramberkensis* resemble *Idmonea* Lamouroux, 1821, a Jurassic–Cretaceous genus with narrow branches with tapered edges formed by kenozooids. It appears that colonies of *R. stramberkensis* begin as a single *Idmonea*-like branch, possibly with a growing tip at both ends; the ridge at the bottom in Figure 4A may be such a primary branch. A radial arrangement of autozooidal ridges separated by kenozooids subsequently develops around this first branch, and the colony spreads outwards as a multiserial sheet. These early astogenetic characters emphasize the close relationship between *Reptoclausa* and *Idmonea*. Indeed, Walter (1970) included material later used as the basis for erecting *Reptoclausa porcata* within the Middle Jurassic type species of *Idmonea*, *I. triquetra*.

Distribution: Early Berriasian and possibly also Tithonian; some colonies were collected from Section B, Bed 22 in the Kotouč Quarry, which belongs to the Early Berriasian Berriasella Jacobi Zone.

Family Plagioeciidae Canu, 1918
Genus *Rugosopora* gen. nov.

Type species: *Berenicea enstonensis* Pitt and Thomas, 1969, Jurassic, Bathonian, Hampen Marly Beds, Oxfordshire, England (Fig. 6).

Diagnosis: Multiserial, sheet-like tubuliporine cyclostomes, unilamellar or multilamellar; colony surface covered by regular transverse ridges separating areas of pseudoporous frontal wall; gonozooids rounded subtriangular to ovoidal, not crossed by the transverse ridges, ooeciopore terminal, slightly smaller than an autozooidal aperture, circular or transversely elliptical.

Etymology: In reference to the transversely ridged, or rugose, colony surface.

Remarks: Hara and Taylor (2009, p. 569) noted the presence in the Jurassic of several cyclostome species of the '*Berenicea*' type with colony surfaces bearing fine but distinct transverse ridges. In stratigraphical order, these species are: *Berenicea enstonensis* Pitt and Thomas, 1969 (mid Bathonian), *Diastopora undulata* Michelin, 1845 (late Bathonian), *Hyporosopora baltovenis* Hara and Taylor, 1996 (Oxfordian), *Berenicea rugosa* d'Orbigny, 1853

(Kimmeridgian) and *Berenicea portlandica* Gregory, 1896 (Tithonian). We here assign all of these species to the new genus *Rugosopora*. The ridges are not simple growth checks (e.g., Hara and Taylor 2009, fig. 8; Zatoń and Taylor 2009, fig. 11B), but instead represent regular thickenings of the frontal wall that are devoid of pseudopores.

The gonozooid in *Rugosopora* is subtriangular, usually transversely elongate (see Hara and Taylor 1996, figs 11, 20, 22), but longitudinally elongate and more ovoidal in *Rugosopora portandica* (see Taylor 1981, text-fig. 2). The ooeciopore is terminal, slightly smaller than the autozooidal apertures and generally a little transversely elongate. While gonozooidal morphology alone would place most or all of these species into *Hyporosopora* Canu and

Bassler, 1929 (see Taylor and Sequeiros 1982), well-defined transverse ridges are absent in *Hyporosopora*.

Colonies of *Rugosopora* are often multilamellar. In the case of *R. undulata*, this is brought about through spiral overgrowth around stationary pivot points (see Taylor 1976), while in some of the younger species of *Rugosopora* multilamellar growth is due to subcolonies being budded eruptively onto the surface of the parent colony (Taylor 1981, pl. 121, fig. 6; Hara and Taylor 2009, fig. 9B) or forming at the edge of the parent colony and subsequently overgrowing it (Hara and Taylor 2009, fig. 9A). The ability to form multilamellar colonies is important in the formation by putative *R. portlandica* of small reefs in the Tithonian Portland Limestone Formation on the Isle of Portland, Dorset (Fürsich *et al.* 1994).
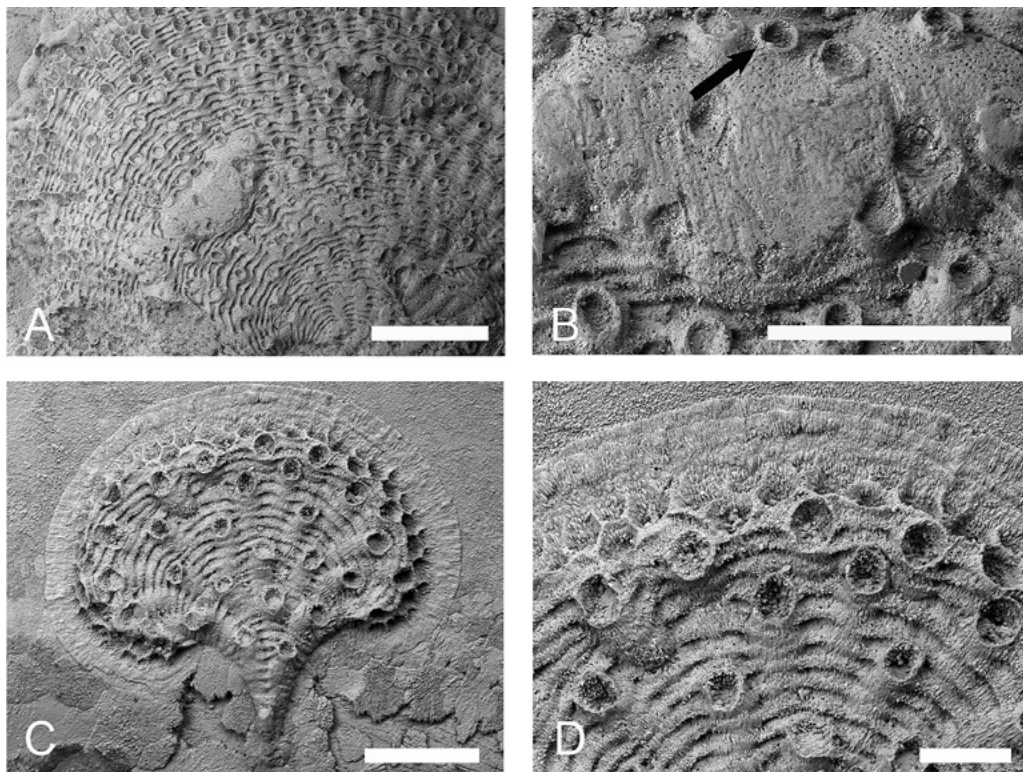

Figure 6. Scanning electron micrographs of *Rugosopora enstonensis* (Pitt and Thomas, 1969), the type species of *Rugosopora* gen. nov., Jurassic, Bathonian, Hampen Formation (= Hampen Marly Beds), Enstone, Oxfordshire. A–B, paratype, NHMUK D51452; (A) colony with one intact and two broken gonozooids; (B) intact gonozooid with ooeciopore arrowed C–D, NHMUK D51449; (C) juvenile colony; (D) growing edge showing distal fringe of basal lamina and colony surface crossed by transverse ridges. Scale bars: A = 1 mm; B, C = 500 µm; C = 200 µm.

A few post-Jurassic cyclostomes have transversely ridged colonies. For example, Walter (1989, pl. 5, fig. 1) figured as *Mesonopora polystoma* (Roemer) a single colony from the French Valanginian with strong transverse ridges, Buge (1979) redescribed the French Eocene (Lutetian) species *Plagioecia plicata* Canu, 1909, which has *Reticulipora*-like erect colonies that are transversely ridged, while Canu and Bassler (1920) introduced two Eocene new species (*Diaperoecia rugosa* and *Exochoecia rugosa*) from Alabama with 'transverse wrinkles'. All of these species require revision before they can be assigned with confidence to *Rugosopora*.

Distribution: Jurassic (Bathonian)–Cretaceous (Berriasian), ?Eocene (Lutetian).

Rugosopora sp.

Fig. 7

Material: NHMUK BZ8886, Early Berriasian, Štramberk Limestone, Section B, Bed 22, Kotouč Quarry, Štramberk. NHMV 1912.VI.169, PDT-5-0002, PDT-5-0003, PDT-5-0004, Štramberk Limestone, Štramberk.

Description: Colonies multiserial, sheet-like, unilamellar or multilamellar, frontal surface bearing prominent transverse ridges spaced 50–95 µm apart (0.06-0.08 mm apart), straight or slightly sinuous.

Autozooids *c.* 0.48–0.70 mm long by 0.13–0.14 mm wide, frontal walls slightly convex distally, otherwise zooidal boundaries ill-defined. Apertures slightly longitudinally elongate, *c.* 0.08–0.10 mm in diameter, often closed by a terminal diaphragm; preserved peristomes short. Pseudopores not visible.
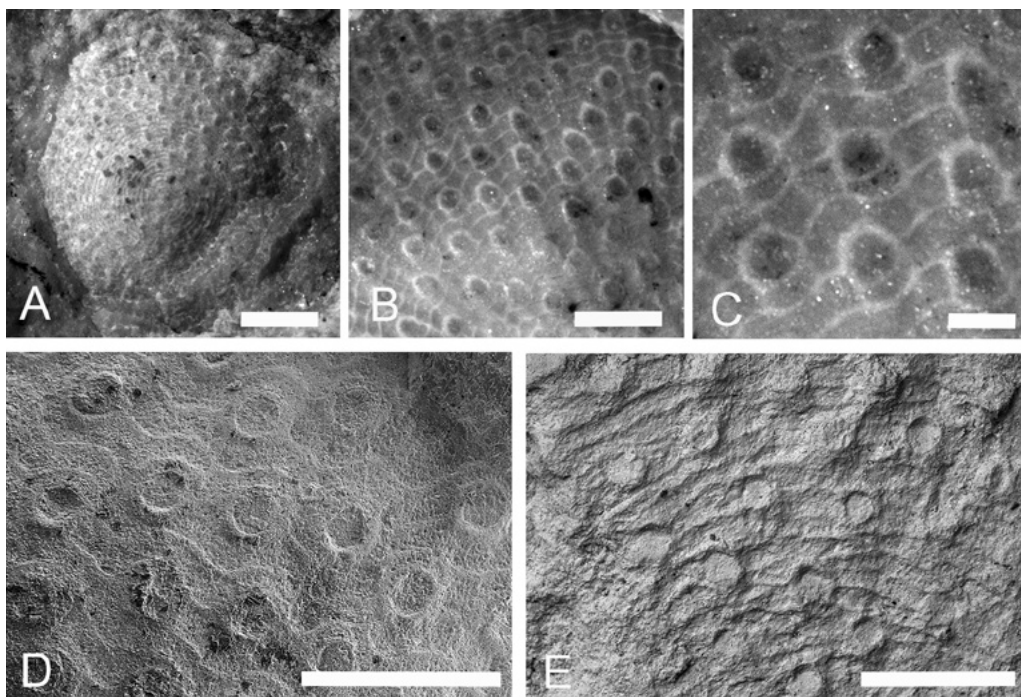
Gonozooids not observed.

Figure 7. Photographic images (A–C) and scanning electron micrographs (D–E) of *Rugosopora* sp., Štramberk Limestone, Štramberk, (A–C) NHMV 1912.VI.169, (A) entire colony; (B) autozooids; (C) detail of autozooids showing apertures and transverse ridges. (D) NHMV PDT-5-0003E, transverse ridges and autozooidal apertures; (E) NHMUK BZ8886, Early Berriasian, Section B, Bed 22, Kotouč Quarry; transverse ridges and autozooids with apertures closed by terminal diaphragms. Scale bars: A = 1 mm; B, D, E = 500 µm; C = 200 µm.
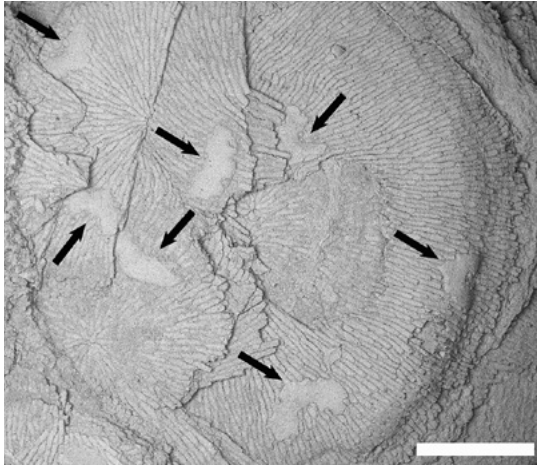
Figure 8. Scanning electron micrograph of abraded, indeterminate, multilamellar plagioeciid with numerous gonozooids (arrowed). NJM PL 2163, Štramberk Limestone, Kotouč Quarry, Štramberk. Scale bar = 2 mm.

Remarks**:** As none of the specimens studied have gonozooids, we are reluctant to assign the Štramberk *Rugosopora* to a species. The size of the autozooids is variable, which might suggest that more than one species is present. However, zooidal size is also variable among specimens of what appear to be a single species of this genus in the Portland Limestone Formation of southern England: the type specimen of *Rugosopora portlandica* has longer and wider autozooids than most other colonies from the same formation. Larger suites of specimens coupled with morphometric analyses

are needed to evaluate the taxonomic significance of zooid size variability in *Rugosopora* from both the Štramberk and Portland limestones.

Plagioeciidae indet.
Fig. 8

Remarks**:** A large number of cyclostomes of the '*Berenicea*' type in the Štramberk Limestone have poor surface preservation, many with frontal walls completely lacking to reveal only the calcite cement infilling the zooidal chambers. These cannot be identified; although some may be *Rugosopora*, without preservation of surface ridges this cannot be proven. A few colonies are fertile, including the multilamellar colony depicted in Figure 8 in which the shape of the numerous gonozooids shows it to belong in Plagioeciidae. Others with closely packed zooids radiating from centres of overgrowth resemble the genus *Cellulipora* d'Orbigny, 1849 (see Buge and Voigt 1972).

Family Heteroporidae Waters, 1880
Genus *Ceriopora* Goldfuss, 1826

'*Ceriopora*' sp.
Fig. 9

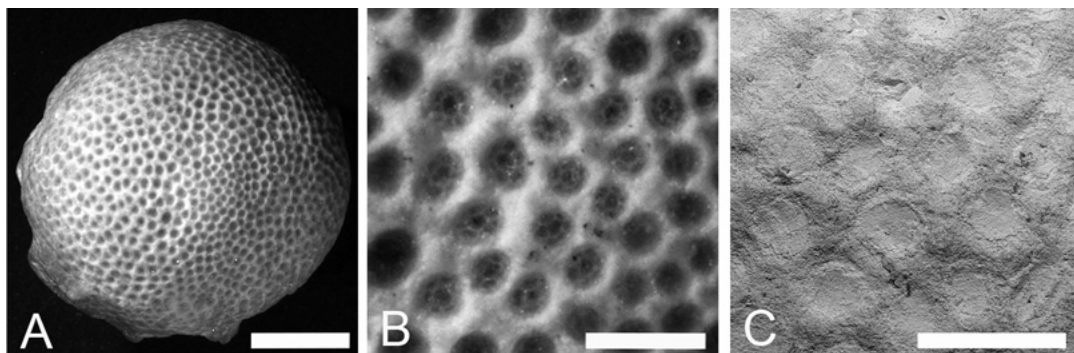***Material*****:** NHMV 1910.V.25, Štramberk Limestone, Štramberk.

Figure 9. Photographic images (A–B) and scanning electron micrograph (C) of '*Ceriopora*' sp. NHMV 1910.V.25, Štramberk Limestone, Štramberk. (A) upper surface of small, dome-shaped colony; (B) thick zooidal walls with tubercles and subdivision of apertures indicative of intrazooecial fission; (C) apertures plugged by calcite. Scale bars: A = 2 mm; B, C = 500 μm.

Description: Colony dome-shaped, small, about 6.8 mm in diameter. Zooids apparently monomorphic, although clusters of smaller than average sized apertures are visible on the colony surface.

Autozooids polygonal, thick walled, with broad tubercles developed at corners. Apertures circular or subcircular, 0.15–0.23 mm in diameter, some containing a thin ring linked by about 6–8 radial walls to the apertural wall.

Gonozooids not observed.

Remarks: Several *Ceriopora*-like fossils have been observed in collections from Štramberk but it is by no means clear whether these are all bryozoans. However, the specimen described and figured here can be confidently identified as a bryozoan on account of the presence of apertures containing a ring defining a central chamber that is surrounded by 6–8 smaller chambers separated by radial walls (Fig. 9B). This morphology is characteristic of zooidal budding by 'intrazooecial fission', as described in the cyclostomes *Reptomulticava* and *Canalipora* and the trepostome *Stenoporella* by Hillmer *et al.* (1975). Attribution of this Štramberk bryozoan informally to '*Ceriopora*' is based on the dome-shaped colony and monomorphic zooids.

Genus *Semimulticavea* d'Orbigny, 1853

?*Semimulticavea* sp.
Fig. 10

Material: NHMV 1912.VI.170, Štramberk Limestone, Štramberk; R. Wessely Collection.

Description: Colony columnar, rounded distally, 21 mm high by 12 mm in maximum width, multilamellar, consisting of at least 4 layers each comprised of laterally fused subcolonies. Subcolonies polygonal in outline, *c*. 3.5–4.7 mm wide, gently convex with
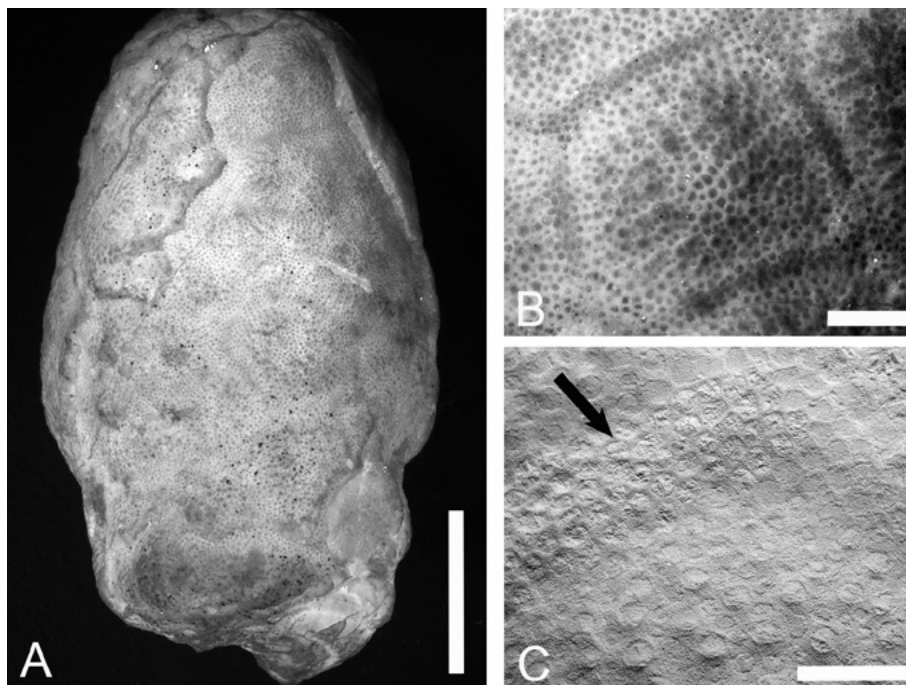

Figure 10. Photographic images (A–B) and scanning electron micrograph (C) of ?*Semimulticavea* sp., NHMV 1912.VI.170, Štramberk Limestone, Štramberk. (A) colony with partial exfoliation of layers; (B) polygonal subcolony; (C) edge of subcolony with marginal zone of kenozooids (arrow). Scale bars: A = 5 mm; B = 1 mm; C = 500 μm.

a slightly depressed centre that is about 1.1–1.25 mm wide and formed exclusively by kenozooids, surrounded by a zone containing kenozooids and autozooids. Edges of subcolonies comprising a slightly raised zone of kenozooids 0.5–0.75 mm wide.

Autozooidal apertures arranged in poorly defined radial rows, occasionally connate but more usually not in contact, about 0.09–0.11 mm in diameter.

Gonozooid unknown.

Remarks: Only one specimen of this distinctive cyclostome is known. The morphology of the colony, comprising multiple layers of laterally fused polygonal subcolonies, is characteristic of several predominantly Early Cretaceous genera including *Semimulticavea* d'Orbigny, 1853, *Multifascigera* d'Orbigny, 1853, *Multicrescis* d'Orbigny, 1854 and *Reptomulticava* d'Orbigny, 1854. The Štramberk specimen, which is infertile, is provisionally assigned to the first of these genera pending the discovery of fertile colonies and, preferably, material that could be thin sectioned to reveal the internal structure.

DISCUSSION

The Štramberk Limestone hosts a rare example of a bryozoan fauna of latest Jurassic to earliest Cretaceous age. Unfortunately, surface preservation of the bryozoans is poor, hindering taxonomic description and interpretation. Indeed, only one of the species found was deemed to be both well enough preserved and sufficiently distinctive to warrant formal description as a new species, *Reptoclausa stramberkensis* sp. nov.

We here report the presence of at least 8 species from the Štramberk Limestone, which is surely an underestimate of its true diversity. Focused collecting and examination of shell substrates from different horizons in the Štramberk Limestone, supplemented by a programme of thin sectioning of limestones containing promising bioclasts, would no doubt yield further species. Nodular fossils consisting of tightly packed tubes are common in the Štramberk Limestone but require thin sectioning and detailed study to determine whether they are calcareous algae, calcified demosponges, hydrozoans or bryozoans.

All of the known Štramberk species are cyclostomes, apart from rare examples of putative ctenostome borings (NHMV 1912.VI.604 and 1908.IX.106). One of the main initial motivations for studying the Štramberk Limestone was the prospect of discovering Jurassic cheilostomes to add to the two species of *Pyriporopsis* already known. Unfortunately, no cheilostomes were found. Nearshore and/or clastic-rich facies host the majority of early, pre-Cenomanian cheilostomes and it may be that cheilostomes took longer to spread into offshore, pure carbonate, reefal facies like the Štramberk Limestone.

REFERENCES

BASSLER, R.S. 1935. Bryozoa. *Fossilium Catalogus. 1: Animalia* **67**, 1–229 pp.

BRONN, H.G. 1825. *System der urweltlichten Pflanzenthiere durch Diagnose, Analyse und Abbildung der Geschlechter erläutert*. Heidelberg, 47 pp.

BROOKFIELD, M.E. 1973. The life and death of *Torquirhynchia inconstans* (Brachiopoda, Upper Jurassic) in England. *Palaeogeography, Palaeoclimatology, Palaeoecology* **13**, 241–259.

BUGE, E. 1979. Découverte du gonozoïde et position systématique de «*Reticulipora*» *plicata* Canu de l'Éocène du Bassin de Paris (Bryozoa Cyclostomata). *Annales de Paléontologie, Invertébrés, Paris* **65**, 43–51.

BUGE, E. AND VOIGT, E. 1972. Les *Cellulipora* (Bryozoa, Cyclostomata) du Cénomanien française et la famille des Celluliporidae. *Geobios* **5**, 121–150.

BUSK, G. 1852. An account of the Polyzoa and Sertularian Zoophytes collected in the voyage of the Rattlesnake on the coast of Australia and the Louisiade Archipelago. In: J. MacGillivray, *Narrative of the Voyage of H.M.S. Rattlesnake, commanded by the late Captain Owen Stanley, during the years 1846-1850* **1**, 343–402. London, Boone.

CANU, F. 1909. Bryozoaires des terrains tertiaires des environs de Paris. *Annales de Paléontologie* **4**, 29–68.

CANU, F. 1918. Les ovicelles des bryozoaires cyclostomes. Études sur quelques familles nouvelles et anciennes. *Bulletin de la Société Géologique de France, Paris*, (4) **16**, 324–335.

CANU, F. AND BASSLER, R.S. 1920. North American Early Tertiary Bryozoa. *Bulletin of the United States National Museum* **106**, 1–879.

CANU, F. AND BASSLER, R.S. 1929. Etude sur les ovicelles des Bryozoaires jurassiques. *Bulletin de la Société Linnéenne de Normandie* (8) **2**, 113–131.

FÜRSICH, F.T., PALMER, T.J. AND GOODYEAR, K.L. 1994. Growth and disintegration of bivalve-dominated patch reefs in the Upper Jurassic of southern England. *Palaeontology* **37**, 131–171.

GOLDFUSS, G.A. 1826–33. *Petrefacta Germaniae, Abbildung und Beschreibungen der Petrefacten Deutschlands und der angreuzenden* Länder. *Teil 1*. Dusseldorf, Arnz & Co., 76 pp.

GREGORY, J.W. 1896. A revision of the British Jurassic Bryozoa. Part III. The genus *Berenicea*. *Annals and Magazine of Natural History* (6) **17**, 41–49.

HALLAM, A. 1986. The Pliensbachian and Tithonian extinction events. *Nature* **319**, 765–768.

HALLAM, A. AND WIGNALL, P.B 1997. *Mass Extinctions and their Aftermath*. Oxford, Oxford University Press.

HARA, U. AND TAYLOR, P.D. 1996. Jurassic bryozoans from Baltów, Holy Cross Mountains, Poland. *Bulletin of The Natural History Museum, London, Geology Series* **52**, 91–102.

HARA, U. AND TAYLOR, P.D. 2009. Cyclostome bryozoans from the Kimmeridgian (Upper Jurassic) of Poland. *Geodiversitas* **31**, 555–575.

HILLMER, G., GAUTIER, T.G. AND MCKINNEY, F.K. 1975. Budding by intrazooecial fission in the stenolaemate bryozoans *Stenoporella*, *Reptomulticava* and *Canalipora*. *Mitteilungen aus dem Geologisch-Paläontologisches Institut der Universität Hamburg* **44**, 123–132.

HOFFMANN, M., KOŁODZIEJ, B. AND SKUPIEN, P. 2017. Microencruster-microbial framework and synsedimentary cements in the Štramberk Limestone (Carpathians, Czech Republic): Insights into reef zonation. *Annales Societatis Geologorum Poloniae* **87**, 325–347.

HOUSA, V. AND NEKVASILOVA, O. 1987. Epifauna cemented to corals and bivalves from the Tithonian of Štramberk (Czechoslovakia). *Casopis pro mineralogii a geologii* **32**, 47–58.

LAMOUROUX, J. 1821. *Exposition méthodique des genres de l'ordre des polypiers*. Paris, Agasse, 115 pp.

MICHELIN, H. 1841–48. *Iconographie zoophytologique, Description par localitès et terrains des polypiers fossiles de France et pays environnants*. Paris, Bertrand, viii + 348 pp., 79 pls.

MILNE EDWARDS, H. 1838. Mémoire sur les Crisies, les Hornères et plusieurs autres Polypes. *Annales des Sciences Naturelles* **9**, 193–238.

ORBIGNY, A. D' 1849. Description de quelques genres nouveaux de mollusques bryozoaires. *Revue et Magasin de Zoologie* (2) **1**, 499–504.

ORBIGNY, A. D' 1851–4. *Paléontologie Française. Terrains Crétacés. 5. Bryozoaires*. Paris, Masson, 1191 pp., pls 600-800.

PERGENS, E. AND MEUNIER, A. 1886. La faune des Bryozoaires garumniens de Faxe. *Annales de la Société Royale Malacologique de Belgique* **12**, 181–242.

PICHA, F.J., STRÁNÍK, Z., AND KREJČÍ, O. 2006. Geology and hydrocarbon resources of the outer western Carpathians and their foreland, Czech Republic. *American Association of Petroleum Geologists Memoir* **84**, 49–175.

PITT, L.J. AND TAYLOR, P.D. 1990. Cretaceous Bryozoa from the Faringdon Sponge Gravel (Aptian) of Oxfordshire. *Bulletin of the British Museum (Natural History), Geology Series* **46**, 61–152.

PITT, L.J. AND THOMAS, H.D. 1969. The Polyzoa of some British Jurassic clays. *Bulletin of the British Museum (Natural History) (Geology Series)* **18**, 29–38.

POHOWSKY, R.A. 1973. A Jurassic cheilostome from England. In: G.P. Larwood (ed.), *Living and fossil Bryozoa*. London, Academic Press, pp. 447–461.

REMEŠ, M. 1902. Nachtrage zur Fauna von Stramberg. I. Die Fauna des rothen Kalksteins. *Beiträge zur Paläontologie und Geologie Österreich-Ungarns und des Orients* **14**, 195–217.

RILEY, S. AND THOMAS, J. 1987 A new bryozoan from Tilly Whim Caves not previously recorded from the British Portlandian. *Proceedings of the Dorset Natural History and Archaeological Society* **108**, 209.

RUBAN, D.A. 2006. Taxonomic diversity dynamics of the Jurassic bivalves in the Caucasus: regional trends and recognition of global patterns. *Palaeogeography, Palaeoclimatology, Palaeoecology* **239**, 63–74.

SHARPE, D. 1854. On the age of the fossiliferous sands and gravels of Faringdon and its neighbourhood. *Quarterly Journal of the Geological Society, London* **10**, 176–198.

SKUPIEN, P. AND SMARŽOVÁ, A. 2011. Palynological and geochemical response to environmental changes in the Lower Cretaceous in the Outer Western Carpathians; a record from the Silesian unit, Czech Republic. *Cretaceous Research* **32**, 538–551.

TAYLOR, P.D. 1976. Multilamellar growth in two Jurassic cyclostomatous Bryozoa. *Palaeontology* **19**, 293–306.

TAYLOR, P.D. 1980. Two new Jurassic Bryozoa from southern England. *Palaeontology* **23**, 699–706.

TAYLOR, P.D. 1981. Bryozoa from the Jurassic Portland Beds of England. *Palaeontology* **24**, 863–875.

TAYLOR, P.D. 1994. An early cheilostome bryozoan from the Upper Jurassic of Yemen. *Neues Jahrbuch für Geologie und Paläontologie Abhandlungen* **191**, 331–344.

TAYLOR, P.D. AND ERNST, A. 2008. Bryozoans in transition: the depauperate and patchy Jurassic biota. *Palaeogeography, Palaeoclimatology, Palaeoecology* **263**, 9–23.

TAYLOR, P.D. AND SEQUEIROS, L. 1982. Toarcian bryozoans from Belchite in north-east Spain. *Bulletin of the British Museum (Natural History) (Geology Series)* **37**, 117–129.

TAYLOR, P.D. AND ZATOŃ, M. 2008. Taxonomy of the bryozoan genera *Oncousoecia*, *Microeciella* and *Eurystrotos* (Cyclostomata: Oncousoeciidae). *Journal of Natural History* **42**, 2557–2574.

TENNANT, J.P., MANNION, P.D., UPCHURCH, P., SUTTON, M.D. AND PRICE, G.D. 2017. Biotic and environmental dynamics through the Late Jurassic–Early Cretaceous transition: evidence for protracted faunal and ecological turnover. *Biological Reviews* **92**, 776–814.

TODD, J.A., TAYLOR, P.D. AND FAVORSKAYA, T.A. 1997. A bioimmured ctenostome bryozoan from the Early Cretaceous of the Crimea and the new genus *Simplicidium*. *Geobios* **30**, 205–213.

TOWNSON, W.C. 1975. Lithostratigraphy and deposition of the type Portlandian. *Journal of the Geological Society of London* **131**, 619–638.

VAŠÍČEK, Z. AND SKUPIEN, P. 2005. Supplements to history of geological and paleontological research of Štramberk Territory. *Sbornik vedeckych praci Vyoske skoly banske – Technicke iniverzity Ostrava, cislo 1, rok 2005, rocnik* LI, 1–6.

VAŠÍČEK, Z. AND SKUPIEN, P. 2016. Tithonian–eearly Berriasian perisphinctoid ammonites from the Štramberk Limestone at Kotouc Quarry near Štramberk, Outer Western Carpathians (Czech Republic). *Cretaceous Research* **64**, 12–29.

VAŠÍČEK, Z., SKUPIEN, P. AND JAGT, J.W.M. 2018. Current knowledge of ammonite assemblages from the Štramberk Limestone (Tithonian–lower Berriasian) at Kotouč Quarry, Outer Western Carpathians (Czech Republic). *Cretaceous Research* **90**, 185–203.

VISKOVA, L.A. 2009. New data on the colonial morphology of the Jurassic bryozoans of the Class Stenolaemata. *Paleontological Journal* **43**, 543–549.

WALTER, B. 1970. Les Bryozoaires Jurassiques en France. *Documents des Laboratoires de Géologie de la Faculté des Sciences de Lyon* **35** (for 1969), 1–328.

WALTER, B. 1972. Les bryozoaires neocomiens du Jura Suisse et Français. *Geobios* **5**, 277–354.

WALTER, B. 1989. Les Diastoporidae bereniciformes neocomiens du Jura Franco-Suisse. *Palaeontographica Abteilungen A* **207**, 107–145.

WALTER, B. 1997. Une faune berriasienne de bryozoaires à Musièges, (Jura méridional, Haute-Savoie). *Geobios* **30**, 371–377.

WATERS, A.W. 1880. Note on the genus *Heteropora*. *Annals and Magazine of Natural History* (5) **6**, 156–157.

ZATOŃ, M. AND TAYLOR, P.D. 2009. Middle Jurassic cyclostome bryozoans from the Polish Jura. *Acta Palaeontologica Polonica* **54**, 267–288.

Celleporiform Bryozoa (Cheilostomata) from the early Miocene of Austria

Norbert Vávra

Institute for Palaeontology, Geozentrum, University of Vienna, Austria [e-mail: norbert.vavra@univie.ac.at]

ABSTRACT

Celleporiform colonies are among the most common bryozoan fossils in the Austrian Neogene. Due to their poor state of preservation they are often extremely difficult to determine and are therefore often neglected in faunal descriptions. If there is any possibility to utilize them as a source for additional information in respect to palaeoecology, palaeobiogeographical studies, or perhaps even biostratigraphical purposes, their morphologies needs to be revised. A summary of the present state of knowledge will be a first step into this direction.

INTRODUCTION

Celleporiform bryozoans are among the most common fossils in the Austrian Neogene: already Reuss (1847) summarized under the name *Cellepora globularis* different shapes of zoaria from various localities (Nußdorf, Baden, Grinzing, Eisenstadt, Mörbisch, Kroisbach, Wieliczka and a few others). With this report a 'never-ending' story started, a story including confusions, uncertainties, proposals, and suggestions. The last author (Pouyet 1973) who presented a revision summarizing fossil and Recent taxa from Europe included also *Cellepora globularis* in her detailed studies. She realized that the collections of the Museum of Natural History at Vienna contained a number of specimens under this name in the Reuss-collection, which obviously belonged to quite different taxa. The determination had obviously been done on the basis of the zoarial shape; according to Pouyet (1973)

the type material had been lost ('Le type est perdu', p. 125). Nevertheless she maintained the taxon, although – with the genus in quotation marks now: *"Cellepora globularis* (Bronn, 1837)*"*. In fact it would result in a very long story to discuss all the details and localities from which *Cellepora globularis* had been reported. To give one more example for an unsatisfactory revision by this author concerning the taxon *Turbicellepora krahuletzi* Kühn, 1925: the type locality of this species is Grübern, from sand-pits exposing sediments of the Eggenburgian stage (according to a definition established for the Paratethys area (e.g. Steininger and Seneš 1971), i.e. from the lower Miocene. Pouyet (1973, pp. 107–108), however, offers a revision on the basis of material from the collection at Lyon from Eisenstadt and Steinebrunn in Austria of Badenian age (middle Miocene!), material which she probably had been collecting herself during her visit to Austria a few years before this publication was issued. As the holotype of this taxon cannot be relocated, and since a paratype, which is kept in the collections of the Austrian Geological Survey, is extremely poorly preserved, the situation remains rather difficult and far from being really satisfying. But while it is easy to critize, it is very difficult (if not impossible) to offer better results. Therefore these few remarks should be regarded only as examples for the situation concerning taxonomical studies of celleporiform bryozoans in general. The state of preservation being usually rather poor, however, they have been often neglected by authors dealing with Bryozoa from the

Austrian Miocene– which is another possibility to deal with this problematical group. The outstanding monographical description of the bryozoan fauna of the Langhian (Miocene) of the Czech Republic by Zágoršek (2010) includes only three taxa of celleporids: *Buffonellaria kuklinskii, B. holubicensis* and *Turbicellepora coronopus*) – possibly the Czech strata studied contain more taxa, however. *Buffonellaria holubicensis* has also been found in material from the early Miocene of Austria meanwhile (locality: Brugg); it is a celleporid taxon, but due to its erect bilaminar colonies it is not considered here further on. Another possibility to deal with this rather problematical and very difficult situation is shown by Schneider *et al.* (2009) for a bryozoan fauna from the Bavarian Molasse Zone of comparable age: a few colonies could be identified as belonging to the genus *Celleporina*, whereas the remaining three zoaria are summarized as Celleporidae gen. et sp. indet. As already confirmed by Kühn (1925), celleporiform colonies are at many localities of the Eggenburg area (i.e. in our early Miocene) the most common and conspicuous group of Bryozoa. A Recent study of a bryozoan fauna from Sigmundsherberg yielded about 75% (weight-%) of celleporiform taxa; a careful counting of zoarial fragments from Unter-Nalb (Sands of Retz) yielded 29% for celleporiform colonies and 49% for *Myriapora truncata* (Vávra 2008). Will future studies show that this group of cheilostomatous Bryozoa has any value in respect to biostratigraphy, paleoecology or paleobiogeography? Nobody knows for sure at the present time. Realizing all these troubles and difficulties, the celleporiforms offer nevertheless a permanent challenge – the following report can only be regarded as another contribution to this never-ending but rather fascinating story.

LOCALITIES/STRATIGRAPHY

The different bryozoan localities mentioned in this text are situated in the NW part of Lower Austria, where sediments of early Miocene age lie transgressively on crystalline rocks of the Bohemian Massif. In this area are the stratotypes of the 'Eggenburgian' as established and described in Steininger and Seneš (1971), and more recently summarized in Wessely (2006). All bryozoan localities belong to the late Eggenburgian, perhaps even to the early Ottnangian (Tabel 1). A detailed map of these bryozoan localities is given in Vávra (2013), a publication in which you can also find a short description giving more information concerning important bryozoan localities (e.g. Brugg, Grübern, Oberdürnbach). Brugg and Oberdürnbach, yielding lots of rather well-preserved zoaria, are attributed to the lower Ottnangian now (Key *et al.* 2012).

Table 1. Stratigraphy of the Miocene of the Molasse Zone in Lower Austria (Wessely 2006).
Bryozoan Localities (e.g. Brugg, Grübern, Limberg, Oberdürnbach, Sands of Retz) belong
to the Uppermost Eggenburgian/Lowest Ottnangian.

Epochs	Age (in Ma)	Stages	Stages of the Central Paratethys	Planktonic Foraminifera
↑ Middle Miocene	16.4	Langhian	↑ Badenian	↑ M5 (N8)
	17.2		Karpatian	M4 (N7)
	18.8	Burdigalian	Ottnangian	M3 (N6)
Early Miocene	20.5		Eggenburgian	M2 (N5)
	23.8	Aquitanian	Egerian ↓	

SYSTEMATICS

Family Lepraliellidae Vigneaux, 1949
Genus *Celleporaria* Lamouroux, 1821

Celleporaria albirostris Smitt, 1872

Discopora albirostris Smitt, 1872: p. 70, pl. 70, figs 233–239.
Holoporella albirostris (Smitt) – Kühn 1925: p. 29.
Celleporaria albirostris (Smitt)– Vávra 1977: p. 154.

Material Examined: No material available for studies.

Description: This species has only been claimed by Kühn (1925) to occur in the early Miocene of Austria. He gives a rather short description without any pictures or figures. The size of the zoaria is given (length may reach 3 cm, 0.5 to 2 cm thick), a fine channel as a result of a former algal substrate is mentioned, around which the zoaria are developing. Size of zooecia (0.40-0.50 versus 0.30-0.40 mm) and size of aperture (0.15 mm) is given; the form of the apertures is described as crescent-shaped, hoof-shaped or round. No more details are given, however.

Discussion: To prove the correctness of this determination would be very important indeed. Realizing the data to which Kühn (1925) refers in respect to the occurrence of this taxon in space and time (Oligocene to Recent; Panama-area, Pliocene of New Zealand and Florida; Recent in the Pacific, Atlantic and Indian Ocean as well) would justify further studies. However, such a wide temporal and geographic distribution of a brooding bryozoan species is completely impossible– most probably Kühn's determination had been completely wrong.

Distribution: Kühn (*l.c.*) mentions that this species is very common in the area of Grübern, rarer however in the area of Eggenburg and Klein-Meiseldorf. No material available for a revision, no comments can be given.

Celleporaria* cf. *foraminosa Reuss, 1847

cf. *Cellepora foraminosa* m. Reuss, 1847: pp. 76–77, pl. 9, fig. 16.
Celleporaria foraminosa (Reuss) – Pouyet 1973: p. 92, pl. 15, fig. 4.
Celleporaria foraminosa (Reuss) – David and Pouyet 1974: p. 210.
Celleporaria foraminosa (Reuss) – Vávra 1977: pp. 154-155.

Lectotype/Paratypes: NHMW-1867.XI.142 (determined by Pouyet, 1973).

Locus typicus: Rudelsdorf (= Rudoltice) situated about 4 km SW of Landskron (= Landskroun) in Bohemia (Czech Republic).

Material examined: Material kept in the collections at Vienna (NHMW-1867.XI.142; NHMW-1867.XL.193) has been studied by the author; more recently, additional material – the very first finds from the Austrian Miocene – has now been found in a sample from Brugg.

Description/Discussion: The description to be given on the basis of material available at present time is rather poor: abrasion has left a zoarial surface with a rather typical pattern of pores. Therefore, only a tentative determination can be given at the moment.

Distribution: The type locality is situated in sediments from the middle Miocene of the Czech Republic; additional material from the Eggenburgian of a drilling at Znojmo (UWPI) can be mentioned as one more occurrence of this taxon. The material recently detected in a sample from Brugg would mark the first occurrence in Austria.

Family Celleporidae Johnston, 1838
Genus *Cellepora* LINNAEUS, 1767

"Cellepora" globularis Bronn, 1837

Cellepora globularis Bronn – Reuss 1847: p. 76, pl. 9, fig. 11-15.

Celleporaria globularis (Bronn) – Manzoni 1877: p. 51, pl. 1, fig. 2.

Holoporella globularis (Bronn) – C. & B. Kühn, 1955: pp. 241–242.

"*Cellepora*" *globularis* Bronn – David & Pouyet 1974: p. 216.

"*Cellepora*" *globularis* Bronn– Vávra 1977: pp. 158–159.

Material examined: Hundreds of specimens from Eggenburgian and Badenian localities as well: obviously this taxon has been used (for closer discussion see below) to summarize finds of celleporiform zoaria with a rather low state of preservation permitting no closer determination at all.

Diagnosis and description: Depending on the state of preservation of the material there is no closer description possible: abrasion of the surface of zoaria does not permit to give any information concerning ovicells, avicularia etc. Often authors seem to have summarized under this designation celleporiform zoaria of globular shape.

Discussion: Reuss (1847) describes and figures such zoaria – no occurrence concerning localities from the early Miocene is given, however. Manzoni (1877) is obviously the very first author who studied also specimens from the early Miocene: Himmelreich, a locality close to the city of Eggenburg. Another locality mentioned by this author – Gaudenzdorf – results possibly from a mistake: Gaudenzdorf is a former village, later being part of the twelfth district of Vienna. Possibly this should be "Gauderndorf" – a well-known fossiliferous locality close to Eggenburg. Kühn (1955), referring to Manzoni (1877), repeats these two names (Gaudenzdorf, Himmelreich) without any new data, but he gives for *Cellepora globularis* a few additional localities from the Eggenburgian: Grübern and three names of localities in the sands of Retz: Ober-Nalb, Unter-Nalb, and Pillersdorf. He emphasizes for this material

that its state of preservation is very poor. Pouyet (1973, p. 125) mentions in the course of her revision that "*Cellepora*" *globularis,* as used by Reuss (1847), includes different taxa – an opinion also repeated by Vávra (1977) – but both authors don't suppress this taxon. Sometimes this name has been used to describe small 'pisiform' zoaria of celleporids (Braga 1963, 1988), thus extending a possible stratigraphical range considerably (Priabonian to Pliocene); other authors, however (e.g. Schneider *et al.* 2009, p. 85), preferred however to use "Celleporidae" or even "*Celleporina* sp." for pisiform zoaria of celleporids.

In the collection of Michelin (Paris; UP – no number), a tiny pisiform zoarium from the locality "Nußdorf" has been detected by the author – obviously an early find corresponding to the information given by Reuss (1847).

Cellepora polythele Reuss, 1847

Cellepora polythele m. Reuss, 1847: pp. 77–78, pl. 9, fig. 18.

Celleporaria polythele (Reuss) – Manzoni 1877: p. 52, pl.1, fig. 3.

Holoporella polythele (Reuss) – Kühn 1925: pp. 29-30, pl. 2, fig.5.

Holoporella polythele (Reuss) – Kühn 1955: p. 242–243.

Cellepora polythele Reuss – Vávra 2004: pp. 23–33, fig. 1, A–E.

Type specimen: NHMW 1859.XLV.657 (Lectotype, Pouyet, 1973).

Type locality: Hlohovec (= Bischofswart), 10 km ESE Mikulov (=Nikolsburg), Moravia, Czech Republic.

Stratum typicum: Badenian (middle Miocene).

Material Examined: Kühn (1925) has obviously been the first author mentioning this species from the Eggenburgian of Austria; he mentions Gauderndorf (situated 2 km N of Eggenburg) as the locality where this specimen of considerable size (10 cm diameter)

had been found. He later confirmed the occurrence of this taxon also for Groß-Reipersdorf (situated near Pulkau, 10 km SW of Retz) and for Pillersdorf (situated 5 km SW of Retz). The only one specimen available for our studies had been the zoarium from Groß-Reipersdorf, the other specimens could not be relocated. This specimen is kept in the collections of the Institute of Palaeontology of the University of Vienna (No. 1545, misspelled in the publication as 'Groß-Reisperbach'). Other Material available in the old collections of the institute may probably originate from Bischof(s)wart (= Hlohovec, Czech Republic) and therefore from the Badenian (middle Miocene). Through continued collecting activity during many years additional material showing the typical shape of the zoarium could be found among material from other localities of the Eggenburgian: Grübern, Brugg (three specimens).

Discussion: A detailed description of this species is given in Vávra (2004); a short summary of its characteristics will be given here nevertheless. The outline of the aperture is usually orbicular, a different shape being simulated depending on the degree of abrasion. The frontal shields of single zooecia cannot be described in detail due to rather poor preservation. Kühn (1925) mentioned already the occurrence of ovicells in his material from Gauderndorf, but unfortunately he did not give any closer description. Neither in Pouyet (1973) nor in David and Pouyet (1974) are ovicells mentioned: 'ovicelle inconnue'. In material collected at Hlohovec a number of ovicells could be observed and described (Vávra 2004). Suboral avicularia are discussed by Pouyet (1973), of rather greater taxonomical interest would be the occurrence of interzooecial avicularia; in this respect Pouyet (1973) suggested that rather large, oval-shaped orifices may correspond to (former) interzooecial avicularia. According to some sort of a 'ranking list' as given by Pouyet (1973) the shape of the zoarium is one of the poorest morphological criteria – but in respect to *Cellepora polythele* this is sometimes most obvious and – even if the state of preservation is rather poor – the only one criterium to be observed. A critical remark must be added however: the type of zoarium as shown by *Cellepora polythele* is rather often the only criterium for the occurrence of this taxon at any one locality. Careful further studies are required, however, to confirm such determinations; such data may therefore have only a preliminary character sometimes. As already mentioned by Hayward and Ryland (1999) such types of nodular zoaria may also occur in *Turbicellepora*, to give but one example.

Distribution: New finds of *Cellepora polythele* at localities belonging to the early Miocene confirmed an earlier occurrence of this taxon, which had first been established for the Badenian. In respect to the occurrence of this taxon in several other countries (Egypt, France, Hungary, Italy, San Marino) no revision can be given, mainly due to the lack of material.

Cellepora **cf.** *pumicosa* (Pallas, 1766)

cf. *Millepora pumicosa* Pallas, 1766: p. 254.
cf. *Cellepora pumicosa* (Pallas) – Hayward and Ryland 1999: p. 320, figs. 147, 148 A,B.

Material Examined: Small pisiform zoaria (12 specimens) from Brugg (Lower Austria).

Description/Discussion: A few zoaria from Brugg show a rather striking similarity to this taxon: the shape of the primary orifice being of circular form showing sometimes at its proximal edge a sinuate, shallowly concave widening. Very often avicularia are developed as a conspicuous spiked process. Lateral avicularia are sometimes situated at the top of columnar-like elevations, almost perpendicular to the orifice plane. Such specimens are sometimes very similar to *Celleporina hassallii* indeed.

Distribution: Eggenburgian (early Miocene).

Genus *Celleporina* Gray, 1848

Celleporina sp.
(Fig. 1, B , E , F)

Among material from Brugg a number of 'pisiform' zoaria could be found which show, depending on their degree of abrasion, a number of morphological details giving a fair chance to attribute them to the genus *Celleporina*. The size of these zoaria being rather small (e.g. Fig. 1, E), a number of details can be observed, however. The primary orifices show a distinct sinuate shape of different width, and there are often remainders of (sometimes paired), flanking adventitious avicularia to be observed (Fig. 1, B, E). The pictured ooecium (Fig. 1, D) is strikingly similar to pictures as given by Hayward and Ryland (1999) for *Celleporina.* Also in respect to vicarious avicularia two different types do occur: a rather tiny with a 'key-hole-like' shape and a rather big one of a rather broadly spatulate shape (Fig. 1, F). In this respect it is worth mentioning that pisiform zoaria of small size have been mentioned already by Schneider *et. al.* (2009) from the Ottnangian of Bavaria; they compared them with *Celleporina caminata* from Recent Mediterranea faunas but did neither give any closer descriptions nor any picture. This is at any case an item to be followed in the course of future research. At the moment this rather short description together with a few pictures given must be sufficient.

Genus *Turbicellepora* Ryland, 1963

Turbicellepora coronopus (Wood, 1844)

Cellepora coronopus Wood, 1844: p. 18.
Schismopora coronopus (Wood) – Kühn 1925: p. 30.
Osthimosia coronopus (Wood) – Lagaaij 1952: p. 137
Turbicellepora coronopus (Wood) – Pouyet 1973: pp. 105-107.
Turbicellepora coronopus (Wood) – David and Pouyet 1974: pp. 212-213.
Turbicellepora coronopus (Wood) – Vávra 1977: p. 157.
Turbicellepora coronopus (Wood) – Hayward 1978: pp. 575-577, Fig. 13.
Turbicellepora coronopus (Wood) – Zágoršek 2010: pp. 160-161, pl. 126, fig.1-5.

Lectotype: coll. Wood, NHMUK B.1606 (chosen by Lagaaij 1952), pictured by Busk (1859: pl. 9, fig. 1a).

Type locality: Sutton (Suffolk, England, Great Britain)

Stratum typicum: Coralline Crag, Pliocene.

Material: Collection Reuss/Manzoni (NHMW-1859.L.758,), MP-coll. Canu (Paris), Pouyet (FSL-130371, 130390, 130396, 130434), David and Pouyet (FSL-260262, 260675).

Description: The description as given by Hayward (1978) for recent material from Europe is also valid for fossil material from Austria so far.

Discussion: A first report concerning the occurrence of this taxon in the early Miocene of Austria has been given already by Kühn (1925: 30) based on material from Klein-Meiseldorf. This occurrence is also reported by Vávra (1977) based on material curated in the collections of Vienna (NHMW-1859.L.758). Following a few critical remarks as given by Zágoršek (2010) in respect to the morphology of finds from the Miocene in general makes a revision of the occurrence of this species necessary in the future.

Distribution: Eggenburgian (early Miocene): Klein-Meiseldorf (Lower Austria), Badenian (middle Miocene): Eisenstadt (Burgenland), Baden (Lower Austria), Miocene (General): Egypt, France, Italy, Poland, Portugal, Slovakia (Devínsjka Nová Ves). Pliocene: England, Italy, Netherlands, Pleistocene: Greece (Rhodes), Italy.
Recent: Atlantic Ocean (England to Morocco), Mediterranean Sea.

Turbicellepora krahuletzi (Kühn, 1925)
(Fig. 1, A)

Schismopora Krahuletzi nov.sp., Kühn, 1925: p. 30, text-fig. 7, pl. 2, fig.6.

Schismopora krahuletzi Kühn – Udin 1964: p. 413, pl. 2, fig. 3.

Turbicellepora krahuletzi (Kühn) – Pouyet 1973: pp. 107–108, pl. 13, fig. 5, pl. 19, fig. 5.

Turbicellepora krahuletzi (Kühn) – David and Pouyet 1974: p. 213.

Turbicellepora krahuletzi (Kühn) – Vávra 1977: p. 158.

Material Examined: Type material kept at Krahuletz-Museum, Eggenburg, Lower Austria: cannot be relocated, possibly lost?
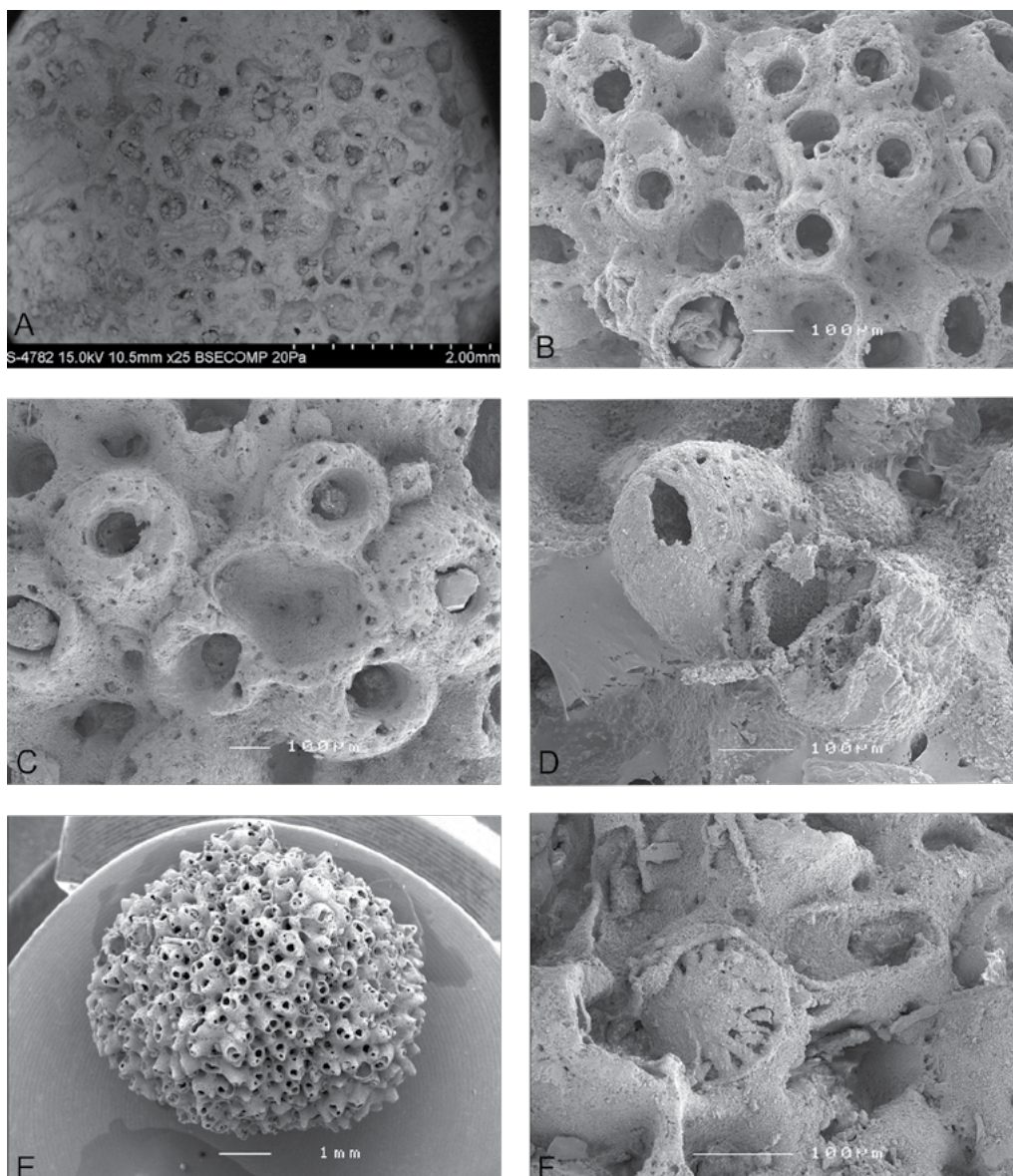
Figure 1. (A) *Turbicellepora krahuletzi* (Paratype): showing the extremely poor preservation, uncoated specimen (Grübern, GBA No.2007/208/5). **(B)** *Celleporina* sp.: sinuate primary orifices, traces of suboral avicularia, interzooecial, keyhole-shaped avicularium. **(C–D)** Turbicellepora sp.: two paired, suboral avicularia, primary orifice with a slit-like sinus, ovicell with a few scattered pores **(E–F)** Celleporina sp., ovicell and spatulate, interzooecial avicularium.

Paratype: Austrian Geological Survey (= Geologische Bundesanstalt): No. 2007/208/5.

Coll. Udin (Inst. for Palaeontology, University of Vienna): UWPI-2307.

Further material (not studied by the author): FSL-130385 (Pouyet, 1973: pl. 13, fig. 5, pl. 19, fig. 5), 130386, 130432, 130393, 130432, 260671 (David and Pouyet, 1974).

Type Locality: Grübern near Maissau, Lower Austria.

Stratum Typicum: Eggenburgian (early Miocene).

Occurrence: Eggenburgian (early Miocene): Grübern (type locality).
Badenian (middle Miocene): Eisenstadt, Oslip (both: Burgenland), Steinebrunn (Lower Austria).

Description: Original description, as given by Kühn (1925: 30), translated by the author – "Big colonies, globular or egg-shaped, diameter up to 5 cm, at the basis often showing a recess. The zooecia are erect, little prominent. The opening (aperture) is circular and has a diameter of 0.16-0.2 mm; adjacent to it is situated a smaller avicularium with a diameter of 0.05-0.08 mm. The aperture has a broad, flat margin with an irregular, somewhat triangular outline. Interzooecial avicularia do not occur. The species is reminiscent in respect to shape of colony, triangular outline of the border of the aperture and by the missing interzooecial avicularia of *Schismopora globosa* from the North American Paleogene; it differs however from this species by the considerable larger size of colonies, the circular aperture (in *S. globosa* it is oval) and the smaller avicularia (in *S. globosa* same size as aperture). *Schismopora Krahuletzi* is one of the most common bryozoa at Grübern."

Redescription/Criticism:
This description is at any case insufficient according to standards of modern taxonomy: the holotype being not available, the probable paratype (GBA 2007/208/5) being poorly preserved (Fig. 1A), and the only one modern revision (Pouyet 1973) being subject to some criticism. This revision has been done on the basis of material from Eisenstadt and possibly also from Steinebrunn (both localities: Badenian, i.e. Middle Miocene) – both localities not identical with the type area of this species. Thus this modern description represents something like a personal opinion of this author, what this species may have looked like. Anyway at present a really satisfactory solution of this problem is not possible. Extensive collecting activities in the type area (Grübern, sand-pit Fiedler) performed by the author achieved some results, however. Among hundreds of celleporid zoaria most are simply undeterminable. One remarkable result of all this rather time-consuming activities has been the fact that there resulted something like a 'taxonomic feeling' what *Turbicellepora krahuletzi* may have looked like. According to Kühn this taxon is the most common species at Grübern, according to my personal experience it is certainly the most common in the whole Eggenburgian (early Miocene) at all. In fact material from other bryozoan localities of comparable age and not very far away from the type area has contributed to these studies essentially: Oberdürnbach near Maissau and Brugg, being situated in a somewhat greater distance from the type area of Grübern are to be mentioned. *T. krahuletzi* has, in the meantime, been identified also in material from Pulkau.

The general problem with material from the type area is the preservation, i.e. the state of fossilization achieved already. The marginal pores on the frontal shield – one of the characteristics of the genus – are not visible due to calcification processes. The shape of the primary orifice showing the proximal sinus, the laterally situated avicularia are mostly not to be seen, however, due to heavy abrasion of the surface. An additional and important problem is the occurrence of any vicarious large avicularia with their spatulate mandibles. Pouyet (1973) has obviously been the very first author to describe them – Kühn, however, mentioned their absence. Pouyet found them on zoaria from the Badenian, which, however, has already been criticized (see above). We

have now observed a few of them in zoaria from the Eggenburgian (early Miocene), they are obviously rather rare and situated close to the branching of arborescent zoaria. In any case, according to our own observations, *Turbicellepora krahuletzi,* is in respect to its morphology very close to *T. coronopus*: this seems to be also true for its vicarious avicularia. In *T. coronopus* they are rather common, whereas in *T. krahuletzi* they are rather rare – in both taxa they are of nearly identical shape, however. Unfortunately until now we cannot give any details concerning the ovicells (they have still not been found) and in respect to any basal pore-chambers. A first step into this direction may be the discovery of an ovicell of the type to be expected for *Turbicellepora* (Fig. 1, D).

MATERIAL/ABBREVIATIONS

Specimens mentioned are curated in collections of the following institutions:

GBA: Collections of the Austrian Geological Survey, Vienna;

FSL: Collections of the Laboratoire de Géologie de Lyon, Faculté des Sciences, Lyon;

MP: collections of the Galerie de Paléontologie et d'Anatomie Comparée, (coll. Canu, Buge, Michelin);

NHMUK: Collections of the British Museum of Natural History, London.

NHMW: Collections of the Museum of Natural History, Vienna, Geology & Palaeontolgy Department;

UWPI: Collections kept at the Institute of Palaeontology, Geozentrum, University of Vienna; most material of these collections will be transferred to the Museum of Natural History, Vienna in the near future.

ACKNOWLEDGEMENTS

REFERENCES

BRAGA, G. 1963. I Briozoi del Terziario Veneto. Ie contributo. *Bollettino della Società Paleontologica Italiana* **2**(1), 16–55.

BRAGA, G. 1988. Les Bryozoaires du Priabonien Stratotypique (Province Vicenza, Italie). *Revue de Paléobiologie* **7**(2), 495–556.

BRONN, H.G. 1837. *Lethaea geognostica. Oder Abbildungen und Beschreibungen der für die Gebirgsformationen bezeichnendsten Versteinerungen. Erster Band, Dritte Periode, Oolith- Gebirge*, 2. Aufl., Stuttgart, Schweizerbart, pp. 195–544.

BUSK, G. 1859. *A monograph of the Fossil Polyzoa of the Crag.* London, Monographs of the Palaeontological Society of London.

CANU, F. AND BASSLER, R.S. 1927. Classification of the Cheilostomatous Bryozoa. *Proceedings of the U.S. National Museum* **69**(14), 1–42.

CANU, F. AND LECOINTRE, G. 1925. Les Bryozoaires cheilostomes des Faluns de Tourraine et d'Anjou. *Mémoires de la Societé Géologique de France, n.s.* **3**. 1–18.

DAVID, L. AND POUYET, S. 1974. Révision des Bryozoaires cheilostomes miocènes du Bassin de Vienne – Autriche. *Documents des Laboratoires de Géologie de la Faculté des Sciences de Lyon* **60**, 83–257.

GRAY, J.E. 1848. *List of the Specimens of the British Animals in the Collection of the British Museum. Centroniae or Radiated Animals.* London, British Museum.

HAYWARD, P. 1978. Systematic and morphological studies on some European species of *Turbicellepora* (Bryozoa, Cheilostomata). *Journal of Natural History* **12**, 551–590.

HAYWARD, P.J. AND RYLAND, J.S. 1999. Cheilostomatous Bryozoa Part 2 Hippothooidea – Celleporoidea. In: R.S.K. Barnes and J.H. Crothers (eds), *Synopses of the British Fauna (New Series), No. 14 (Second Edition).* London, Linnean Society of London etc. pp. 1–416.

JOHNSTON, G. 1838. *A history of the British Zoophytes,* 2nd edition. Edinburgh, Lizars, London and Dublin, Curry, pp. 1-341.

KEY, M.M., JR., ZÁGORŠEK, K. AND PATTERSON, W.P. 2012. Paleoenvironmental reconstruction of the Early to Middle Miocene Central Paratethys using stable

isotopes from bryozoan skeletons. *International Journal of Earth Science* **102**(1), 305–318.

KÜHN, O. 1925. Die Bryozoen des Miocäns von Eggenburg. In: F.X. Schaffer (ed.), DasMiocän von Eggenburg. *Abhandlungen der k. und k. Geologischen Reichsanstalt* **22**(3), 21–39.

KÜHN, O. 1955. Die Bryozoen der Retzer Sande. *Sitzungsberichte der Österreichischen Akademie der Wissenschaften, Mathematisch-Naturwissenschaftliche Klasse, Abteilung 1* **164**(4, 5), 231–248.

LAGAAIJ, R. 1952. The Pliocene Bryozoa oft he Low Countries and their Bearing on the Marine Stratigraphy of the North Sea Region. *Mededelingen van de geologische Stichting, Serie C,* V – **5**, 1–233.

LAMOUROUX, J.V.F. 1821. *Exposition méthodique des genres de l'ordre des polypiers avec leur description et celles des principales espèces figurées dans 84 planches; les 63 premiere de zoophytess appartenant a l'histoire naturelle des zoophytes d'Ellis et Solander.* Paris, V, Agasse.

LINNAEUS, C. 1767. *Systema Naturae, per regna tria naturae: secundum classes, ordines, genera, species….. ed. 12.* Holmiae [= Stockholm].

MANZONI, A. 1877. I Briozoi fossili del Miocene d'Austria ed Ungheria, II. *Denkschriften der Kaiserlichen Akademie der Wissenschaften, Mathematisch-naturwissenschaftliche Classe* **37**, 49–78.

PALLAS, P.S. 1766. *Elenchus zoophytorum sistens generum adumbrations generaliores et specierum cognitarum succintas descriptiones cum selectis auctorum synonymis.* Hagae Comitum, Petrum van Cleef.

POUYET, S. 1973. Révision systématique des Cellépores (Bryozoa, Cheilostomata) et des espèces fossiles Européennes. Analyse de quelques populations à Cellépores dans le Néogène du Bassin Rhodanien. *Documents des Laboratoires de Géologie de la Faculté des Sciences de Lyon* **55**, 1-266.

REUSS, A.E. 1847. Die fossilen Polyparien des Wiener Tertiärbeckens. *Naturwissenschaftliche Abhandlungen* **2**, 1–109.

RYLAND, J.S. 1963. Systematic and biological studies on Polyzoa (Bryozoa) from western Norway. *Sarsia* **14**, 1–59.

SCHNEIDER, S., BERNING, B., BITNER, M.A., CARRIOL, R-P., JÄGER, M, KRIWET, J., KROH, A. AND WERNER, W. 2009. A parautochthonous shallow marine fauna from the Late Burdigalian (early Ottnangian) of Gurlan (Lower Bavaria, SE Germany): Macrofaunal inventory and paleoecology. *Neues Jahrbuch für Geologie und Paläontologie. Abhandlungen* **254**(1-2), 63–103.

SMITT, F.A. 1872. Floridan Bryozoa collected by Count L.F. de Pourtalès, I. *Konglinga Svenska Vetenskaps-akademiens Handlingar.* **10**(11), 1–20.

STEININGER, F. AND SENEŠ, J. 1971. *M1 Eggenburgien. Die Eggenburger Schichtengruppe und ihre Stratigraphie. Chronostratigraphie und Neostratotypen, Miozän der zentralen Paratethys 2.* Bratislava, Vydavatelstvo Slovenskej akadémie vied.

UDIN, A.R. 1964. Die Steinbrüche von St.Margarethen (Burgenland) als fossiles Biotop. I. Die Bryozoenfauna. *Sitzungs-Berichte der österreichischen Akademie der Wissenschaften, mathematisch-naturwissenschaftliche Klasse, Abt. 1* **173**, 383–439.

VÁVRA, N. 1977. Bryozoa tertiaria. In: H. Zapfe (ed.), *Catalogus Fossilium Austriae, Vb/3.* Wien, Österreichische Akademie der Wissenschaften, pp. 210.

VÁVRA, N. 2004. *Cellepora polythele*, a cheilostomate bryozoan species from the Neogene of Moravia (Czech Republic). *Scripta Facultatis Scientiarum Naturalium Universitatis Masarykianae Brunensis* **31-32**(2001-2002), 23–33.

VÁVRA, N. 2008. Bryozoans of the Retz Formation (Early Miocene, Austria) – a high-energy environment case study. In: S.J. Hageman, M.M. Key, jr. and J.E. Winston (eds), *Bryozoan Studies 2007.* Proceedings of the 14th International Bryozoology Association Conference, Boone, North Carolina, July 1-8, 2007. *Virginia Museum of Natural History, Special Publications* **15**, 311–319.

VÁVRA, N. 2013. The use of Early Miocene Bryozoan Faunal Affinities in the Central Paratethys for inferring climatic change and seaway connections. In: A. Ernst, P. Schäfer and J. Scholz (eds), *Bryozoan Studies 2010.* Berlin, Heidelberg, Springer, pp. 401–418.

VIGNEAUX, M. 1949. Révision des Bryozoaires néogènes du Bassin d'Aquitaine et essai de classification. *Mémoires de la Societé géologique de France* (=Mém.60), Paris, N.S. **28** (1-3): 1–155.

WESSELY, G. 2006. *Geologie der österreichischen Bundesländer. Niederösterreich.* Wien, Geologische Bundesanstalt.

WOOD, S.V. 1844. Descriptive Catalogue of the Zoophytes from the Crag. *Annals and Magazine of Natural History (1)* **13**, 10–21.

ZÁGORŠEK, K. 2010. Bryozoa from the Langhian (Miocene) of the Czech Republic. Part I: Geology of the studied sections, systematic description of the orders Cyclostomata, Ctenostomata and "Anascan" Cheilostomata (Suborders Malacostega Levinsen, 1902 and Flustrina Smitt, 1868). Part II: Systematic description of the Suborder Ascophora Levinsen, 1909 and paleoecological reconstruction of the studied environment. *Sborník Národního Muzea v Praze, Rada B – Přírodni védy* **66** (1-4), 1–255.

Bryozoan Skeletal Index (BSI): a measure of the degree of calcification in stenolaemate bryozoans

Patrick N. Wyse Jackson[1]*, Marcus M. Key, Jr.[2] and Catherine M. Reid[3]

[1] Department of Geology, Trinity College, Dublin 2, Ireland
[*corresponding author: e-mail: wysjcknp@tcd.ie]
[2] Department of Earth Sciences, Dickinson College, Carlisle, Pennsylvania 17013-2896, USA
[e-mail: key@dickinson.edu]
[3] School of Earth and Environment, University of Canterbury, Private Bag 4800, Christchurch, New Zealand [e-mail: catherine.reid@canterbury.ac.nz]

ABSTRACT

The Upper Ordovician of the Cincinnati Arch region of the United States has yielded a highly diverse bryozoan fauna, and which provides an excellent data source for use in this study that proposes a novel measure of the degree of skeletal material in Palaeozoic stenolaemate bryozoans. This study is based on 16 trepostome species and one cystoporate species described from the Dillsboro Formation (Maysvillian to early Richmondian, Cincinnatian) of Indiana and in 20 species (15 trepostomes and five cystoporates) from the Lexington Limestone and Clays Ferry Formation (Middle to Upper Ordovician respectively) of Kentucky. The Bryozoan Skeletal Index (BSI) is derived from measurement of three characters readily obtainable from colonies: (1) maximum autozooecial apertural diameter at the zoarial surface or in shallow tangential section [MZD], (2) thickness of the zooecial wall between adjacent autozooecial apertures [ZWT], and (3) the exozone width [EW] in the formula:

$$BSI = ((EW*ZWT)/MZD)*100$$

This provides a measure of the relative proportion of skeleton to open space in the exozonal portion of the colony. The endozonal skeletal contribution to the overall colony skeletal budget is regarded as being minimal. In this study the differences observed in BSI between trepostome and cystoporate species in the Cincinnatian is significant, and ramose colonies show a higher BSI than encrusting zoaria in the same fauna.

INTRODUCTION

Bryozoans of the Class Stenolaemata are characterised by having autozooecial chambers that are broadly tubular in nature. They were significant members of the Palaeozoic faunas appearing in the Ordovician when there was a rapid diversification into six orders (Ernst 2019, fig. 1). While the majority of these groups disappeared at the Permo-Triassic boundary, some trepostomes, cystoporates, and one cryptostome survived in reduced diversity into the Triassic (Boardman 1984, Powers and Pachut 2008), while the cyclostomes took advantage of vacated niches and diversified rapidly in the Mesozoic before they declined and members of the Class Gymnolaemata overtook them in terms of diversity (Ernst 2019).

Within the stenolaemates classes, the trepostomes together with the esthonioporids developed the greatest degree of calcification in their colonies, followed by the cystoporates, cryptostomes, and

cyclostomes, whereas the fenestrates were least calcified. All of these orders with the exception of the cyclostomes have recently been assembled together into the subclass Palaeostomata (Ma *et al.*, 2014). As Taylor *et al.* (2015) note, these are skeletally rather different from the cyclostomes which have frontal walls that are calcified.

Key (1990) developed a morphometric approach to quantifying the amount of skeleton in ramose trepostomes colonies using ZWT and MZD compared between the endozone and exozone. That study showed that the endozonal skeletal contribution to the overall colony skeletal budget is minimal. This study takes a more generic approach that is applicable to ramose, encrusting, frondose, and massive stenolaemates of all classes. Herein we establish the Bryozoan Skeletal Index (BSI), a novel measure of the degree of exozonal skeletal material in stenolaemate bryozoans.

This current study is one of a continuum of papers by the authors on various aspects of Cincinnatian bryozoans which together with other recent studies have added to our understanding of the inter-relationship of these bryozoans with endoskeletozoans (Erickson and Bouchard 2003; Wyse Jackson *et al.* 2014; Wyse Jackson and Key 2019) and epizoozoans (Baird *et al.* 1989; Wyse Jackson *et al.* 2014), and the character of their growth, branching and reasons for colony fragmentation (Key *et al.* 2016) as well as their palaeoecological setting (Buttler and Wilson 2018). The Ordovician was a time of calcite seas and bryozoans thrived during the Cincinnatian, so much so that Taylor and Kuklinski (2011) asked whether trepostomes had become hypercalcified at this time. Bryozoans that in life encrusted on living aragonitic molluscs have yielded much information about the host shells that rapidly dissolved in these calcitic seas and their early stage epibionts and endobionts which are known only from the bryoimmurations (Wilson *et al.* 2019). This recent research adds to the wealth of information on Cincinnatian bryozoans published since the late nineteenth century (see Key *et al.* 2016, p. 400 for summary).

Size of bryozoan colonies and skeletal materials have been the focus of various studies that have taken specific avenues. Key (1990, 1991) examined parameters that influenced skeletal size in trepostome bryozoans, Cheetham (1986) showed that Cenozoic cheilostomes developed the ability to thicken branches, and Cheetham and Hayek (1983) discussed the ecological implications of being able to produce robust and erect bryozoan colonies. Key *et al.* (2001) showed how a Permian trepostome with a notably wide exozone achieved this size not by secreting more skeleton but by inserting exilazooecia within maculae. Cuffey and Fine (2005, 2006) reconstructed the largest trepostomes colonies from fragments.

Thus, understanding the architecture and abundance of skeleton in stenolaemates is important for a number of reasons, and the BSI proposed here which is straight forward to derive, allows for rapid comparison between taxa of different stenolaemates. Amongst a number of aspects, the BSI can be utilised as a measure of strength of zoaria and ability to withstand infestation by endoskeletozoans. If a higher BSI allows upward vertical growth with the ramose zoarial habit, then those colonies have access to resources in the water column that are not available to encrusting colonies confined to the substrate (Jackson 1979). The robustness of the BSI is tested here utilising a suite of Ordovician trepostome and cystoporate bryozoans.

MATERIALS
The Cincinnatian of the Upper Ordovician of the United States has yielded a highly diverse bryozoan fauna with a range of morphological forms (Fig. 1) that has been extensively reported since the 1850s, and thus provides an excellent database for use in this study that proposes a novel measure of the degree of skeletal material in Palaeozoic stenolaemate bryozoans.

This study is based on bryozoans described from the Lexington Limestone and Clays Ferry Formation (Middle [Sandbian] to Upper Ordovician [Sandbian-Katian] respectively) of Kentucky (Karklins 1984) and the Dillsboro Formation (Maysvillian to early

Richmondian [Katian], Cincinnatian) of south-eastern Indiana (Brown and Daly 1985). Karklins (1984) reported on 36 species in 22 genera (16 trepostomes and six cystoporates) while Brown and Daly (1985) provided detailed taxonomic descriptions for 53 species in 18 genera of which 17 belonged to the Order Trepostomata and one to the Order Cystoporata. These two taxonomic studies provide a suite of data (a total of 37 species, Table 1) that

allow for initial testing of the robustness of the BSI formula prior to it being utilised in further and larger studies (see below).

METHODS

The Bryozoan Skeletal Index (BSI) is derived from three measures: (1) maximum autozooecial apertural diameter at the zoarial surface or in shallow tangential
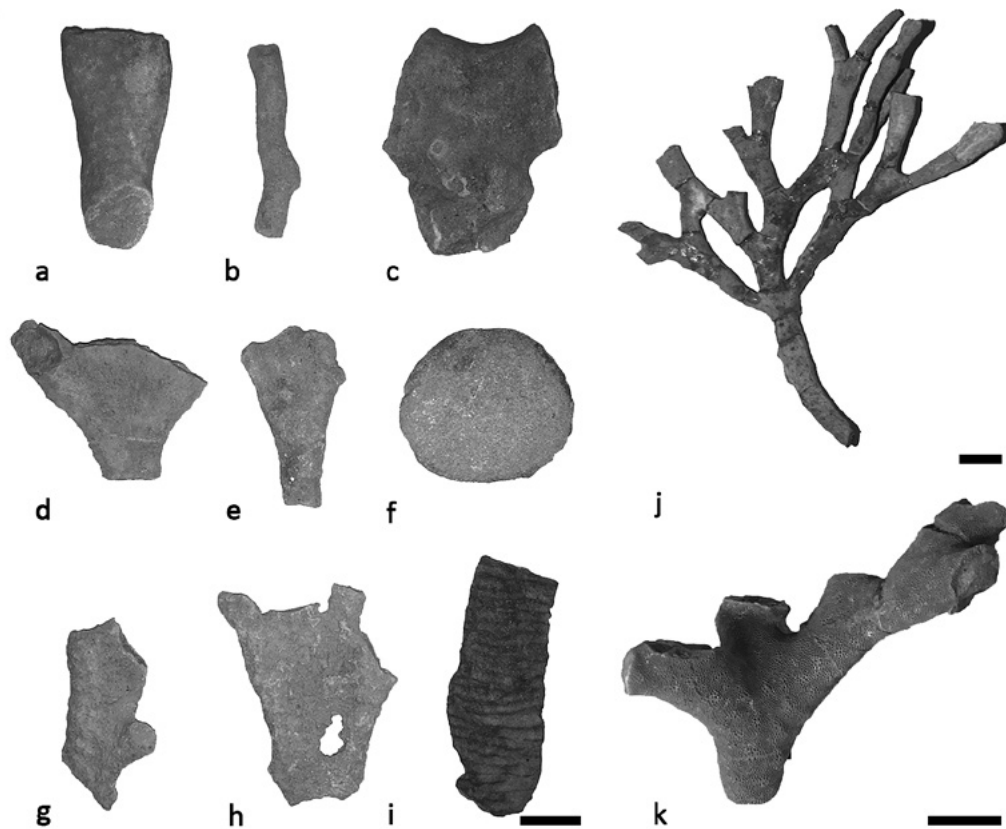

Figure 1. Cincinnatian Bryozoa (a-c) ramose trepostomes; (d-e) foliose trepostomes; (f) domed trepostome; (g-h) foliose cystoporate (*Constellaria* sp.); (i) bifoliate cryptostome (*Escharopora hilli*) from the Lexington Limestone, Kentucky, USA, (a-e, g-i) from Stafford, Kentucky, road-cut on west side highway 150 (37°34.97N 84°42.68W); (f) from Danville, Kentucky, junction 150 and bypass, Danville sign (37°38.73N 84°46.59W), Geological Museum, Trinity College Dublin. (j) re-assembled ramose trepostome *Hallopora andrewsi* (Nicholson, 1874) from Southgate Member, Kope Formation, Western corner of the intersection of Rt. 9 (AA Highway) and Kentucky Rt. 709 (US 27-AA Highway Connector Rd.) adjacent to Alexandria, KY; on slope leading down to Rt. 709; 38.988753°N, 84.396203°W, CMC IP72749. (k) ramose trepostome *Hallopora subplana* (Ulrich, 1882), Mount Hope Member, Fairview Formation, Covington, Kentucky, USNM 40364. (j, from Key et al., 2016, fig. 1.5). Scale bars = 10mm.

Table 1. Bryozoan Skeletal Index (BSI) index for Cincinnatian (Katian) stenolaemate bryozoans. Abbreviations: MZD = mean autozooecial apertural diameter (in mm); EW = mean exozone width (mm); ZWT = mean thickness of the zooecial wall between adjacent autozooecial apertures at zoarial surface or in shallow tangential section (in mm); B & D = Brown and Daly.

Order	Taxon	Zoarial form	MZD	EW	ZWT	BSI	Source	Lithological unit (Stage)
Trepostomata	*Orbignyella lamellosa*	encrusting	0.216	2.976	0.017	23	B & D, 1985	Dillsboro (Katian)
Trepostomata	*Mesotrypa patella*	encrusting	0.216	1.810	0.010	8	B & D, 1985	Dillsboro (Katian)
Trepostomata	*Leptotrypa minima*	encrusting	0.217	2.146	0.010	10	B & D, 1985	Dillsboro (Katian)
Trepostomata	*Monticulipora mammulata*	massive	0.210	2.488	0.015	18	B & D, 1985	Dillsboro (Katian)
Trepostomata	*Peronopora vera*	bifoliate	0.197	2.238	0.049	56	B & D, 1985	Dillsboro (Katian)
Trepostomata	*Amplexopora septosa*	ramose	0.231	1.333	0.038	22	B & D, 1985	Dillsboro (Katian)
Trepostomata	*Parvohallopora ramosa*	ramose	0.220	0.950	0.080	35	B & D, 1985	Dillsboro (Katian)
Trepostomata	*Batostomella gracilis*	ramose	0.154	1.463	0.075	71	B & D, 1985	Dillsboro (Katian)
Trepostomata	*Batostoma varians*	ramose	0.279	2.585	0.098	90	B & D, 1985	Dillsboro (Katian)
Trepostomata	*Cyphotrypa madisonensis*	ramose	0.287	1.317	0.015	7	B & D, 1985	Dillsboro (Katian)
Trepostomata	*Dekayia catenulata*	ramose	0.199	1.503	0.018	14	B & D, 1985	Dillsboro (Katian)
Trepostomata	*Nicholsonella vaupeli*	ramose	0.271	0.976	0.065	23	B & D, 1985	Dillsboro (Katian)
Trepostomata	*Rhombotrypa quadrata*	ramose	0.250	1.050	0.033	14	B & D, 1985	Dillsboro (Katian)
Trepostomata	*Stigmatella interporosa*	ramose-frondescent	0.213	0.650	0.020	6	B & D, 1985	Dillsboro (Katian)
Trepostomata	*Heterotrypa subfrondosa*	frondescent	0.204	1.303	0.029	19	B & D, 1985	Dillsboro (Katian)
Trepostomata	*Homotrypa flabellaris*	frondescent	0.163	1.415	0.047	41	B & D, 1985	Dillsboro (Katian)
Cystoporata	*Constellaria polystomella*	frondescent	0.133	1.317	0.062	61	B & D, 1985	Dillsboro (Katian)
Trepostomata	*Mesotrypa angularis*	domal	0.2450	5.9000	0.0360	87	Karklins, 1994	Lexington Ls. (Sandbian)
Trepostomata	*Cyphotrypa acervulosa*	globular	0.2687	2.5000	0.0110	10	Karklins, 1994	Lexington Ls. (Sandbian)
Trepostomata	*Prasopora falesi*	hemispherical	0.2513	3.0000	0.0173	21	Karklins, 1994	Lexington Ls./Clays Ferry Fm. (Sandbian-Katian)
Trepostomata	*Peronopora vera*	bifoliate	0.1860	1.6180	0.0583	51	Karklins, 1994	Lexington Ls./Clays Ferry Fm. (Sandbian-Katian)
Trepostomata	*Homotrypella granulifera*	ramose	0.1380	1.3110	0.0880	84	Karklins, 1994	Lexington Ls. (Sandbian)
Trepostomata	*Parvohallopora nodulosa*	ramose	0.2296	0.7529	0.0718	24	Karklins, 1994	Lexington Ls./Clays Ferry Fm. (Sandbian-Katian)
Trepostomata	*Eridotrypa mutabilis*	ramose	0.1888	0.9370	0.0961	48	Karklins, 1994	Lexington Ls./Clays Ferry Fm. (Sandbian-Katian)
Trepostomata	*Tarphophragma multitabulata*	ramose	0.2552	0.7188	0.0470	13	Karklins, 1994	Lexington Ls. (Sandbian)
Trepostomata	*Heterotrypa foliacea*	ramose	0.1950	1.2200	0.0496	31	Karklins, 1994	Lexington Ls./Clays Ferry Fm. (Sandbian-Katian)
Trepostomata	*Homotrypa cressmani*	ramose	0.1260	1.0200	0.0840	68	Karklins, 1994	Lexington Ls./Clays Ferry Fm. (Sandbian-Katian)
Trepostomata	*Atactoporella newportensis*	ramose	0.1500	0.2125	0.0580	8	Karklins, 1994	Lexington Ls./Clays Ferry Fm. (Sandbian-Katian)
Trepostomata	*Amplexopora* aff. *winchelli*	ramose	0.2078	1.7000	0.0367	30	Karklins, 1994	Lexington Ls. (Sandbian)
Trepostomata	*Balticopora tenuimurale*	ramose	0.2665	1.3000	0.0429	21	Karklins, 1994	Lexington Ls./Clays Ferry Fm. (Sandbian-Katian)
Trepostomata	*Dekayia epetrima*	ramose	0.2120	3.0000	0.0240	34	Karklins, 1994	Lexington Ls. (Sandbian)
Trepostomata	*Stigmatella multispinosa*	subconical	0.2095	0.8333	0.0140	6	Karklins, 1994	Lexington Ls. (Sandbian)
Cystoporata	*Ceramoporella distincta*	encrusting	0.2915	0.3963	0.0260	4	Karklins, 1994	Lexington Ls. (Sandbian)
Cystoporata	*Crepipora venusta*	encrusting	0.2530	0.5800	0.0452	10	Karklins, 1994	Lexington Ls./Clays Ferry Fm. (Sandbian-Katian)
Cystoporata	*Acanthoceramoporella valliensis*	globular	0.2300	1.0500	0.0288	13	Karklins, 1994	Lexington Ls. (Sandbian)
Cystoporata	*Ceramophylla alternatum*	ramose?	0.2133	0.5000	0.0940	22	Karklins, 1994	Lexington Ls./Clays Ferry Fm. (Sandbian-Katian)
Cystoporata	*Constellaria teres*	ramose	0.1198	1.8333	0.0175	27	Karklins, 1994	Lexington Ls./Clays Ferry Fm. (Sandbian-Katian)

section [MZD], (2) thickness of the zooecial wall between adjacent autozooecial apertures [ZWT], and (3) the width of the exozone [EW] all measured in mm (Fig. 2). Parameter 1 is a measure of the open space in the exozonal region, whereas parameters 2 and 3 are features of largely solid skeletal material.

$$BSI = ((EW*ZWT)/MZD) *100$$

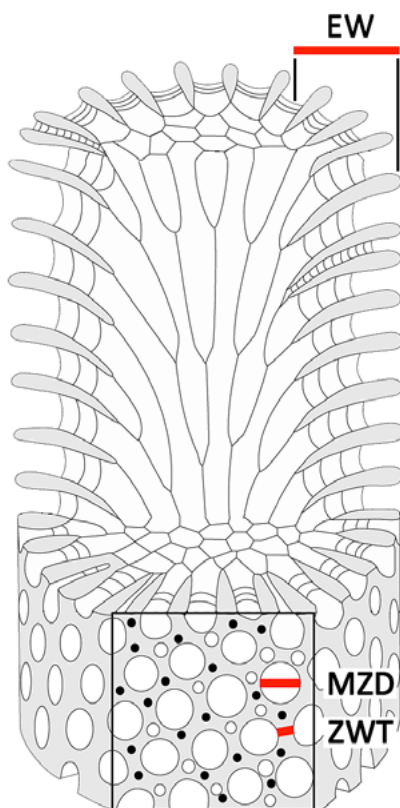The resultant computation is multiplied by 100 so as to give a whole number.

Figure 2. Morphological characters used to compute the Bryozoan Skeletal Index (BSI) (modified from Ernst and Carrera 2012, after Boardman 1984). Abbreviations: MZD: maximum autozooecial apertural diameter at the zoarial surface or in shallow tangential section; ZWT: thickness of the zooecial wall between adjacent autozooecial apertures; EW: thickness of the exozone.

In many of these stenolaemate bryozoans, colonies are made up of an innermost endozone with thinner walls surrounded (or overlain as in the case of encrusting zoaria) by an outer exozonal rim of thickened skeleton. In contrast to these, in some globular and dome-shaped trepostomes such as *Diplotrypa* the endozone comprises a thin, recumbent layer at the base and exozonal walls generally are thin. In any one taxon, the thickness of the exozone is given to remain proportionally constant to that of the colony diameter.

The three parameters above were chosen to provide a measure of the relative proportion of skeleton to open space in the exozonal portion of the colony. No endozone parameters (e.g., endozone diameter, branch diameter, axial ratio, etc.) were included as the zooecial walls in the endozone of trepostomes are significantly thinner (i.e., less skeletalised) than those in the exozone (Key 1990, fig. 3). The endozonal skeletal contribution to the overall colony skeletal budget is considered to be minimal. Axial Ratio (Boardman 1960, p. 21) may be calculated from ramose colonies but not from encrusting forms. Additionally, adoption of this measure is problematic as it cannot be computed in zoaria that have been subjected to post-depositional crushing, where the endozone collapses but the exozonal width is unaffected (Key *et al.* 2016, fig. 2.6). This would reduce the number of specimens collected from many faunas that otherwise could be added to the data suite.

Details of these three parameters are usually reported in taxonomic literature as they are easy to acquire. For this study, data was taken from only one species per genus reported in Karklins (1984) and Brown and Daly (1985); that for which data on each of the relevant parameters was selected, and where several taxa presented this complete data, the type species if described was favoured. Otherwise, then the species for which the greatest number of morphometric measurements was reported was selected; an abundant species is most likely to yield robust morphometric data on the three parameters than from a rarer species. Karklins (1984) tabulated

data for primary types separately to that for hypotypes (specimens not part of the original type suite), and in this case we selected the morphometric data derived from the largest number of measurements, which resulted in not necessarily selecting data from primary holotypes or paratypes. Where not all relevant character values for BSI computation were reported in the published data tables, these were obtained from the figured plates where scale bars scales were provided, or by collating data from a suite of specimens reported in the papers.

During data gathering for this study, additional information was compiled on lithostratigraphy (from the original publication), chronostratigraphic stage (Haq 2007), geological age (Cohen *et al.* 2013), and palaeolatitude (van Hinsbergen *et al.* 2015). This will allow for the determination of trends in the BSI through space and time in a further on-going study to be published elsewhere.

It may be considered that the BSI would be more accurate if it was based on three-dimensional characters such as the volume of space occupied by autozooecial, mesozooecial or exilazooecial chambers, as well as the volume of exozonal and endozonal walls, the portions of acanthostyles that extend beyond the surficial margins of autozooecial walls, and any intrazooecial features such as widely spaced monilae in the exozone, skeletal diaphragms, hemiphragms, and cystiphragms (Boardman 2001; Boardman and Buttler 2005). The effect of these features on the BSI values could be computed by adding those additional characters composed of solid skeleton such as acanthostyles to the left-hand side of the equation alongside EW and ZWT and those of the open spaced features (exilazooecia and mesozooecia) to the right-hand side in combination with MZD. Similarly, the effect of maculae on skeletal volume could be tested. Some monticulate maculae may be skeletal rich (Fig. 1g-h), whereas others that contain numerous exilazooecia and which are flush with the zoarial surface probably add little to the skeletal budget of zoaria (Fig. 3g). For this paper, that establishes the BSI, it was felt prudent to derive a simple equation and to test its

effectiveness. The equation as proposed nonetheless allows for additional extrazooidal characters such as those outlined above, to be added in the future as desired.

The overall geometry of autozooecial chambers varies from taxon to taxon, with many chambers being cone-shaped and others more parallel sided and so cylindrical in form. Quantification of three-dimensional volumes would be complex, time-consuming and prone to high levels of measurement error. Many trepostome taxa possess autozooecial and mesozooecial chambers that contain intrazooecial divisions such as diaphragms (e.g., *Hallopora*) and cystiphragms (e.g., *Prasopora*), and cystoporate genera typically possess vesicular tissue between adjacent autozooecial chambers. For the purpose of this study we consider that the overall volume contributed by these intra- and extrazooecial elements to be negligible compared to the volume of skeleton contained in the autozooecial walls throughout the depth of the exozone. Boardman (2001) noted that structural diaphragms can be extensively developed in some trepostome taxa, although these are very narrow and so contribute low levels of skeleton overall. If necessary a factor could be added to the BSI calculation to account for their development in some taxa. Users applying the BSI should also note that proximal portions of colonies may have thickened walls and endozones compared to younger distal regions, and measuring in areas of macular development may modify the resultant BSI values. Additionally, while the monographs utilised in this study are detailed, information on all the intra and extra-zooecial parameters above is rarely provided for every taxon.

Supporting greater accuracy to BSI calculations would be to consider the nature of the skeletal ultrastructure, which as Taylor *et al.* (2015) reviewed is somewhat varied within the members of the Palaeostomata and more so between them and the other stenolaemate order, the cyclostomes. In this study we have not attempted to quantify palaeostomate ultrastructure, and it has not been used as a BSI parameter.

RESULTS

The BSI of these 37 Cincinnatian stenolaemates ranges from values of 4 to 90 (mean = 30.5; standard deviation = 24.2, Table 1). The lowest BSI in an encrusting species was 4 in the cystoporate *Ceramoporella distincta* from the Lexington Limestone whereas the highest was 23 in the trepostome *Orbignyella lamellosa* (Fig. 3a-b) from the Dillsboro Formation. In ramose trepostomes the lowest BSI was 6 in *Stigmatella interporosa* (Fig. 3i-k) and the highest was 90 in *Batostoma*

varians (Fig. 3e-f) both from the Dillsboro. One species *Peronopora vera* which formed bifoliate colonies was common to both of the original studies investigated with the BSI 51 in the Lexington Limestone/Clays Ferry material and slightly higher at 56 in the Dillsboro Formation.

Encrusting bryozoans in the stratigraphically older successions of Kentucky recorded BSIs of 4–10 (n = 2, mean = 7.0, standard deviation = 4.9) as compared to those from the younger Dillsboro Formation of Indiana with BSI of 8–23 (n=3,
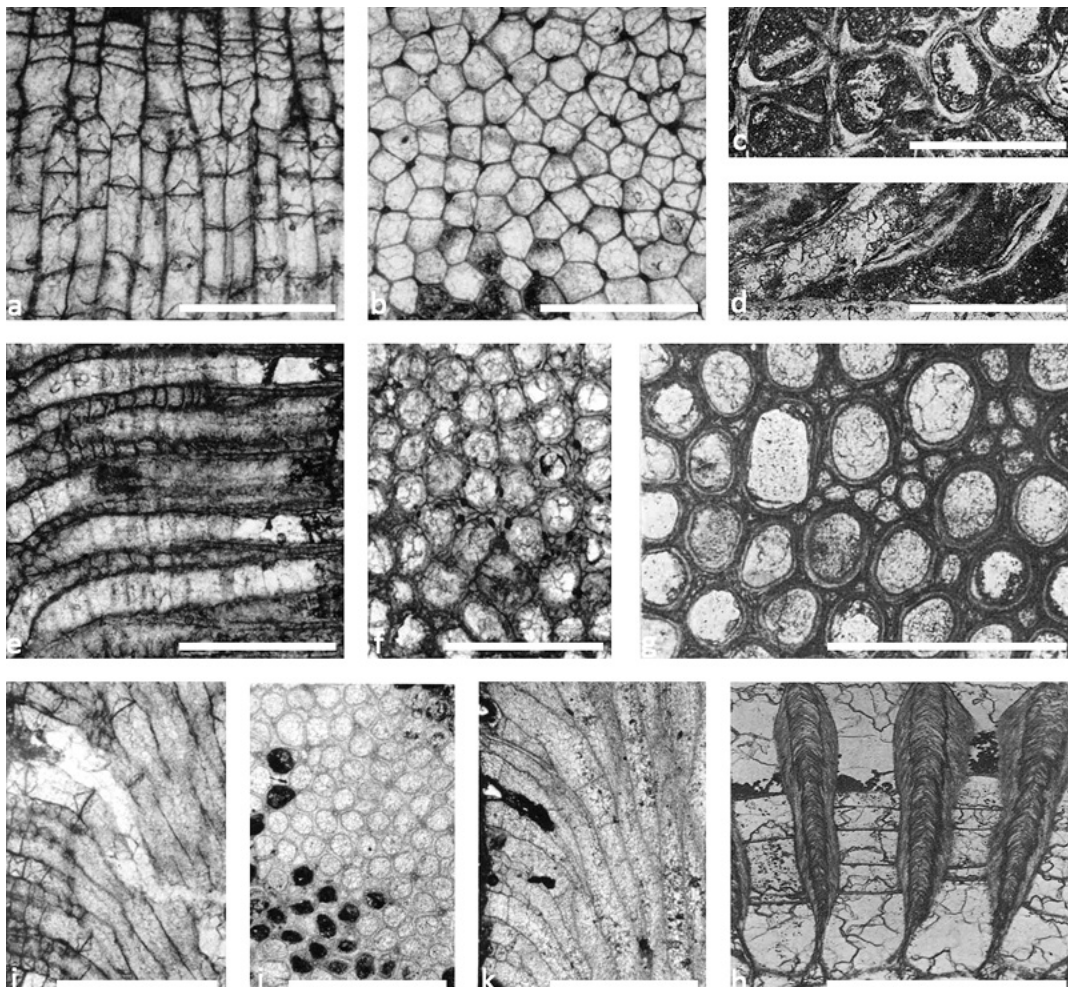

Figure 3. (a-d) Encrusting bryozoans; (e-k) Ramose bryozoans. (a-b) *Orbignyella lamellosa* (Ulrich, 1890); (c-d) *Crepipora venusta* (Ulrich, 1878); (e-f) *Batostoma varians* (James, 1878), (g-h) *Parvohallopora ramosa* (d'Orbigny, 1850); (i-k) *Stigmatella interporosa* Ulrich and Bassler, 1904. [c-d, g-h from Karklins, 1984; a-b, e-f, i-k from Brown and Daly, 1985). Scale bars = 0.5mm (c, d, h), 1mm (a, b, e-f, i-k).

mean= 13.9, standard deviation=8.3). Ramose bryozoans in the two units exhibited nearly identical BSI ranges: 8–84 (n = 13, mean = 31.9, standard deviation=22.6) as against 6–90 (n = 14, mean = 31.3, standard deviation = 29.8). Domed, globular, massive or hemispherical zoaria from the older unit ranged in value from 10 to 87 (n = 4, mean = 32.7, standard deviation=36.3) and frondose colonies in the Dillsboro had a BSI range of 19–61 (n = 3, mean = 40.2, standard deviation = 21.5).

The cystoporates (n = 6), regardless of zoarial habit or stratigraphic range, generally had lower BSI values (range = 4-61, mean = 22.9, standard deviation=18.8) than the trepostomes (n = 31, range = 6-90, mean = 32.0, standard deviation = 24.9), but it they were not significantly different (t-Test, P = 0.371, Fig. 4a, 5a). Adding data from cystoporates in other faunas might demonstrate that they exhibit a similarly broad range as do the trepostomes measured in this study. A wider assessment in terms of taxa in space and time will be undertaken in a future study.

The encrusting taxa (n = 5) (Fig. 3a-d), regardless of stratigraphic age and taxonomy, generally showed a lower BSI with a range of 4–23 (mean = 11.1; standard deviation = 6.6, Table 1), and conversely
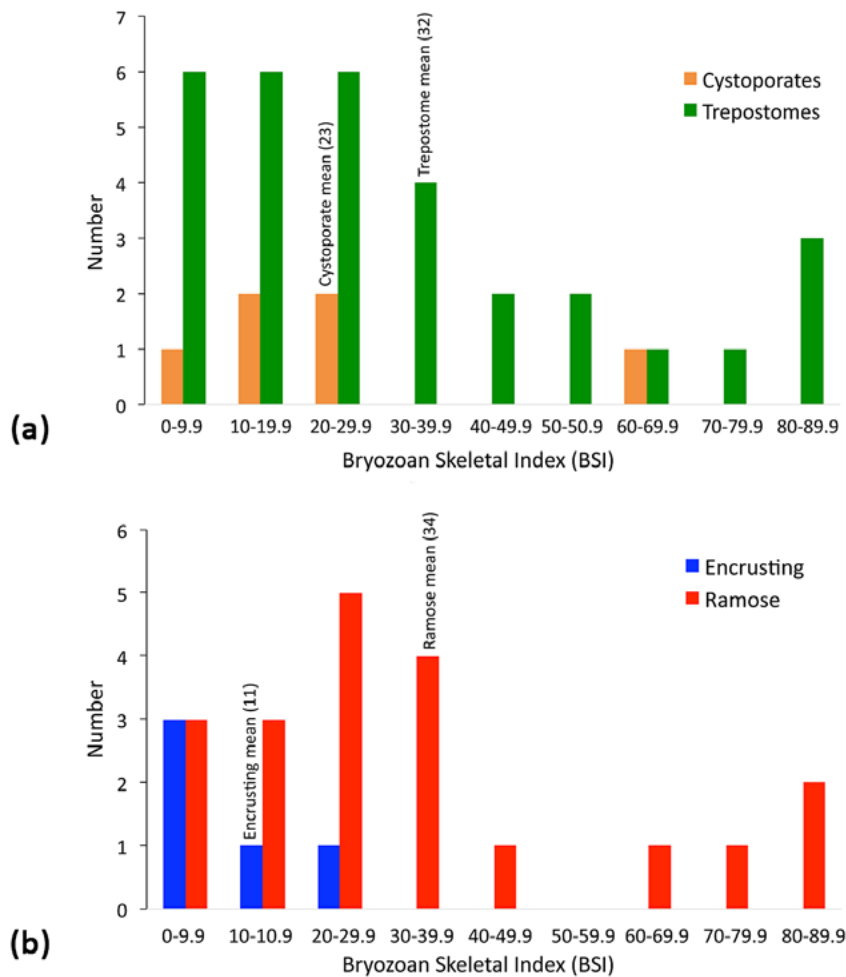

(a)

(b)

Figure 4. Frequency histograms show the numbers of taxa within groupings of BSI for (a) cystoporates and trepostomes and (b) encrusting and ramose colonies.

ramose zoaria (n = 20) (Fig. 3e-j) yielded higher BSI values in the range 7–90 (mean = 34.2; standard deviation=24.3, Table 1). The mean BSI of ramose colonies was significantly higher than that of encrusting colonies (t-Test, P = 0.002, Fig. 4b, 5b).

To test whether endozonal characters would influence the BSI results, three hypothetical ramose zoaria of 5mm in diameter but with different exozone thicknesses (Fig. 6a-c) were analysed. In these, ZWT is 0.5mm and MZD is 1mm, but EW varies from 0.5mm (Fig. 6a), 1mm (Fig. 6b) or 2mm (Fig. 6c). BSI for these zoaria is 25, 50 and 100 respectively. If Endozone Diameter (ED) is added to the formula (i.e.,

BSI = ((EW*ZWT)/(MZD*ED))*100) the BSI values are 6.25, 16.7 and 100. If Axial Ratio (AR) is added to the original formula (i.e., BSI = ((EW*ZWT)/(MZD*AR))*100) the values compute as 6.25, 33.3 and 200. In both cases, addition of endozonal characters does not alter the relative ranking of BSI, and given, as is outlined above, the difficulties of obtaining such data from these parameters, the BSI based on MZD, ET and IWT is sufficiently robust. If exozone thickness (EW) remains constant but endozone diameter decreases, i.e. overall branch diameter decreases (Fig. 6d-f), there is no change in BSI using the formula proposed here.
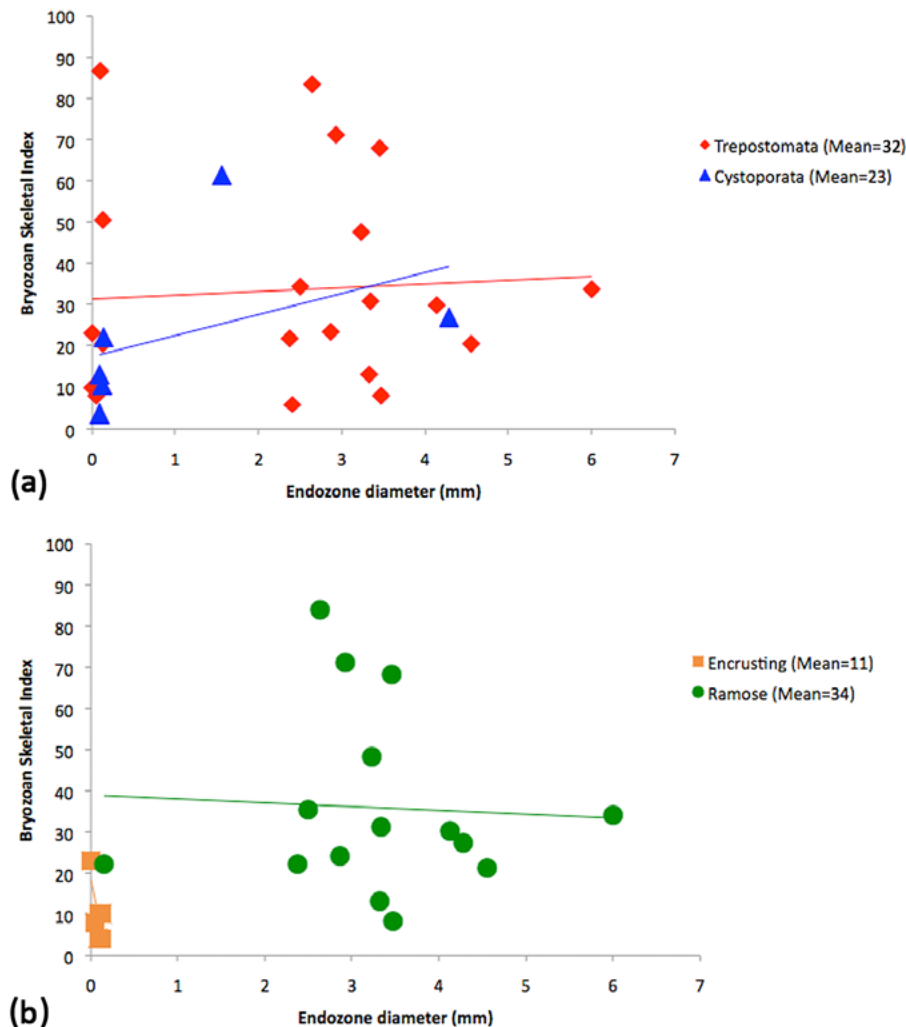

Figure 5. Plots of BSI against endozone diameter (in mm) for (a) cystoporates and trepostomes and (b) encrusting and ramose colonies.

DISCUSSION

BSI is highest in ramose trepostomes rather than ramose cystoporates or encrusing trepostomes as they have proportionally more exozone in branches and thus a lower axial ratio than do cystoporates. The differences in BSI between ramose and encrusting bryozoans are manifested in the formers' need for the skeleton to provide enough strength to allow for erect growth, and to maintain strength in water currents (Key 1991). Encrusters simply require skeleton to separate and isolate autozooecial chambers for the filter feeding lophophores; most of the strength of these colonies is provided by the foundation substrate (shell, cobble, hardground). This is also true of dome-shaped colonies such as *Diplotrypa* in which the exozonal walls are lightly calcified (Mänill 1961; Boardman and Utgaard 1966; Wyse Jackson and Key 2007) or in the turbinate *Dianulites* where the endozone and exozone cannot be distinguished on the basis of wall thickness (Taylor and Wilson 1999).

Though this study focuses on skeletal volume, it has implications for computation and assessment of colony strength (Key 1991), the biomechanics of space filling (Key *et al.* 2001), and resistance to bioerosion (Wyse Jackson and Key 2007, 2019).

The findings of this study suggest that there is merit in the adoption of the BSI in future examination of stenolaemate bryozoans, as the data generated may throw light on questions of palaeoecology, biogeochemistry, biomechanics, and biotic interactions:

 (1) The volume of skeletal material in bryozoans may be related to depth, although this hypothesis remains untested for specific taxa from known different palaeo-bathymetric regimes. Branch diameter in cyclostome bryozoans has been shown to increase in cyclostome with depth (Taylor *et al.* 2007), and Figuerola *et al.* (2015) demonstrated depth-related differences in the levels of skeletal Mg-calcite in modern Antarctic bryozoans, but does the BSI vary with depth? Similarly, colony morphology
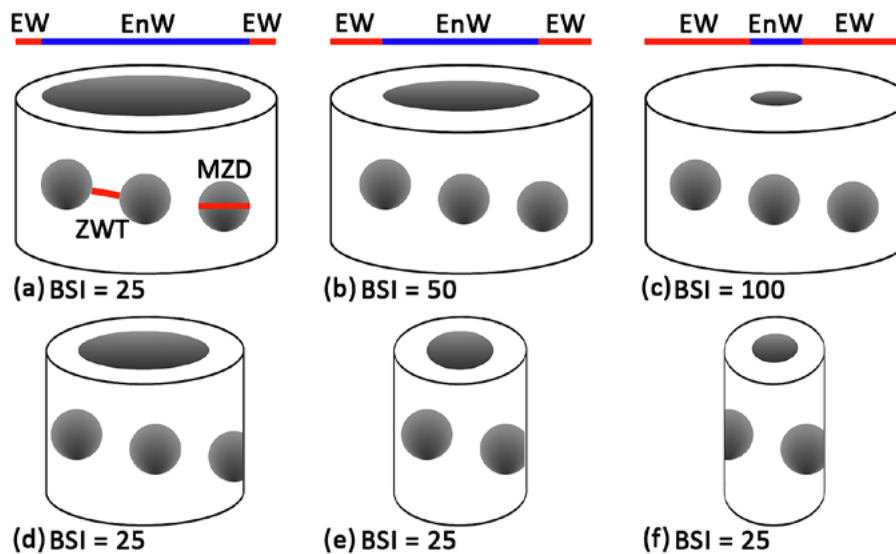

Figure 6. Stylised ramose trepostome bryozoans with (a-c) exozone of different widths (EW),
(a) = 0.5mm, (b) = 1mm, (c) = 2mm in branches of 5mm diameter; (d-f) constant exozone width 0.5mm
in branches of different diameter (d) = 3mm, (e) = 2mm, (f) = 1.5mm. In each colony,
MZD is 1.0mm, and ZWT is 0.5mm. Abbreviation: EW: Exozone width; EnW: Endozone width;
MZD: maximum autozooecial apertural diameter;
ZWT: zooecial wall thickness between adjacent autozooecial apertures.

in stromatolites (Andres and Reid 2006; Jahnert and Collins 2012) varies with depth, and the ability or otherwise to lay down skeleton in bryozoans may be reflected in observable differences in zoarial or zooecial morphology.

(2) Some taxa have shown considerable plasticity in zoarial form in response to changes in environmental conditions through a small stratigraphical interval or even within reefal systems of tens of metres high. *Leioclema* a Mississippian reef of North Wales formed ramose colonies in the deepest basal facies, unilaminar sheets and bifoliate zoaria in the mid-depth facies and unilaminar sheets in the upper shallowest water zone (Wyse Jackson *et al.* 1991). While initial observations on this material suggest that BSI is similar in all zoarial forms, this needs further quantification and confirmation. Similarly, Hageman and Sawyer (2006) in a study of *Leioclema punctatum* from the Mississippian, recorded that exozone thickness was approximately the same in all specimens examined. It would be interesting to determine if there was any discernible variation in exozonal thickness between the encrusting portions of zoaria as against the erect ramose branches which subsequently developed from the bases. If so, then BSI may be able to indicate subtle changes in environmental conditions.

(3) The ability of modern bryozoans to build the hard parts of their colonies is also linked to the chemistry and levels of acidification of the oceanic waters in which they live (Smith 2009, 2014; Lombardi *et al.* 2015 and references therein). This leads to two questions: could BSI be utilised as a proxy for past oceanic chemistry or acidification, or does ocean acidification effect BSI in live bryozoan colonies or only after death through the taphonomic process?

Taylor and Kuklinski (2011) used two proxies (diameter of branches and exozonal wall thickness) in a test for hypercalcification. They concluded that these proxies either didn't demonstrate hypercalcification in the Ordovician calcite sea, or that trepostome stenolaemates didn't become hypercalcified at all. However, use of branch diameter as a proxy in this regard may be problematic as it can be altered taphonomically which results in branch flattening and loss of endozonal interiors. BSI might be a more accurate proxy for the presence or otherwise of calcite seas as it can be applied to crushed specimens.

(4) Implications of strength from skeleton. The biomechanical architecture of bryozoan colonies is one element determining strength. Cheetham and Thomsen (1981) concluded that skeletal ultrastructure and mineralogy were not demonstrable contributors to strength of colonies and their breakage under energy regimes but that the overall design of branches was more important. In ramose trepostomes, there is a positive relationship between autozooecial wall thickness and exozone width with branch strength, (Key 1991), and this study has implications for the biomechanics of space filling (Key *et al.* 2001). Quantification of the skeletal contribution via the BSI to bryozoan zoaria can add quantifiable measures for strength and the behaviour of bryozoans under different hydrodynamic regimes.

(5) It would be interesting to determine if there is a correlation between BSI and gross colony size.

(6) A high BSI may affect the ability of epibionts to penetrate zoaria and so become endoskeletozoans, and the susceptibility of these zoaria to bioerosion may thus be lessened (see Wyse Jackson and Key, 2019). This would be particularly true if epibionts attempted boring transversely across the walls, or if the diameter of the borer was greater than the autozooecial apertural diameter (MZD) where it attempted to penetrate perpendicular to the zoarial surface. Conversely, thin-walled zoaria may be more easily bored, but would have a high breakage potential and so may not be favoured by endoskeletozoans. This hypothesis will be investigated in a future study that will document BSI for Ordovician to Triassic stenolaemates from various palaeogeographic areas and draw on data on the geological record and distribution of bio-eroding organisms. Assembly of this geologically wider database may also yield evolutionary patterns of skeletal development in bryozoans.

Application of the BSI in future studies drawing on data derived from earlier literature as well as from measurements taken by the current authors, will test further potential limitations of the measure such as, what are the effects of exilazooecia, mesozooecia, diaphragms and maculae on results, and is zoarial plasticity in a single taxon reflected in a variance of BSI and in the incidence of boring?

CONCLUSION

The Bryozoan Skeletal Index (BSI) is established to provide a measure of the degree of skeletal material or calcification in stenolaemate bryozoans and is formulated from three frequently measured and thus readily available morphological characters. A study of two faunas from the Cincinnatian (Upper Ordovician) of North America has shown that the differences in BSI values between encrusting and ramose taxa is significant while that between trepostome and cystoporate taxa is not. The use of the BSI may have potential as a proxy for zoarial strength, size, and endoskeletozoan infestation as well as for investigating patterns of calcification and biomineralisation throughout the geological record of stenolaemate bryozoans.

ACKNOWLEDGMENTS

REFERENCES

ANDRES, M.S. AND REID, R.P. 2006. Growth morphologies of modern marine stromatolites: a case study from Highborne Cay, Bahamas. *Sedimentary Geology* **185**, 319–328.

BAIRD, G.C., BRETT, C.E. AND FREY, R.W. 1989. "Hitchhiking" epizoans on orthoconic nautiloids: preliminary review of the evidence and its implications. *Senckenbergiana lethaea* **69**, 439–465.

BOARDMAN, R.S. 1960. Trepostomatous Bryozoa of the Hamilton Group of New York State. *United States Geological Survey Professional Paper* **340**, 1–87.

BOARDMAN, R.S. 1984. Origin of the post-Triassic Stenolaemata (Bryozoa): a taxonomic oversight. *Journal of Paleontology* **58**, 19–39.

BOARDMAN, R.S. 2001. The growth and function of skeletal diaphragms in the colony life of Lower Paleozoic Trepostomata (Bryozoa). *Journal of Paleontology* **75**, 225–240.

BOARDMAN, R.S. AND BUTTLER, C.J. 2005. Zooids and Extrazooidal Skeleton in the Order Trepostomata (Bryozoa). *Journal of Paleontology* **79**, 1088–1104.

BOARDMAN, R.S. AND UTGAARD, J. 1966. A revision of the Ordovician bryozoan genera *Monticulipora*, *Peronopora*, *Heterotrypa*, and *Dekayia*. *Journal of Paleontology* **40**, 1082–1108.

BROWN, G.D., JR. AND DALY, E.J. 1985. Trepostome Bryozoa from the Dillsboro Formation (Cincinnatian Series) of southeastern Indiana. *Geological Survey of Indiana, Special Report* **33**, 1–95.

BUTTLER, C.J. AND WILSON, M.A. 2018. Paleoecology of an Upper Ordovician sunmarine cave-deweeling bryozoan fauna and its exposed equivalents in northern Kentucky, USA. *Journal of Paleontology* **92**, 568–576.

CHEETHAM, A.H. 1986. Branching, biomechanics and bryozoan evolution. *Proceedings of the Royal Society of London, Series B, Biological Sciences* **228**, 151–171.

CHEETHAM, A.H. AND HAYEK, L.-A.C. 1983. Geometric consequences of branching growth in adeoniform Bryozoa. *Paleobiology* **9**, 240–260.

CHEETHAM, A.H. AND THOMSEN, E. 1981. Functional morphology of arborescent animals: strength and design of cheilostome bryozoan skeletons. *Paleobiology* **7**, 355–383.

COHEN, K.M., FINNEY, S.C., GIBBARD, P.L. AND FAN, J.-X. 2013. The ICS International Chronostratigraphic Chart. *Episodes* **36**, 199–204.

CUFFEY, R.J. AND FINE, R.L. 2005. The largest known fossil bryozoan reassembled from near Cincinnati. *Ohio Geology* **2005**(1), 1, 3–4.

CUFFEY, R.J. AND FINE, R.L. 2006. Reassembled trepostomes and the search for the largest bryozoan colonies. *International Bryozoology Association Bulletin* **2**(1), 13–15.

ERICKSON, J.M. AND BOUCHARD, T.D. 2003. Description and interpretation of *Sanctum laurentiensis*, new ichnogenus and ichnospecies, a domichnium mined into Late Ordovician (Cincinnatian) ramose bryozoan colonies. *Journal of Paleontology* **77**, 1002–1010.

ERNST, A. 2019. Fossil record and evolution of Bryozoa. In: A. Schmidt-Rhaesa (ed.), *Handbook of Zoology Online*. Berlin, De Gruyter.

ERNST, A. AND CARRERA, M. 2012. Upper Ordovician (Sandbian) bryozoan fauna from Argentine Precordillera. *Journal of Paleontology* **86**, 721–752.

FIGUEROLA, B., KUKLINSKI, P. AND TAYLOR, P.D. 2015. Depth patterns in Antarctic bryozoan skeletal

Mg-calcite: can they provide an analogue for future environmental changes? *Marine Ecology Progress Series* **540**, 109–120.

HAGEMAN, S.J. AND SAWYER, J.A. 2006. Phenotypic variation in the bryozoan *Leioclema punctatum* (Hall, 1858) from the Mississippian ephemeral host microcommunities. *Journal of Paleontology* **80**, 1047–1057.

HAQ, B.U. 2007. *The Geological Time Scale*, 6ᵗʰ revised edition. Amsterdam, Elsevier.

JACKSON, J.B.C. 1979. Morphological strategies of sessile animals. In: G.P. Larwood and B.R. Rosen (eds), *Biology and Systematics of Colonial Organisms.* London, Academic Press, pp. 499–555.

JAHNERT, R.J. AND COLLINS, L.B. 2012. Characteristics, distribution and morphogenesis of subtidal microbial systems in Shark Bay, Australia. *Marine Geology* **303–306**, 115–136.

KARKLINS, O.L. 1984. Trepostome and cystoporate bryozoans from the Lexington Limestone and the Clay Ferry Formation (Middle to Upper Ordovician) of Kentucky. *United States Geological Survey Professional Paper* **1066-I**, 1–105.

KEY, M.M., JR. 1990. Intracolony variation in skeletal growth rates in Paleozoic ramose trepostome bryozoans. *Paleobiology* **16** (4), 483–491.

KEY, M.M., JR. 1991. How to build a ramose trepostome. In: F.P. Bigey and J.-L. d'Hondt (eds), Bryozoaires actuels et fossiles: Bryozoa living and fossil. *Bulletin de la Société des Sciences Naturelles de l'Ouest de la France. Mémoire HS* **1**, 201–207.

KEY, M.M., JR., THRANE, L. AND COLLINS, J.A. 2001. Space-filling problems in ramose trepostome bryozoans as exemplified in a giant colony from the Permian of Greenland. *Lethaia* **34**(2), 125–135.

KEY, M.M., JR., WYSE JACKSON, P.N. AND FELTON, S. 2016. Intracolony variation in zoarial morphology in reassembled fossil ramose stenolaemate bryozoans from the Upper Ordovician (Katian) of the Cincinnati Arch region, USA. *Journal of Paleontology* **90**(3), 400–412.

LOMBARDI, C., COCITO, S., GAMBI, M.C. AND TAYLOR, P.D. 2015. Morphological plasticity in a calcifying modular organism: evidence from an *in situ* transplant experiment in a natural CO_2 vent system. *Royal Society Open Science* **2**, 140413.

MA, J., BUTTLER, C.J. AND TAYLOR, P.D. 2014. Cladistic analysis of the 'trepostome' Suborder Estonioporina and the systematics of Palaeozoic bryozoans. *Studi Trentini di Scienze Naturali* **94**, 153–164.

MÄNNIL, R.M. 1961. On the morphology of the hermispherical Bryozoa of the Order Trepostomata. *Eesti NSV Teaduste Akadeemia Geoloogia Instituudi Uurimused* **6**, 113–140.

POWERS, C.M. AND PACHUT, J.F. 2008. Diversity and distribution of Triassic bryozoans in the aftermath of the end-Permian mass extinction. *Journal of Paleontology* **82**, 362–371.

SMITH, A.M. 2009. Bryozoans as southern sentinels for ocean acidification: a major role for a minor phylum. *Marine and Freshwater Research* **60**, 475–482.

SMITH, A.M. 2014. Growth and calcification of marine bryozoans in a changing ocean. *Biological Bulletin* **226**, 203–210.

SMITH, A.M. 2018. Bryozoans and ocean acidification. In: P.L. Cook, P.E. Bock, D.P. Gordon and H.J. Weaver (eds), *Australian Bryozoa Volume 1: Biology, Ecology and Natural History*. Clayton South, Victoria, CSIRO publishing, pp. 139–144.

TAYLOR, P.D. AND KUKLINSKI, P. 2011. Seawater chemistry and biomineralisation: did trepostome bryozoans become hypercalcified in the 'calcite sea' of the Ordovician? *Palaeobiodiversity and Palaeoenvironments* **91**, 185–195.

TAYLOR, P.D., KUKLINSKI, P. AND GORDON, D.P. 2007. Branch diameter and depositional depth in cyclostome bryozoans: testing a potential paleobathymetric tool. *Palaios* **22**, 220–224.

TAYLOR, P.D. LOMBARDI, C. AND COCITO, S. 2015. Biomineralization in bryozoans: present, past and future. *Biological Reviews* **90**, 1118–1150.

TAYLOR, P.D. AND WILSON, M.A. 1999. *Dianulites* Eichwald, 1829: an unusual Ordovician bryozoan with a high-Magnesium Calcite skeleton. *Journal of Paleontology* **73**, 38–48.

VAN HINSBERGEN, D.J.J., DE GROOT, L.V., VAN SCHAIK, S.J., SPAKMAN, W., BIJL, P.K., SLUIJS, A., LANGEREIS, C.G. AND BRINKHUIS, H. 2015. A Paleolatitude Calculator for Paleoclimate Studies. *PLoS ONE* **10**(6), 1–21 [Model version 2.1 online: www.paleolatitude.org]

WILSON, M.A., BUTTLER, C.J. AND TAYLOR, P.D. 2019. Bryozoans as taphonomic engineers, with examples from the Upper Ordovician (Katian) of Midwestern North America. *Lethaia* **52**, 403–409.

WYSE JACKSON, P.N., BANCROFT, A.J. AND SOMERVILLE, A.J. 1991. Bryozoan zonation in a trepostome-dominated buildup from the Lower Carboniferous of North Wales. In: F.P. Bigey and J.-L. d'Hondt (eds), Bryozoaires actuels et fossiles: Bryozoa living and fossil. *Bulletin de la Société des Sciences Naturelles de l'Ouest de la France. Mémoire HS* **1**, 551–559.

WYSE JACKSON, P.N. AND KEY, M.M., JR. 2007. Borings in trepostome bryozoans from the Ordovician of Estonia: two ichnogenera produced by single maker, a case of host morphology control. *Lethaia* **40**, 237–252.

WYSE JACKSON, P.N. AND KEY, M.M., JR. 2019. Epizoan and endoskeletozoan distribution across reassembled ramose stenolaemate bryozoan zoaria from the Upper Ordovician (Katian) of the Cincinnati Arch region, USA. *Memoirs of the Association of Australasian Palaeontologists* **52**, 169–178.

WYSE JACKSON, P.N., KEY, M.M., JR. AND COAKLEY, S.P. 2014. Epizoozoan trepostome bryozoans on nautiloids from the Upper Ordovician (Katian) of the Cincinnati Arch Region, U.S.A.: an assessment of growth, form and water flow dynamics. *Journal of Paleontology* **88**(3), 475–487.